SYNTHESIS, CHARACTERIZATION OF TRANSITION METAL-DITHIOETHER COMPLEXES AND CATALYTIC APPLICATIONS IN ORGANIC REACTIONS

A Thesis submitted to the University of North Bengal

For the Award of

Doctor of Philosophy

in

Chemistry

By

Sankar Saha

GUIDE

Prof. Basudeb Basu

Department of Chemistry
University of North Bengal

JULY, 2019

Dedicated
TO
My Parents
&
Family members

DECLARATION

I declare that the thesis entitled **SYNTHESIS, CHARACTERIZATION OF TRANSITION METAL-DITHIOETHER COMPLEXES AND CATALYTIC APPLICATIONS IN ORGANIC REACTIONS** has been prepared by me under the guidance of Prof. Basudeb Basu, Professor of Chemistry (Retired), University of North Bengal. No Part of this thesis has formed the basis for the award of any degree or fellowship previously.

Sankar Saha
29/7/2019

Sankar Saha
Department of Chemistry
University of North Bengal
Darjeeling, 734013
West Bengal, India

ENLIGHTENMENT TO PERFECTION

UNIVERSITY OF NORTH BENGAL

Accredited by NAAC with Grade A

DEPARTMENT OF CHEMISTRY

P.O. NORTH BENGAL UNIVERSITY, Raja Rammohunpur, Dist. Darjeeling, West Bengal, India, PIN - 734013.
PHONE : (0353) 2776 381, Fax: (0353) 2699 001

Ref. No.....

Dated 26/07/2019

CERTIFICATE

I certify that Mr. **SANKAR SAHA** has prepared the thesis entitled, **SYNTHESIS, CHARACTERIZATION OF TRANSITION METAL-DITHIOETHER COMPLEXES AND CATALYTIC APPLICATIONS IN ORGANIC REACTIONS** for the award of Ph.D. degree of the University of North Bengal, under the guidance of Prof. (Dr.) Basudeb Basu. He has carried out the work at the Department of Chemistry, University of North Bengal. No part of this thesis has formed the basis for the award of any degree or fellowship previously.

Professor (Retired)
Department of Chemistry
University of North Bengal
Darjeeling - 734013, India

26/7/19

Professor (Dr.) B. Basu, Ph.D., FAScT (Retired)
Department of Chemistry
University of North Bengal
Darjeeling 734013, India
Visiting Professor, Raiganj University (Presently)
Mobile: +91 9434428477
Alternative E-mail: basudeb.basu@gmail.com

URKUND

Urkund Analysis Result

Analysed Document: Sankar Saha_Chemistry.pdf (D54476791)
Submitted: 7/18/2019 1:29:00 PM
Submitted By: nbuplg@gmail.com
Significance: 5 %

Sources included in the report:

http://doczz.fr/doc/167390/curve-di-portata---service-frigorifice
https://www.depts.ttu.edu/aaec/icac/archive/pdf/Ginning_optimized/Charges/Rates_for_Ginning_and_Wrapping_American_Cotton_and_Related_Data_Seasons_1928-29_to_1935-36.pdf
fcea3381-bf82-4064-a8d0-e90af1c28bee
fc88f6a0-9ae7-4d5b-a5c6-f23a1ae7bbfb
5ebcc06c-943b-472a-baa9-eca6ea0eed88

Instances where selected sources appear:

17

26/7/2019

Professor (Retired)
Department of Chemistry
University of North Bengal
Darjeeling - 734013, India

Sankar Saha
29/7/2019

26/7/19

Head
Department of Chemistry
University of North Bengal
Darjeeling - 734013, India

ABSTRACT

The research work embodied in this thesis entitled, **SYNTHESIS, CHARACTERIZATION OF TRANSITION METAL-DITHIOETHER COMPLEXES AND CATALYTIC APPLICATIONS IN ORGANIC REACTIONS** is primarily focused on the development of new dithioether ligands, their transition metal complexes and the characterization of these complexes by various methods like NMR, HRMS and Single Crystal XRD techniques. Another important aspect was to introduce these transition metal–dithioether complexes as catalytic system in various organic reactions. The overall work delineated herein has been divided into four chapters.

As a prelude to present work, the **Chapter I** covers a brief review on the recent development and trends towards the synthesis of dithioether ligands, various transition metal complexes of these ligands and catalytic applications of these Coordination Clusters, Metal Organic Frameworks towards various organic reactions. 1D, 2D, 3D–frameworks of various coordination polymers of these dithioether ligands with copper, silver, gold etc. and their coordination architectures has been well discussed under this chapter. Catalytic application of these coordination polymers towards various organic transformation has been also illustrated.

Chapter II depicts the preparation of a new 1D CuI–1,3–dithioether coordination polymer complex, characterization of the complex by NMR, HRMS and single crystal X–ray structure determination, and finally its efficient role as catalyst in azide–alkyne cycloaddition (AAC) reaction. Although few examples of other dithioether–based Cu(I) complexes are known in the literature, the present 1,3–dithioether ligand–based Cu(I) complex is not known, and there is no example of such complexes used as the catalyst for the AAC reaction. The present study therefore establishes a new and convenient catalytic system for the one–pot AAC in multi–component manner. The yields of the cycloadducts are excellent in diverse array of reactants. The applicability of the catalyst was also extended and 1,2,3–triazole compound with sulfur functionalized arms was synthesized in a multicomponent approach in one–pot two–step process.

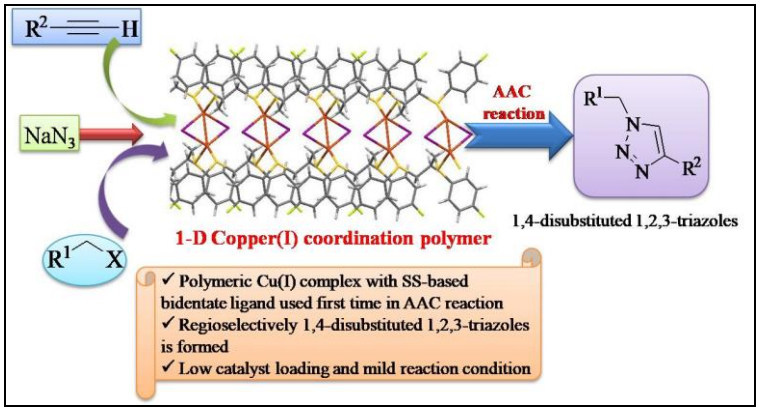

Chapter III describes the synthesis of a new 2D CuI–1,2–dithioether coordination polymeric complex synthesized from CuI and 1-(1-{4-chlorophenylthio}propan-2-ylthio)-4-chlorobenzene, $([(CuI)_2\{ArSCH_2CH(CH_3)SAr\}_2]_n$, Ar = 4-Cl-$C_6H_4$), and characterized by NMR, high resolution mass spectrometry (HRMS) and single crystal X–Ray Diffraction technique. The complex compound has been employed as suitable catalyst for solvent-free one-pot three-component A^3 coupling reaction. Variety of aromatic and aliphatic aldehydes, terminal alkynes and aliphatic cyclic secondary amines have been employed to prepare a library of propargylamines using the 2D–Cu complex at significantly low concentration (0.2 mol%).

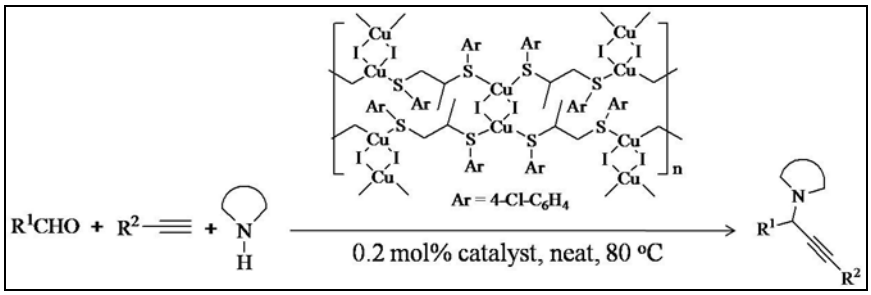

In **Chapter IV** a simple and green method for the preparation of stabilized cuprous oxide nanoparticles (NPs) fairly dispersed and anchored with macroporous poly–ionic resins is developed (named as Cu_2O@ARF) and characterized by FT–IR, PXRD, XPS, HRTEM and ICP–AES. It was employed as an efficient recyclable heterogeneous catalyst for "on–water" three–component click reaction leading to the formation of diversely functionalized 1,2,3–triazoles. The resins with counter formate anions are believed to reduce Cu(II) to Cu(I) species and also help in stabilization the Cu_2O NPs and provide necessary immobilizing ambience on polymeric matrices thus negating additional reductant, ligands and capping agents. We further extended the reaction scope towards the synthesis of a dithiocarbamate based bio–active triazole compound possessing antitumor activity.

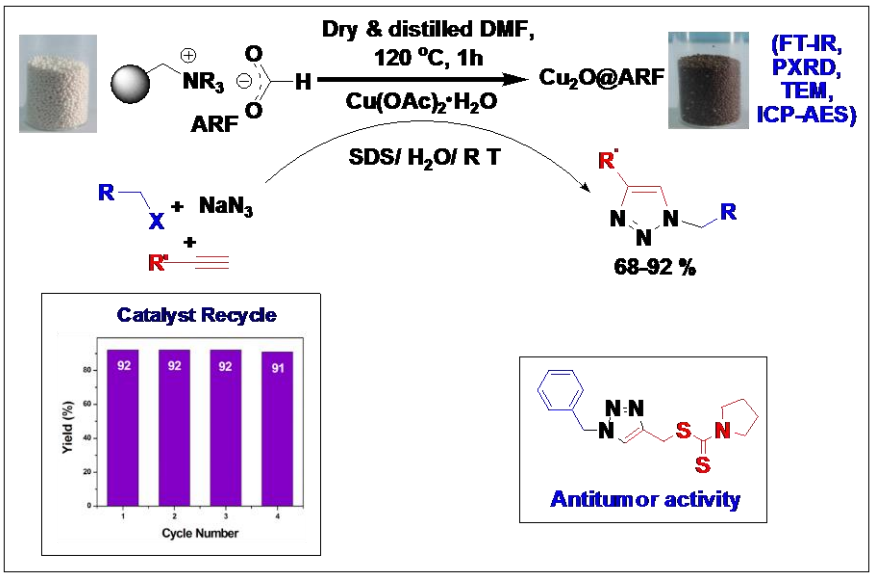

PREFACE

Research on variety of transition metal–dithioether complex synthesis, their characterization and their catalytic applications has revealed much attention now a days. Copper complexes of thioether–based ligands with structural diversities like 1D, 2D– and 3D–coordination copolymer (CP) networks are of much interest. The copper–dithioether coordination polymers with definite topology and geometry (metal–organic frameworks, MOFs) could be used as potential catalyst in organic reactions.

The present research work describes development of the transition metal–dithioether based complexes and their catalytic applications in various organic transformations. This thesis begins with **Chapter I**, which introduces a brief review on synthesis, characterization of transition metal–dithioether based complexes and their catalytic applications towards organic transformations. **Chapter II** describes the synthesis, characterization of a new 1,3–dithioether based 1D–Copper(I) coordination polymer and its catalytic activity towards one–pot AAC reaction. **Chapter III** illustrates synthesis, characterization of another novel 1,2–dithioether based 2D–copper(I) coordination polymer and its catalytic application towards solvent–free A^3–coupling reaction to synthesize propargylamines. **Chapter IV** deals with the synthesis and characterization of Cu_2O@ARF nanocomposite (Cu_2O nanoparticles embedded on polymeric macroporous resin surface) and its catalytic application in one–pot three–component click reaction in water for the regioselective synthesis of 1,4–disubstituted–1,2,3–triazoles.

ACKNOWLEDGEMENT

This thesis is the outcome of a long rigorous journey in which I have been encouraged and supported by many peoples who actually make my dream possible. It is really pleasure moment for me to express my full gratitude for them.

Primarily, I would like to express my deep and sincere gratitude to my supervisor Dr. Basudeb Basu, Professor, Department of Chemistry, University of North Bengal, Darjeeling, for his Inspiring guidance, parental attitude, solicitude behaviour and constant encouragement throughout my work..

I wish to express my warm and sincere thanks to Dr. Goutam De, Chief Scientist & Head, Nano-Structured Materials Division, CSIR-CGCRI, Kolkata, for his help to characterize our metal nanocatalyst.

I express my full gratitude to Prof. Ashutosh Ghosh, University of Calcutta, Kolkata and Mayukh Deb, IIT Delhi for carrying out the single crystal XRD.

I gratefully acknowledge to Prof. Pranab Ghosh and Dr. Sajal Das for recording and interpreting NMR spectra.

I offer my special thanks to Shreyasi Chattopadhyay, Kolkata for her valuable contribution in my scientific work.

I also thank Swarnali Roy, IICB, Kolkata for helping me to interprete HRMS data.

I would like to thank my labmates Dr. Kinkar Biswas, Dr. Sujit Ghosh, Debashish Da, Samirda Suchandra and Prasun for their help and active co-oparation throughout my research period.

I would like to express my thanks to University of North Bengal for providing the infrastructural facilities and DST, New Delhi.

I express my full gratitude to Head and all respected teachers of Department of Chemistry, University of North Bengal.

I really acknowledge my sister for his constant inspiration throughout my life.

I would like to thank my wife Aparna for her constant selflessness, love and support.

The single largest contribution in properly shaping me what I am today comes from the faith, hope and pride of my parents. Words are inadequate for expressing such feelings.

TABLE OF CONTENTS

	Page No.
Abstract	i-ii
Preface	iii
Acknowledgement	iv
List of Tables	xi
List of Schemes	xii-xiv
List of Figures	xv-xvii
List of Appendices	xviii
Appendix A: List of Research Publications	xix
Appendix B: Oral Presentations	xx
Abbreviation	xxi-xxii

CHAPTER I

Brief review on synthesis, characterization of transition metal-dithioether based complexes and their catalytic applications towards organic transformations			**1-19**
I.1.	Dithioethers and their synthesis		2
I.2.	Coordination polymers or Metal Organic Framework (MOF)		4
I.3.	Synthesis of various dithioether based metal complexes		5-18
	I.3.1.	Iridium complex with chiral dithioether compounds	5
	I.3.2.	Zirconium(IV) and Titanium(IV) complexes with [OSSO] type ligands	6-7
	I.3.3.	Ruthenium(II) dithioether complex	8
	I.3.4.	Tin(IV) dithioether complexes	8

I.3.5. Silver(I) coordination polymers with dithioether ligands 9

I.3.6. Gold(I) complexes of dithioether ligands 9-10

I.3.7. Copper complexes of dithioether-based ligands 11-18

I.4. Catalytic application of transition metal dithioether complexes towards organic transformations 18-19

I.5. References 19

CHAPTER II

Synthesis of a new 1,3-dithioether based 1D- Copper(I) coordination polymer and its catalytic activity towards one–pot AAC reaction **20-52**

II.1. Introduction 21-22

II.2. Background and Objectives 22-25

II.3. Present Work: Result and Discussion 25-35

II.3.1. Synthesis of 1,3–bis(4–fluorophenylthio) –propane ligand (L) 25

II.3.2. Synthesis of polymeric coordination complex catalyst CuI–1,3–bis(4–fluorophenylthio)–propane 25

II.3.3. Characterization of complex catalyst 25-29

II.3.3.1. NMR and HRMS spectroscopy 25-26

II.3.3.2. Single crystal X–ray diffraction 26-29

II.3.4. Catalytic application 29-33

II.3.5. One–pot two–step process for the synthesis of sulfur functionalized 1,2,3–triazole derivative 33-34

II.3.6. Mechanism 34-35

II.4. Conclusion 35-36

II.5.	Experimental Section		36-52
	II.5.1.	General Information	36
	II.5.2.	General procedure of preparing 1,3-bis(4-fluorophenylthio)-propane (L)	36
	II.5.3.	General procedure of preparing 1,3-bis(4-fluorophenylthio)-propane (L) ligated CuI-coordination complex	36-37
	II.5.4.	General procedure for one-pot three component AAC reaction	37
	II.5.5.	Characterization data of the ligand (L) and the 1D-polymeric complex	37-44
	II.5.6.1	Scanned copy of HRMS spectra of polymeric copper complex	45
	II.5.6.2.	Scanned copies of ^{1}H NMR, ^{13}C NMR of Table II.5, Entry 4 and 9 and HRMS of entry 9	46-52
II.6.	References		52

CHAPTER III

1,2-dithioether based 2D-copper(I) coordination polymer catalysed A^3-coupling reaction: Solvent-free synthesis of propargylamines			**53-95**
III.1.	Introduction		54-58
III.2.	Background and Objectives		58-62
III.3.	Present Work: Result and Discussion		62-73
	III.3.1.	Synthesis of 1,2–bis(4-chlorophenylthio) –propane ligand (L)	62
	III.3.2.	Synthesis of polymeric coordination complex catalyst CuI–1,2–bis(4- chlorophenylthio)–propane	62
	III.3.3.	Characterization of complex catalyst	62-67

III.3.3.1. ^{1}H NMR, ^{13}C NMR and HRMS spectroscopy 62

III.3.3.2. Single crystal X–ray diffraction 63-67

III.3.4. Catalytic application 67-72

III.3.5. Mechanism 72-73

III.4. Conclusion 73

III.5. Experimental Section 73-95

III.5.1. General Information 73-74

III.5.2. General procedure of preparing 1,2-bis(4-chlorophenylthio)-propane (L) 75

III.5.3. General procedure of preparing 1,2-bis(4-chlorophenylthio)-propane (L) ligated CuI-coordination complex 75

III.5.4. General procedure for A^3-coupling reaction 75

III.5.5. Characterization data of the ligand (L) and the 2D-polymeric complex 76

III.5.6. Physical properties and spectroscopic data of various propargyl amine products 77-84

III.5.7.1. Scanned copy of HRMS spectra of polymeric copper complex 85

III.5.7.2. Scanned copies of ^{1}H NMR, ^{13}C NMR and HRMS of Table III.5, Entry 6 and 7 86-95

III.6. References 95

CHAPTER IV

Stabilized Cu_2O nanoparticles on macroporous poly–styrene resins (Cu_2O@ARF) as heterogeneous catalyst towards click reaction for the synthesis of triazoles in aqueous medium **96-131**

IV.1. Introduction 97

IV.2. Background and Objectives 98-104

IV.3. Present Work: Result and Discussion 104-117

IV.3.1. Preparation of Cu_2O@ARF 104-105

IV.3.2. Characterization of Cu_2O@ARF 105-108

IV.3.2.1. FT–IR spectroscopy 105

IV.3.2.2. Powder X–ray diffraction (PXRD) pattern 106

IV.3.2.3. TEM analysis 106-107

IV.3.2.4. ICP–AES analysis 107

IV.3.2.5. XPS analysis 107-108

IV.3.3. Catalytic activity of Cu_2O@ARF nanocomposite in three–component click reaction 109-113

IV.3.4. Reusability and stability of Cu_2O@ARF 113-115

IV.3.5. Plausible mechanism 116

IV.3.6. Comparison of catalytic activity 116-117

IV.3.7. Application towards the synthesis of bio–active 1,2,3–triazole 117

IV.4. Conclusion 117-118

IV.5. Experimental Section 118-131

IV.5.1. General Information 118

IV.5.2. General procedure for the synthesis of 1,2,3−triazole derivative 118-119

IV.5.3. Procedure for recovery and reusability of the catalyst [Cu_2O@ARF] 119

IV.5.4. Procedure for the synthesis of dithiocarbamate based triazole compound (2) 119

IV.5.5. Physical properties and spectroscopic data of triazole compounds 120-127

IV.5.6. Scanned copies of ^{1}H NMR, ^{13}C NMR of Table IV.5, 128-131

Entry 1d and compound (1)

IV.6. References 131

Bibliographic References

References for Chapter I 132-134

References for Chapter II 134-136

References for Chapter III 136-139

References for Chapter IV 139-143

Index 144-147

LIST OF TABLES

Table No.	Title	Page No.
Table I.1.	Ligands used and Dimensionality of Coordination polymers obtained	16-17
Table II.1.	Crystal Data, Data Collection and Structure Refinement for the complex catalyst	26-27
Table II.2.	Selected bond length	27-28
Table II.3.	Selected bond angle	28-29
Table II.4.	Optimization of reaction conditions for the one–pot azide–alkyne click reaction.	29-30
Table II.5.	Catalytic activity of the complex in the AAC reaction	31-33
Table III.1.	Crystal Data, Data Collection and Structure Refinement for the complex catalyst	63-64
Table III.2.	Selected bond length	65-66
Table III.3.	Selected bond angle	66-67
Table III.4.	Optimization of reaction conditions for the 2D- Cu(I)-polymeric complex catalyzed A^3-coupling reaction	68-69
Table III.5.	Catalytic activities of the 2D- Cu(I)-polymeric complex catalyzed A^3-coupling reaction	69-72
Table IV.1.	Optimization of the reaction conditions for the synthesis of triazole	109-110
Table IV.2.	Cu_2O@ARF catalyzed three–component click reaction in aqueous and aerobic conditions at room temperature	111-113
Table IV.3.	Catalyst recycling experiments	114
Table IV.4.	Comparison of on–water triazole synthesis using some Cu(I) catalytic systems and our catalyst at room temperature (without reducing source)	116-117

LIST OF SCHEMES

Scheme No.	Title	Page No.
Scheme I.1.	Ruthenium catalysed synthesis of vicinal dithioethers	2
Scheme I.2.	Synthesis of 1,3-dithioethers from alkynes	2
Scheme I.3.	Preparation of vicinal-dithioethers from norbornene derivatives	3
Scheme I.4.	Hypervalent iodine catalysed 1,2-dithioether synthesis	3
Scheme I.5.	Gallium trichloride catalysed vicinal dithioether preparation	3
Scheme I.6.	Lewis acid catalysed disulfenylation of alkenes	4
Scheme I.7.	Preparation of 1,2- and 1,3-dithioether in silica support	4
Scheme I.8.	Synthesis of a Zirconium complex with [OSSO]-type ligand	7
Scheme I.9.	Ruthenium(II) complexes containing 1,10-phenanthroline and di-thioether ligand	8
Scheme I.10.	Synthesis of different CuI-dithioether complexes	12
Scheme I.11.	Formation of various framework depending upon the metal to ligand ratio	14
Scheme I.12.	Formation of 1D- and 2D- frameworks with two different dithioether ligands	15
Scheme I.13.	Formation of Cu(I) coordination polymers with 1,3–dithiane ligands L_1 and L_2	18
Scheme I.14.	CuBr with PhSMe catalysed click reaction	19
Scheme I.15.	CuI-1,3-dithioether catalysed AAC reaction	19
Scheme II.1.	Huisgen's 1,3–dipolar cycloaddition reaction	21
Scheme II.2.	CuBr.PhSMe–catalyst system for AAC reaction	22
Scheme II.3.	Preparation of CuX_2(SNS) catalysts and application towards azide–alkyne click reaction	23
Scheme II.4.	Cu–NS catalyst for one–pot azide–alkyne cycloaddition reaction	24
Scheme II.5.	"Click–and–click" – hybridised 1,2,3–triazoles supported Cu(I) coordination polymers for azide–alkyne cycloaddition	25
Scheme II.6.	One–pot two–step synthesis of sulfur functionalized 1,2,3–	34

	triazole derivative	
Scheme II.7.	A plausible mechanistic path for the Cu(I)–complex catalyzed one–pot three–component AAC reaction.	35
Scheme III.1.	SIPr–CuCl–catalyzed A^3 coupling reaction	56
Scheme III.2.	CuCN–catalyzed A^3 coupling reaction in [bmim][PF_6]	56
Scheme III.3.	CuI–catalyzed of AA^3 coupling reaction	57
Scheme III.4.	CuI–catalyzed by A^3 coupling reaction of salicylaldehyde	57
Scheme III.5.	MW–irradiated intramolecular A^3 coupling reaction	58
Scheme III.6.	1,2-dithioether based Cu(I) halide complex catalyzed aminomethylation of phenylacetylene	59
Scheme III.7.	Diallylphosphine-tetramer copper(I) complex catalyzed A^3-coupling reaction	59
Scheme III.8.	Nitrogen ligated 1D-Cu(I)-coordination polymer catalyzed A^3 coupling reaction	60
Scheme III.9.	Benzotriazole based 1D- polymeric Cu(II) catalyzed A^3 coupling	60
Scheme III.10.	2-(picolyliminomethyl)pyrrole based dicopper (I) complex catalyzed A^3 coupling reaction	61
Scheme III.11.	SS-based bidentate 1,2-dithioether- Cu(I) coordination polymer catalyzed A^3 coupling	62
Scheme III.12.	A plausible mechanism for the Cu(I)-complex catalyzed A^3-coupling reaction	73
Scheme IV.1.	Huisgen and Sharpless or Meldal approach for 1,2,3–1*H*–triazole formation	98
Scheme IV.2.	PS–C22–CuI–catalyzed three–component click reaction	99
Scheme IV.3.	Three–component click reaction catalyzed by $NiFe_2O_4$–supported glutamate–Cu	99
Scheme IV.4.	Three–component click reaction catalyzed by NHC–Cu(I) complex of vitamin B_1	100
Scheme IV.5.	Three–component azide–alkyne click reaction catalyzed by NHC–Cu(I) complex	101
Scheme IV.6.	Three–component click reaction catalyzed by magnetic nano Fe_3O_4@TiO_2/Cu_2O	101
Scheme IV.7.	Cu@PyIm-SBA-15 catalyzed click reaction	102

Scheme IV.8.	Three–component click reaction by MNP@ImAc/Cu	102
Scheme IV.9.	Three–component click reaction by (RGO/Cu_2O) nanocomposite	103
Scheme IV.10.	PVA–Cu_2O composite catalyzed three–component click reaction	103
Scheme IV.11.	Cu_2O@ARF catalyzed three–component on–water click reaction at room temperature	104
Scheme IV.12.	Synthesis of pharmaceutically active triazole compound (2) catalyzed by Cu_2O@ARF	117

LIST OF FIGURES

Figure No.	Title	Page No.
Figure I.1.	Various types of metal–organic framework (MOF)	5
Figure I.2.	Chiral dithioether ligands for asymmetric hydrogenation	6
Figure I.3.	[OSSO] type ligand and its [ONNO] Salan type analogue	6
Figure I.4.	[OSSO]–type ligands used to synthesize enantiomeric pure Titanium complex	7
Figure I.5.	Association of discrete molecules into 1D– or 2D–networks by aurophilic interactions	10
Figure I.6.	1,4–Dithioether ligands used for synthesis of polymeric complex with CuI	12
Figure II.1.	View of (a) monomeric picture of the complex and (b) infinite 1–D chain of the complex incorporating dinuclear Cu(μ_2–I)$_2$Cu motifs along '*b*' axis.	27
Figure II.2.	HRMS of 1,3–bis(4–fluorophenylthio)–propane (L) ligated CuI–coordination complex	45
Figure II.3.	^{1}H–NMR spectra of [1, 3–bis(4–fluorophenylthio)–propane] ligand(L) in d_6–DMSO	46
Figure II.4.	^{1}H–NMR spectra of the complex catalyst in d_6–DMSO	47
Figure II.5.	^{1}H NMR spectra of 1–benzyl–4–(4–nitrophenyl)–1*H*–1,2,3–triazole	48
Figure II.6.	^{13}C NMR spectra of 1–benzyl–4–(4–nitrophenyl)–1*H*–1,2,3–triazole	49
Figure II.7.	^{1}H NMR spectra of 1–(*E*)–Cinnamyl–4–(*p*–tolyl)–1*H*–1,2,3–triazole	50
Figure II.8.	^{13}C NMR spectra of 1–(*E*)–Cinnamyl–4–(*p*–tolyl)–1*H*–1,2,3–triazole	51
Figure II.9.	HRMS of 1–(*E*)–Cinnamyl–4–(*p*–tolyl)–1*H*–1,2,3–triazole	52
Figure III.1.	Structure of monoamine oxidase (MAO) type–B inhibitors	54
Figure III.2.	Schematic approaches for the synthesis of various *N*–containing heterocyclic molecules from different propargylamines	55

Figure III.3.	Schematic representation of A^3–coupling reaction	55
Figure III.4.	a) ORTEP diagram of the ($[(CuI)_2\{ArSCH_2CH(CH_3)SAr\}_2]_n$, Ar = 4–Cl–$C_6H_4$) complex, b) Part of the two–dimensional framework of complex, c) The asymmetric unit of polymeric complex and d) unit cell of polymeric matrix. Color code: Cu (brown), I (purple), Cl (green), S (yellow), C (black), H (grey).	65
Figure III.5.	HRMS of 1–(1–(4–chlorophenylthio)propan–2–ylthio)–4–chlorobenzene (L) ligated CuI–coordination complex	85
Figure III.6.	^{1}H NMR spectra of ligand 1–(1–(4–chlorophenylthio)propan–2–ylthio) –4–chlorobenzene (L)	86
Figure III.7.	^{13}C NMR spectra of ligand 1–(1–(4–chlorophenylthio)propan–2–ylthio) –4–chlorobenzene (L)	87
Figure III.8.	^{1}H NMR spectra of 1–(1–(4–chlorophenylthio)propan–2–ylthio)–4–chlorobenzene (L) ligated CuI–coordination complex (1)	88
Figure III.9.	^{13}C NMR spectra of 1–(1–(4–chlorophenylthio)propan–2–ylthio)–4–chlorobenzene (L) ligated CuI–coordination complex (1)	89
Figure III.10.	^{1}H NMR spectra of 4–(1–(3,5–dibromophenyl)–3–phenyl prop–2–ynyl)morpholine	90
Figure III.11.	^{13}C NMR spectra of 4–(1–(3,5–dibromophenyl)–3–phenyl prop–2–ynyl)morpholine	91
Figure III.12.	HRMS of of 4–(1–(3,5–dibromophenyl)–3–phenyl prop–2–ynyl)morpholine	92
Figure III.13.	^{1}H NMR spectra of 4–(3–(4–bromophenyl)–1–(4–methoxyphenyl)prop–2–ynylmorpholine	93
Figure III.14.	^{13}C NMR spectra of 4–(3–(4–bromophenyl)–1–(4–methoxyphenyl)prop–2–ynylmorpholine	94
Figure III.15.	HRMS of 4–(3–(4–bromophenyl)–1–(4–methoxyphenyl)prop–2–ynylmorpholine	95
Figure IV.1.	Biologically active 1,4–disubstituted–1,2,3–1*H*–triazole molecules	97
Figure IV.2.	Digital images of different steps during preparation of Cu_2O@ARF	105
Figure IV.3.	FT–IR spectra of ARF and Cu_2O@ARF	105
Figure IV.4.	PXRD pattern of Cu_2O@ARF	106
Figure IV.5.	(a) TEM image of the composite material showing the Cu_2O nanoparticles embedded in the resin. Inset of (a) shows the EDS pattern of the sample. It	107

	confirms presence of C, O and Cu from the sample; A part of C and Mo are coming from the carbon coated Mo grid used for TEM analysis. (b) HR-TEM showing the lattice fringes of Cu_2O nanoparticles. Magnified views of (110) lattice plane is shown in the inset of (b)	
Figure IV.6.	XPS spectra of the fresh catalyst Cu_2O@ARF. (a) high resolution Cu2p spectrum showing two distinct peaks for Cu^+ and (b) deconvoluted high resolution O1s spectrum consistent with the presence of Cu_2O chemical state	108
Figure IV.7.	Recyclability of the heterogeneous catalyst Cu_2O@ARF	114
Figure IV.8.	Three sets of mid-way filtration test at different time intervals showing conversion of triazole with or without the catalyst	115
Figure IV.9.	Comparison of Powder XRD of Cu_2O@ARF before and after the reaction	115
Figure IV.10.	Proposed mechanism of the three–component click reaction using Cu_2O@ARF	116
Figure IV.11.	^{1}H NMR spectra of (1–Benzyl–1*H*–1,2,3–triazol–4–yl) methyl acetate	128
Figure IV.12.	^{13}C NMR spectra of (1–Benzyl–1*H*–1,2,3–triazol–4–yl) methyl acetate	129
Figure IV.13.	^{1}H NMR spectra of (1–Benzyl–1*H*–1,2,3–triazol–4–yl)methyl pyrrolidine–1–carbodithioate	130
Figure IV.14.	^{13}C NMR spectra of (1–Benzyl–1*H*–1,2,3–triazol–4–yl)methyl pyrrolidine–1–carbodithioate	131

APPENDICES

APPENDIX A:

List of Research Publications

APPENDIX B:

Oral and Poster Presentations

APPENDIX A:

List of Publications :

1. "1D–copper(I) coordination polymer based on bidentate 1,3–dithioether ligand: Novel catalyst for azide–alkyne–cycloaddition (AAC) reaction", **Sankar Saha**, Kinkar Biswas and Basudeb Basu*, *Tetrahedron Letters*, **2018**, *59*, 2541–2545.
2. "New 1,2–dithioether based 2D copper(I) coordination polymer: From synthesis to catalytic application in A^3–coupling reaction", **Sankar Saha**, Kinkar Biswas, Pranab Ghosh and Basudeb Basu*, *Journal of coordination chemistry*, **2019**, *72*, DOI: 10.1080/00958972.2019.1627339.
3. "Stabilized Cu_2O Nanoparticles on Macroporous Polystyrene Resins [Cu_2O@ARF]: Improved and Reusable Heterogeneous Catalyst for On–Water Synthesis of Triazoles via Click Reaction", Sujit Ghosh, **Sankar Saha**, Debasish Sengupta, Shreyasi Chattopadhyay, Goutam De* and Basudeb Basu*, *Industrial and Engineering Chemistry Research*, **2017**, *56*, 11726–11733.

APPENDIX B

Oral Presentations :

1. "Transition Metal–Dithioether Complexes and their Catalytic Applications in Organic Synthesis", in the National Seminar "*Frontiers in Chemistry–2017*" organized by the Department of Chemistry, University of North Bengal and funded by UGC and SAP (DRS–III), held at University of North Bengal, Darjeeling, India, February 20–21, 2017.
2. "Stabilised Cu_2O nanoparticles on poly–ionic macroporous resins: An excellent reusable heterogeneous catalyst for azide–alkyne click reaction", in the National Seminer on "*Frontiers in Chemistry 2017–18*" organized by the Department of Chemistry, University of North Bengal and sponsored by UGC, held at University of North Bengal, Darjeeling, India, September 14, 2017.

ABBREVIATION

AAC	Azide–alkyne cycloaddition
AA^3	Asymmetric A^3
AAS	Atomic absorption spectra
ARF	Amberlite resin formate
[bmim][PF_6]	1–Butyl–3–methylimidazolium hexafluorophosphate
^oC	Degree Celsius
CCs	Coordination clusters
CP	Coordination polymer
Cy	Cyclohexyl
d	doublet
1D	One dimensional
2D	Two dimentional
3D	Three dimensional
dd	doublet of a doublet
DMF	*N*, *N*–Dimethylformamide
DMSO	Dimethyl sulphoxide
eqv	equivalent
h	hour / hours
HPLC	High performance liquid chromatography
HRMS	High resolution mass spectrometry
HRTEM	High resolution transmission electron microscopy
Hz	Hertz
ICP–AES	Inductively coupled plasma–atomic emission spectroscopy
IR	Infrared spectroscopy
MCR	Multicomponent reaction
mg	milligram
MHz	Mega hertz

min	minute / minutes
mmol	millimole
MOF	Metal organic framework
mol%	mole percent
MW	Microwave
NHC	N–heterocyclic carbene
NMR	Nuclear magnetic resonance
NPs	Nanoparticles
ORTEP	Oak ridge thermal ellipsoid plot program
PPDA	Polyphenylene diamine
ppm	Parts per million
PVA	Polyvinyl alcohol
PXRD	Powder X–ray diffraction
q	Quintet
RGO	Reduced grapheme oxide
s	singlet
SCXRD	Single crystal X–ray diffraction
SEM	Scanning electron microscope
SDS	Sodium dodecyl sulfate
t	triplet
TBAB	n–tetrabutyl ammonium bromide
TEM	Transmission electron microscope
THF	Tetrahydrofuran
TLC	Thin layer chromatography
TMS	Tetramethylsilane
TOF	Turnover frequency
XPS	X–ray photoelectron spectroscopy

CHAPTER I

Brief review on synthesis, characterization of transition metal–dithioether based complexes and their catalytic applications towards organic transformations

I.1. Dithioethers and their synthesis:

Sulfur containing organic molecules are important constituents of various biologically active compounds.[1] Versatile applications of organosulfur compounds are known in various fields of chemistry. That is why preparation of various dithioether ligands draw much attention to the field of organic synthesis. Various procedures have been developed to synthesize these dithioethers. Vicinal dithioethers can be synthesized by the nucleophilic substitution of 1,2–dihalides with suitable thiols or thiolate ions.[2–3] The consecutive hydrothiolation of alkynes either by nucleophilic or radical–induced conditions gave vicinal dithioether.[3–4] These can be synthesized by the addition of disulfides to alkenes catalyzed by transition metal.[5–6]

Kondo *et al.* developed a ruthenium catalyst, Cp*RuCl(cod) which catalyzed addition of disulfides to certain alkenes to give syn addition products with high stereoselectivity. The products are the corresponding vicinal dithioethers.[7] This has been shown in scheme I.1.

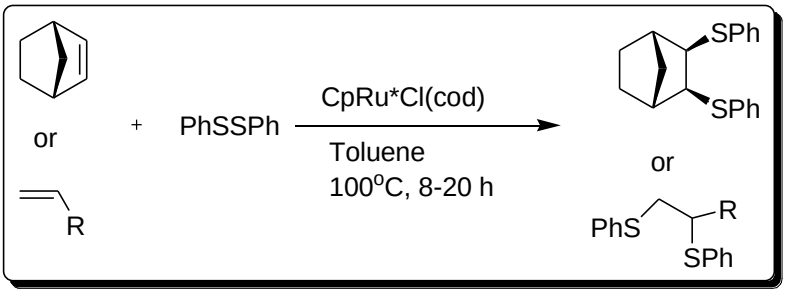

Scheme I.1. *Ruthenium catalyzed synthesis of vicinal dithioethers*

G. B. Hammond *et al.* reported a reaction methodology where various thiols were reacted with a wide range of alkynes to produce 1,3–dithioethers in aqueous medium and under mild conditions.[8]

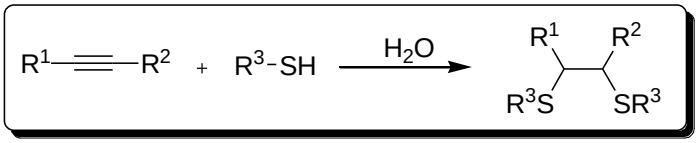

Scheme I.2. *Synthesis of 1,3–dithioethers from alkynes*

S. Poulain *et al.* prepared vicinal–dithioethers from norbornene derivatives. The sulfuration process of norbornene derivatives was done in presence of catalytic amount of $Ni(NH_3)_6Cl_2$ in DMF to produce the corresponding trithiolanes selectively. The trithiolanes obtained in this procedure were reduced to 1,2–dithiolate which was subsequently quenched to produce vicinal–dithioethers.[9]

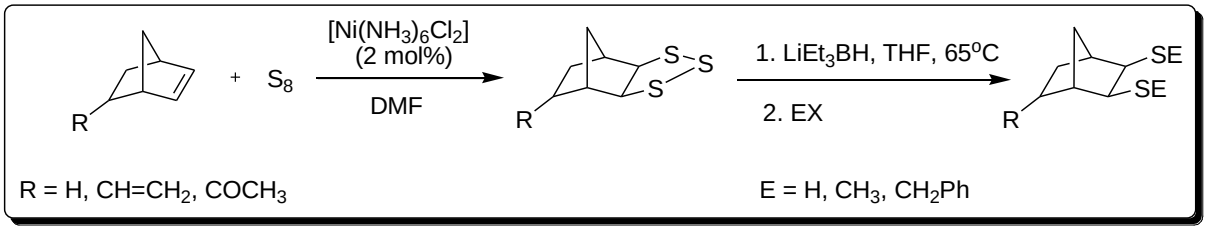

Scheme I.3. *Preparation of vicinal–dithioethers from norbornene derivatives*

T. Kitamura and H. Taniguchi *et al.* illustrated an addition reaction of disulphide moiety with alkenes induced by hypervalent iodine compound, [PhIO–TfOH] to produce certain vicinal dithioethers.[10]

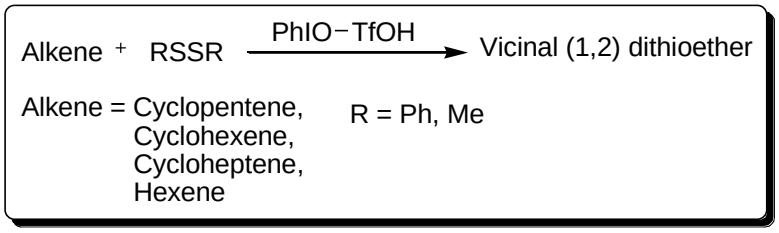

Scheme I.4. *Hypervalent iodine catalyzed 1,2–dithioether synthesis*

K. Oshima *et al.* reported a disulfidation reaction of PhSSPh with alkynes and alkenes catalysed by a transition metal catalyst gallium trichloride.[11] Alkenes react with phenyl disulfide to form the *trans* adduct selectively. Here we represent one example in scheme I.5.

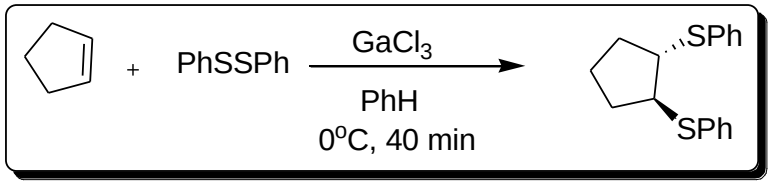

Scheme I.5. *Gallium trichloride catalyzed vicinal dithioether preparation*

N. Yamagiwa and Y. Torisawa *et al.* investigated about the disulfenylation of alkenes catalyzed by some common lewis acids such as $FeCl_3$ and $AlCl_3$. Cycloalkenes and other alkenes reacted excellently with $FeCl_3$. The substrates for which the conversion was poor with $FeCl_3$, obtained effective conversion with lewis acid catalyst $AlCl_3$.

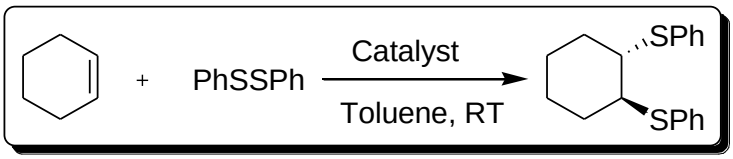

Scheme I.6. *Lewis acid catalyzed disulfenylation of alkenes*

Silica supported highly selective synthetic procedure to synthesize 1,2 or 1,3–dithioethers has been developed by our group.[13] Reactions of an allyl bromide with excess thiol in silica at room temperature in solvent–free condition leads to the formation of 1,2 or 1,3–dithioethers. This method produces either 1,2 or 1,3–dithioethers by altering the reaction condition.

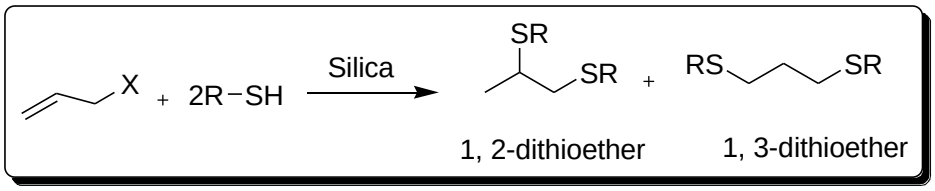

Scheme I.7. *Preparation of 1,2– and 1,3–dithioether in silica support*

I.2. Coordination polymers or Metal Organic Framework (MOF)

Now a days, the designs and constructions of oligo– and poly (nuclear) coordination architectures attract much attention because of their new structural topologies and fascinating architectures. It has been used in optoelectronic devices,[14] microporous materials,[15] and catalysis.[16] The smart combination of organic ligand "spacers" and metal ion "nodes" has been considered as one of the most common strategy to synthesize various types of coordination polymeric networks (Figure I.1).[17]

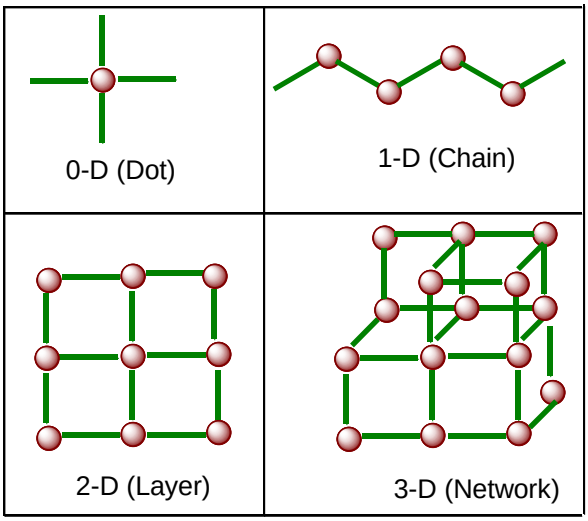

Figure I.1.*Various types of metal–organic framework (MOF)*

The advantage of constructing these metal–organic framework (MOF) is to allow diverse electronic properties and coordination geometry of the metal ions, as well as versatile functions and structures of organic ligands. This is one of the interesting parts of crystal engineering where the control of the topology and geometry of the networks formed due to sensible choice of ligand, metal salt and synthetic conditions etc.[18] The dithioether based ligands have excellent capability to form various metal–complexes and metal–organic frameworks (MOFs).[19–23]

I.3. Synthesis of various dithioether based metal complexes

Research on this variety of transition metal–dithioether complex formation, their characterization and their applications has revealed much attention now a days.[24–46] Various transition metal based dithioether complexes and also MOFs have been synthesized and factors affecting their polymeric propagations are also well described by various groups.

I.3.1. Iridium complex with chiral dithioether compounds

A. Ruiz *et al.* prepared new type of chiral dithioether compounds. The addition of these dithioether compounds to $[Ir(cod)_2]BF_4$ in CH_2Cl_2 produced chiral complexes having formulla $[Ir(cod)\{(-)–degusme\}]BF_4$, $[Ir(cod)\{(-)–degus pr^i\}]BF_4$. CH_2Cl_2 and $[Ir(cod)\{(+)–degusph\}]BF_4$**.** These complexes are active to the process asymmetric hydrogenation at room temperature with 68% enantiomeric excess.[24]

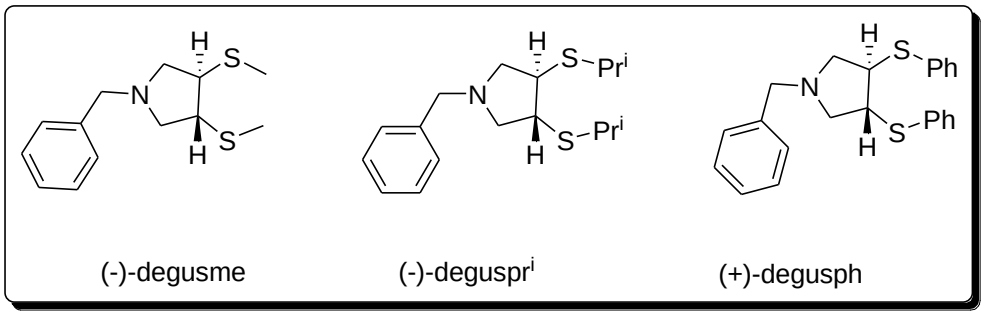

Figure I.2. *Chiral dithioether ligands for asymmetric hydrogenation.*

I.3.2. Zirconium(IV) and Titanium(IV) complexes with [OSSO] type ligands

M. Kol *et al.* synthesized a new [OSSO]–type ligand which represents an S analogue of the [ONNO]–type ligands. The [OSSO]H_2 ligand on reaction with titanium(IV) isopropoxide and zirconium(IV) tert–butoxide produces the corresponding [OSSO]–M$(OR)_2$ type complexes. The reaction between the [OSSO]–type ligand and tetrabenzyl zirconium formed a dibenzyl complex [OSSO]–Zr$(bn)_2$ that was found to be an active catalyst for the polymerization of 1–hexene when activated with $B(C_6F_5)_3$.[25]

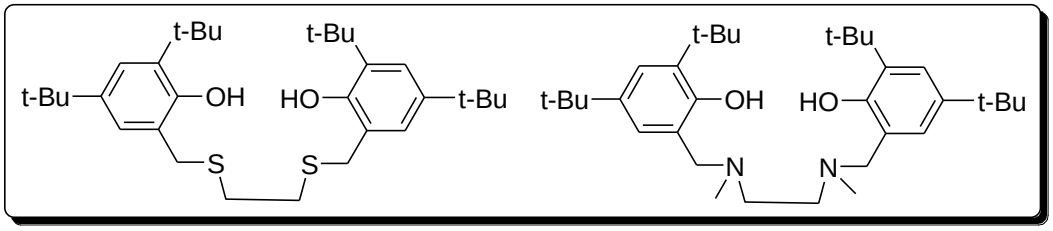

Figure I.3. *[OSSO] type ligand and its [ONNO] Salan type analogue*

A. Ishii *et al.* synthesized a zirconium Complex of an [OSSO]–type ligand.[26] It possess a *trans*–1,2–cyclooctanediylbis(thio) core that has been given in scheme I.8.

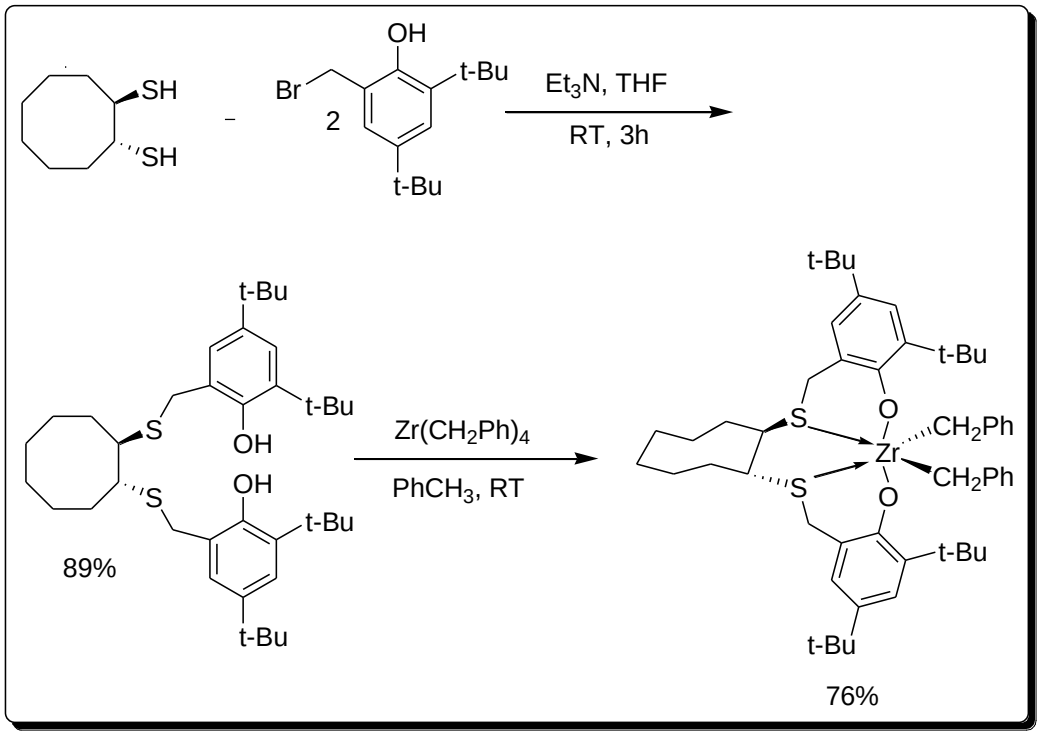

Scheme I.8. *Synthesis of a Zirconium complex with [OSSO]–type ligand*

J. Okuda and his group synthesized and characterized enantiomerically pure [OSSO]–type bis(phenolate) ligand containing titanium complexes. Complexation of the ligands ($[OSSO]H_2$, R_1= *t*–Bu, *i*–Pr, H; R_2= *t*–Bu, *i*–Pr, Me) with the TiX_4 where X= Cl, O^iPr occurs to produce the enantiomeric complexes.[27]

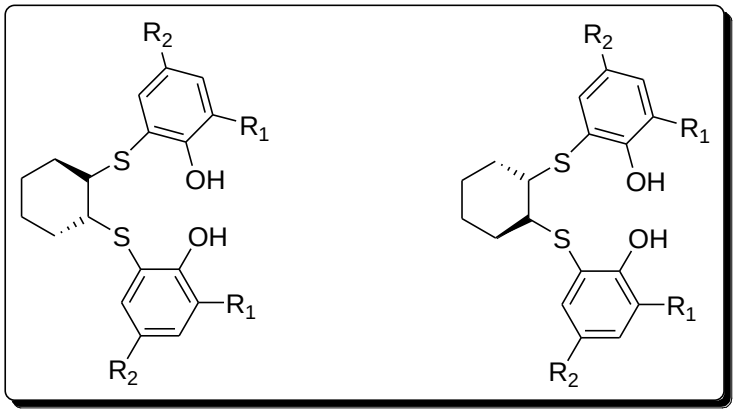

Figure I.4. *[OSSO]–type ligands used to synthesize enantiomeric pure Titanium complex*

I.3.3. Ruthenium(II) dithioether complex

J. –P. Collin and J. –P. Sauvage prepared and characterized ruthenium(II) complexes that possess two 1,10-phenanthroline and one di–thioether ligand. Two complexes of that kind was perfectly characterized by X–ray crystallography.[28] Photosubstitution reaction of di–thioether chelate was achieved, when the complexes were treated in presence of chloride anions. The preparation procedure and the photosubstitution reaction has been depicted in Scheme I.8.

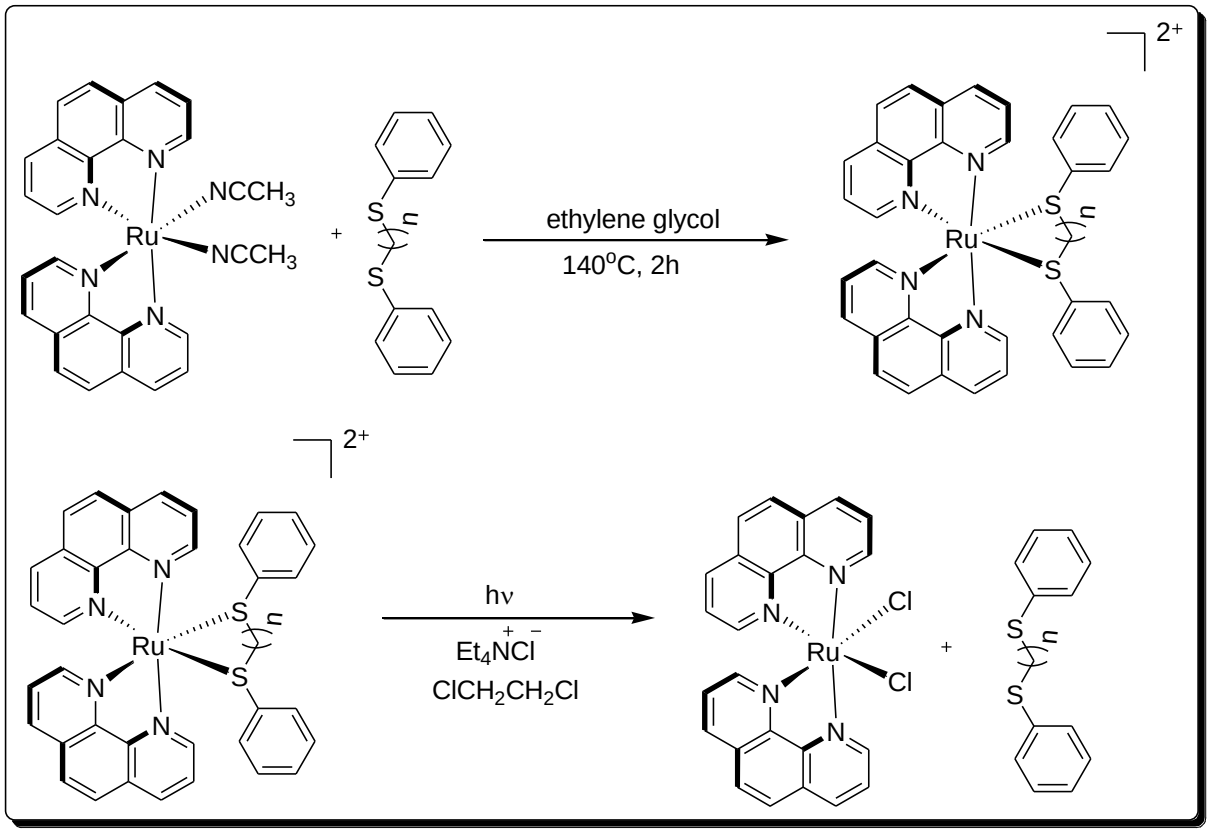

Scheme I.9. *Ruthenium(II) complexes containing 1,10–phenanthroline and di–thioether ligand*

I.3.4. Tin(IV) dithioether complexes

G. Reid *et al.* prepared and characterized tin(IV) complexes of the type $[SnCl_4\{MeS(CH_2)_2SMe)]$, $[SnC1_4\{o–C_6H_4(SMe)_2\}]$, $[SnCl_4\{MeS(CH_2)_3SMe)]$, $[SnBr_4\{MeS(CH_2)_3SMe\}]$ and $[SnCl_4(PhS(CH_2)_3SPh)]$. The compounds were obtained by the reaction of one mole dithioether with SnX_4 in $CHCl_3$ to achieve the six–co–ordinate complexes.[29]

I.3.5. Silver(I) coordination polymers with dithioether ligands

Xian–He Bu *et al.* prepared four Ag(I) 2D–coordination polymers by the reaction of Ag(I) salts with ligand L [1,4–bis(phenylthio)butane], $PhS(CH_2)_4SPh$ in various conditions. Four complexes, $[Ag_2\mathbf{L}_3(ClO_4)_2]_\infty$, $[Ag_2\mathbf{L}_3(ClO_4)_2.\ CH_3OH]_\infty$, $\{[Ag\mathbf{L}_2](ClO_4)\}_\infty$ and $[Ag\mathbf{L}NO_3]_\infty$ were obtained by the procedure when solvents, counter anions, metal to ligand ratios etc. parameters were varied. Structures of the co–ordination polymers of silver were confirmed by single–crystal XRD technique. Every AgI centre possess tetra coordination geometry in all the four complexes which were synthesized in this procedure. The 2D–networks are built up with macro–metallacyclic ring structures with honeycomb–like structures or networks consisting large channels which can accommodate phenyl rings, solvent methanol and the corresponding counteranion.[30]

I.3.6. Gold(I) complexes of dithioether ligands

Awaleh *et al.* reported synthesis, characterization and luminescence properties of various gold(I) complexes produced by the reaction of gold chloride with various dithioether ligands like bis(phenylthio)methane, bis(methylthio)methane, 1,3–bis(phenylthio)propane, 1,2 bis(phenylthio)–ethane, 1,3–bis–(methylthio)propane 1,4–bis(phenylthio)butane etc. Various polymeric complexes of gold(I) species like [Au{bis(methylthio)methane}Cl] (1), $[Au_2${1,2 bis(phenylthio)ethane}$Cl_2]$ (2), $[Au_2${1,3–bis(phenylthio)propane}$Cl_2]$ (3), $[Au_2${bis(phenylthio)methane}$Cl_2]$ (4), $[Au_2${1,4–bis(phenylthio)butane}$Cl_2]$ (5), [Au{1,3–bis(methylthio)propane}Cl] (6) were obtained in this process. The complex (1) is 1D–polymeric, and the complex (2) is 2D–supramolecular polymeric in nature. Complex (3), (4), (5) possess nearly identical 1D–polymeric nature as found from the single crystal XRD analyses.[31] They selected dithioether ligands of the type $RS(CH_2)_nSR$, where n = no. of methylene group between the sulfur atoms and R is alkyl or aryl group. These ligands have the following advantages. First of all the soft acid Au(I) have strong tendency to coordinate with the soft thioether ligands. As the number of methylene group increases between the sulfur atoms the flexibility of the ligand increases resulting various coordination polymers. The bulk of the R group also controls the structure of the gold coordination polymers. Complex (1), (2) and (6) also showed solid–state luminescence property. The strenghth of the Au(I)–Au(I) interactions and the no. of Au–Au bonds are the factors which control the electronic properties of the complexes.[32–34]

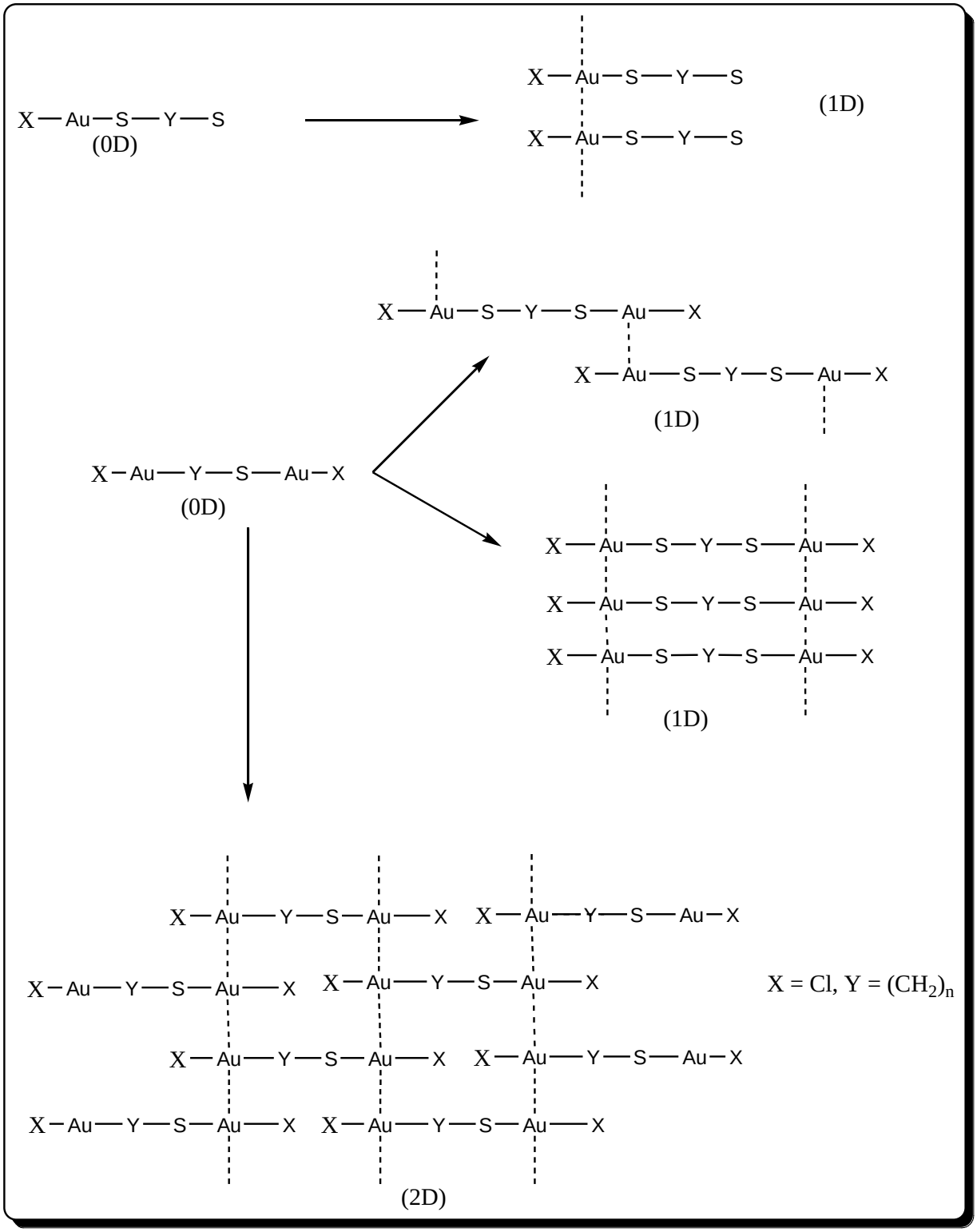

Figure I.5. *Association of discrete molecules into 1D– or 2D– networks by aurophilic interactions*

I.3.7. Copper complexes of dithioether–based ligands:

The coordination polymers of CuI attract much attention now a days. Its clusters with various ligands are well known.[35] Most of the widely used ligands are basically amine, phosphine functionalities or containing multi–functional groups in one ligand.[36] The coordination clusters exhibiting the general structure $Cu_4X_4L_4$ with mono–dentate ligand.[35a,37] The rhombic Cu_2I_2 and closed–cubane Cu_4I_4 clusters are the most encountered motifs whereas the open–flower busket Cu_4I_4 cubane and the hexagonal Cu_6I_6 clusters are scare.[35a] Apart from these structures step–cubane tetramer, partially opened cubane tetramer, capped square, staircase polymer, flower–basket–shaped partially opened cubane and hexagonal prism cluster has been well documented.[35b] The exact structures of the solids having stoichiometries $Cu_xX_yL_z$ yet to be known. Unique 2D–double–layered polymer containing helical chains were introduced by Dai and his group.[38]

Potenza *et al.* first reported the formation of coordination clusters between CuI and dimethyl sulfide.[39] The sulfur or thioether based ligands attract much attention to the field of coordination clusters formation.[40] Due to strong coordination power of sulfur atoms, thioether ligands are generally used for the preparation of Cu(I)–coordination polymer. Coordination chemistry of CuI towards dithioether ligands of the type $RS(CH_2)_nSR$ attracts more interest.

Kim *et al.* prepared cyclohexyl thiol based three different complexes having different structural network with CuI such as descrete, 2D–infinite brick wall, 1D–loop chain containing Cu_4I_4 cubane like coordination polymers (Scheme I.10).[41] 1,2–Bis(cyclohexylthiomethyl)benzene, 1,3–Bis(cyclohexylthiomethyl)benzene, 1,4–Bis(cyclohexylthiomethyl)benzene these three ligands were reacted with CuI to form the complex polymers.

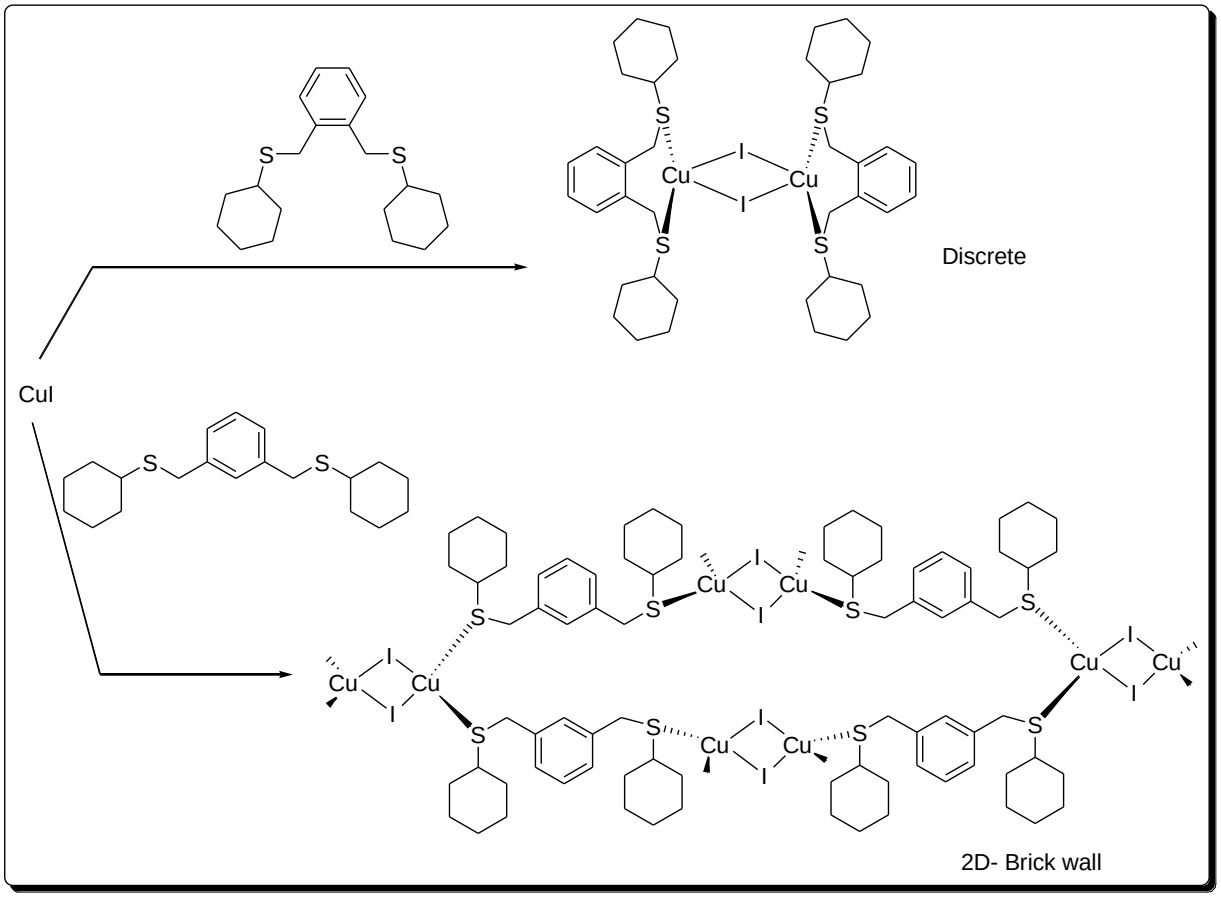

Scheme I.10. *Synthesis of different CuI–dithioether complexes*

Chen and his coworkers examined the adducts between CuI and two 1,4–dithioether ligands, $EtS(CH_2)_4SEt$ (1) and $PhCH_2S(CH_2)_4SCH_2Ph$ (2). The complex of ligand (1) possess 2D–network whereas that of (2) a 3D–framework both containing $(CuI)_4$ cubane unit as the secondary building block with dithioether as bridging unit. Different metal to ligand molar ratio were taken to prepare varying frameworks for the polymeric complexes.[42]

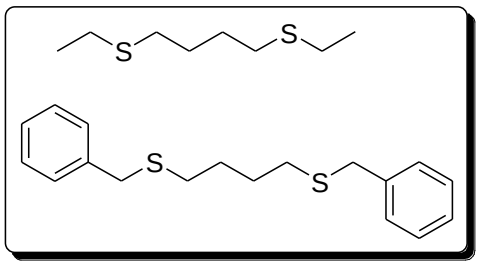

Figure I.6. *1,4–Dithioether ligands used for synthesis of polymeric complex with CuI*

Knorr. *et al.* investigated and illustrated the structure and luminescence properties of a wide range of coordination polymers with Cu_2Br_2, Cu_2I_2, Cu_4Br_4, Cu_4I_4 units ligated with flexible dithioether ligands $ArS(CH_2)_nSAr$ where n = 3,5 and Ar = Ph, *p*–Tol (Scheme I.11).[40a]

They found that the reaction of CuI and $PhS(Ch_2)_3Ph$ in a ratio 1:1 yields a 2D–sheet–like coordination polymer having formula $[\{Cu(\mu_2\text{–}I)_2Cu\}\{\mu\text{–}PhS(CH_2)_3SPh\}_2]_n$ whereas a 2D–coordination polymer having formula $[Cu_4I_4\{\mu\text{–}PhS(CH_2)_3SPh\}_2]_n$ with strong luminescence property results when two equivalent of the ligand was taken. When this ligand was reacted with CuBr it formed 1D–coordination polymer $[\{Cu(\mu_2\text{–}Br)_2Cu\}\{\mu\text{–}PhS(CH_2)_3SPh\}_2]_n$. When CuI was mixed with $PhS(CH_2)_5SPh$ in 2:1, it resulted 1D–polymeric complex $[Cu_4I_4\{\mu\text{–}PhS(CH_2)_5Ph\}_2]_n$ that possess cubane like $Cu_4(\mu_3\text{–}I)_4$ units bridged with the dithioether ligand forming 1D–necklace–like structure. But keeping the metal to ligand ratio 1:1 they prepared 1D–coordination polymer with formula $[\{Cu(\mu_2\text{–}I)_2Cu\}\{\mu\text{–}PhS(CH_2)_5SPh\}_2]_n$ containing rhomboid Cu_2I_2 units. 1D–polymeric complex $[\{Cu(\mu_2\text{–}Br)_2Cu\}\{\mu\text{–}PhS(CH_2)_5SPh\}_2]_n$ was produced by the reaction of CuBr with the 1,5–dithioether ligand. Moreover 1,5–bis(*p*–tolylthio)pentane and CuI were mixed in the ratio 1:2 and 1:1 to form $[Cu_4I_4\{\mu\text{–}p\text{–}TolS(CH_2)_5STol\text{–}p\}_2]_n$ and 2D–polymeric $[\{Cu(\mu_2\text{–}I)_2Cu\}_2\{\mu\text{–}p\text{–}TolS(CH_2)_5STol\text{–}p\}_2]_n$ respectively. $[Cu_4I_4\{\mu\text{–}p\text{–}TolS(CH_2)_5STol\text{–}p\}_2]_n$ possess strong luminescent property. 1D–polymeric complex $[\{Cu(\mu_2\text{–}Br)_2Cu\}\{\mu\text{–}pTolS(CH_2)_5STol\text{–}p\}_2]_n$ was produced by the reaction of CuBr with 1,5–bis(*p*–tolylthio)pentane keeping the reaction condition unchanged.

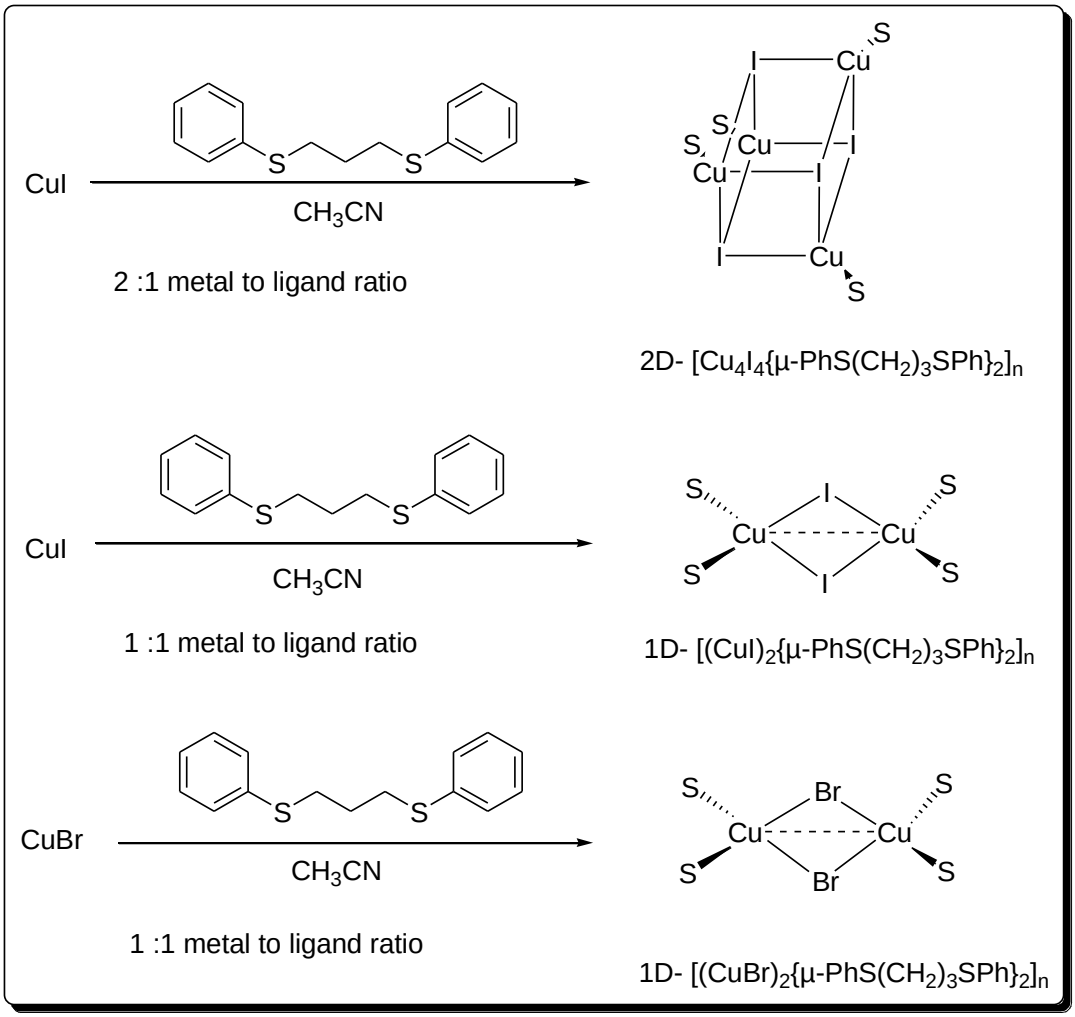

Scheme I.11. *Formation of various framework depending upon the metal to ligand ratio*

M. Knorr and his group also synthesized and characterized 1D– and 2D–Cu(I) coordination polymers which incorporates CuI ligated with $PhSCH_2SPh$ and $PhS(CH_2)_2SPh$ type dithioethers. The one dimensional necklace–like coordination framework, $[Cu_4I_4\{\mu–PhSCH_2SPh\}_2]_n$ was formed by the linking of $Cu_4(\mu^3–I)_4$ units with dithioether ligands. Whereas the reaction of CuI with $PhS(CH_2)_2SPh$ produces 2D–framework of $[(CuI)_2\{\mu–PhS(CH_2)_2SPh\}_2]_n$ that contains Cu_2I_2 building units bridged with 1,2–bis(phenylthioethane) ligand. The first coordination polymer exhibits strong luminescence spectrum whereas the second one is weakly active (Scheme I.12).[43]

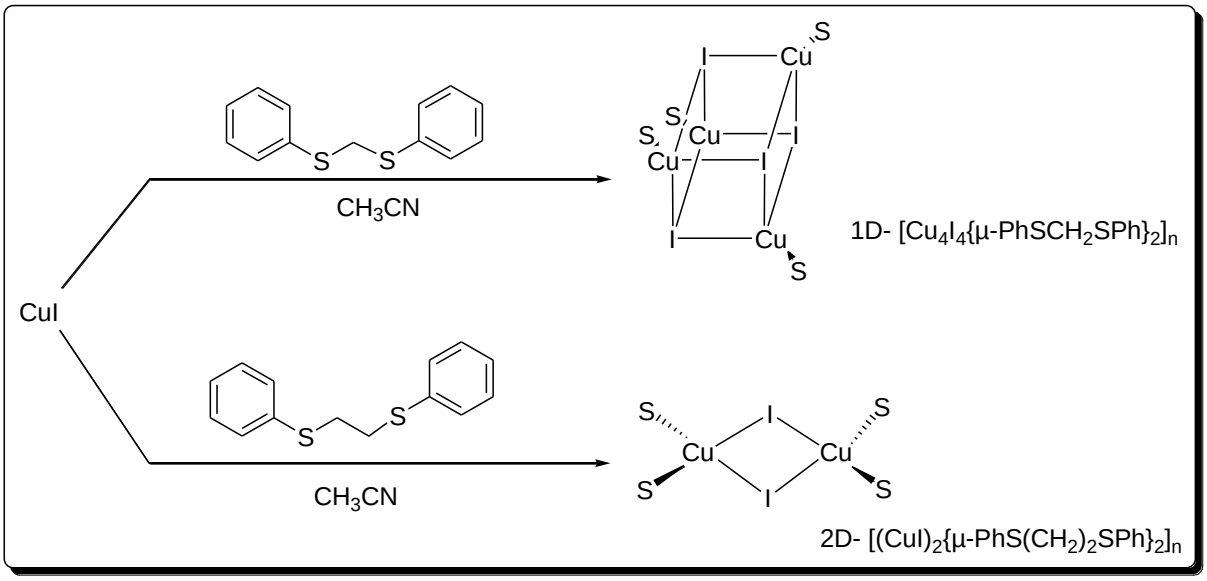

Scheme I.12. *Formation of 1D– and 2D–frameworks with two different dithioether ligands*

Thus the cluster size was controlled by changing the metal–to–ligand ratio, the nature of the halide, the number of sulfur atoms on the ligand (mono– vs. di–) and the number of methylene groups in the alkane chain in $ArS(CH_2)_nSAr$ (Ar = aromatic; n = 1–5)[40a,42,43] The reactivity of the aromatic dithioether ligands $PhS(CH_2)_nSPh$ (m = 1, 2, 4) toward CuI is influenced by the spacer on the resulting framework.[43] The insertion of additional spacer units between the SAr groups may change the dimensionality, cluster nuclearity and the luminescence properties of the metal–organic framework (MOF).[40a]

It has been also observed that the bulkiness of the R group in the dithioether of the type $RS(CH_2)_4SR$ affects the luminescent properties of the resulting coordination polymers. As for example a blue shift in the emission band of solid state luminescent spectra has been observed changing from R = *n*–Bu to R = *t*–Bu.[44]

In a recent investigation A. Raghuvanshi *et al.* synthesized and characterized various Cu(I) coordination polymers having 0D to 3D architectures where various 1,3–dithiane ligands were used with varying reaction conditions. 1D–coordination polymer $[\{Cu(\mu_2\text{–}I)_2Cu\}\text{–}\ (\mu_2\text{–}L_1)_2]_n$ (CP1) was obtained when the ligand 1,3–dithiane (L_1) was treated with CuI. Another coordination polymer with similar structure, $[\{Cu(\mu_2\text{–}Br)_2Cu\}(\mu_2\text{–}L_1)_2]_n$ (CP2) resulted upon reaction of CuBr with the ligand L_1. But 2D–polymeric $[\{Cu(\mu_2\text{–}Cl)_2Cu\}(\mu_2\text{–}L_1)]_n$ (CP3) was

obtained on treatment CuCl with L_1, where every sulfur atom works as a 4–electron donor. When 2–methyl–1,3 dithiane (L_2) was reacted with CuBr and CuCl, coordination polymers $[\{Cu(\mu_2–X)_2Cu\}(\mu_2–L_2)_2]_n$ (CP7, X = Br, and CP8, X = Cl) with 1D–architecture resulted which resembles the CuI homologue $[\{Cu(\mu_2–I)_2Cu\}(\mu_2–L_2)_2]_n$(CP5) that has been reported previously. A 2D–CP $[\{Cu(\mu_2–CN)_2Cu\}(\mu_2–L_2)_2]_n$ (CP9) has been obtained when CuCN was taken. Complexation of CuI with ligand 2–isobutyl–1,3–dithiane (L_3) generates a new 2D–CP $[\{Cu_3(\mu_3–I)(\mu_2–I)_2(\mu_2–L_3)_2\}]_n$ (CP10) which contains trinuclear μ_3–I–capped Copper centre in its clusters. But 2D–coordination polymers $[\{Cu(\mu_2–Br)_2Cu\}(\mu_2–L_3)_2]_n$ (CP11) and $[\{Cu(\mu_2–Cl)_2Cu\}(\mu_2–L_3)_2]_n$ (CP12) resulted when similar ligand was treated with CuBr and CuCl respectively. Reaction of 2–Me_3Si–1,3–dithiane (L_4) with CuX resulted a series of coordination polymers, $[\{Cu_2(\mu_4–X)(\mu_2–X)\}(\mu_2–L_4)]_n$ (CP13−CP15). 2–phenyl–1,3–dithiane (L_5), reacted with CuI in different reaction conditions which results a 1D–ribbon $[\{Cu(\mu_2–I)_2Cu\}(MeCN)_2(\mu_2–L_5)_2]_n$ (CP16) when CuI was treated with L_5 in MeCN, whereas 2D–CP $[\{Cu_3(\mu_3–I)(\mu_2–I)_2(\mu_2–L_5)_2\}]_n$ (CP17) was obtained when CuI was treated with L_5 in EtCN. The CP16 structure varried from triclinic to monoclinic when the same reaction was monitored at different temperatures range between 100 and 300 K. A 0D dinuclear coordination complex $[\{Cu(\mu_2–I)_2Cu\}(\eta^1–L_6)_2(MeCN)_2]$ was obtained when Ligand L_6 with 2–ferrocenyl functionality was treated with 1 equiv of CuI, whereas 2 equiv of CuI afforded an 1D–CP $[\{Cu(\mu_3–I)_2Cu\}(\mu–L_6)]_n$ (CP18).[45]

Table I.1. Ligands used and Dimensionality of Coordination polymers obtained

Ligand	X of CuX	Coordination Polymer	Dimentionality
 L1	I	CP1	1D
	Br	CP2	1D
	Cl	CP3	2D
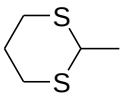 L2	I	CP4	2D
		CP5	1D
		CP6	3D
	Br	CP7	1D
	Cl	CP8	1D

	CN	CP9	2D
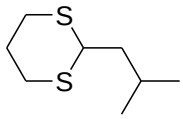 L3	I	CP10	2D
	Br	CP11	2D
	Cl	CP12	2D
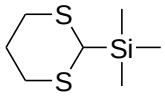 L4	I	CP13	1D
	Br	CP14	1D
	Cl	CP15	1D
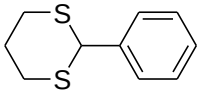 L5	I	CP16	1D
		CP17	2D
	Br	CP18	2D
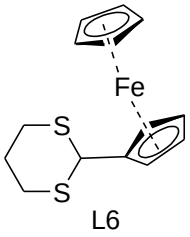 L6	I	D1	0D
		CP19	1D

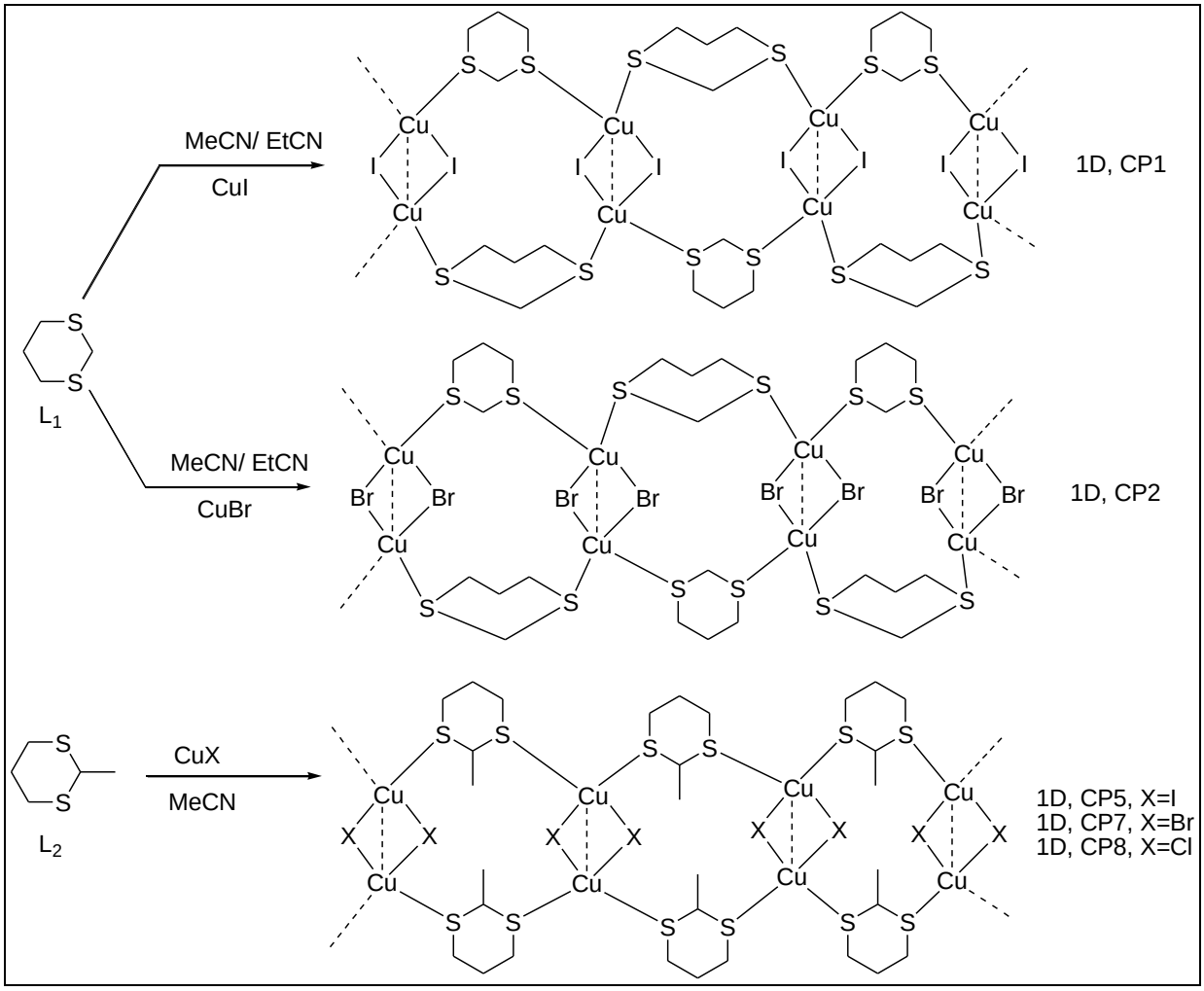

Scheme I.13. *Formation of Cu(I) coordination polymers with 1,3–dithiane ligands L_1 and L_2*

I.4. Catalytic application of transition metal dithioether complexes towards organic transformations

Applications of this dithioether based transition metal coordination complex polymers are yet to be focused. However there are few examples where thioethers have been employed as ligand along with metal salt.

Zhao and co–workers developed a CuBr–PhSMe catalyst which can efficiently catalyze cycloaddition of aliphatic or aromatic azides and alkynes (click reaction) in aqueous medium (Scheme I.14).[46]

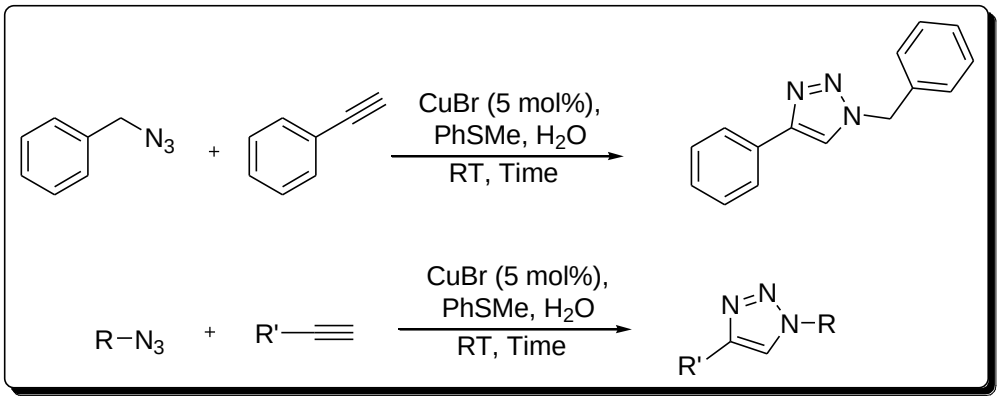

Scheme I.14. *CuBr with PhSMe catalyzed click reaction*

Basu *et al.* first synthesized and characterized a new 1,3–dithioether based 1D–coordination polymer having formula $[(CuI)_2\{ArS(CH_2)_3SAr\}_2]_n$, Ar = 4–F–$C_6H_4$ and used it as an excellent catalyst system towards three component AAC reaction (Scheme I.15).[47]

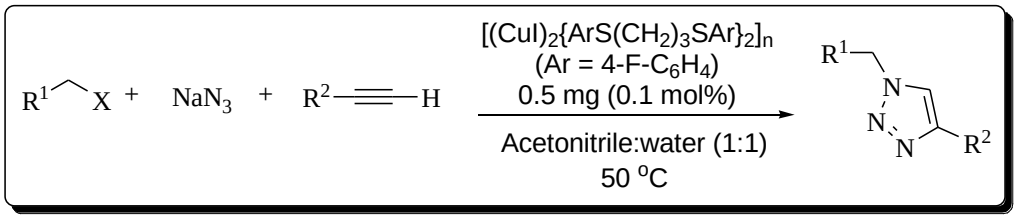

Scheme I.15. *CuI–1,3–dithioether catalyzed AAC reaction*

I.5. References

References are given in BIBLIOGRAPHY under Chapter I page no. 132–134.

CHAPTER II

Synthesis of a new 1,3–dithioether based 1D–Copper(I) coordination polymer and its catalytic activity towards one–pot AAC reaction

II.1. Introduction

The 1,2,3–triazoles are very important heterocyclic compounds from various biological and pharmaceutical aspects. They plays vital role like H_1–antihistamine,[1] anti–HIV,[2] anti–bacterial activity[3] and β3–adrenergic receptor agonism in selective manner.[4] Rolf Huisgen developed the model reaction for the synthesis of 1,2,3–triazole in 1984 from alkynes and organyl azides which is generally known as the Huisgen [3+2] cycloaddition reaction or AAC reaction (Scheme II.1).[5]

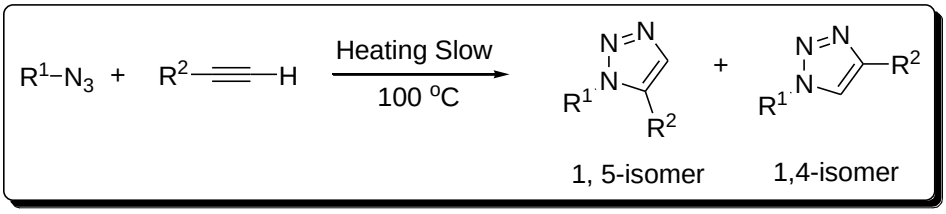

Scheme II.1. *Huisgen's 1,3–dipolar cycloaddition reaction*

But high temperature requirement for the reaction and the lack of regioselectivity (as both 1,4 and 1,5 substituted 1,2,3–triazoles are produced in this method) are two major drawbacks of this method. The application of Cu(I) catalysts under mild conditions form the 1,4–disubstituted 1,2,3–triazoles selectively and the formation of the mixture of 1,4– and 1,5–disubstituted 1,2,3–triazoles can be avoided. This procedure is known as 'click reaction'. Various metal catalysts were introduced from last few decades to make the AAC reaction regioselective. Copper salts or catalysts were found to be the best catalyst for this reaction among these various transition metal salts/catalysts. Various methods are developed where copper acetate, copper chloride or simple salts of Cu(I) or Cu(II) were used as catalyst system. Cu(I) catalyzed triazole synthesis was simply achieved by the use of excess $CuSO_4$ along with sodium ascorbate which reduces the Cu(II) species to Cu(I) species and also inhibits the aerobic oxidation of Cu(II) species. Various ligands like P–, S– and polydentate N–based molecules have been used. But unwanted Staudinger reaction was the main problem of using P–based ligands.[6]

Using polymer supported Cu(I) composite, Cu(I)–*p*PDA (*p*PDA: polyphenylene diamine) Mallick and his co–workers showed azide alkyne cycloaddition (AAC) reaction by microwave irradiation technique under solvent free condition. Both domestic as well as laboratory

microwave worked well to afford 1,2,3–triazole derivatives. The reaction was believed to proceed through the formation of Cu(0) acetylide complex intermediate.[7]

The multicomponent approach towards the AAC reaction is more convenient over two component Huisgen [3+2] cycloaddition method because it avoids the direct use of toxic and explosive organic azides which are difficult to handle and tedious to isolate and purify.[8]

Preformed stable Cu(I) complexes with phosphines or nitrogen ligands could be employed by small proportion. Many homogeneous and heterogeneous copper catalysts are reported for AAC reactions.[9] But the catalytic use of polymeric Cu catalysts (coordination polymer of Cu) in AAC reaction is a new interesting aspect.

II.2. Background and Objectives

PPh_3, NHC, imidazole, sulfur and nitrogen based molecules are among the most used ligands for various well–defined catalyst system.[10] The sulfur–based ligands attract much attention in the vicinity of copper complex formation and subsequently on click reaction because of the reducing power of sulfur group. It also reduces the chance of aerobic oxidation of Cu(I) to Cu(II) in the absence of any kind of base. Thus Cu–thioamide catalyzed click reaction has been explored recently.[11]

H. Fu and his group introduced a catalytic system, CuBr and thioanisole which catalyzed on–water cycloaddition of water–insoluble aliphatic and aryl azides excellently. They tried with various sulfur ligands in this protocol but thioanisole was the best one under this catalytic condition (Scheme II.2).[12]

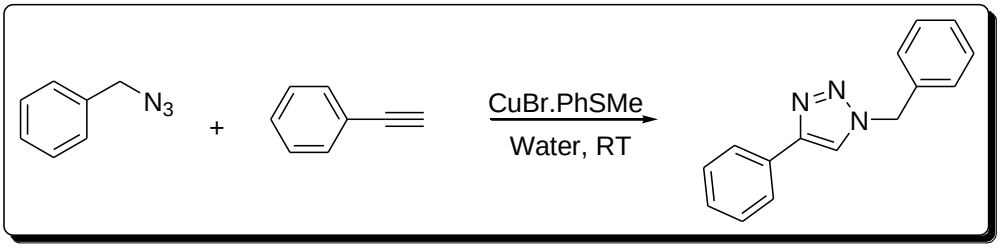

Scheme II.2. *CuBr.PhSMe–catalyst system for AAC reaction*

SNS ligand based copper catalysts, which have been found to be efficient for AAC reaction were introduced by T. S. A. Hor and his group. The hybrid SNS ligand with an amine moiety and two sulfur moieties can effectively form an one–dimentional mononuclear polymer with

copper having formula [CuX_2(SNS)]. They have synthesized four different copper complexes with SNS ligands and the complexes were characterized (Scheme II.3). They also studied the catalystic activity of these catalysts in azide–alkyne cycloaddition reaction in a multicomponent approach between benzyl chloride, phenyl acetylene and sodium azide. The substrates scope is limited here.[13]

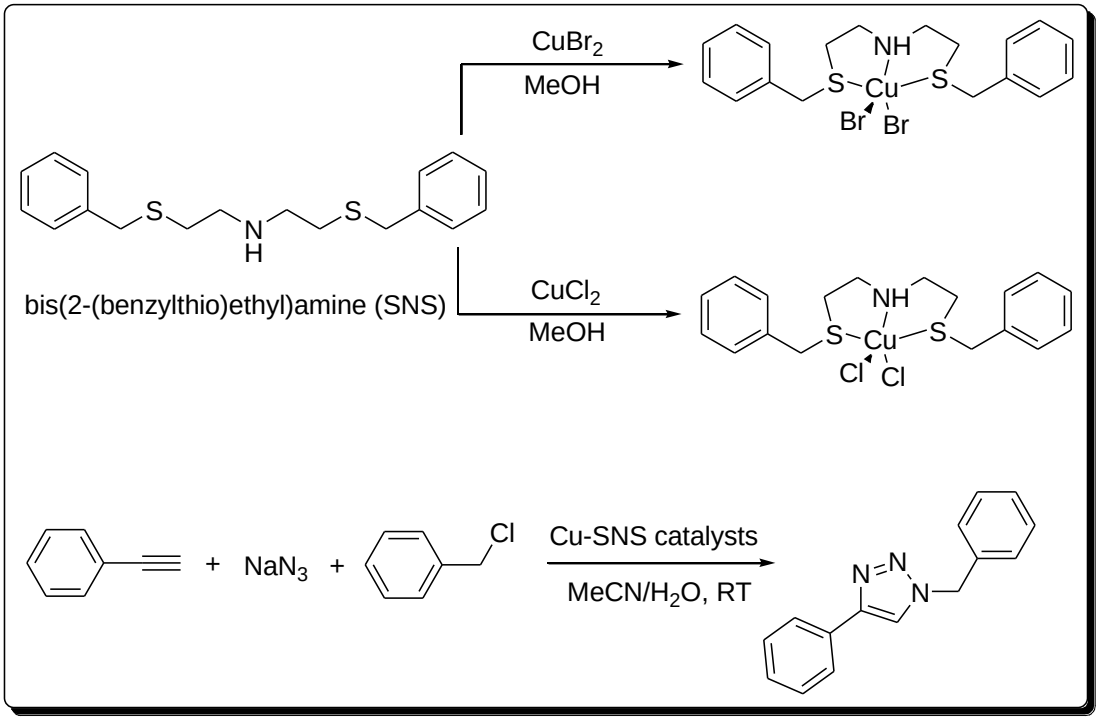

Scheme II.3. *Preparation of CuX_2(SNS) catalysts and application towards azide–alkyne click reaction*

A new class of NS ligands possessing excellent complex formation ability with copper were reported by S.–Q. Bai and T. S. A. Hor *et al*. (Scheme II.4). These hybrid NS–ligands are promising in catalytic reactions because of the assembling of hard and soft donors. These ligands were able to coordinate with CuI, CuBr and CuCl salts. The copper complexes appeared to be polymeric units and these catalyzed one–pot AAC reaction very effectively.[14]

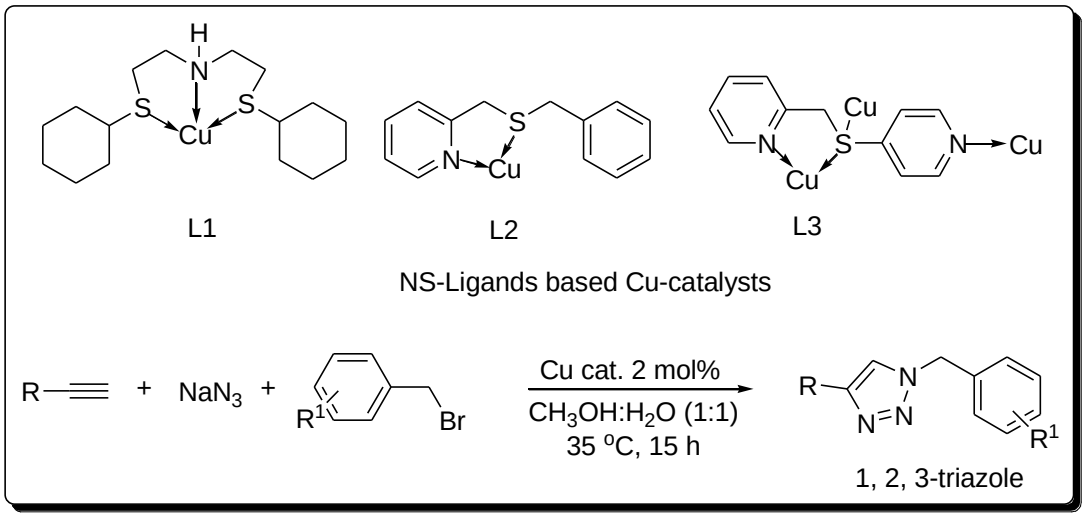

Scheme II.4. *Cu–NS catalyst for one–pot azide–alkyne cycloaddition reaction*

Pyridyl and thioether hybridized 1, 2, 3–triazole ligands were synthesized by click reaction. These compounds were further utilized to prepare a new type of dithioether based CuI coordination complexes by T. S. A. Hor and his group (Scheme II.5). The complexes obtained by this method were further used as catalyst in one–pot AAC reactions. Though the reactions took long time for completion but this methodology opened a new dimension for the polymeric coordination complex catalyzed click reactions.[15]

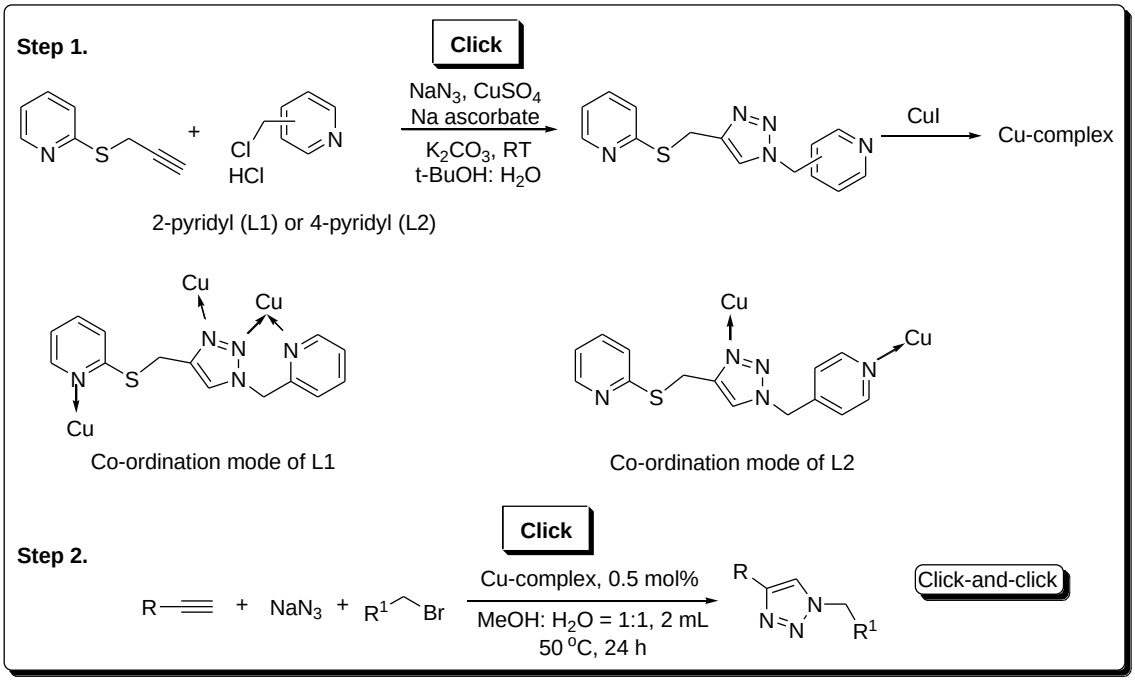

Scheme II.5. *"Click–and–click" –hybridised 1,2,3–triazoles supported Cu(I) coordination polymers for azide–alkyne cycloaddition*

1,3–Dithioether ligands play a vital role for the preparation of coordination clusters due to strong coordination power of sulfur atoms.[16] The coordination mode of aromatic bisthioether ligands of the type $PhS(CH_2)_nSPh$ was first illustrated by Knorr *et al.*[17] They have wide applications in the field of phtophysical phenomena,[16a,c] and in bio–inorganic chemistry.[18] But, 1,3–dithioether based CuI polymeric complexes have never been used for 1,3–dipolar cycloaddition reaction. Here, we describe a new methodology for the synthesis of 1,2,3–triazole molecules in presence of 1,3–dithioether based CuI polymeric coordination complex. Our 1,3–bis(4–fluorophenylthio)–propane ligand based CuI coordination complex having molecular formula, $([(CuI)_2\{ArS(CH_2)_3SAr\}_2]_n$, Ar = 4–F–$C_6H_4$) was first synthesized and characterized by NMR, HRMS spectroscopy and single crystal X–ray diffraction pattern. The catalyst undergoes a smooth azide–alkyne cycloaddition reaction in base–free condition in water–acetonitrile (1:1, v/v) solvent mixture at 50 ^oC. It produces selectively 1,4–disubstituted 1,2,3–triazole products. Only 0.5 mg (0.1 mol %) of the catalyst is required for the complete conversion of the product. Thus a new polymeric Cu(I) complex with SS–based bidentate ligand was developed and found as an excellent catalyst in the AAC reaction.

II.3. Present work: Results and Discussion

II.3.1. Synthesis of 1,3–bis(4–fluorophenylthio)–propane ligand (L)

The ligand (L) 1,3–bis(4–fluorophenylthio)–propane was prepared by following our previously reported technique.[19] It was also characterized by ^1H– and ^{13}C–NMR spectroscopy. The procedure for the synthesis of the ligand has been illustrated in the experimental section.

II.3.2. Synthesis of polymeric coordination complex catalyst CuI–1,3–bis(4–fluorophenylthio)–propane

The procedure for the synthesis of the polymeric catalyst is given in the experimental section in details.

II.3.3. Characterization of complex catalyst

II.3.3.1. NMR and HRMS spectroscopy

The polymeric complex was characterized by several techniques such as ^{1}H– and ^{13}C–NMR, HRMS spectroscopy and by single crystal XRD techniques. ^{1}H– and ^{13}C–NMR spectra of the polymeric complex and the ligand 1,3–bis(4–fluorophenylthio)–propane (L) were taken separately in d_6–DMSO solvent. Some changes were observed in ^{1}H–NMR spectra between L and the polymeric complex. which indicates the complex formation between ligand L and CuI. The ^{1}H–NMR spectra of L and the complex are given in Figure II.3 and Figure II.4. In ^{1}H–NMR spectrum of L, a clear splitting into a triplet at δ 3.02 (for 4H, $2CH_2$) and a quintet at δ 1.77 (for 2H, $1CH_2$) are observed but in ^{1}H–NMR spectrum of the complex these patterns are absent rather quite different pattern with a doublet δ 3.02 (for 4H, $2CH_2$) and a singlet at δ 1.76 (for 2H, CH_2) are observed. This indicates the coordination may happen between CuI and sulfur donor atoms of the ligand L. The spectra also indicate the presence of the Cu(I) in the polymeric Copper complex rather than Cu(II). HRMS calculation also supports the formation of the complex catalyst.

II.3.3.2. Single crystal X–ray diffraction

The polymeric co–ordination complex crystallizes in the monoclinic space group P $2_{1/c}$. It also shows a polymeric propagation in the form of $[(CuI)_2\{ArS(CH_2)_3SAr\}_2]_n$ metallopolymer (Fig II.1). This 1D–network of the co–ordination polymer is built up upon dimeric Cu_2I_2 units and these units are interconnected by dithioether ligands. The framework is made of $Cu_2(\mu–I)_2$ prismatic part which is connected with the dithioether ligands. The bond lengths of Cu─I range between 2.5867 (5) and 2.6443 (12) Å within the cluster core. The distance between the two adjacent Cu (I) centers, 2.7812 (10) Å that is significantly below the sum of the vander Waals radius (2.8 Å). The mean Cu─S bond length of range between 2.3339 (11) to 2.3551 (12) Å similar to $[\{Cu(\mu–I)_2Cu\}_2\{\mu–PhS(CH_2)_3SPh\}_2]_n$ (2.3465 Å).[17a] The angle between Cu…I…Cu is 64.23° and I…Cu…I 115.77° in the metallocluster.

Table II.1. Crystal Data, Data Collection and Structure Refinement for the complex catalyst

Formula	$C_{15}H_{14}CuF_2IS_2$	Cell volume/Å^3	1684.06 (12)
Formula weight	486.83	Cell formula units Z, Z$'$	4, 0
Temperature/K	293 (2)	density (calculated) g/cm^3	1.920

Description	Prismatic	θ range for data collection/deg	1.43–25.07
Colour	White	F(000)	944.0
Crystal system	Monoclinic	crystal size/mm	0.08, 0.12, 0.24
Space group	P $2_{1/C}$	Absorption co–efficient (μ)	3.387
a/Å	16.2003(7)	index ranges	$-19 \leq h \leq 15$ $-8 \leq k \leq 8$ $-18 \leq l \leq 18$
b/Å	7.4990(3)	reflections collected	20413
c/Å	15.7177(7)	independent reflections	2989
Cell angle (α)	90^{o}	refinement method	full–matrix least–squares on F^2
Cell angle (β)	118.12^{o} (2)	R–equivalents	0.0424
Cell angle (γ)	90^{o}	Sigma I/net I	0.0265

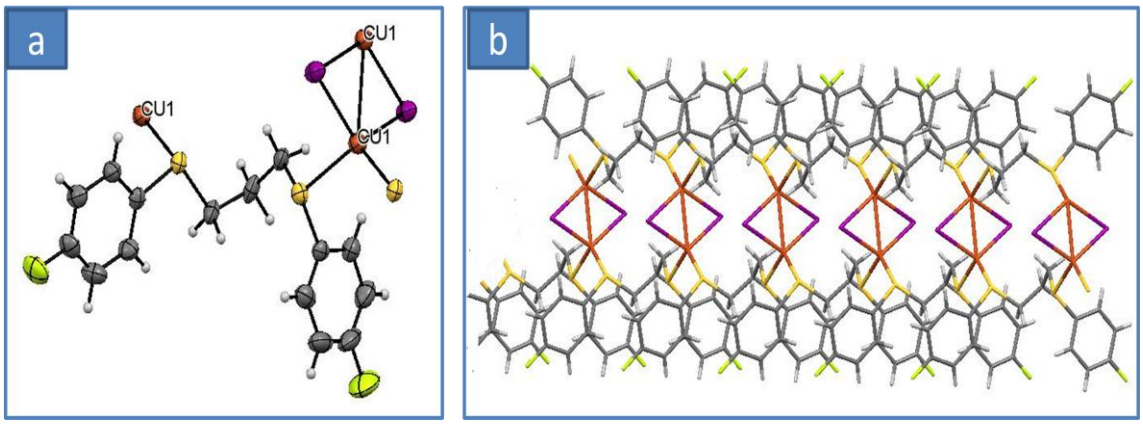

Figure II.1. *View of (a) monomeric picture of the complex and (b) infinite 1–D chain of the complex incorporating dinuclear Cu(μ_2–I)$_2$Cu motifs along 'b' axis.*

Selected bond lengths and bond angles are also given in the Tables below.

Table II.2. Selected bond length

Bond	Length	Bond	Length

I1–Cu1	2.5867 (5)	C10–C11	1.362 (7)
I1–Cu1	2.6443 (6)	C13–C12	1.377 (6)
Cu1–S1	2.339 (11)	C13–C14	1.384 (6)
Cu1–S2	2.3551 (12)	C14–C15	1.395 (6)
Cu1–I1	2.6443 (6)	C20–C19	1.373 (6)
S2–C19	1.782 (4)	C20–C21	1.394 (7)
S2–C22	1.813 (4)	C24–C23	1.524 (6)
S1–C13	1.775 (4)	C24–S1	1.813 (4)
S1–C24	1.813 (4)	C19–C18	1.399 (6)
F1–C10	1.366 (5)	C18–C17	1.363 (7)
F2–C16	1.355 (6)	C11–C12	1.389 (7)
C22–C23	1.507 (7)	C17–C16	1.381 (9)
C10–C15	1.348 (7)	C16–C21	1.345 (9)

Table II.3. Selected bond angle

Bond	**Angle**	**Bond**	**Angle**
Cu1–I1–Cu1	64.23 (2)	C11–C10–F1	117.9 (4)
S1–Cu1–S2	108.26 (4)	C12–C13–C14	119.9 (4)
S1–Cu1–I1	113.87 (3)	C12–C13–S1	124.3 (3)
S2–Cu1–I1	111.66 (3)	C14–C13–S1	115.9 (3)
S1–Cu1–I1	105.37 (3)	C13–C14–C15	119.8 (4)
S2–Cu1–I1	100.87 (3)	C19–C20–C21	119.9 (5)
I1–Cu1–I1	115.77 (2)	C23–C24–S1	110.9 (3)
S1–Cu1–Cu1	128.93 (4)	C20–C19–C18	120.5 (4)
S2–Cu1–Cu1	121.50 (4)	C20–C19–S2	117.4 (3)
I1–Cu1–Cu1	58.89 (18)	C18–C19–S2	122.1 (3)
I1–Cu1–Cu1	56.88 (18)	C17–C18–C19	119.3 (5)
C19–S2–C22	101.3 (2)	C22–C23–C24	116.1 (4)
C19–S2–Cu1	109.32 (14)	C10–C11–C12	118.3 (4)
C22–S2–Cu1	103.62 (15)	C18–C17–C16	118.8 (5)

C13–S1–C24	102.8 (2)	C13–C12–C11	120.1 (4)
C13–S1–Cu1	104.03 (13)	C10–C15–C14	118.5 (4)
C24–S1–Cu1	110.61 (15)	C21–C16–F2	118.6 (6)
C23–C22–S2	114.7 (3)	C21–C16–C17	123.4 (5)
C15–C10–C11	123.3 (4)	F2–C16–C17	117.9 (6)
C15–C10–F1	118.8 (4)	C16–C21–C20	118.1 (5)

II.3.4. Catalytic application

The polymeric co–ordination complex catalyst exhibits excellent catalytic activity towards the one–pot multicomponent azide alkyne cycloaddition reaction under base–free conditions. The reaction condition was optimized by taking the model reaction of benzyl bromide, NaN_3 and phenylacetylene. Various catalyst loading was checked under different temperature conditions and various solvents was also used as shown by Table II.4. At the very first time the reaction was done in neat condition and the temperature was kept as 60 °C with catalyst amount 5 mg. In this condition, the product yield isolated was 84% after 5 hours (entry 1). Relatively the conversion was less in methanol compared to the neat condition (70%, entry 2). In same reaction conditions when we used acetonitrile and water as solvent consecutively the yield found to be 87% and 80% respectively (entry 3 & 4). A (1:1) solvent mixture of acetonitrile and water gave excellent yield within 30 minutes (entry 5). When the same experiment was done in microwave reactor, the yield was less than the conventional thermal heating technique (entry 6). When the reaction was done keeping the temperature as 50 ^{o}C, the product yield was excellent (97%) in 3 hours (entry 7). The conversion of the triazole product was dropped to 85% at room temperature (entry 8). The catalyst loading was also checked by taking only 0.5 mg of the complex catalyst from entry 8 to entry 10 and the catalytic activity has been found to be excellent with the reaction conditions illustrated as entry 11. The yield of the product of same reaction was found to be decreased (83%) in the presence of CuI (entry 12). When the reactants amount were doubled keeping the catalyst amount same that is 0.5 mg, the yield found to be poor (65%, entry 13).

Table II.4. Optimization of reaction conditions for the one–pot azide–alkyne click reaction.

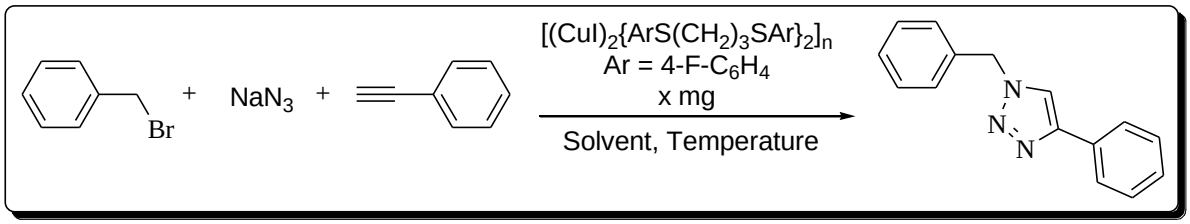

Entry	Solvent	Complex/CuI in (mg)	Temp. (^oC)	Time (h)	Yield[a] (%)
1	Neat	5	60	5	84
2	Methanol	5	60	5	70
3	Acetonitrile	5	60	5	87
4	Water	5	60	8	80
5	Acetonitrile: water	5	60	3	97
6	Acetonitrile: water	5	60	0.5	92[b]
7	Acetonitrile: water	5	50	3	97
8	Acetonitrile: water	5	RT	5	85
9	Acetonitrile: water	3	50	3	97
10	Acetonitrile: water	1	50	3	96
11	**Acetonitrile: water**	**0.5**	**50**	**3**	**96**
12[c]	Acetonitrile: water	0.5	50	3	79
13[d]	Acetonitrile: water	0.5	50	4	65

Reaction conditions: Phenyl acetylene (1 mmol), NaN_3 (1.2 mmol) and benzyl bromide (1.1 mmol), Cu–complex (5.0 to 0.5 mg), Acetonitrile:H_2O (1:1, 2 mL). [a]Isolated yield after purification through column chromatography by silica gel. [b]Reaction tried on focused microwave reactor. [c]CuI was used as catalyst. [d]Phenyl acetylene(2 mmol), NaN_3 (2.4 mmol) and benzyl bromide (2.2 mmol).

The complex is found to be very much air stable and the reaction was done with a range of benzyl, alkyl, allyl and cinnamyl halides (Table II.5). The terminal alkynes like phenyl acetylene, 4–ethanyl toluene and 2–bromo phenyl acetylene reacted very smoothly and the yields were also high (entry 1 to 3). 4–nitro–phenyl acetylene also gave 91% yield (entry 4).

Alphatic alkynes also responded effectively and a significant amount of yield was isolated in each case (entries 5, 13 and 14). Allyl bromide reacted effectively with phenyl acetylene, 4–ethanyl toluene as given in entry 6 and 7 respectively. Benzyl chlorides was also reactive as benzyl bromides (entry 8 and 9). When the same reaction was carried out with diphenyl acetylene an internal alkyne, the reaction did not occur even after 12 hours (entry 10). Cinnamyl chloride was found to be an excellent partner of terminal alkyne for this three component AAC reaction (entry 11 and 12). An aliphatic halide *n*–Octyl iodide also responded well to the AAC reaction (entry 15). These reactions proceeded without any difficulties. All the products were isolated in good to excellent yields and purified through column chromatography.

Table II.5. Catalytic activity of the complex in the AAC reaction.[a]

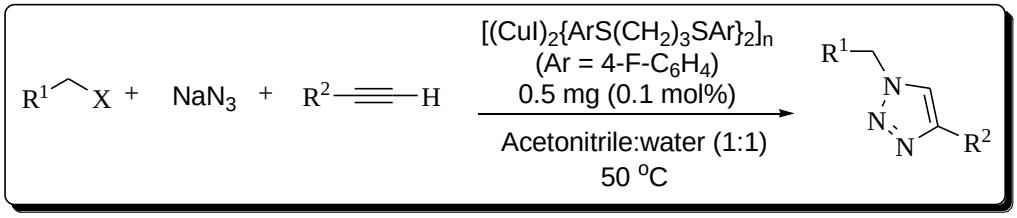

Entry	Alkyl Halide	Alkyne	Time (h)	Product	Yield [a] (%)
1	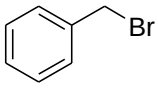	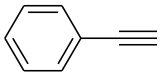	3	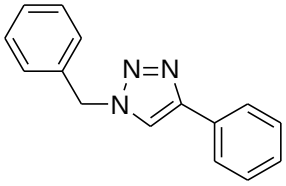	97
2	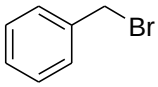	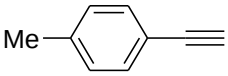	3	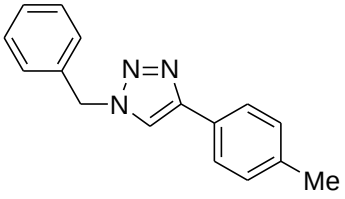	96
3	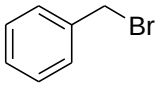	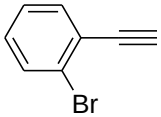	4	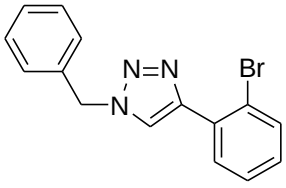	96

4	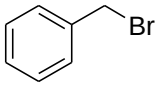		4	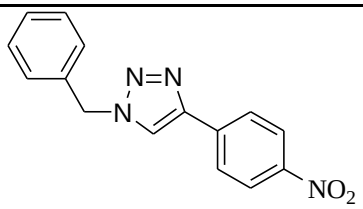	91
5	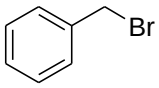	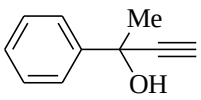	4	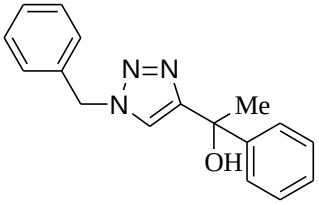	90
6	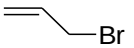	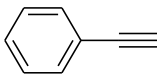	4	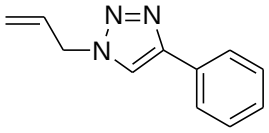	81
7	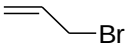	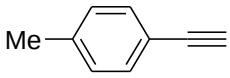	4	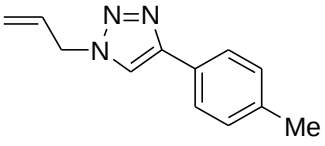	83
8	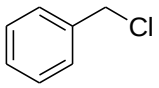	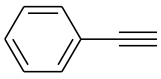	3.5	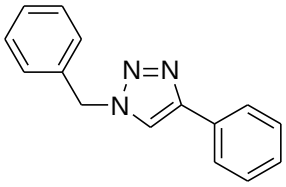	95
9	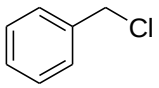	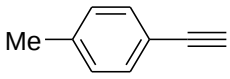	3.5	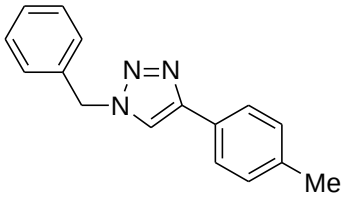	94
10	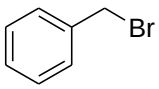	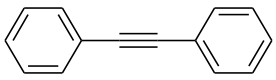	12	NR	–
11	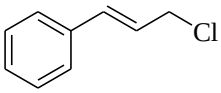	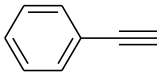	4	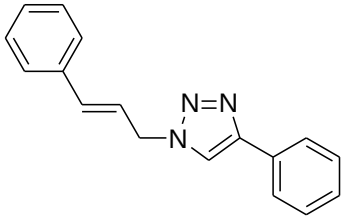	84

12	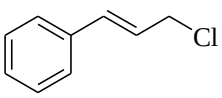	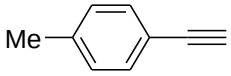	4	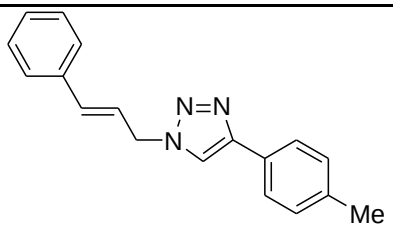	85
13	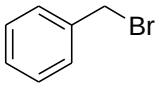	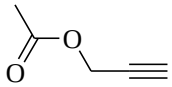	4	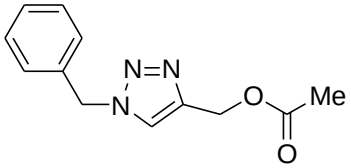	72
14	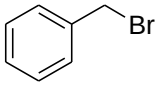	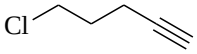	4	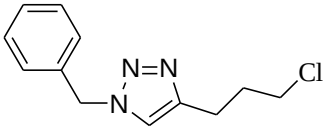	81
15	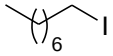	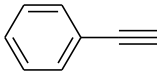	4	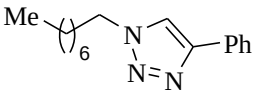	76

Reaction conditions: Terminal alkynes (1 mmol), NaN_3 (1.2 mmol) and benzyl/allyl/cinnamyl/alkyl halide (1.1 mmol), Cu–complex (0.5 mg, 0.1 mol%), Acetonitrile:H_2O (1:1, 2 mL). [a]Isolated yield after purification through column chromatography by silica gel. [Entries 1, 2, 3, 4, 5, 6, 12, 14, 15 were synthesized by presenting author and the rest of the entries were performed by the co–author K. Biswas.]

II.3.5. One–pot two–step process (GP4) for the synthesis of sulfur functionalized 1,2,3–triazole derivative

1,2,3–triazoles having various functional groups acts as steel corrosion inhibitors and these are used as suitable ligands for transition–metal chemistry.[30] 1,2,3–triazole compound with sulfur functionalized arms is synthesized by our group in a multicomponent approach by using our catalyst in one–pot two–step manner. At first benzenethiol (1.1 mmol) was reacted with propargyl bromide (1 mmol) in presence of triethyl amine (2 mmol) as base at room temperature using water medium. After 2 hours, benzyl bromide (1.1 mmol) and sodium azide (1.2 mmol) and Cu(I)–complex catalyst (0.5 mg) were added. TLC was used to monitor the progress of the reaction. Finally the desired triazole product was isolated through column chromatography in 82% yield. Scheme II.6 illustrates the preparation methodology.

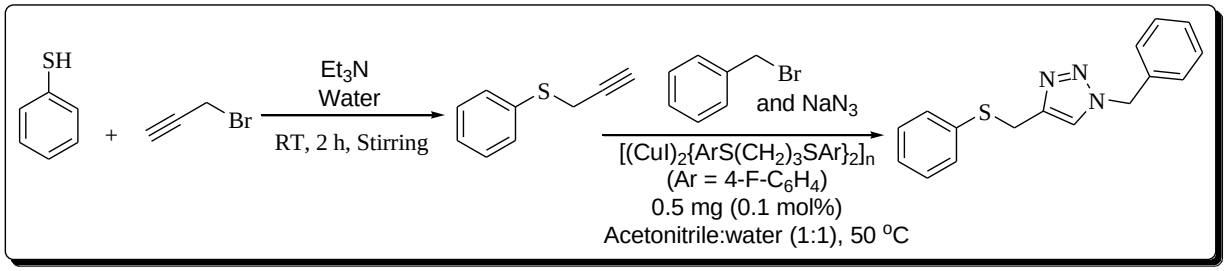

Scheme II.6. *One–pot two–step synthesis of sulfur functionalized 1,2,3–triazole derivative*

II.3.6. Mechanism

A probable mechanistic pathway for this multicomponent AAC reaction is proposed in Scheme II.7. Here the copper (I) species plays the vital role. At first, phenylacetylene forms copper acetylide in the presence of 1D–CuI dithioether polymeric complex by metallation process. Then, by substitution reaction between benzyl/ alkyl/ allyl/ cinnamyl halide and sodium azide occurs to form benzyl/ alkyl/ allyl/ cinnamyl azide *in situ*. In the next step, the polymeric copper acetylide reacts with benzyl/ alkyl/ allyl/ cinnamyl azide which was formed *in situ*. In the last step formation of the 1,4–disubstituted 1,2,3–triazoles occurs in the presence of proton with simultaneous elimination of the polymeric complex catalyst.[20]

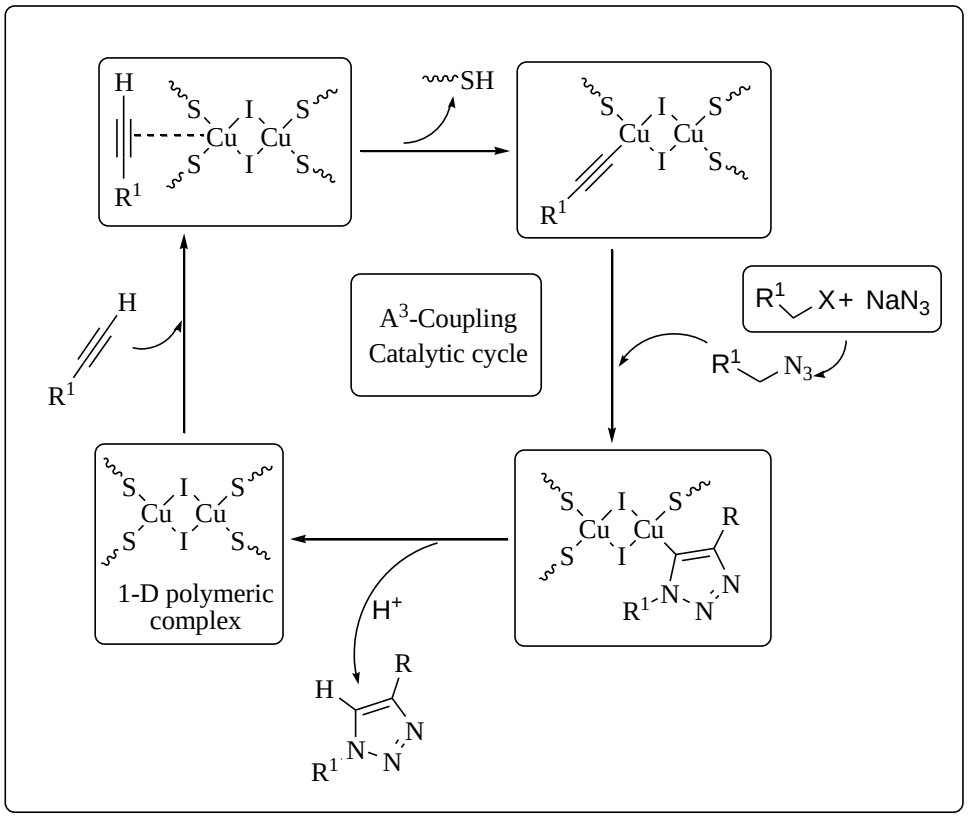

Scheme II.7. *A plausible mechanistic path for the Cu(I)–complex catalyzed one–pot three–component AAC reaction.*

II.4. Conclusion

We have synthesized SS–type bidentate dithioether ligand based Cu(I) coordination polymer, which is very efficient as catalyst for azide alkyne cycloaddition reaction. The new polymeric complex has been characterized by various techniques like ^{1}H NMR, ^{13}C NMR, Single Crystal XRD, HRMS etc. It was also applied as catalytic system in variety of substrates to produce various 1,4–disubstituted 1,2,3–triazole products in excellent yields. Low temperature and low catalyst loading are the significant features for this reaction methodology. The applicability of the catalyst was also extended and 1,2,3–triazole compound with sulfur functionalized arms was synthesized in a multicomponent approach in one–pot two–step process. This triazole compounds can be used to bind metal ions to synthesize new metal–complex system.

These work has been also selected by the editorial board of ***SYNFACTS*** *for its importance towards synthetic organic chemistry. The electronic reprint of the article has been published in*

SYNFACTS *issue 09/2018, highlighting some aspect of our original paper* ***Tetrahedron Letters****, 2018, 59, 2541–2545.*

II.5. Experimental section

II.5.1. General Information

All the reagents required for synthesis were commercially available and employed in reaction without further purification. The solvents were also purchased from commercial suppliers and used after distillation. All the products were purified by column chromatography on 60–120 mesh silica gels (SRL, India). Merck plates coated with silica gel 60, F_{254} were used for TLC. Single crystal XRD data were collected on a SIEMENS D5005 X–ray diffractometer with Cu–Kα radiation (λ = 1.5406 Å). FT–IR spectra were recorded with a FT–IR–8300 SHIMADZU spectrophotometer using a KBr pellet for solid compounds and neat for liquid compounds. The ^{1}H– & ^{13}C–NMR spectra were recorded at 300 MHz and 75 MHz respectively on Bruker AV 300 spectrometer in $CDCl_3$ and d_6–DMSO. Splitting patterns of protons were described as s (singlet), d (doublet), t (triplet), bs (broad singlet), dd (doublet of doublet) and m (multiplet). Chemical shifts (δ) were reported in parts per million (ppm) relative to TMS as internal standard. *J* values (coupling constant) were reported in Hz (Hertz). ^{13}C–NMR spectra were recorded with complete proton decoupling ($CDCl_3$: δ 77.0 ppm). HRMS was performed by Micromass Q–TOF Spectrometer under ESI (positive mode). Atomic Absorption Spectroscopy (AAS) was measured by Varian Spectra AA 50B Atomic Absorption Spectrometer.

II.5.2. General procedure (GP1) of preparing 1,3–bis(4–fluorophenylthio)–propane (L)

A mixture of allyl bromide (240 mg, 2 mmol) and 4–fluorobenzenethiol (640 mg, 5 mmol) was mixed with silica gel with mesh size 60–120 (1 g), which was moistened with few drops of water and stirred magnetically by using a spin magnetic bar for 16 h. The progress of the reaction was monitored by using thin layer chromatography. The product was then purified by column chromatography after completion of the reaction. The product was eluted with light petroleum and we got the 1,3–bis(4–fluorophenylthio)–propane ligand (L). It was characterized by ^{1}H– and ^{13}C–NMR and compared with literature data.[20]

II.5.3. General procedure (GP2) of preparing 1,3–bis(4–fluorophenylthio)–propane (L) ligated CuI–coordination complex

1:2 metal to ligand ratio was used to prepare 1,3–bis(4–fluorophenylthio)–propane (L) ligated CuI–coordination complex. CuI (190 mg, 1 mmol) was added and stirred in dry and distilled acetonitrile (10 mL) solvent at room temperature for 1 hour. Then the ligand L (2 mmol, 256 mg) was added to the solution. The reaction mixture was then stirred under refluxing condition for 20 hours. After that the reaction mixture was kept at room temperature for a while. Finally distilled petroleum ether was added drop wise to the reaction mixture and it was kept into refrigerator. White crystals were found on the petroleum ether part. These crystals were separated by simple filtration and dried under vacuum. The yield of the complex was found to be 78%.

II.5.4. General procedure (GP3) for one–pot three component AAC reaction

To a solution of 0.5 mg of the complex catalyst in Acetonitrile:H_2O (1:1), 1.1 mmol of benzyl/ alkyl/ allyl/cinnamyl halide and 1.2 mmol of NaN_3 were added. The reaction mixture was then stirred for few minutes at room temperature. Then 1.0 mmol of terminal alkyne was added to the reaction mixture. The reaction mixture was then heated at 50 ^oC for 3 hours in a round–bottomed flask fitted with condenser and maintaining gentle magnetic stirring. The progress of the reaction was monitored by TLC. After completion of the reaction, the mixture was diluted by water (2 mL) and the filtrate was extracted with ethyl acetate (4 x 10 mL) and the combined organic parts were washed with brine (1 x 5 mL), dried over anhydrous Na_2SO_4 and concentrated under vacuum. The residue was purified by passing through a short silica gel column chromatography and eluted with mixture of ethyl acetate–light petroleum to afford the desired triazole product. All products were characterized by spectral data as well as melting points and compared the same with literature.

II.5.5. Characterization data of the ligand 1,3–bis(4–fluorophenylthio)–propane (L)

NMR spectra of ligand (L)[19]

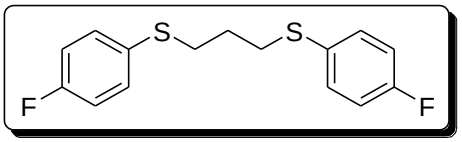

^{1}H NMR (d_6–DMSO, 300 MHz): δ 1.77 (quintet, J = 6.9 Hz, 2H, CH_2), 3.02 (t, J = 6.9 Hz, 4H, $2CH_2$, 7.11–7.18 (m, 4H, ArH), 7.34–7.39 (m, 4H, ArH); **^{13}C NMR (d_6–DMSO, 75**

MHz): δ 28.4, 32.3, 116.5 (d, J = 22.5 Hz, 1C, C–C–F coupling), 131.3–131.4 (1C), 131.7–131.9 (1C), 159.7–162.9 (d, J = 240 Hz, 1C, C–F *ipso* coupling) .

^{1}H NMR, ^{13}C NMR and HRMS spectral data of the copper 1D–polymeric complex

^{1}H NMR (d_6–DMSO, 300 MHz): δ 1.76 (s, 2H, CH_2), 3.02 (d, J = 6.0 Hz, 4H, $2CH_2$), 7.13 (d, J = 7.2 Hz, 4H, ArH), 7.37 (d, J = 4.5 Hz, 4H, ArH); **^{13}C NMR (d_6–DMSO, 75 MHz):** δ 28.1, 32.9, 116.5 (d, J = 21.74 Hz, 1C, C–C–F coupling), 131.0, 132.1, 161.4–163.1 (d, J = 127.5 Hz, 1C, C–F ipso coupling).

HRMS:[2] m/z $[M - I]^+$ calcd for $C_{15}H_{14}CuF_2IS_2$, 358.9801; found, 358.5771.

1–Benzyl–4–phenyl–1*H*–1,2,3–triazole (Table II.5, entry 1):

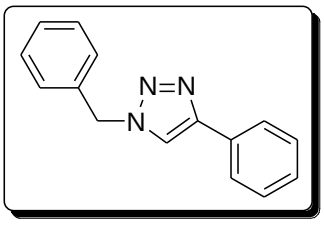

This compound was obtained by following the general procedure **GP3** in 97% yield as a white crystalline needle with melting point 128–130 ^{o}C. The MP and NMR data obtained are in quite agreement with that reported in the literature previously.[21] **^{1}H NMR ($CDCl_3$, 300 MHz)** δ 5.47 (s, 2H), 7.19–7.33 (m, 8H), 7.58 (s, 1H), 7.70–7.72 (m, 2H); **^{13}C NMR ($CDCl_3$, 75 MHz)** δ 54.1, 119.5, 125.6, 127.9, 128.1, 128.7, 128.8, 129.1, 130.5, 134.6, 148.1; **FT−IR (KBr)** ν_{max} 3128, 3029, 2924, 1638, 1465, 1357, 1227, 1075, 767, 730, 692 cm^{-1}.

1–Benzyl–4–(*p*–tolyl)–1*H*–1,2,3–triazole (Table II.5, entry 2):

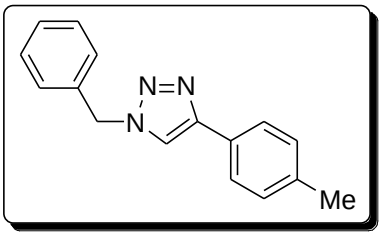

Obtained by using general procedure **GP3** in 96% yield as white crystalline solid with melting point 142–144 ^{o}C as compared to 150 ^{o}C reported in the literature. The NMR data also agrees with that repoted previously.[21] **^{1}H NMR ($CDCl_3$, 75 MHz)** δ 2.26 (s, 3H), 5.44 (s, 2H), 7.10 (d, *J* = 7.8 Hz, 2H), 7.18–7.28 (m, 5H), 7.53 (s, 1H), 7.6 (d, *J* = 8.1 Hz, 2H); **^{13}C NMR ($CDCl_3$, 75 MHz)** δ 21.2, 54.1, 119.1, 125.5, 127.6, 127.9, 128.6, 129.0, 129.4, 134.7, 137.9, 148.2; **FT–IR (KBr)** ν_{max} 3144, 2921, 1631, 1496, 1431, 1224, 1047, 825, 794, 721, 510 cm^{-1}.

1–Benzyl–4–(2–bromophenyl)–1*H*–1,2,3–triazole (Table II.5, entry 3):

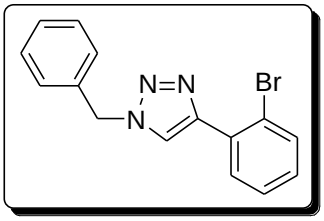

This compound was obtained using the general procedure **GP3** as pale yellow crystal in 96% yield and melts at 80–82 ^{o}C. The NMR data also corroborates with that previously reported one.[22] **^{1}H NMR ($CDCl_3$, 75 MHz)** δ 5.58 (s, 2H), 7.12–7.18 (m, 1H), 7.25–7.39 (m, 6H), 7.6 (d, *J* = 7.8, 1H), 8.07–8.15 (m, 2H); **^{13}C NMR ($CDCl_3$, 75 MHz)** δ 54.2, 121.2, 123.1, 127.7, 127.9 128.7, 129.1, 129.4, 130.6, 131.3, 133.5, 134.7, 145.7; **FT–IR (KBr)** ν_{max} 3119, 3083, 2950, 1632, 1496, 1460, 1418, 1227, 1026, 831, 756, 730, 700 cm^{-1}.

1–benzyl–4–(4–nitrophenyl)–1*H*–1,2,3–triazole (Table II.5, entry 4):

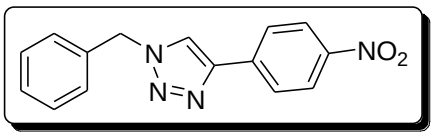

It was obtained by following the general procedure **GP3** as pale yellow crystal in 91% yield, having melting point 171–172 ^{o}C which supports the literature data. The NMR data also corroborates with the literature reports.[23] **^{1}H NMR (d_6–DMSO, 300 MHz)** δ 5.69 (s, 2H), 7.34–7.38 (m, 5H), 8.11–8.14 (m, 2H), 8.28–8.31 (m, 2H), 8.91 (s, 1H); **^{13}C NMR (d_6–DMSO,**

75 MHz) δ 53.7, 124.1, 124.8, 126.4, 128.5, 128.7, 129.3, 136.2, 137.5, 145.2, 147.1; **FT–IR (KBr)** ν_{max} 3135, 3100, 2935, 2830, 2438, 2357, 1605, 1506, 1461, 1332, 1230, 1206, 1108, 1049, 973, 821, 731 cm^{-1}.

1–(1–benzyl–1*H*–1,2,3–triazol–4–yl)–1–phenylethanol (Table II.5, entry 5):

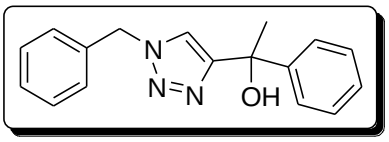

This compound was obtained by using the general procedure **GP3** in 90% yield as white solid which melts at 133–135 °C. The NMR data are in good agreement with that one reported in the literature.[24] **^{1}H NMR (d_6–DMSO, 300 MHz)** δ 1.81 (s, 3H), 5.54 (s, 2H), 5.85 (s, 1H), 7.18–7.21 (m, 1H), 7.26–7.37 (m, 7H), 7.45–7.48 (m, 2H), 7.89 (s, 1H); **^{13}C NMR (d_6–DMSO, 75 MHz)** δ 31.3, 53.1, 71.4, 122.1, 125.6, 126.8, 128.2, 128.5, 128.6, 129.2, 136.6, 148.8, 155.9; **FT–IR (KBr)** ν_{max} 3318, 3122, 2981, 2929, 1599, 1491, 1442, 1334, 1217, 1159, 1121, 1052, 1013, 829, 729, 698, 570 cm^{-1}.

1–Allyl–4–phenyl–1*H*–1,2,3–triazole (Table II.5, entry 6):

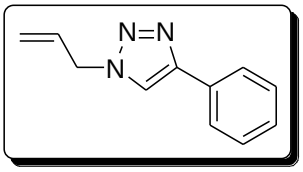

Obtained by the general procedure **GP3** in 81% yield as white crystalline solid with melting point 62–64 °C. The NMR data are in agreement with those reported previously in literature. [25] **^{1}H NMR ($CDCl_3$, 75 MHz)** δ 4.96 (d, 2H), 5.26–5.34 (m, 2H), 5.95–6.08 (m, 1H), 7.28–7.42 (m, 3H), 7.76–7.83 (m, 3H); **^{13}C NMR ($CDCl_3$, 75 MHz)** δ 52.7, 119.7, 120.1, 125.7, 128.1, 128.8, 130.6, 131.3, 147.9; **FT–IR (KBr)** ν_{max} 3122, 3093, 2945, 1640, 1420, 1224, 1077, 991, 943, 763, 691 cm^{-1}.

1–Allyl–4–(*p*–tolyl)–1*H*–1,2,3–triazole (Table II.5, entry 7):

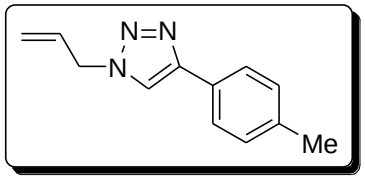

This compound was obtained following the general procedure **GP3** in 83% yield as white crystalline solid with melting point 88–90 ^{o}C. The MP and NMR data are in good agreement with the literature.[26] **^{1}H NMR ($CDCl_3$, 75 MHz)** δ 2.36 (s, 3H), 4.97–5.01 (m, 2H), 5.29–5.38 (m, 2H), 5.98–6.11 (m, 1H), 7.02–7.26 (m, 2H), 7.69–7.72 (m, 3H); **^{13}C NMR ($CDCl_3$, 75 MHz)** δ 21.3, 52.7, 119.1, 120.1, 125.6, 127.8, 129.5, 131.4, 138.0, 148.1; **FT–IR (KBr)** ν_{max} 3102, 3043, 2945, 1644, 1630, 1457, 1433, 1226, 1050, 948, 817, 776, 513 cm^{-1}.

1–(*E*)–Cinnamyl–4–phenyl–1*H*–1,2,3–triazole (Table II.5, entry 11):

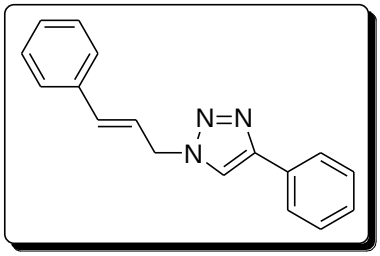

Obtained by the general procedure **GP3** in 84% yield as white solid with melting point 136–137 ^{o}C. The MP and NMR data are in agreement with the literature report.[26] **^{1}H NMR ($CDCl_3$, 75 MHz)** δ 5.11–5.13 (m, 2H), 6.29–6.41 (m, 1H), 6.66 (d, J = 15.9 Hz, 1H), 7.24–7.47 (m, 8H), 7.79–7.83 (m, 3H); **^{13}C NMR ($CDCl_3$, 75 MHz)** δ 52.4, 119.5, 121.9, 125.7, 126.8, 128.2, 128.6, 128.8, 128.9, 130.6, 135.4, 135.5, 148.1; **FT–IR (KBr)** ν_{max} 3133, 3023, 2951, 1608, 1465, 1448, 1220, 1076, 975, 761, 696 513 cm^{-1}.

1–(*E*)–Cinnamyl–4–(*p*–tolyl)–1*H*–1,2,3–triazole (Table II.5, entry 12):

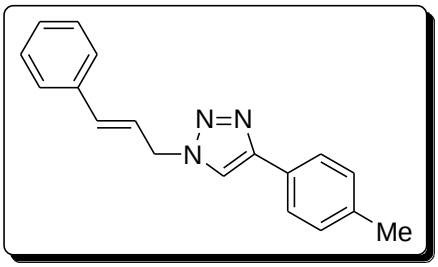

It was obtained by following the general procedure **GP3** in 85% yield as a white solid with melting point 145–147 ^{o}C. The HRMS data obtained also corroborates the calculated value. **^{1}H NMR ($CDCl_3$, 75 MHz)** δ 2.35 (s, 3H), 5.11–5.14 (m, 2H), 6.30–6.4 (m, 1H), 6.67(d, *J* = 15.6 Hz, 1H), 7.19–7.36 (m, 7H), 7.69–7.75 (m, 3H); **^{13}C NMR ($CDCl_3$, 75 MHz)** δ 21.3, 52.4, 119.1, 122.0, 125.6, 126.7, 127.8, 128.5, 128.7, 129.5, 135.3, 135.5, 137.9, 148.1; **FT–IR (KBr)** ν_{max} 3132, 2977, 1657, 1468, 1431, 1229, 1051, 823, 698 cm^{-1}; **HRMS: m/z [M + Na]$^{+}$** Calcd for $C_{18}H_{17}N_3$, 298.1320; found, 298.2050.

(1–Benzyl–1*H*–1,2,3–triazol–4–yl) methyl acetate Table II.5, entry 13):

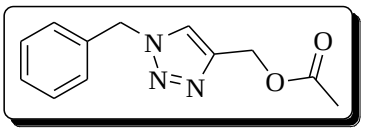

It was obtained by the general process **GP3** in 72% yield as a light yellow viscous oil. The NMR data well supports that obtained from literature.[27] **^{1}H NMR ($CDCl_3$, 75 MHz)** δ 2.20 (s, 3H), 5.16 (s, 2H), 5.51 (s, 2H), 7.26–7.36 (m, 5H), 7.72 (s, 1H); **^{13}C NMR ($CDCl_3$, 75 MHz)** δ 20.8, 54.1, 57.6, 123.7, 128.1, 128.7, 129.1, 134.5, 143.1, 170.7; **FT–IR (Neat)** ν_{max} 3143, 2960, 1740, 1643, 1455, 1367, 1230, 1035, 722 cm^{-1}.

1–benzyl–4–(3–chloropropyl)–1*H*–1,2,3–triazole (Table II.5, entry 14):

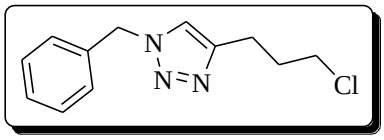

This compound was synthesized by following the procedure **GP3** and obtained as Colourless viscous oil in 81% yield. The spectral data are in well agreement to the literature report.[28] **^{1}H**

NMR ($CDCl_3$, 75 MHz) δ 2.09–2.18 (m, 2H), 2.85 (t, *J* = 7.2 Hz, 2H), 3.55 (t, *J* = 6.3 Hz, 2H), 5.49 (s, 2H), 7.26 (s, 3H), 7.35 (s, 3H); **^{13}C NMR ($CDCl_3$, 75 MHz)** δ 22.7, 31.8, 44.2, 54.0, 121.1, 128.0, 128.7, 129.1, 134.8, 146.8; **FT–IR (Neat)** ν_{max} 3112, 3062, 2956, 2860, 2418, 1887, 1552, 1495, 1450, 1336, 1307, 1275, 1215, 1177, 1132, 1057, 836, 765, 715, 672, 572 cm^{-1}.

1–octyl–4–phenyl–1*H*–1,2,3–triazole (Table II.5, entry 15):

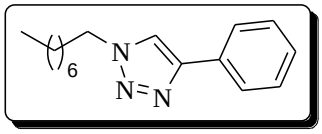

It was obtained by using the general procedure **GP3**. The compound is a white solid in nature with melting point 70–72 ^{o}C. The MP and spectral data are in well agreement with the previously reported literature.[29] **^{1}H NMR ($CDCl_3$, 75 MHz)** δ 0.84–0.87 (d, *J* = 6.9 Hz, 2H), 1.26–1.32 (m, 10H), 1.92 (bs, 2H), 4.63 (t, *J* = 7.2 Hz, 2H), 7.31 (t, *J* = 7.2 Hz, 1H), 7.38–7.43 (m, 2H), 7.75 (s, 1H), 7.83 (d, *J* = 7.5 Hz, 2H); **^{13}C NMR ($CDCl_3$, 75 MHz)** δ 14.1, 22.6, 26.5, 29.0, 29.1, 30.4, 31.7, 50.4, 119.5, 125.7, 128.1, 128.9, 130.8, 147.7; **FT–IR (KBr)** ν_{max} 3119, 3090, 2952, 2917, 2847, 1609, 1464, 1356, 1215, 1191, 1078, 1052, 976, 839, 762, 724, 695, 526 cm^{-1}.

1–benzyl–4–((phenylthio)methyl)–1*H*–1,2,3–triazole (Scheme II.6, Sulfur functionalised triazole):

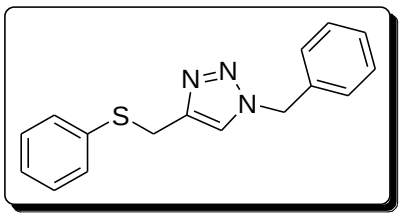

This triazole compound with sulfur containing pendent arm was synthesized to broaden the scope of the reaction as this compound may act as a good ligand for binding metal ions. It was obtained as white crystalline solid with melting point 75–76 ^{o}C by following the general

process **GP4**. MP and NMR data supports the literature reports.[30] **^{1}H NMR ($CDCl_3$, 75 MHz)** δ 4.19 (s, 2H), 5.44 (s, 2H), 7.13–7.35 (m, 11H); **^{13}C NMR ($CDCl_3$, 75 MHz)** δ 29.04, 29.08 ($–SCH_2$), 54.1 ($–NCH_2$), 122.0, 126.5, 127.9, 128.7, 128.93, 128.95, 129.1, 129.8, 129.9, 134.7, 135.4, 145.3; **FT–IR (KBr)** ν_{max} 3141, 3070, 2918, 1569, 1549, 1438, 1428, 1337, 1207, 1106, 1046, 814, 734, 471 cm^{-1}.

II.5.6.1. Scanned copy of HRMS spectra of polymeric copper complex

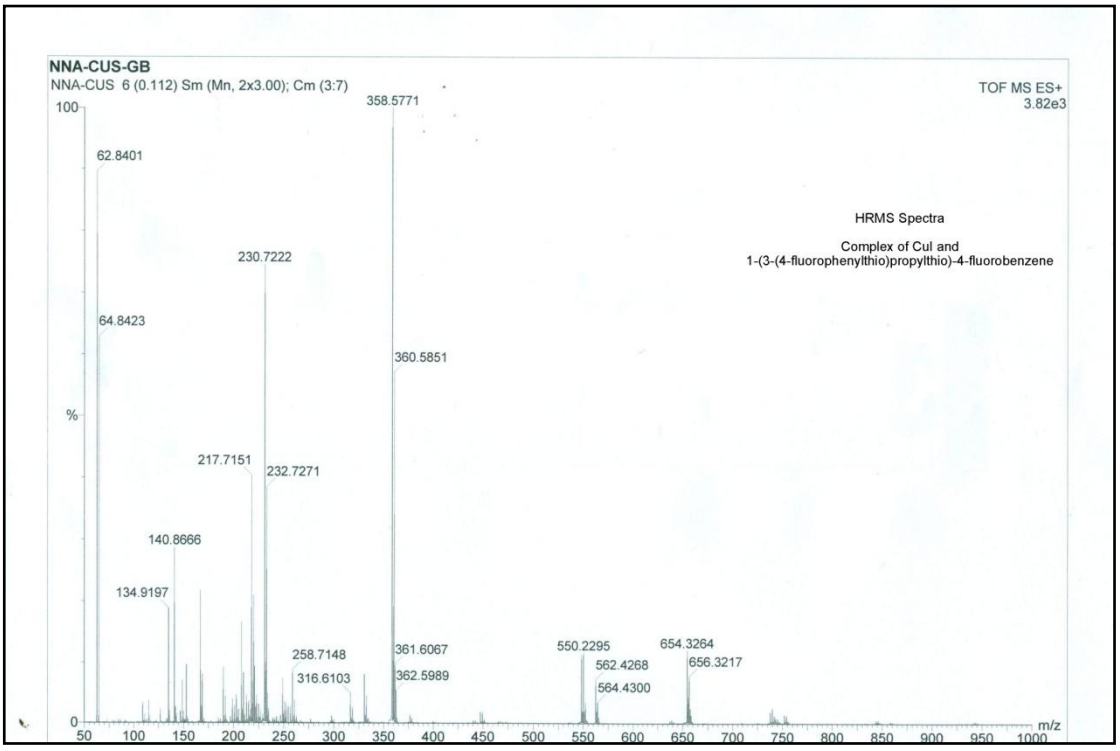

Figure II.2. *HRMS of 1,3–bis(4–fluorophenylthio)–propane (L) ligated CuI–coordination complex*

II.5.6.2. Scanned copies of ^{1}H–NMR, ^{13}C–NMR of Ligand (L), complex; Table II.5, Entry 4, 9 and HRMS of entry 9

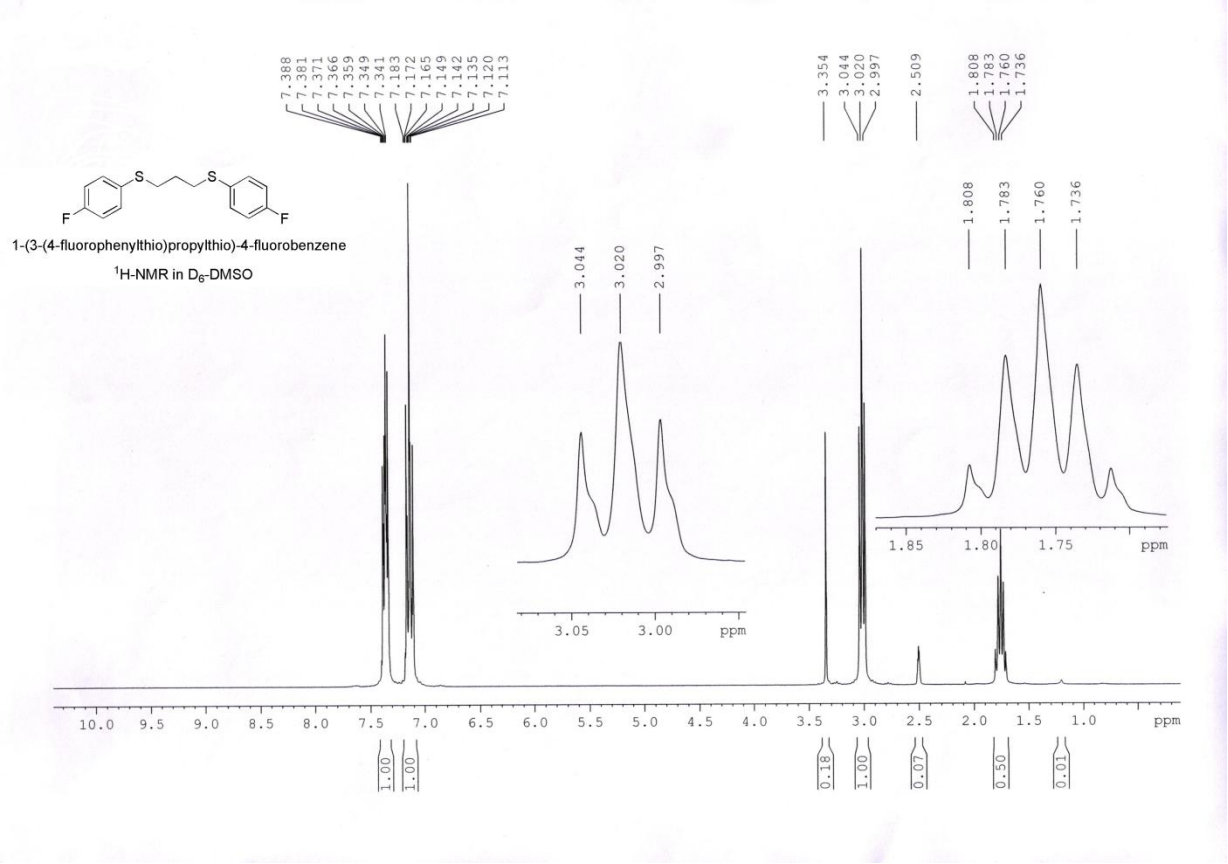

Figure II.3. *^{1}H–NMR spectra of [1, 3–bis(4–fluorophenylthio)–propane] ligand(L) in d_6–DMSO*

Figure II.4. *^{1}H–NMR spectra of the complex catalyst in d_6–DMSO*

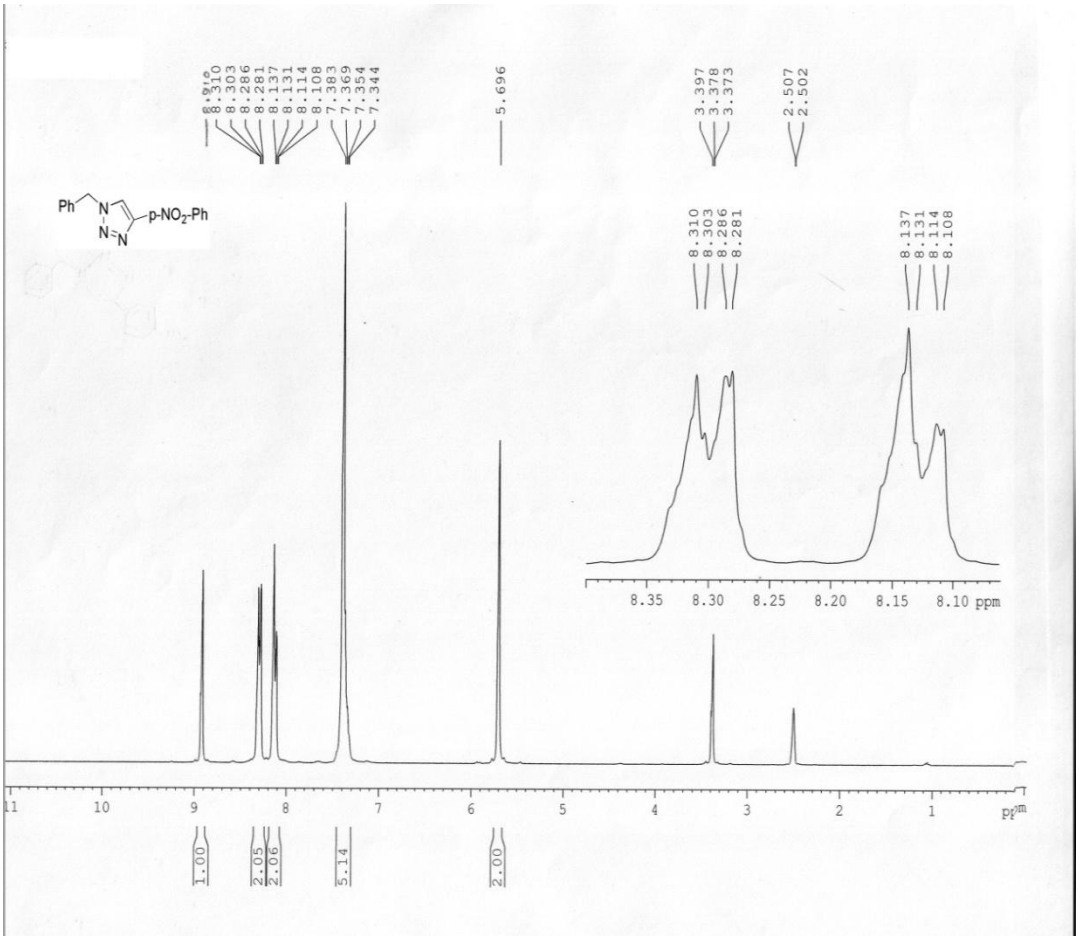

Figure II.5. *^{1}H NMR spectra of 1–benzyl–4–(4–nitrophenyl)–1H–1,2,3–triazole*

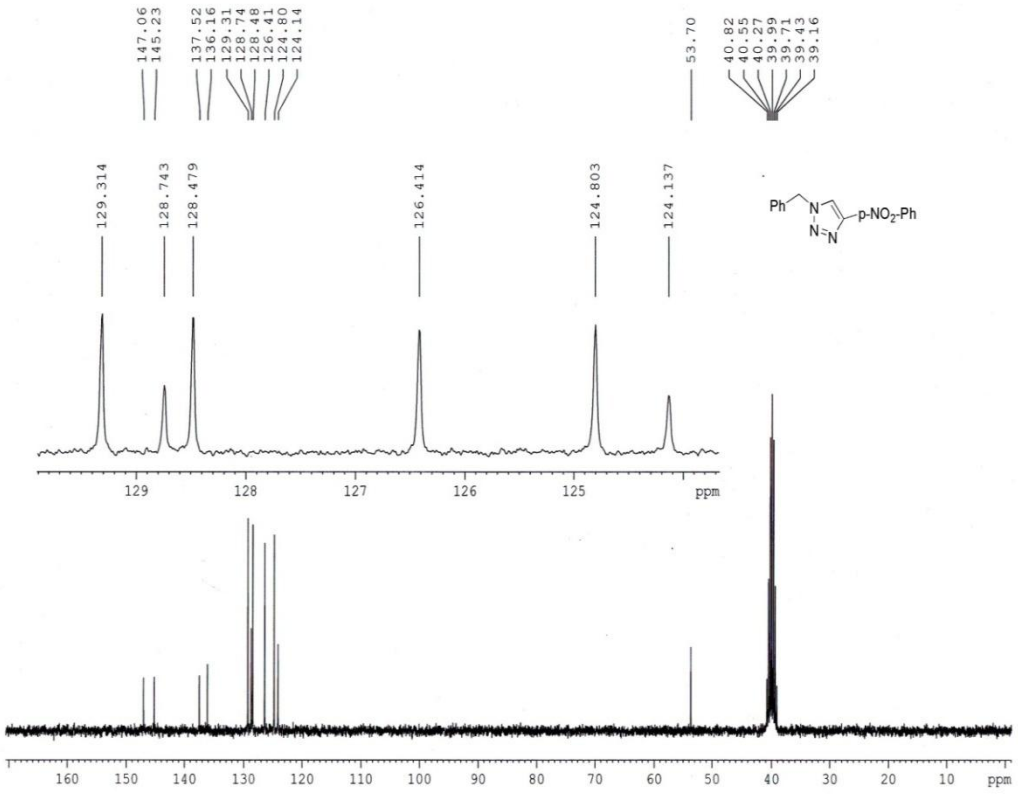

Figure II.6. *^{13}C NMR spectra of 1–benzyl–4–(4–nitrophenyl)–1H–1,2,3–triazole*

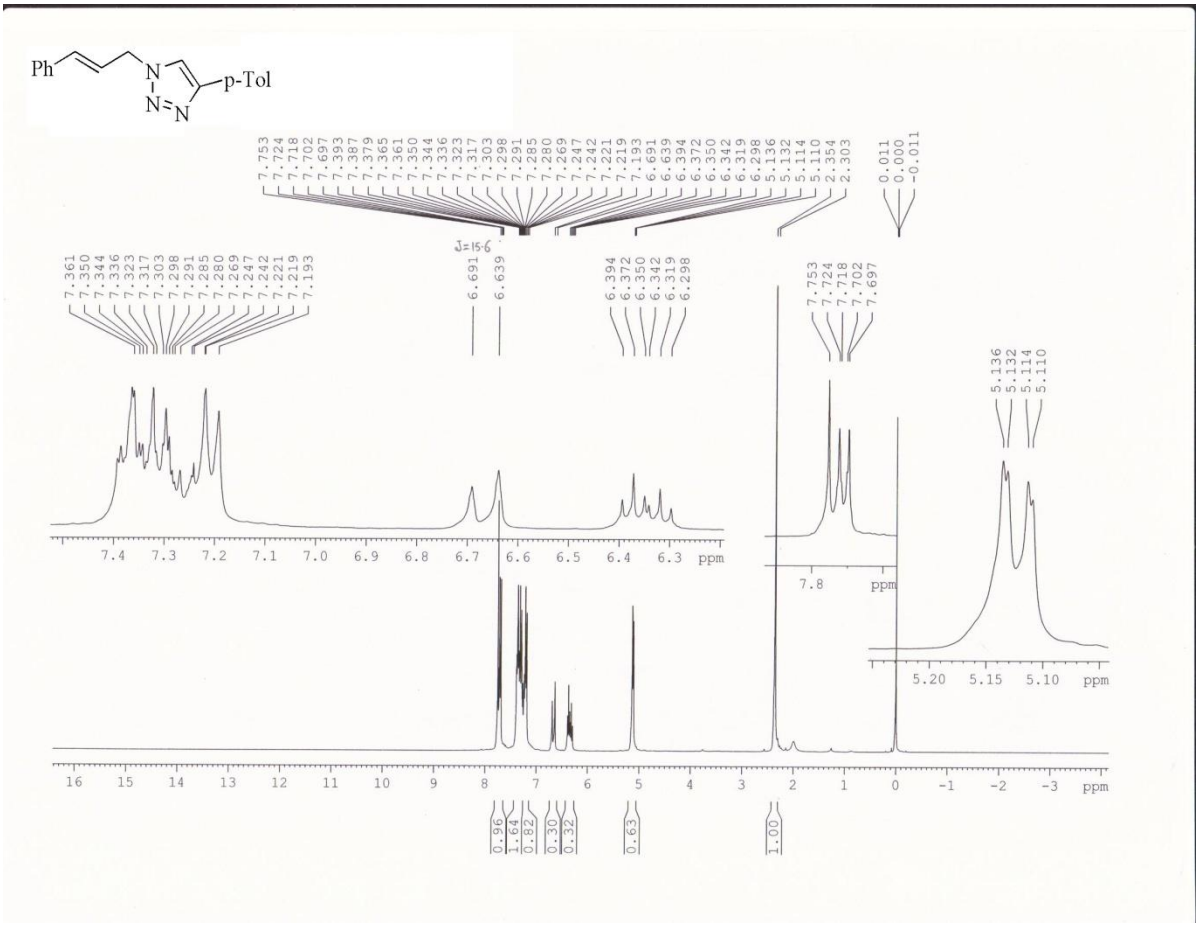

Figure II.7. *^{1}H NMR spectra of 1–(E)–Cinnamyl–4–(p–tolyl)–1H–1,2,3–triazole*

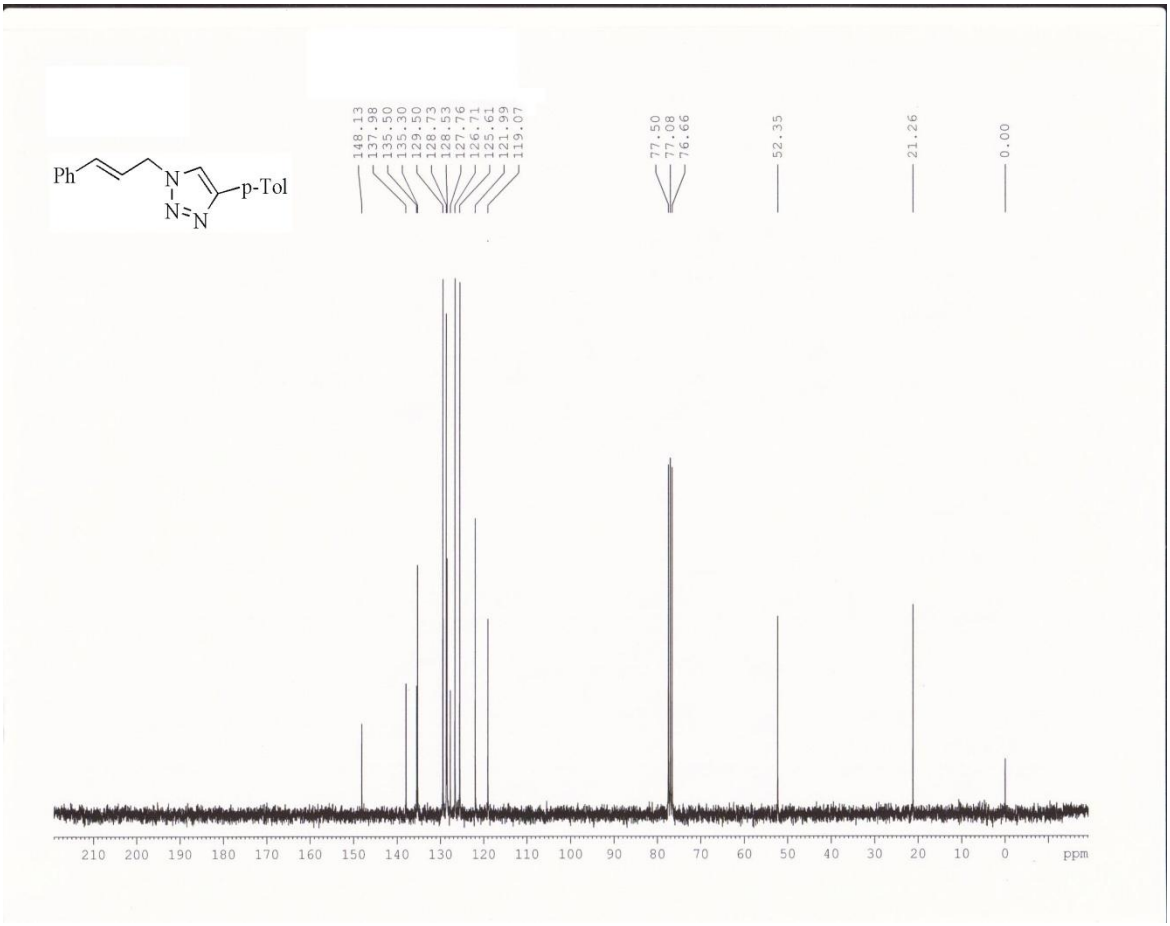

Figure II.8. *^{13}C NMR spectra of 1–(E)–Cinnamyl–4–(p–tolyl)–1H–1,2,3–triazole*

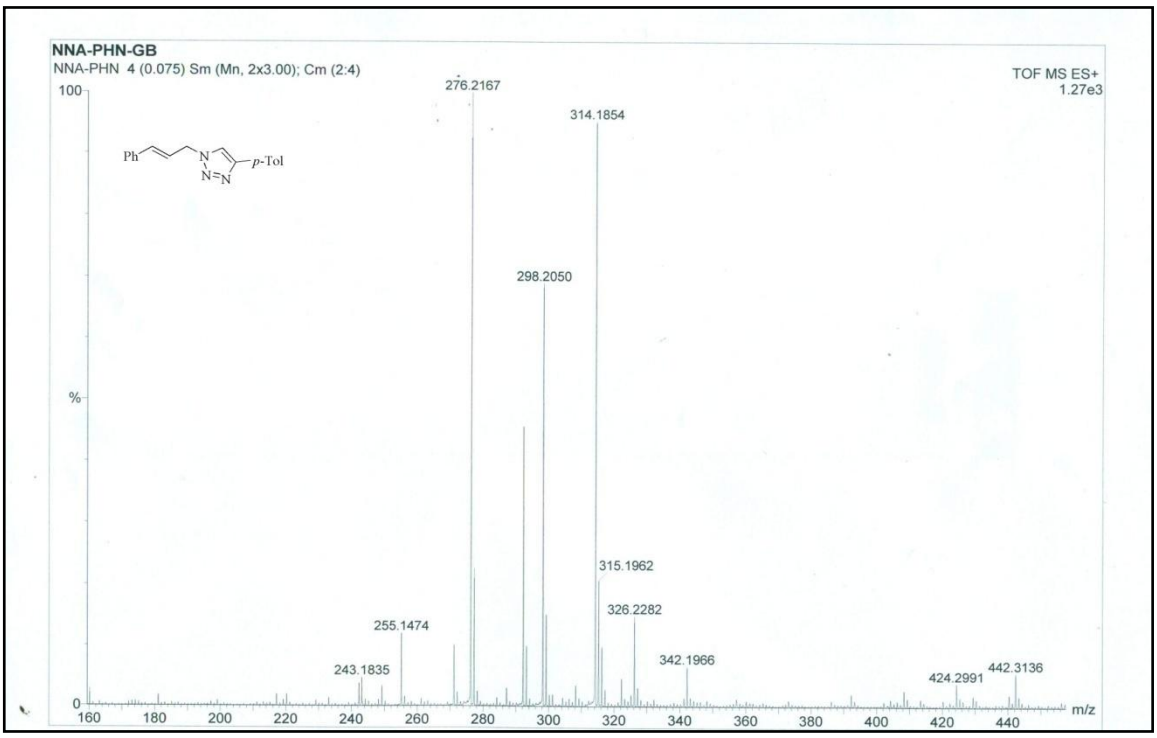

Figure II.9. *HRMS of 1–(E)–Cinnamyl–4–(p–tolyl)–1H–1,2,3–triazole*

II.6. References

References are given in BIBLIOGRAPHY under Chapter II page no. 134–136.

CHAPTER III

1,2–dithioether based 2D–copper(I) coordination polymer catalyzed A^3–coupling reaction: Solvent–free synthesis of propargylamines

III.1. Introduction

Propargylamines are used in organic chemistry as precursors and versatile building blocks for the preparation of various nitrogen–containing heterocyclic compounds as well as key intermediates for the synthesis of biologically active pharmaceuticals and natural products.[1–3] They also act as key intermediates for the construction of biologically active compounds like isosteres, *β*–lactams, oxotremorine substrates, conformationally restricted peptides and therapeutic drug molecules.[4] Several propargylamines such as Resagiline and Deprenyl (Figure III.1.) have been shown to be highly potent and irreversible selective monoamine oxidase type–B inhibitors.[5] Some propargylamines have been used for the treatment of neuropsychiatric disorders such as Parkinson's and Alzheimer's disease.[6,7]

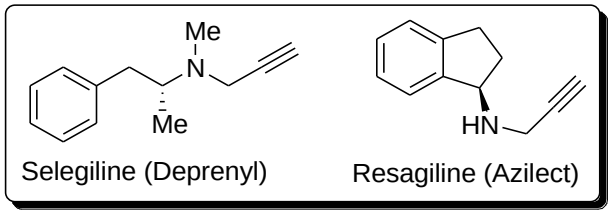

Figure III.1. *Structure of monoamine oxidase (MAO) type–B inhibitors*

These alkynyl amines are also important building blocks for the synthesis of *N*–bearing compounds such as *β*–lactam,[8,9] pyrrole,[10] pyrrolidine,[11] pyrrolophane,[12] 3–amino benzofuran,[13] aminoindolizine,[14] 2–aminoimidazole,[15] oxazolidinone,[16] quinoline,[17] etc. Biologically active dibenzoazocines and dibenzoazepines have been synthesized by intramolecular A^3–coupling reaction.[18]

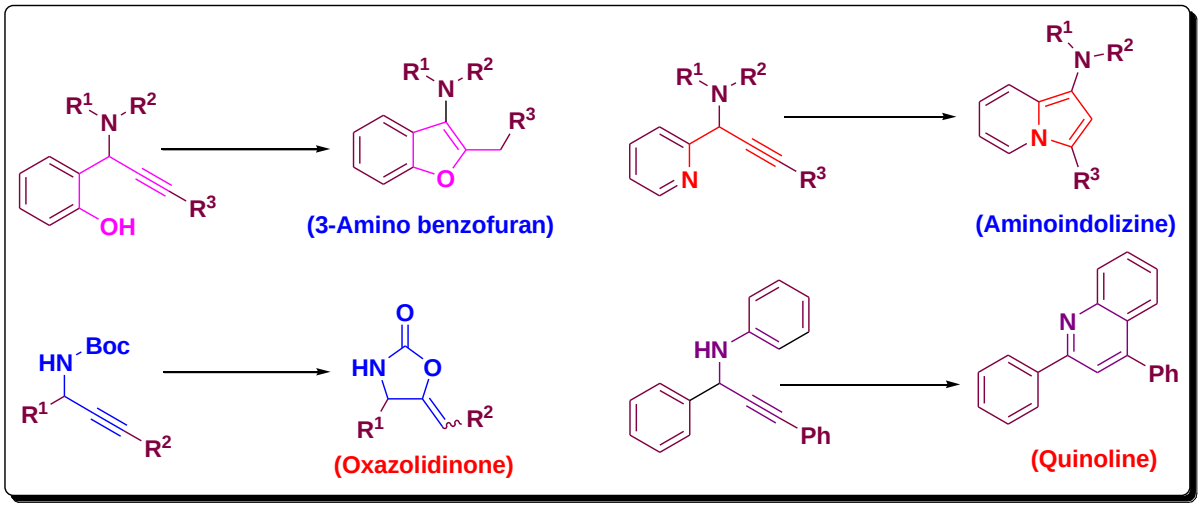

Figure III.2. *Schematic approaches for the synthesis of various N–containing heterocyclic molecules from different propargylamines*

Because of their immense importance, many synthetic methods have been developed so far.[19–22] Classically, propargylamines were synthesized by simple nucleophilic addition of a metal alkynylide to C=N electrophilic moiety. In this case, stoichiometric amount of highly active organometallic reagents *viz.* organolithium, Grignard reagents,[23] and organozinc reagents[24] are required. Therefore these methodologies are less attractive due to low tolerance of functional groups, harsh reaction conditions and operational difficulty. However, the most direct and efficient method for the preparation of propargylamines through transition–metal catalyzed three–component coupling between an aldehyde, an amine and a terminal alkyne, which is commonly known as A^3–coupling reaction (Figure III.3).[25]

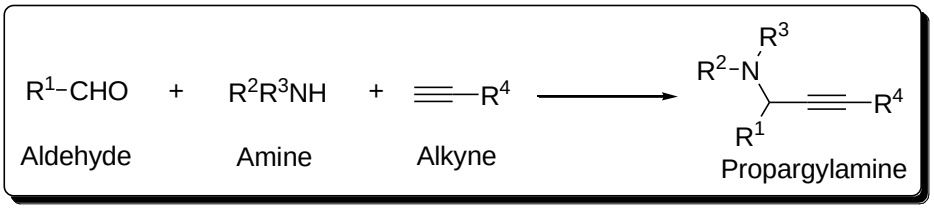

Figure III.3. *Schematic representation of A^3–coupling reaction*

Under homogeneous or heterogeneous conditions, a wide variety of transition metal salts and complexes have been employed in the synthesis of propargylamine via A^3–coupling reaction.[26] This three component coupling reaction is catalyzed by transition metal catalysts like copper,[26–29] silver,[26,30–32] gold,[26,33–35] iron,[36,37] cobalt,[38] nickel,[39] indium,[40,41] zinc,[42] ruthenium,[43] iridium[44] etc.

Out of these catalysts the copper have been most studied because of its easy availability, low cost, low toxicity and high reactivity. Few methodologies where Cu–catalysts have been employed are shown here.

Navarro and Chen reported *N*–heterocyclic carbene (NHC) complex of copper (I) as catalyst for A^3–coupling reaction (Scheme III.1).[28]

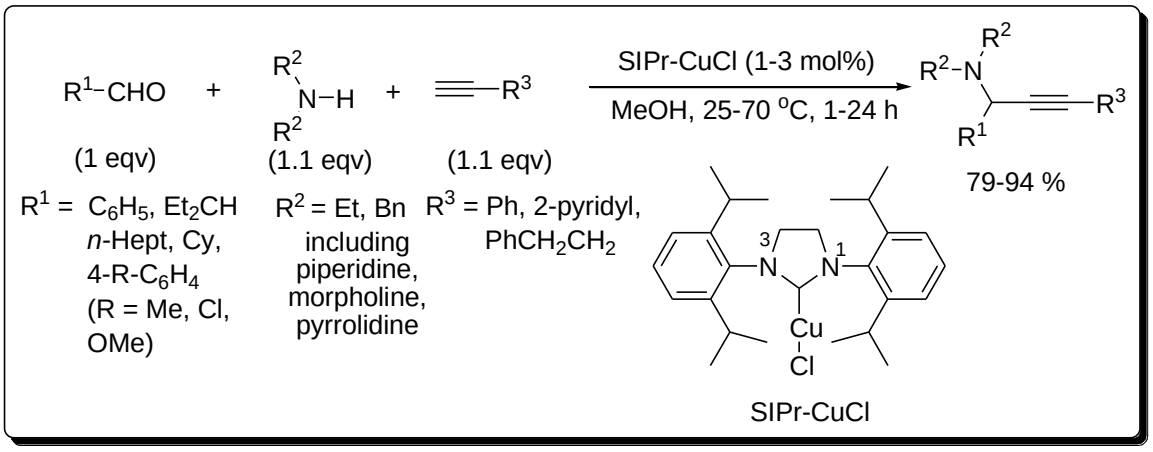

Scheme III.1. *SIPr–CuCl–catalyzed A^3–coupling reaction*

A^3–coupling reaction in ionic liquid solvent 1–butyl–3–methylimidazolium hexafluorophosphate [bmim][PF_6] using CuCN as a source of copper catalyst was reported by Park and Alper. The temperature of the reaction was kept 120°C (Scheme III.2).[27]

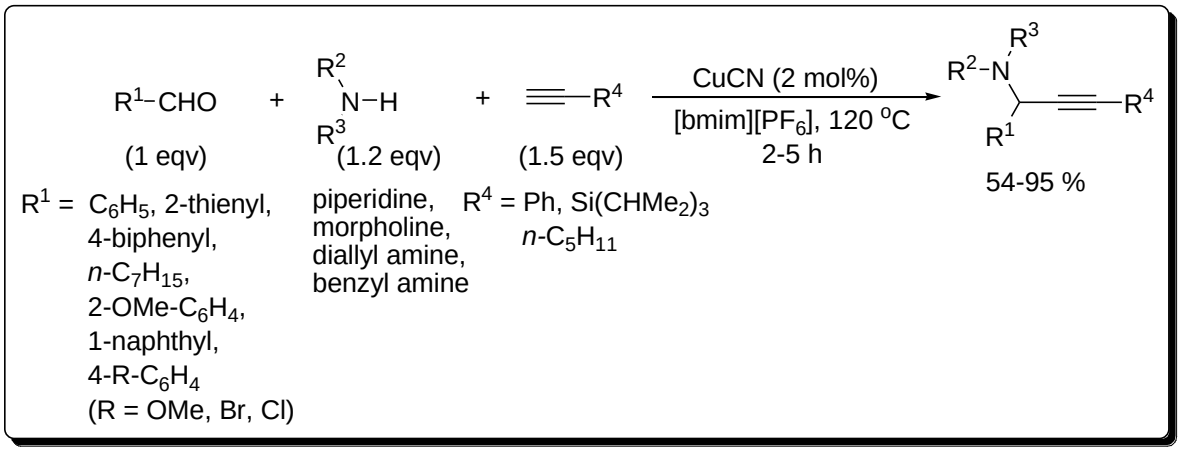

Scheme III.2. *CuCN–catalyzed A^3–coupling reaction in [bmim][PF_6]*

When CuI was used with the combination of a chiral co–catalyst asymmetric A^3–coupling reaction (AA^3 coupling) was achieved. Enantioselective propargylamines were obtained in good to excellent yield with dichloromethane solvent at 0 °C in this procedure (Scheme III.3).[29]

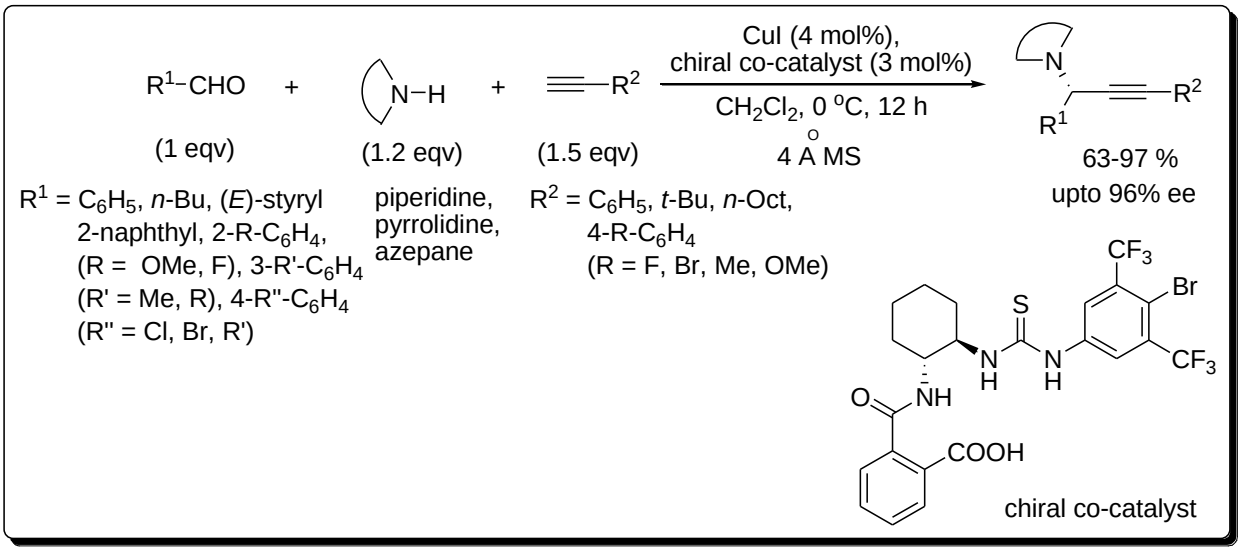

Scheme III.3. *CuI–catalyzed of AA*^{3}*–coupling reaction*

Li *et al*. has shown Cu–catalyzed A^3–coupling reaction of salicylaldehyde and its derivatives. The propargylamines produced by the process contains phenolic OH group and it undergoes cyclization reaction when treated with potassium carbonate base and tetra–*n*–butylammonium bromide (TBAB).[13]

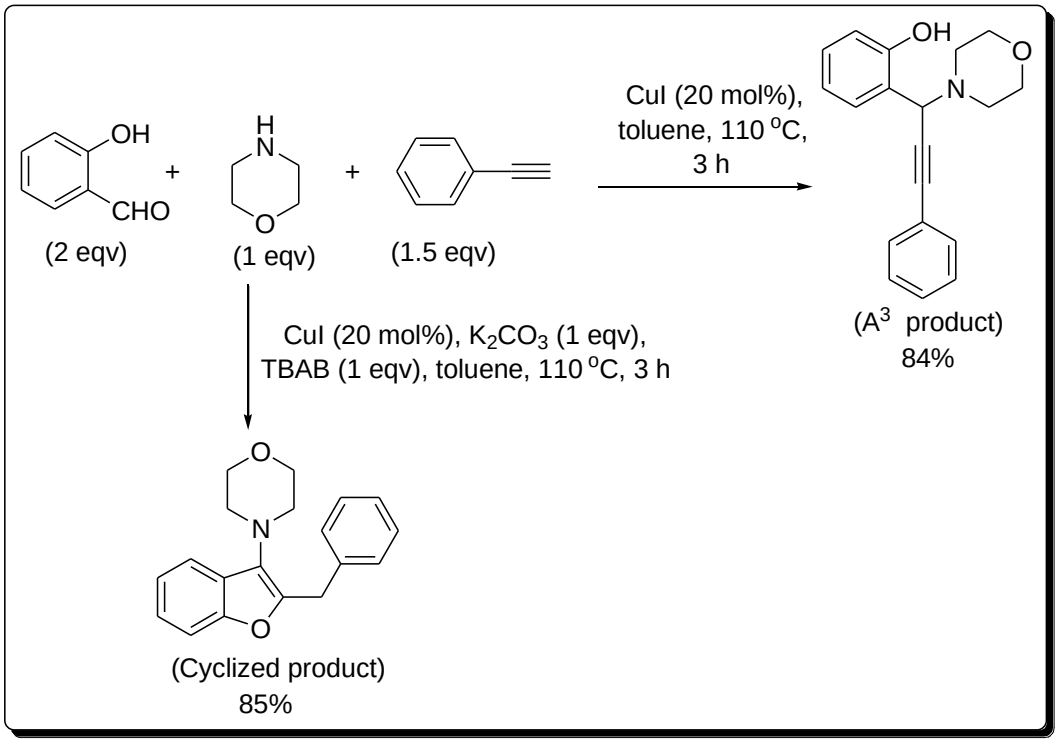

Scheme III.4. *CuI–catalyzed by A*^{3}*–coupling reaction of salicylaldehyde*

Eycken and his co–workers used microwave irradiation technique with CuBr catalyst to achieve intramolecular A^3–coupling reaction (Scheme III.5).[18]

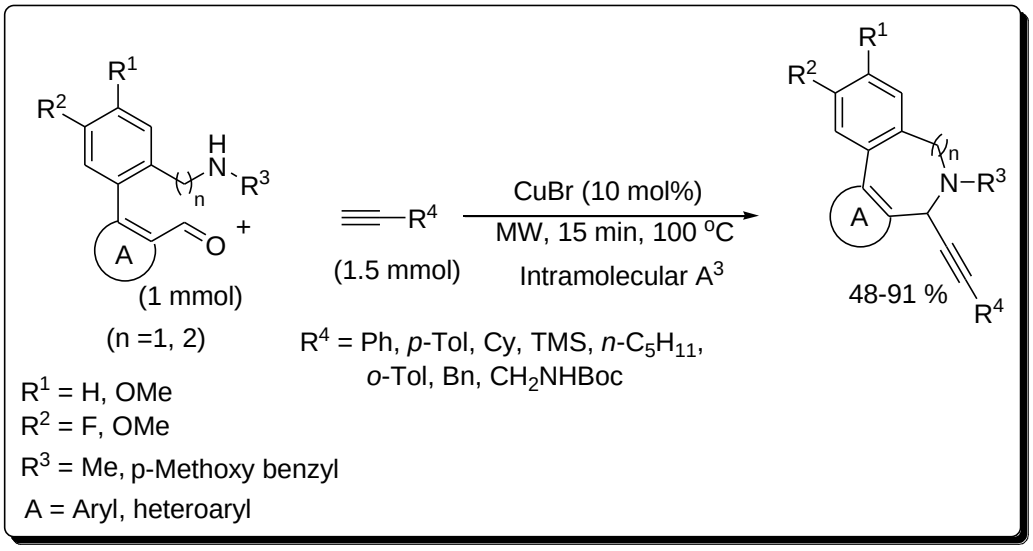

Scheme III.5. *MW–irradiated intramolecular A^3–coupling reaction*

III.2. Background and Objectives

Coordination polymers of copper halides with infinite network structures composed with organic ligands are widely reported due to the presence of their enthralling physical and chemical properties.[45] For example, Cu(I) halides–based compounds have been widely explored due to their attractive structural characteristics and possible applications in luminescence–based sensors, photophysical phenomena and biological probes.[46] They also find catalytic applications in various organic transformations.[47–51] Apparently, Cu–complexes of N– and P–based ligands are employed in catalytic applications.[48–51] Thioether based ligands are rarely synthesized and used as catalysts. Very recently, we demonstrated the synthesis of 1,3–dithioether ligands in making Cu_2I_2 coordination polymers and used as catalyst in AAC reaction.[52]

Another 1,2–dithioether and Cu(I) halides based complexes have been synthesized by Akhmetova *et al.* and its catalytic application in aminomethylation of phenylacetylene was reported (Scheme III.6).[53]

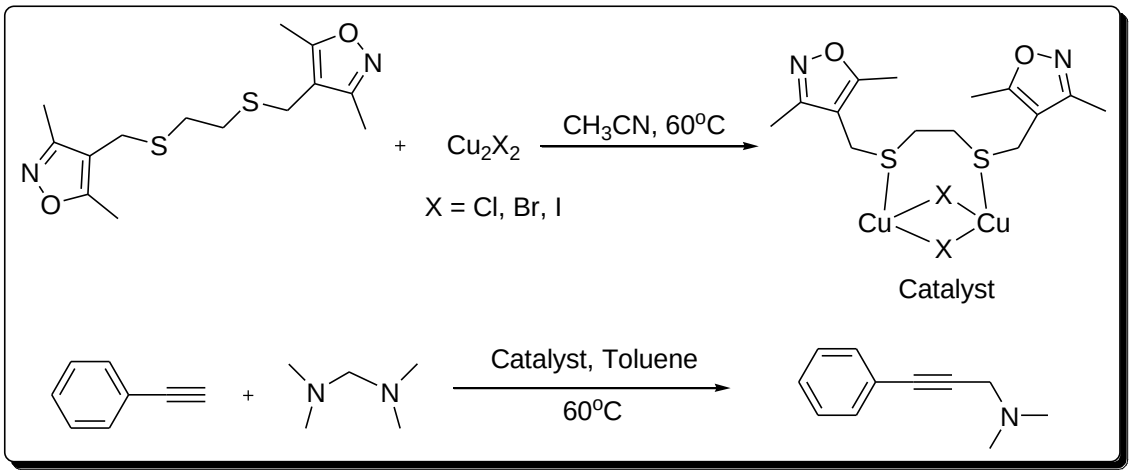

Scheme III.6. *1,2–dithioether based Cu(I) halide complex catalyzed aminomethylation of phenylacetylene*

Trivalent phosphorus ligands have been used to control the metal center, leads to metal catalysts with improved reactivity and stability. Garcia *et al.* reported a diallylphosphine–tetramer copper(I) complex catalyzed A^3–coupling reaction for preparing propargylamine (Scheme III.7).[48]

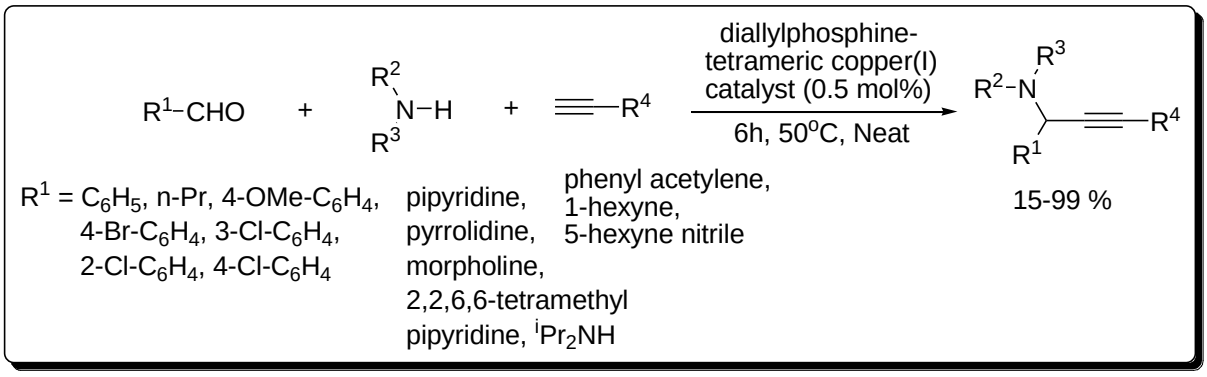

Scheme III.7. *Diallylphosphine–tetramer copper(I) complex catalyzed A^3–coupling reaction*

Apart from the phosphorous ligands, nitrogen ligated Cu(I) compounds have also been used for A^3–coupling reaction. Dong *et al.* has synthesized and characterized a heterogeneous 1D–Cu(I)–coordination polymer which possess outer–hanging copper bromide moiety and it exhibits excellent catalytic activity for A^3–coupling reaction (Scheme III.8).[49]

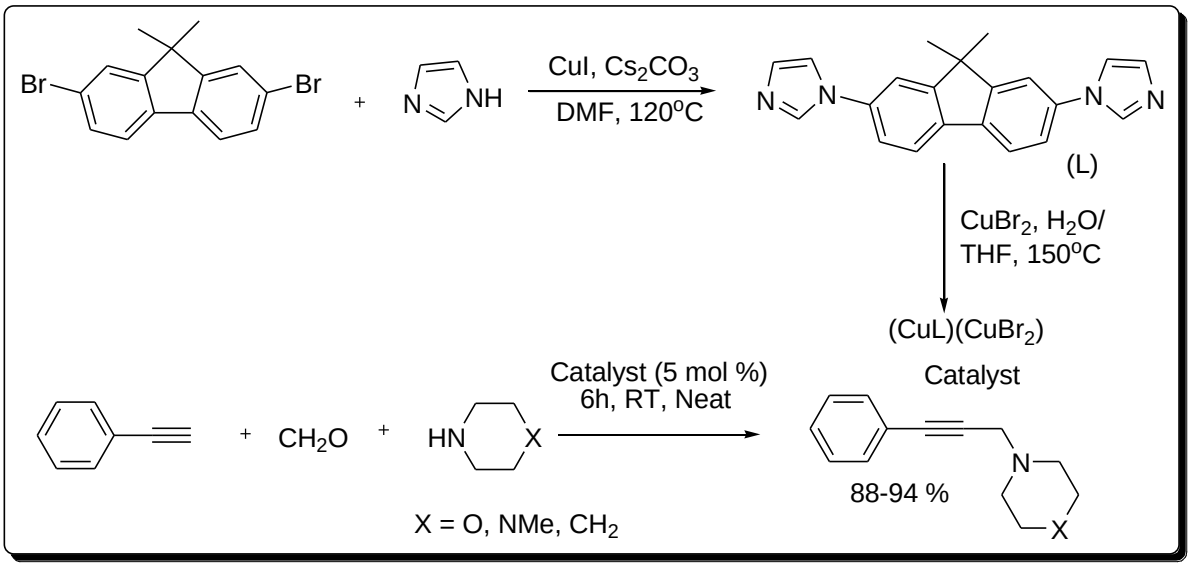

Scheme III.8. *Nitrogen ligated 1D–Cu(I)–coordination polymer catalyzed A^3–coupling reaction*

I. N. Lykakis and G. E. Kostakis has synthesized a series of benzotriazole based homogeneous and air–stable 1D–Cu(II)–coordination polymers and found its excellent catalytic activity towards the formation of various propargylamines via A^3–coupling reaction (Scheme III.9).[50]

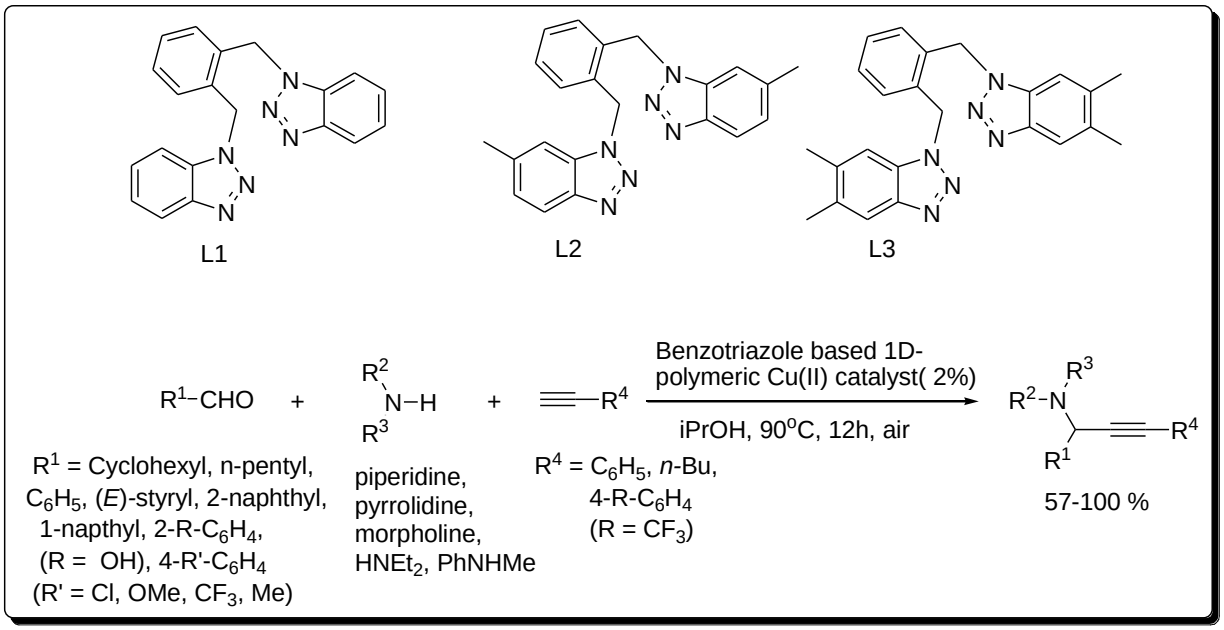

Scheme III.9. *Benzotriazole based 1D–polymeric Cu(II) catalyzed A^3–coupling*

Hong–Bin Chen *et al.* have synthesized and characterized 2–(picolyliminomethyl)pyrrole based dicopper (I) complex which possess excellent catalytic activity towards A^3–coupling reaction (Scheme III.10).[51]

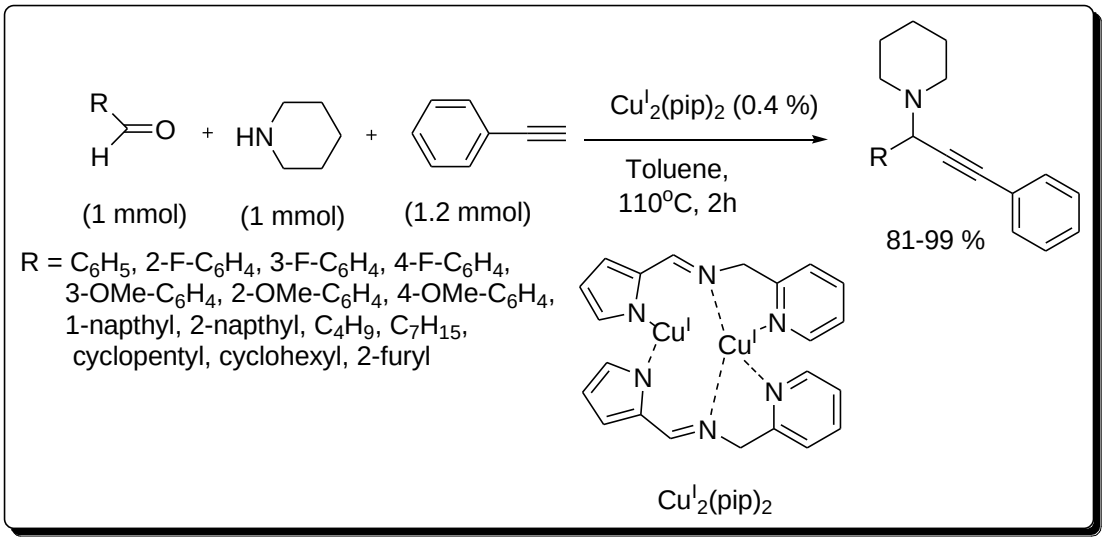

Scheme III.10. *2–(picolyliminomethyl)pyrrole based dicopper (I) complex catalyzed A^3–coupling reaction*

We have synthesized a new coordination polymer of CuI ligated with bidentate 1,2–dithioether [1–(1–(4–chlorophenylthio)propan–2–ylthio)–4–chlorobenzene] and found its excellent catalytic activity towards A^3 coupling reaction (Scheme III.11).[53] ^{1}H–NMR, ^{13}C–NMR, HRMS and single crystal X–ray diffraction (SCXRD) patterns were used to characterize the catalyst. The catalyst works efficiently in A^3–coupling reaction under solvent–free condition at 80 ^{o}C to afford propargylamines in good to excellent yields. As discussed earlier various Cu(I)/Cu(II) monomeric and/or polymeric complexes based on P– and N–ligands have been used as catalyst towards the A^3–coupling reaction. But this is the first example of Cu(I)–1,2–dithioether coordination polymer that has been synthesized and used as catalyst for the synthesis of propargylamines. It opens a new area of research where polymeric Cu(I) complex with SS–based bidentate ligands have been applied as the catalyst for the three component A^3–coupling reaction.

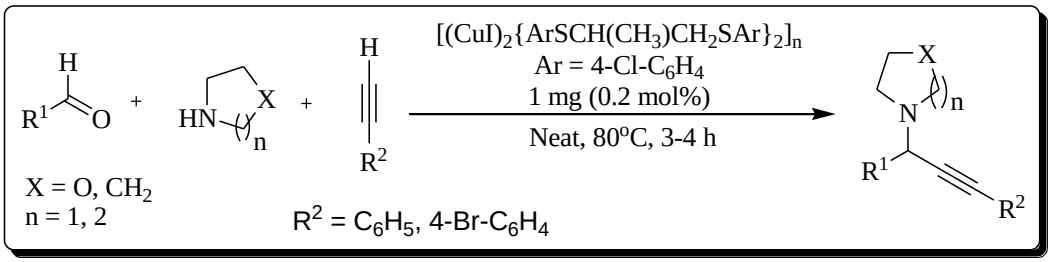

Scheme III.11. *SS–based bidentate 1,2–dithioether–Cu(I) coordination polymer catalyzed A^3–coupling*

III.3. Present work: Results and Discussion

III.3.1. Synthesis of 1–(1–(4–chlorophenylthio)propan–2–ylthio)–4–chlorobenzene ligand (L)

The ligand (L) 1–(1–(4–chlorophenylthio)propan–2–ylthio)–4–chlorobenzene was prepared by following our previously reported technique.[54] It was also characterized by ^{1}H– and ^{13}C–NMR spectroscopy. The procedure for the synthesis of the ligand has been illustrated in the experimental section.

III.3.2. Synthesis of polymeric coordination complex catalyst CuI–1–(1–(4–chlorophenylthio)propan–2–ylthio)–4–chlorobenzene

The procedure for the synthesis of the polymeric catalyst is given in the experimental section in details.

III.3.3. Characterization of complex catalyst

III.3.3.1. ^{1}H NMR, ^{13}C NMR and HRMS spectroscopy

The polymeric complex was characterized by several techniques such as ^{1}H and ^{13}C NMR, HRMS spectroscopy and single crystal XRD techniques. ^{1}H– and ^{13}C–NMR spectra of the polymeric complex and the ligand 1–(1–(4–chlorophenylthio)propan–2–ylthio)–4–chlorobenzene (L) were taken separately in d_6–DMSO solvent. Some changes were observed in ^{1}H–NMR spectra between L and the polymeric complex, which indicates the complex formation between ligand L and CuI. The ^{1}H–NMR spectra of L and the complex are given in Figure III.6 and Figure III.8. The δ values of proton and carbon in complex were shifted to downfield than the ligand (L) in ^{1}H–NMR and ^{13}C–NMR spectra, which indicates the formation of the complex. HRMS calculation also corroborates the formation of the complex catalyst.

III.3.3.2. Single crystal X–ray diffraction

Single crystal X–ray diffraction analysis revealed that the complex crystallizes in the orthorhombic Pbca space group and shows a polymeric propagation in the form of $[(CuI)_2\{ArSCH_2CH(CH_3)SAr\}_2]_n$ metallopolymer. The ORTEP diagram of the complex is given in figure III.4a.[55–57] The 2D–network is built up upon dimeric Cu_2I_2 units which are interconnected via dithioether ligands. Within the cluster core, the Cu–I bond lengths range between 2.6119(4) and 2.6182(4) Å. The interatomic distance between two Cu within the Cu_2I_2 cluster is 2.8979(8) Å, significantly larger than the sum of the vander Waals radius (2.80 Å).[58] The mean Cu–S bond length [range between 2.3539(7) to 2.3990(7) Å] of the as-synthesized Cu–complex is a little excess to $[\{Cu(\mu\text{–}I)_2Cu\}_2\{\mu\text{–}PhS(CH_2)_3SPh\}_2]_n$ (2.3465 Å) and $([(CuI)_2\{ArS(CH_2)_3SAr\}_2]_n$, Ar = 4–F–$C_6H_4$); range between 2.3339 (11) to 2.3551 (12) Å).[52,55] The angle between Cu…I…Cu is 67.296(15) Å and I…Cu…I is 112.705(15) Å in the metallocluster. The polymeric framework of the complex is formed by the connection of Cu_2I_2 unit and four 1,2–dithioether linker **L**. Each 1,2–dithioether coordinates via its S–donor atoms to two Cu_2I_2 units, while each Cu_2I_2 unit connects with four 1,2–dithioether ligands (**L**). This gives rise to a 2D–shaped network matrix topology (Fig. III.4b).

Table III.1. Crystal Data, Data Collection and Structure Refinement for the complex catalyst

Formula	$C_{15}H_{14}Cl_2Cu\ I\ S_2$	Cell volume/Å3	3661.7(4)
Formula weight	519.73	Cell formula units Z	8
Temperature/K	296 (2)	density (calculated) g/cm^3	1.886
Description	block	θ range for data collection/deg	2.42- 27.48
Colour	White	F(000)	2016
Crystal system	orthorhombic	crystal size/mm	0.216, 0.284, 0.320
Space group	Pbca	Absorption co-efficient (μ)	3.389
a/Å	10.0087(5)	index ranges	$-12 \le h \le 13$ $-20 \le k \le 20$ $-30 \le l \le 30$

b/Å	15.4384(10)	reflections collected	62648
c/Å	23.6978(14)	independent reflections	4182
Cell angle (α)	90^{o}	refinement method	full-matrix least-squares on F^2
Cell angle (β)	90 ^{o}	R-equivalents	0.0285
Cell angle (γ)	90 ^{o}	Sigma I/net I	0.0119

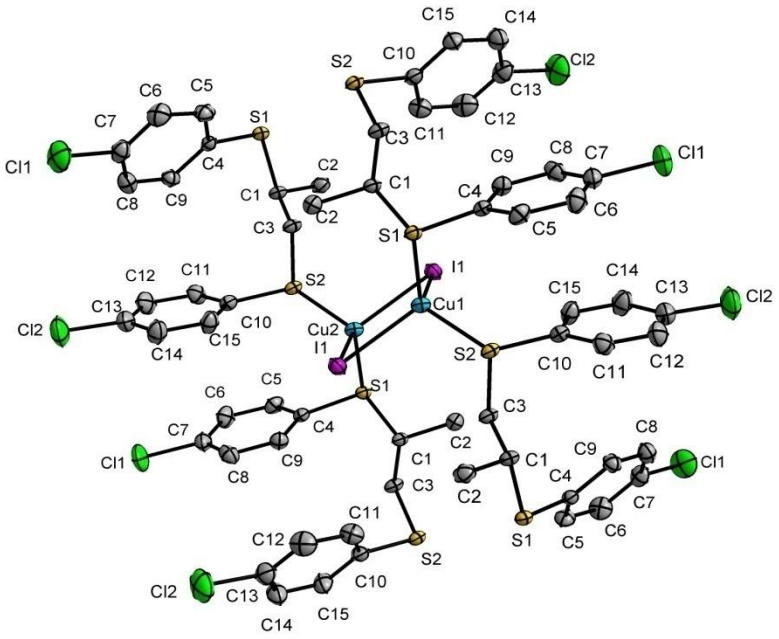

(a)

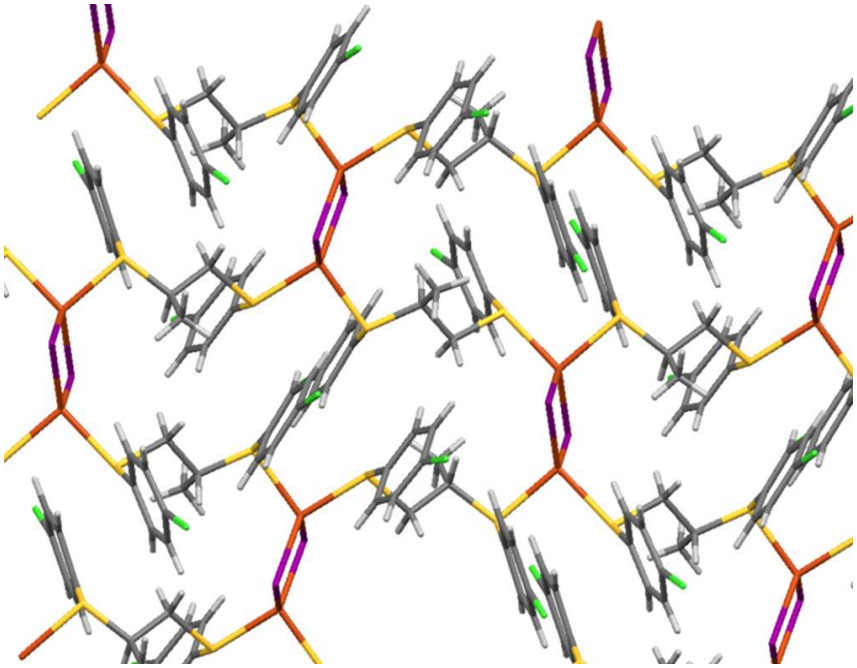

(b)

Fig. III.4. *a) ORTEP diagram of the ($[(CuI)_2\{ArSCH_2CH(CH_3)SAr\}_2]_n$, Ar = 4–Cl–$C_6H_4$) complex, b) Part of the two–dimensional framework of complex*

Selected bond lengths and bond angles are also given in the Tables below.

Table III.2. Selected bond length

Bond	Length	Bond	Length
I3 Cu1	2.6119(4)	C9 H9	0.9300
I3 Cu1	2.6182(4)	C10 C15	1.385(4)
Cu1 S2	2.3539(7)	C10 C11	1.389(4)
Cu1 S1	2.3990(7)	C5 C6	1.381(5)
Cu1 I3	2.6182(4)	C5 H5	0.9300
Cu1 Cu1	2.8979(8)	C2 H2A	0.9600
S1 C4	1.779(2)	C2 H2B	0.9600
S1 C1	1.828(2)	C2 H2C	0.9600
S1 Cu1	2.3990(7)	C11 C12	1.387(5)
S2 C10	1.787(3)	C11 H11	0.9300
S2 C3	1.829(2)	C8 C7	1.385(5)

Cl1 C7	1.749(3)	C8 H8	0.9300
Cl2 C13	1.734(3)	C15 C14	1.376(5)
C4 C5	1.396(4)	C15 H15	0.9300
C4 C9	1.398(4)	C7 C6	1.377(6)
C3 C1	1.518(3)	C6 H6	0.9300
C3 H3A	0.9700	C13 C14	1.364(5)
C3 H3B	0.9700	C13 C12	1.380(6)
C1 C2	1.534(4)	C14 H14	0.9300
C1 H1	0.9800	C12 H12	0.9300
C9 C8	1.368(4)		

Table III.3. Selected bond angle

Bond	**Angle**	**Bond**	**Angle**
Cu1 I3 Cu1	67.296(15)	C15 C10 S2	120.4(2)
S2 Cu1 S1	96.07(2)	C11 C10 S2	119.1(2)
S2 Cu1 I3	123.28(2)	C6 C5 C4	120.5(3)
S1 Cu1 I3	110.344(19)	C6 C5 H5	119.8
S2 Cu1 I3	102.56(2)	C4 C5 H5	119.8
S1 Cu1 I3	110.42(2)	C1 C2 H2A	109.5
I3 Cu1 I3	112.705(15)	C1 C2 H2B	109.5
S2 Cu1 Cu1	133.71(2)	H2A C2 H2B	109.5
S1 Cu1 Cu1	128.94(2)	C1 C2 H2C	109.5
I3 Cu1 Cu1	56.455(13)	H2A C2 H2C	109.5
I3 Cu1 Cu1	56.249(11)	H2B C2 H2C	109.5
C4 S1 C1	104.44(11)	C12 C11 C10	119.5(3)
C4 S1 Cu1	99.81(8)	C12 C11 H11	120.3
C1 S1 Cu1	104.84(8)	C10 C11 H11	120.3
C10 S2 C3	99.43(12)	C9 C8 C7	119.4(3)
C10 S2 Cu1	117.54(9)	C9 C8 H8	120.3
C3 S2 Cu1	106.10(8)	C7 C8 H8	120.3

C5 C4 C9	119.5(2)	C10 C15 C14	119.1(3)
C5 C4 S1	117.8(2)	C10 C15 H15	120.4
C9 C4 S1	122.6(2)	C14 C15 H15	120.4
C1 C3 S2	111.33(16)	C6 C7 C8	122.0(3)
C1 C3 H3A	109.4	C6 C7 Cl1	120.4(3)
S2 C3 H3A	109.4	C8 C7 Cl1	117.5(3)
C1 C3 H3B	109.4	C7 C6 C5	118.5(3)
S2 C3 H3B	109.4	C7 C6 H6	120.8
H3A C3 H3B	108.0	C5 C6 H6	120.8
C3 C1 C2	111.9(2)	C14 C13 C12	120.9(3)
C3 C1 S1	110.36(16)	C14 C13 Cl2	119.3(3)
C2 C1 S1	106.14(17)	C12 C13 Cl2	119.8(3)
C3 C1 H1	109.4	C13 C14 C15	120.6(3)
C2 C1 H1	109.4	C13 C14 H14	119.7
S1 C1 H1	109.4	C15 C14 H14	119.7
C8 C9 C4	120.0(3)	C11 C12 C13	119.3(3)
C8 C9 H9	120.0	C11 C12 H12	120.3
C4 C9 H9	120.0	C13 C12 H12	120.3
C15 C10 C11	120.4(3)		

III.3.4. Catalytic application

The catalytic activity of the complex towards A^3–coupling reaction was optimized by the model reaction of phenyl acetylene, benzaldehyde and morpholine with varying catalyst loading under different temperature and solvent conditions (Table III.4). Initially, the reaction of phenylacetylene (1.1 mmol), benzaldehyde (1.0 mmol) and morpholine (1.0 mmol) was performed in acetonitrile at 60 °C for 8 hours using 5 mg of the complex as catalyst. A trace amount of conversion was achieved (entry 1). Raising the temperature of the medium from 60^o to 80 ^{o}C gave 40% yield of the product (entry 2). Under the polar hydroxylic solvents e.g. ethanol and water, the yield of the product was found to be 50% (entry 3 and 4) in both cases. Under the same condition in binary solvent mixture (Acetonitrile:water=1:1) the conversion was increased to 65% (entry 5). When the reaction was studied at neat condition, the yield of

the product was drastically increased to 91% (entry 6). Decreasing the amount of the catalyst from 3.0 to 1.0 mg did not affect on the overall yield of the product (90% yield in both cases; entries 7 and 8). Now, we have reduced the reaction time from 8 to 6 hours, 88% product was found with 1.0 mg of the catalyst (entry 9). Further reducing the reaction time from 6 to 4 hours, the yield was found to be the same as entry 9 (entry 10). Reaction performed without any catalyst, no conversion was achieved after 24 hours (entry 11). The same reaction carried out under room temperature showed traces of product after 24 hours with 1.0 mg of the catalyst (entry 12). While using CuI as the catalyst, the product was obtained in relatively lower yield, 69% (entry 13).

Table III.4. Optimization of reaction conditions for the 2D–Cu(I)–polymeric complex catalyzed A^3–coupling reaction

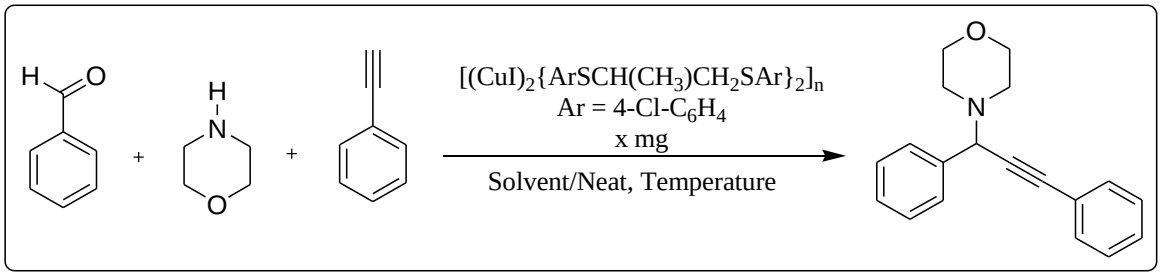

Entry	Solvent	Cu-catalyst (mg)	Temp. (^oC)	Time (h)	Yield[a] (%)
1	Acetonitrile	5	60	8	Traces
2	Acetonitrile	5	80	8	40
3	Ethanol	5	80	8	50
4	Water	5	80	8	50
5	Acetonitrile: water	5	80	8	65
6	Neat	5	80	8	91
7	Neat	3	80	8	90
8	Neat	1	80	8	90
9	Neat	1	80	6	88
10	**Neat**	**1**	**80**	**4**	**88**
11	Neat	-	80	24	No reaction
12	Neat	1	RT	24	Traces

13[b]	Neat	1	80	4	69

Reaction conditions: Phenyl acetylene (1.1 mmol), Benzaldehyde (1.0 mmol) and Morpholine (1.0 mmol), Cu–complex (5 mg to 1 mg), Neat. [a]Isolated yield after purification through column chromatography by silica gel. [b]CuI was used as catalyst.

In order to explore the generality of the optimized reaction conditions, different types of substrates such as secondary amines with different types of aldehydes were reacted with terminal acetylenes. Very good to excellent isolated yields of the products have been achieved under this protocol (Table III.5). In table III.5, it has been clearly evident that various aldehydes including electron releasing or withdrawing groups such as OMe, OH, Br, Cl as well as benzaldehyde were reacted smoothly with terminal alkynes (phenyl acetylene and 4–bromophenyl acetylene) and cyclic secondary amines (morpholine, piperidine and pyrrolidine). Furthermore reaction of alicyclic aldehyde (cyclohexane carboxaldehyde) and straight–chain aliphatic aldehyde (*n*–heptanal) with morpholine and phenylacetylene were performed efficiently and afforded desired products in brilliant yields (entries 9 and 10).

Table III.5. Catalytic activities of the 2D–Cu(I)–polymeric complex catalyzed A^3–coupling reaction

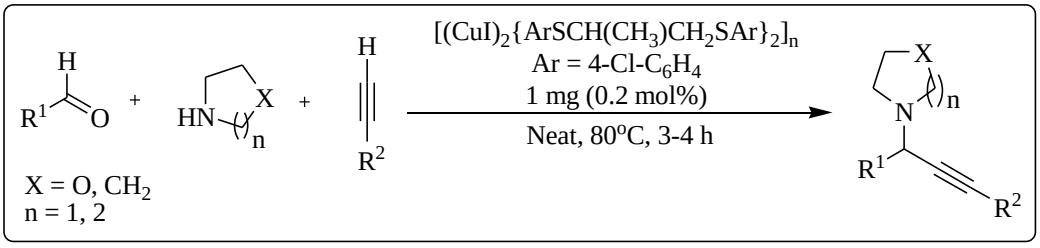

Entry	Aldehyde (1 mmol)	2° Amine (1 mmol)	Alkyne (1.1 mmol)	Time (h)	A^3 Product (Propargylamine)	Yield[a] (%)
1	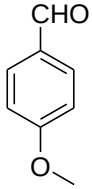	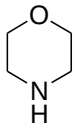	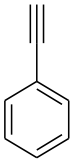	4	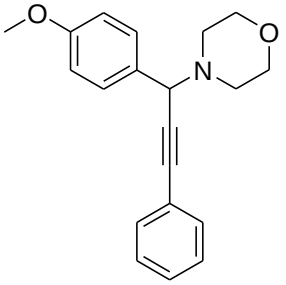	87

2	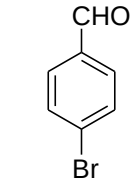	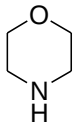	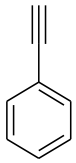	4	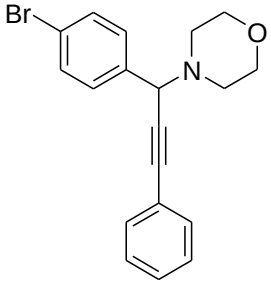	92
3	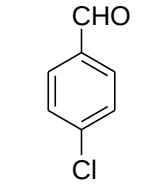	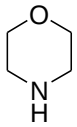	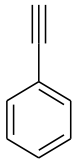	4	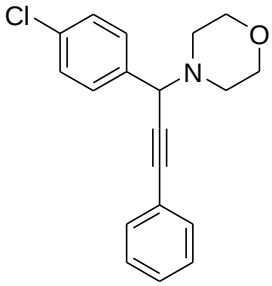	96
4	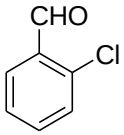	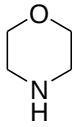	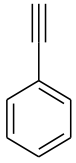	4	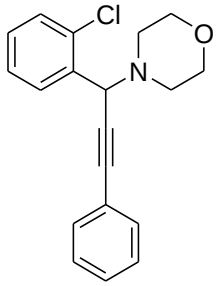	88
5	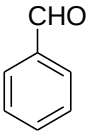	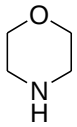	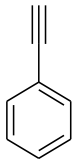	4	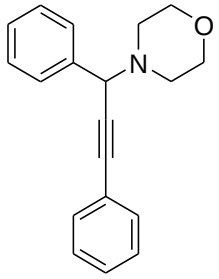	88
6	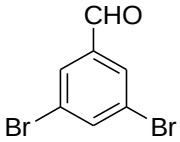	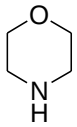	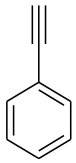	4	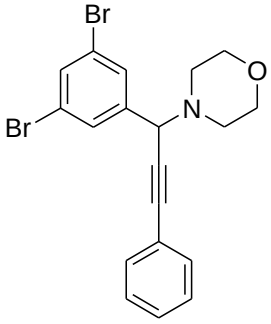	95

7	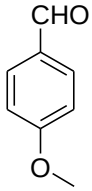	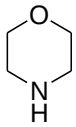	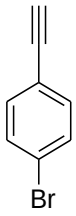	4	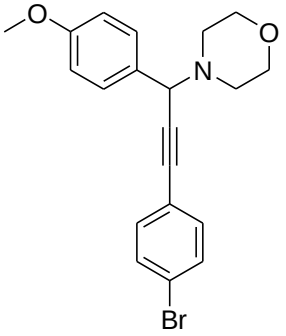	92
8	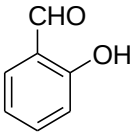	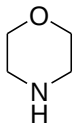	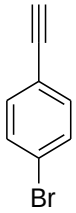	3	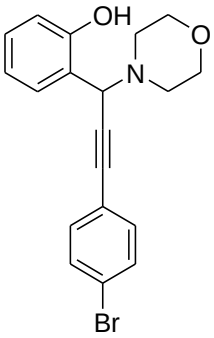	85
9	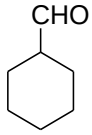	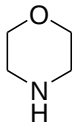	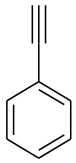	3.5	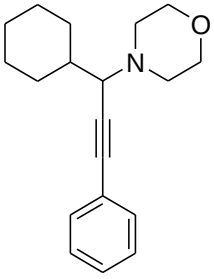	91
10	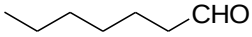	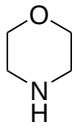	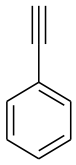	3.5	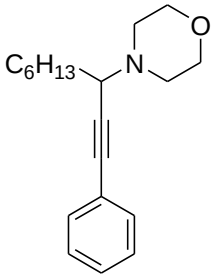	86
11	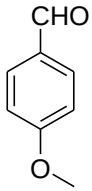	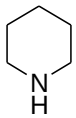	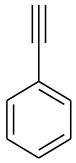	4	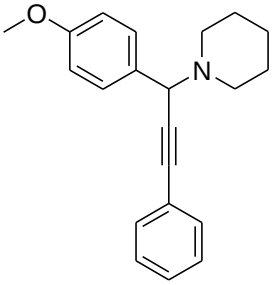	93

12	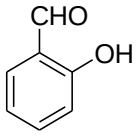	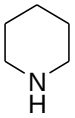	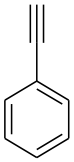	3	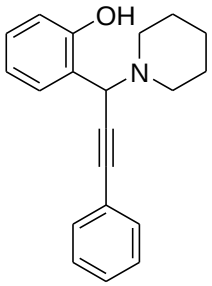	90
13	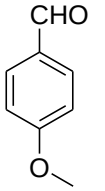	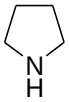	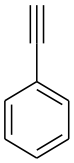	4	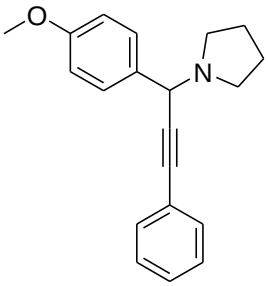	82
14	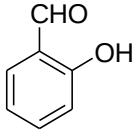	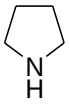	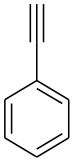	3	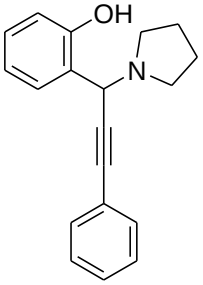	92
15	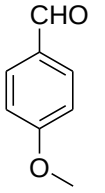	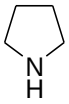	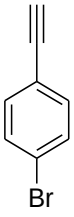	4	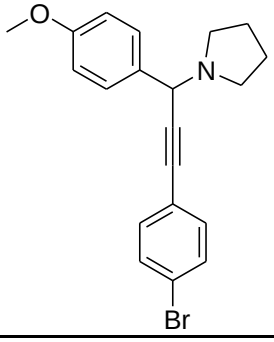	91

Reaction conditions: Phenyl acetylene/4–bromo phenyl acetylene (1.1 mmol), Aldehyde (1.0 mmol) and Morpholine/Piperidine/ Pyrrolidine (1.0 mmol), Cu–complex (1 mg, 0.2 mol%) in neat condition.

[a] *Isolated yield after purification through column chromatography by silica gel.*

III.3.5. Mechanism

Since A^3–coupling reaction is well known, the most suitable mechanism for A^3–coupling reaction has been proposed in Scheme III.12. The Cu(I) species present in the coordination polymer plays the vital role in the mechanism. The reaction proceeds *via* the activation of the C_{sp}–H bond of the terminal alkyne by the 2D–polymeric CuI–1,2–dithioether complex which forms alkynyl–Cu intermediate (copper acetylide). The copper acetylide then reacts with the

iminium ion generated *in situ* from the reaction of aldehyde and secondary amine to produce the corresponding propargylamine product under solvent–free condition. In this step finally the 2D–polymeric CuI–1,2–dithioether complex catalyst is eliminated to further act as catalyst.

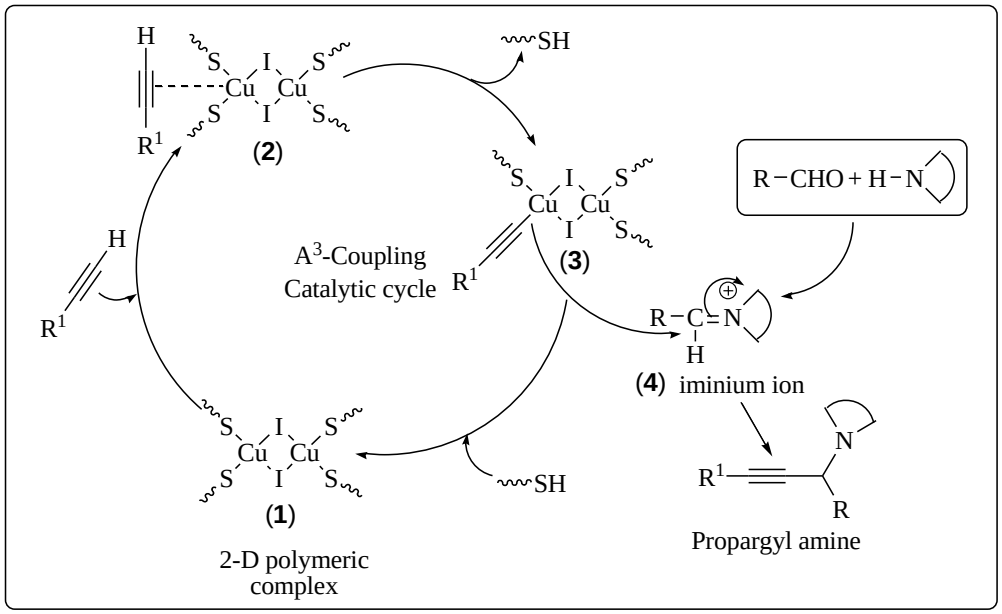

Scheme III.12. *A plausible mechanism for the Cu(I)–complex catalyzed A^3–coupling reaction.*

III.4. Conclusion

In conclusion, we have demonstrated synthesis, characterization of a new 2D–Cu(I) coordination polymer of 1,2–dithioether ligands (SS, bidentate) and its successful catalytic applications in A^3–coupling reaction to form various propargylamine derivatives under solvent–free condition. Although Cu(I) complexes with various P– and N–based mono or bidentate ligands are known to act as the catalysts for A^3–coupling reaction, this is the first example of SS, bidentate ligand–Cu(I) coordination polymer as the catalyst in A^3–coupling reaction. As the reaction is carried out in solvent–free condition and high yield of the propargylamines were obtained under low catalytic concentrations, we believe that the present work opens up further development of Cu(I)–thio 2D–complexes in diverse reactions.

III.5. Experimental section

III.5.1.1. General Information

All the reagents required for synthesis were commercially available and employed without further purification or purified by standard methods prior to use. Phenylacetylene, cyclohexane carboxaldehyde and *p*–bromophenylacetylene were purchased from Sigma–Aldrich and used without further purification. Benzaldehyde and salicylaldehyde were purchased from Merck and used directly as obtained. The rest aldehydes were purchased from SD Fine Chemical Limited, India. 2^o amines such as piperidine, morpholine and pyrrolidine were purchased from Lancaster and used as reagent for A^3–coupling after distillation. The solvents were purchased from Thomas Baker (Chemicals) Pvt. Ltd., India and served the purpose after distillation process. All the products were purified by column chromatography on 60–120 mesh silica gels (SRL, India). For TLC, Merck plates coated with silica gel 60, F_{254} were used. The reagents and the catalyst were weighed accurately by Mettler–Toledo digital balance. Single–crystal diffraction studies were carried out on a Bruker D8 Quest CMOS diffractometer with Mo Kα (λ=0.71073 Å). FT–IR spectra were recorded with a FT–IR–8300 SHIMADZU spectrophotometer using a KBr pellet for solid compounds and neat for semi–solid or liquid compounds. The ^{1}H– & ^{13}C–NMR spectra were recorded at 300 MHz and 75 MHz respectively on Bruker AV 300 spectrometer in $CDCl_3$. Splitting patterns of protons were described as s (singlet), d (doublet), t (triplet), bs (broad singlet), dd (doublet of doublet) and m (multiplet). Chemical shifts (δ) were reported in parts per million (ppm) relative to TMS as internal standard. *J* values (coupling constant) were reported in Hz (Hertz). ^{13}C–NMR spectra were recorded with complete proton decoupling ($CDCl_3$: δ 77.0 ppm). HRMS was performed by Micromass Q–TOF Spectrometer under ESI (positive mode) at Indian Association for the Cultivation of Science.

III.5.1.2. Crystal structure determination of the 1–(1–(4–chlorophenylthio)propan–2–ylthio)–4–chlorobenzene ligated CuI–coordination complex

Suitable crystals of the compounds were obtained by slow evaporation of their saturated solutions in acetonitrile solvent and using the diffusion method. Single–crystal diffraction studies were carried out on Bruker D8 Quest CMOS diffractometer with Mo Kα (λ=0.71073 Å). The data frames were obtained using the program APEX3 and processed using the program SAINT routine in APEX3. The structures were solved by direct methods and refined by the full–matrix least–squares on F^2 using the SHELXTL–2014/7 program.[59–61] All hydrogen atoms were included at the idealized positions, and a riding model was used.

III.5.2. General procedure (GP1) of preparing 1–(1–(4–chlorophenylthio)propan–2–ylthio)–4–chlorobenzene (L)

A mixture of 2.0 mmol of allyl bromide (240 mg) and 5.0 mmol of 4–chlorobenzenethiol (722.5 mg) was mixed with pre–calcined dry activated silica gel with mesh size 60–120 (1.0 g) and stirred magnetically by using a spin magnetic bar for 16 h. The reaction was monitored by tlc. The product was purified by column chromatography after completion of the reaction. The product was eluted with light petroleum and we got the 1–(1–(4–chlorophenylthio)propan–2–ylthio)–4–chlorobenzene ligand (L). It was characterized by ^{1}H– and ^{13}C–NMR and compared with literature data.[54]

III.5.3. General procedure (GP2) of preparing 1–(1–(4–chlorophenylthio)propan–2–ylthio)–4–chlorobenzene (L) ligated CuI–coordination complex (1)

The ligand L, 1–(1–(4–chlorophenylthio)propan–2–ylthio)–4–chlorobenzene was synthesized according to our reported procedure.[54] The 1,2–dithioether based 2D–copper(I) co–ordination polymer, **(1)** was synthesized according to the following procedure. **L** (329 mg, 1.0 mmol), CuI (95 mg, 0.5 mmol) and acetonitrile (2 mL) were mixed in a 50 mL round bottomed flask. The mixture was stirred at room temperature for 4 hours followed by stirring under refluxing condition for 24 hours. The reaction mixture was kept at room temperature. Then distilled petroleum ether was added drop wise to the reaction mixture and kept it into refrigerator. A shining white crystal was found in reaction vessel and it was separated by simple filtration. The yield of the complex was found to be 74%. Finally, the crystals were dried under vacuum for several hours.

III.5.4. General procedure (GP3) for A^3–coupling reaction

A mixture of aldehyde (1.0 mmol), secondary amine (1.0 mmol) and terminal acetylene (1.1 mmol) was magnetically stirred at 80 °C in an open reaction vessel for hours as mentioned in Table III.5. The progress of the reaction was monitored by TLC. After completion of the reaction (disappearance of the alkyne spot on TLC), the reaction mixture was cooled to room temperature. 5 mL of methylene chloride was added to the reaction mixture and was adsorbed on column silica gel. After the evaporation of the solvent, the resulting dry mass was placed on a silica gel column and eluted with light petroleum–ethyl acetate (in varying proportion) which afforded the desired propargylamine.

III.5.5. Characterization data of the ligand (L) and the 2D–polymeric complex

NMR spectra of ligand 1–(1–(4–chlorophenylthio)propan–2–ylthio)–4–chlorobenzene (L)[54]

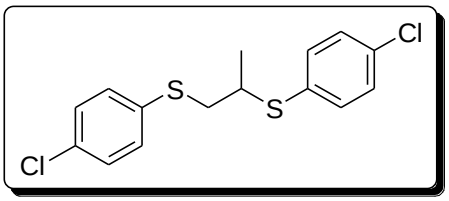

^{1}H NMR (d_6–DMSO, 300 MHz): δ 1.19 (d, J = 6.6 Hz, 3H, CH_3), 2.83–2.90 (m, 1H, CH), 3.02–3.27 (m, 2H, CH_2), 7.09–7.22 (m, 8H, ArH); **^{13}C NMR (d_6–DMSO, 75 MHz):** δ 19.8, 40.9, 42.7, 129.4, 129.5, 130.9, 131.4, 132.7, 133.3, 133.7, 135.2.

^{1}H NMR, ^{13}C NMR and HRMS spectral data of the copper 2D–polymeric complex[62]

^{1}H NMR (d_6–DMSO, 300 MHz): δ 1.21 (d, J = 6.6 Hz, 3H), 2.96–2.99 (m, 1H), 3.04–3.06 (m, 2H), 7.17–7.28 (m, 8H, ArH). **^{13}C NMR (d_6–DMSO, 75 MHz):** δ 20.0, 41.5, 43.0, 129.4, 129.5, 131.3, 131.5, 132.7, 133.4, 133.9, 135.3.

HRMS: m/z $[(C_{15}H_{14}Cl_2S_2)_2Cu - I^-]^+$ calcd for $C_{15}H_{14}CuCl_2IS_2$, 718.9124; found, 719.0043.

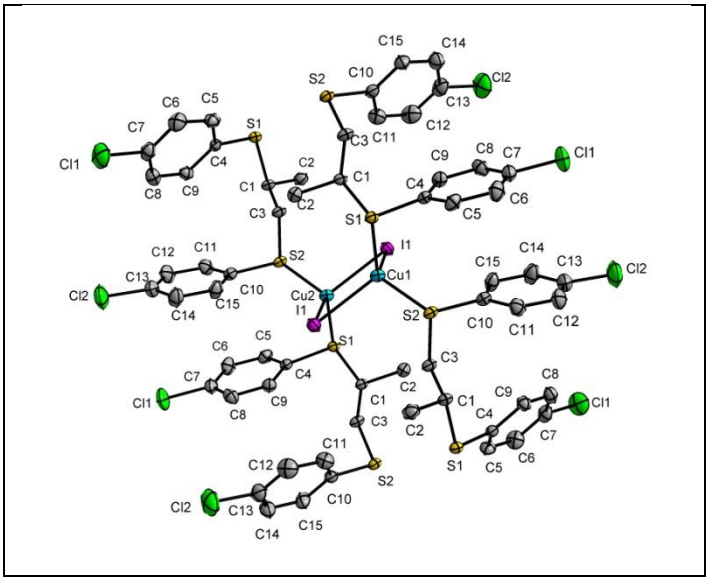

III.5.6. Physical properties and spectroscopic data of various propargyl amine products

4–(1– (4–methoxyphenyl) –3–phenylprop–2–ynyl)morpholine (Table III.5, entry 1)[63]

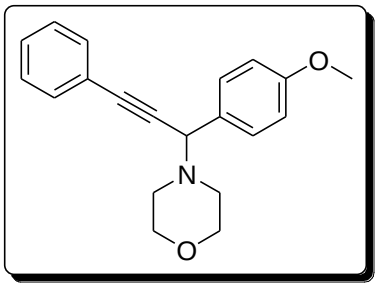

This compound was obtained by following the general procedure **GP3** in 87% yield as a sticky yellow solid. The NMR data obtained are in quite agreement with that reported in the literature previously.[63] **^{1}H NMR ($CDCl_3$, 300 MHz)** δ 2.60 (m, 4H), 3.74 (m, 4H), 3.87 (s, 3H), 4.72 (s, 1H), 6.88–6.98(m, 2H), 7.24–7.33 (m, 3H), 7.41–7.54 (m, 4H); **^{13}C NMR ($CDCl_3$, 75 MHz)** δ 49.8, 55.3, 61.4, 67.2, 85.4, 88.2, 113.6, 123.0, 128.2, 128.3, 129.7, 129.9, 131.8, 159.2; **FT−IR (KBr)** ν_{max} 3055, 2952, 2841, 2022, 1605, 1509, 1487, 1450, 1317, 1244, 1170, 1152, 1034, 1000, 849, 783, 691, 562 cm^{-1}.

4–(1–(4–bromophenyl)–3–phenylprop–2–ynyl)morpholine (Table III.5, entry 2)[63]

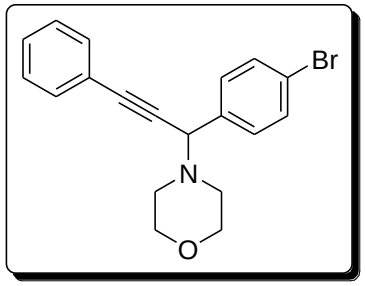

It was obtained by following the general procedure **GP3** in 92% yield as a sticky yellow solid. The NMR data obtained are in quite agreement with that reported in the literature previously.[63] **^{1}H NMR ($CDCl_3$, 300 MHz)** δ 2.60 (t, J = 3.9 Hz, 4H), 3.70–3.76 (m, 4H), 4.72 (s, 1H), 7.31–7.33 (m, 3H), 7.46–7.53 (m, 6H); **^{13}C NMR ($CDCl_3$, 75 MHz)** δ 49.8, 61.4, 67.1, 84.3, 88.9, 121.7, 122.7, 128.3, 128.4, 130.3, 131.3, 131.8, 137.0; **FT−IR (KBr)** ν_{max} 3047, 2841, 2000, 1590, 1483, 1447, 1395, 1317, 1284, 1115, 1067, 967, 849, 812, 753, 687, 562 cm^{-1}.

4–(1–(4–chlorophenyl)–3–phenylprop–2–ynyl)morpholine (Table III.5, entry 3)[63]

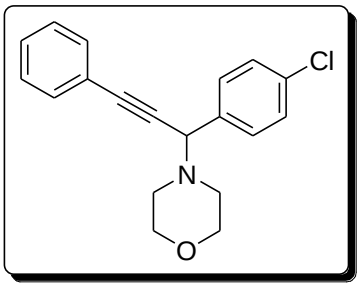

This compound was synthesized by following the general procedure **GP3** in 96% yield as a sticky solid. The NMR data obtained are quite similar with that reported in the literature.[63] **^{1}H NMR ($CDCl_3$, 300 MHz)** δ 2.60 (m, 4H), 3.71–3.72 (m, 4H), 4.74 (s, 1H), 7.32–7.34 (m, 5H), 7.50–7.58 (m, 4H); **^{13}C NMR ($CDCl_3$, 75 MHz)** δ 49.8, 61.4, 67.1, 84.4, 88.9, 122.7, 128.4, 128.5, 129.9, 131.8, 133.6, 136.5; **FT−IR (KBr)** ν_{max} 3040, 2929, 2856, 2000, 1594, 1483, 1443, 1395, 1314, 1284, 1107, 1070, 967, 859, 846, 757, 687, 517 cm^{-1}.

4–(1–(2–chlorophenyl)–3–phenylprop–2–ynyl)morpholine (Table III.5, entry 4)[63]

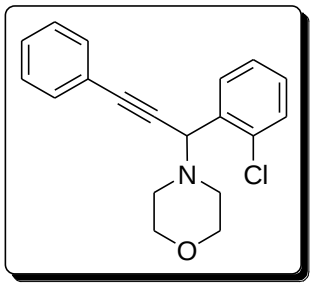

This compound was obtained by following the general procedure **GP3** in 88% yield as a sticky solid. The NMR data obtained are in quite agreement with that reported in the literature previously.[63] **^{1}H NMR ($CDCl_3$, 300 MHz)** δ 1.79–2.0 2 (m, 4H), 2.842 (m, 4H), 4.24 (s, 1H), 6.38–6.53 (m, 5H), 6.61–6.88 (m, 4H); **^{13}C NMR ($CDCl_3$, 75 MHz)** δ 49.2, 58.2, 66.4, 84.0, 87.7, 122.1, 125.7, 127.7, 128.4, 129.2, 131.1, 133.9, 134.8; **FT−IR (KBr)** ν_{max} 3055, 2922, 2811, 1594, 1568, 1487, 1465, 1314, 1270, 1240, 1111, 1067, 1052, 975, 927, 864, 746, 705, 687, 562, 525 cm^{-1}.

4–(1,3–diphenylprop–2–ynyl)morpholine (Table III.5, entry 5)[63]

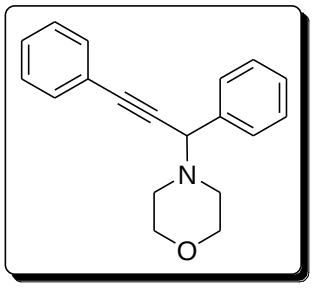

This very compound was synthesized with the general procedure **GP3** as a sticky solid and the yield obtained was 88%. The NMR data obtained are in quite agreement with that reported in the literature previously.[63] **^{1}H NMR ($CDCl_3$, 300 MHz)** δ 2.21–2.62 (m, 4H), 3.70 (m, 4H), 4.77 (s, 1H), 7.31–7.37 (m, 6H), 7.50–7.63 (m, 4H); **^{13}C NMR ($CDCl_3$, 75 MHz)** δ 49.9, 62.0, 67.1, 66.4, 85.1, 88.5, 123.0, 127.6, 128.3, 128.4, 128.6, 131.8, 137.0; **FT−IR (KBr)** ν_{max} 3055, 2952, 2819, 1598, 1487, 1447, 1388, 1317, 1272, 1115, 1070, 1000, 860, 753, 694, 562 cm^{-1}.

4–(1–(3,5–dibromophenyl)–3–phenylprop–2–ynyl)morpholine (Table III.5, entry 6)

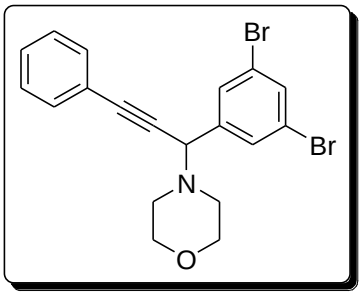

This compound was obtained by following the general procedure **GP3** in 95% yield as a deep brown solid. The compound was synthesized first with the procedure and the HRMS data obtained corroborates the calculated value. **^{1}H NMR ($CDCl_3$, 300 MHz)** δ 2.26–2.70 (m, 4H), 3.62 (m, 4H), 4.60 (s, 1H), 7.22–7.23 (m, 5H), 7.40–7.63 (m, 3H); **^{13}C NMR ($CDCl_3$, 75 MHz)** δ 49.8, 61.0, 67.0, 83.2, 89.7, 122.4, 122.9, 128.5, 128.7, 130.3, 131.9, 133.5, 142.2; **FT−IR (KBr)** ν_{max} 3055, 2937, 2848, 1583, 1550, 1454, 1410, 1316, 1295, 1244, 1185, 1107, 1067, 1000, 875, 846, 757, 687, 525 cm^{-1}; **HRMS** m/z $[M + H]^+$ calcd for $C_{19}H_{17}Br_2NO$, 433.9677; found, 433.9759.

4–(3–(4–bromophenyl)–1–(4–methoxyphenyl)prop–2–ynyl) morpholine (Table III.5, entry 7)

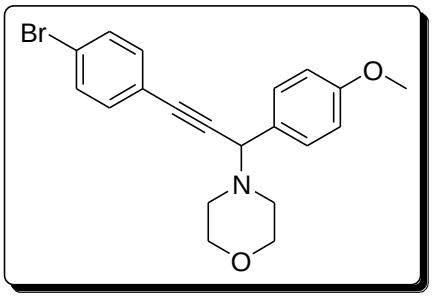

This compound was obtained by following the general procedure **GP3** in 92% yield as a deep yellow sticky solid. As the compound was first synthesized by this procedure, the HRMS was checked. The HRMS data obtained are in quite agreement with the calculated value. **^{1}H NMR ($CDCl_3$, 300 MHz)** δ 2.37–2.60 (m, 4H), 3.49–3.80 (m, 7H), 4.70 (s, 1H), 6.87–6.90 (m, 2H), 7.09–7.25 (m, 2H), 7.33–7.77 (m, 4H); **^{13}C NMR ($CDCl_3$, 75 MHz)** δ 49.8, 55.3, 61.5, 67.1, 86.7, 87.2, 113.6, 121.9, 122.4, 129.6, 129.7, 131.6, 133.3, 159.3; **FT−IR (KBr)** ν_{max} 3065, 2959, 2855, 1609, 1589, 1483, 1291, 1248, 1166, 1111, 1069, 1037, 997, 928, 846, 685, 605, 570, 545, 518 cm^{-1}; **HRMS** m/z $[M + K]^+$ calcd for $C_{20}H_{20}BrNO_2$, 424.0314; found, 424.0433.

2–(3–(4–bromophenyl)–1–morpholinoprop–2–ynyl)phenol (Table III.5, entry 8)[64]

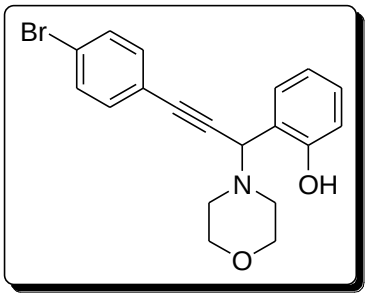

This compound was obtained by following the general procedure **GP3** in 85% yield as a yellow sticky solid. The NMR data obtained are in quite agreement with that reported in the literature previously.[64] **^{1}H NMR ($CDCl_3$, 300 MHz)** δ 2.74 (s, 4H), 3.77 (s, 4H), 5.05 (s, 1H), 6.87–6.91 (m, 2H), 7.21–7.27 (m, 1H), 7.37–7.54 (m, 5H), 10.69 (s, 1H, br, OH); **^{13}C NMR ($CDCl_3$, 75 MHz)** δ 48.7, 60.4, 66.5, 82.8, 89.0, 116.4, 119.2, 120.0, 120.9, 122.8, 128.4, 129.6, 131.5, 133.0, 156.7; **FT−IR (KBr)** ν_{max} 3408, 2842, 2364, 1584, 1471, 1270, 1115, 1073, 999, 844, 746, 584 cm^{-1}

4–(1–cyclohexyl–3–phenylprop–2–ynyl)morpholine (Table III.5, entry 9)[63]

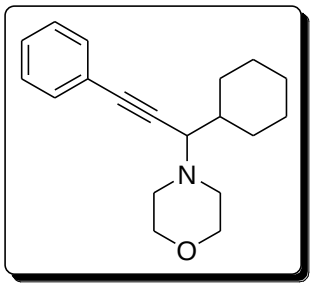

This compound was synthesized by following the general procedure **GP3** in 91% yield as a pale yellow oil. The NMR data obtained are in quite agreement with that reported in the literature previously.[63] **^{1}H NMR ($CDCl_3$, 300 MHz)** δ 1.06–1.10 (m, 2H), 1.21–1.30 (m, 3H), 1.54–1.75 (m, 4H), 1.98–2.12(m, 2H), 2.48–2.52 (m, 2H), 2.67–2.71 (m, 2H), 3.10–3.13 (m, 1H), 3.72–3.77 (m, 4H), 7.27–7.28 (m, 3H), 7.43–7.45 (m, 2H); **^{13}C NMR ($CDCl_3$, 75 MHz)** δ 26.0, 26.2, 26.7, 30.4, 31.0, 39.1, 49.9, 63.9, 67.2, 86.6, 86.8, 123.4, 127.8, 128.2, 131.7; **FT−IR (Neat)** ν_{max} 3409, 2915, 2848, 1590, 1483, 1447, 1317, 1258, 1111, 1074, 1000, 912, 886, 860, 757, 687, 563 cm^{-1}.

4–(1–phenylnon–1–yn–3–yl)morpholine (Table III.5, entry 10)[65]

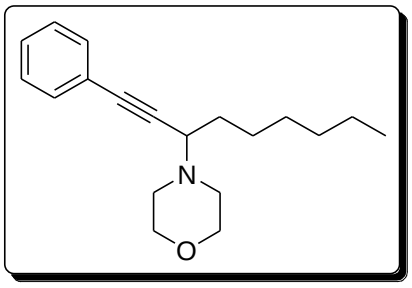

This compound was obtained by following the general procedure **GP3** as a pale yellow oil. The yield of the product was 86%. The NMR data obtained are in quite agreement with that reported in the literature previously.[65] **^{1}H NMR ($CDCl_3$, 300 MHz)** δ 0.96–0.98 (m, 3H), 1.48–1.67 (m, 8H), 1.69–1.72 (m, 2H), 2.54–2.59 (m, 2H), 2.72–2.77 (m, 2H), 3.45–3.50 (m, 1H), 3.70–3.77 (m, 5H), 7.26–7.44 (m, 5H); **^{13}C NMR ($CDCl_3$, 75 MHz)** δ 14.0, 22.6, 26.5, 29.0, 31.7, 32.9, 49.7, 58.1, 67.1, 86.1, 87.2, 123.2, 127.9, 128.2, 131.7; **FT−IR (Neat)** ν_{max} 3476, 2937, 2922, 2848, 2752, 1594, 1483, 1450, 1325, 1255, 1118, 1070, 1000, 912, 860, 753, 587 cm^{-1}.

1–(1–(4–methoxyphenyl)–3–phenylprop–2–ynyl)piperidine (Table III.5, entry 11)[66]

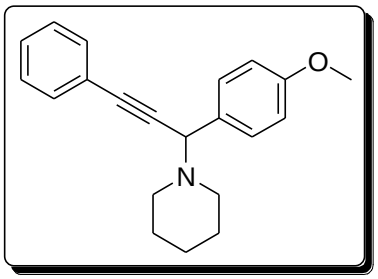

This compound was obtained by following the general procedure **GP3** in 93% yield as a yellow sticky solid. The NMR data obtained are in quite agreement with that reported in the literature previously.[66] **^{1}H NMR ($CDCl_3$, 300 MHz)** δ 1.25–1.58 (m, 6H), 2.54 (bs, 4H), 3.79 (s, 3H), 4.74(m, 1H), 6.87–6.98 (m, 2H), 7.24–7.31 (m, 3H), 7.51–7.54 (m, 4H); **^{13}C NMR ($CDCl_3$, 75 MHz)** δ 24.4, 26.1, 50.6, 55.3, 61.8, 86.4, 87.6, 113.4, 123.4, 128.0, 128.3, 129.7, 130.6, 131.8, 159.0; **FT−IR (KBr)** ν_{max} 3483, 3040, 2797, 1608, 1509, 1487, 1443, 1170, 1107, 1030, 823, 753, 683, 588 cm^{-1}.

2–(3–phenyl–1–(piperidin–1–yl)prop–2–ynyl)phenol (Table III.5, entry 12)[64]

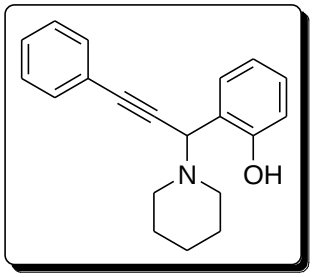

Obtained by the general procedure **GP3** as a yellow liquid and the yield was 90%. The NMR data obtained are in quite agreement with that reported in the literature previously.[64] **^{1}H NMR ($CDCl_3$, 300 MHz)** δ 1.52 (s, br, 2H), 1.67 (s, 4H), 2.72 (t, J = 5.1 Hz), 5.09 (s, 1H), 6.83–6.87 (m, 2H), 7.19–7.25 (m, 1H), 7.34–7.38 (m, 3H), 7.52–7.57 (m, 3H); **^{13}C NMR ($CDCl_3$, 75 MHz)** δ 24.0, 26.0, 61.1, 82.4, 89.8, 116.4, 119.0, 121.3, 122.7, 128.42, 128.45, 128.6, 129.4, 131.9, 157.7; **FT−IR (Neat)** ν_{max} 3055, 2936, 2853, 2221, 1692, 1590, 1464, 1277, 1108, 1084, 974, 754, 691, 670, 543 cm^{-1}.

1–(1–(4–methoxyphenyl)–3–phenylprop–2–ynyl)pyrrolidine (Table III.5, entry 13)[67]

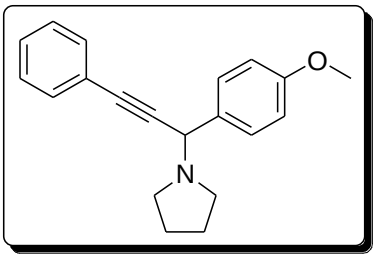

This compound was synthesized by following the general procedure **GP3** in 82% yield as a yellow sticky solid. The NMR data well supports that reported in the literature previously.[67] **^{1}H NMR ($CDCl_3$, 300 MHz)** δ 1.79–1.81 (m, 4H), 2.69–2.71 (m, 4H), 3.78 (s, 3H), 4.84 (s, 1H), 6.86–6.89 (m, 2H), 7.28–7.30 (m, 3H), 7.45–7.53 (m, 4H); **^{13}C NMR ($CDCl_3$, 75 MHz)** δ 23.5, 50.2, 55.3, 58.5, 86.8, 86.9, 87.6, 113.6, 123.3, 128.1, 128.2, 129.5, 131.5, 131.6, 159.1; **FT−IR (KBr)** ν_{max} 2944, 2811, 2361, 1609, 1500, 1487, 1247, 1170, 1107, 1034, 831, 757, 694, 584, 551 cm^{-1}.

2–(3–phenyl–1–(pyrrolidin–1–yl)prop–2–ynyl)phenol (Table III.5, entry 14)[64]

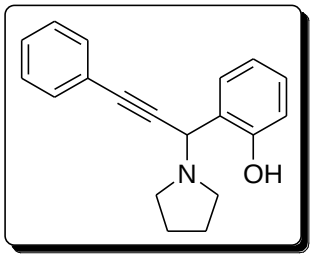

This compound was obtained by following the general procedure **GP3** as a pale yellow semisolid and the yield was 92%. The NMR data obtained are in quite agreement with that reported in the literature previously.[64] **^{1}H NMR ($CDCl_3$, 300 MHz)** δ 1.87–1.90 (m, 4H), 2.79–2.88 (m, 4H), 5.28 (s, 1H), 6.83–6.87 (m, 2H), 7.19–7.27 (m, 2H), 7.35–7.43 (m, 3H), 7.52–7.55 (m, 3H); **^{13}C NMR ($CDCl_3$, 75 MHz)** δ 23.9, 48.9, 57.1, 83.0, 89.1, 116.3, 119.0, 122.2, 122.6, 127.8, 128.4, 128.6, 129.4, 131.9, 157.6; **FT−IR (Neat)** ν_{max} 3367, 3056, 2967, 2845, 2268, 1591, 1489, 1466, 1276, 1095, 1258, 754, 691 cm^{-1}.

1–(3–(4–bromophenyl)–1–(4–methoxyphenyl)prop–2–ynyl) pyrrolidine (Table III.5, entry 15)

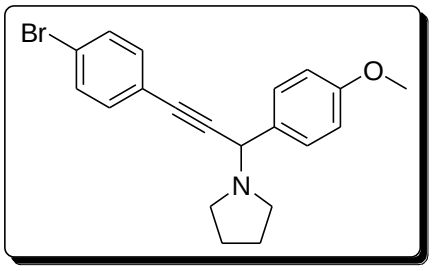

This compound was obtained by following the general procedure **GP3** in 91% yield as a yellow sticky solid. **^{1}H NMR ($CDCl_3$, 300 MHz)** δ 1.78 (s, 4H), 2.66 (s, 4H), 3.79–3.86 (m, 3H), 4.78 (s, 1H), 6.86–6.90 (m, 2H), 7.30–7.33 (m, 2H), 7.41–7.49 (m, 4H); **^{13}C NMR ($CDCl_3$, 75 MHz)** δ 23.4, 50.3, 55.3, 58.6, 85.6, 88.4, 87.6, 113.6, 122.2, 122.3, 129.4, 131.3, 131.5, 133.2, 159.1; **FT−IR (KBr)** ν_{max} 3387, 2952, 2804, 1598, 1505, 1480, 1391, 1299, 1240, 1166, 1111, 1067, 1034, 1008, 820, 772, 683, 595, 565, 517 cm^{-1}.

III.5.7.1. Scanned copy of HRMS spectra of 2D–polymeric copper complex

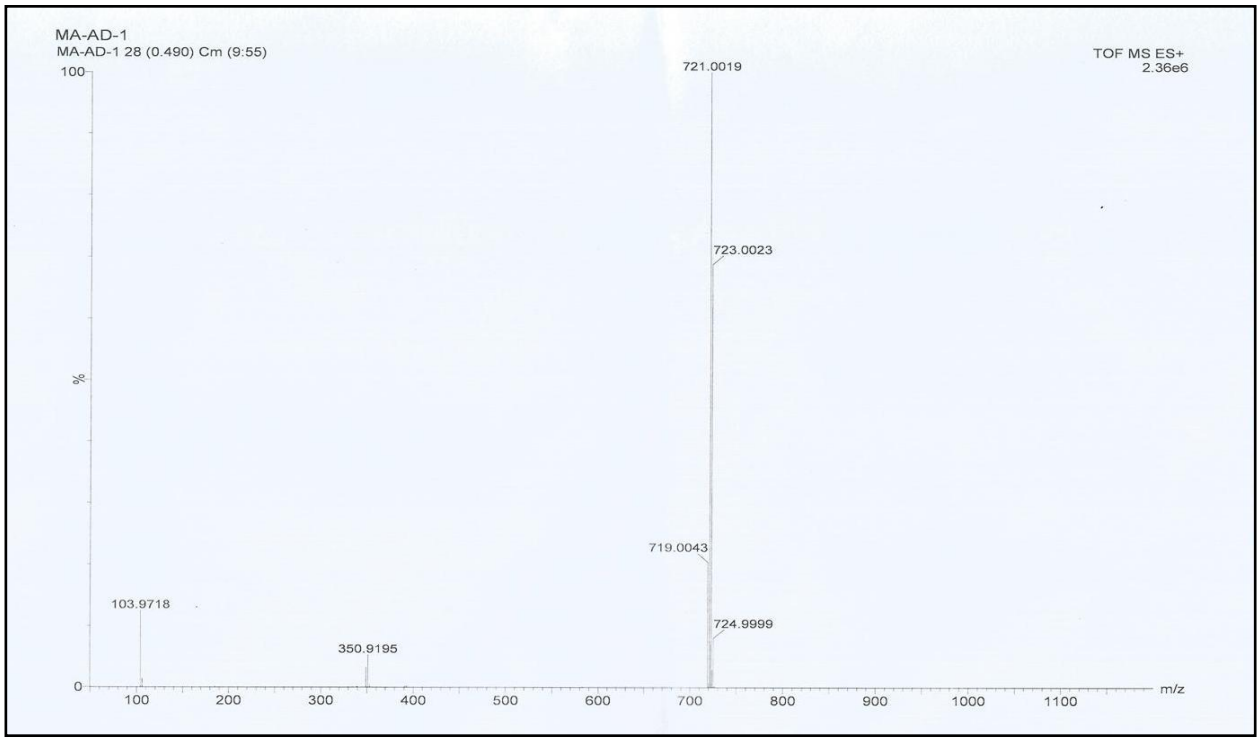

Figure III.5. *HRMS of 1–(1–(4–chlorophenylthio)propan–2–ylthio)–4–chlorobenzene (L) ligated CuI–coordination complex*

III.5.7.2. Scanned copies of ^{1}H–NMR, ^{13}C–NMR spectra of ligand (L), complex; Table III.5, Entry 6, 7 and HRMS of entry 6, 7

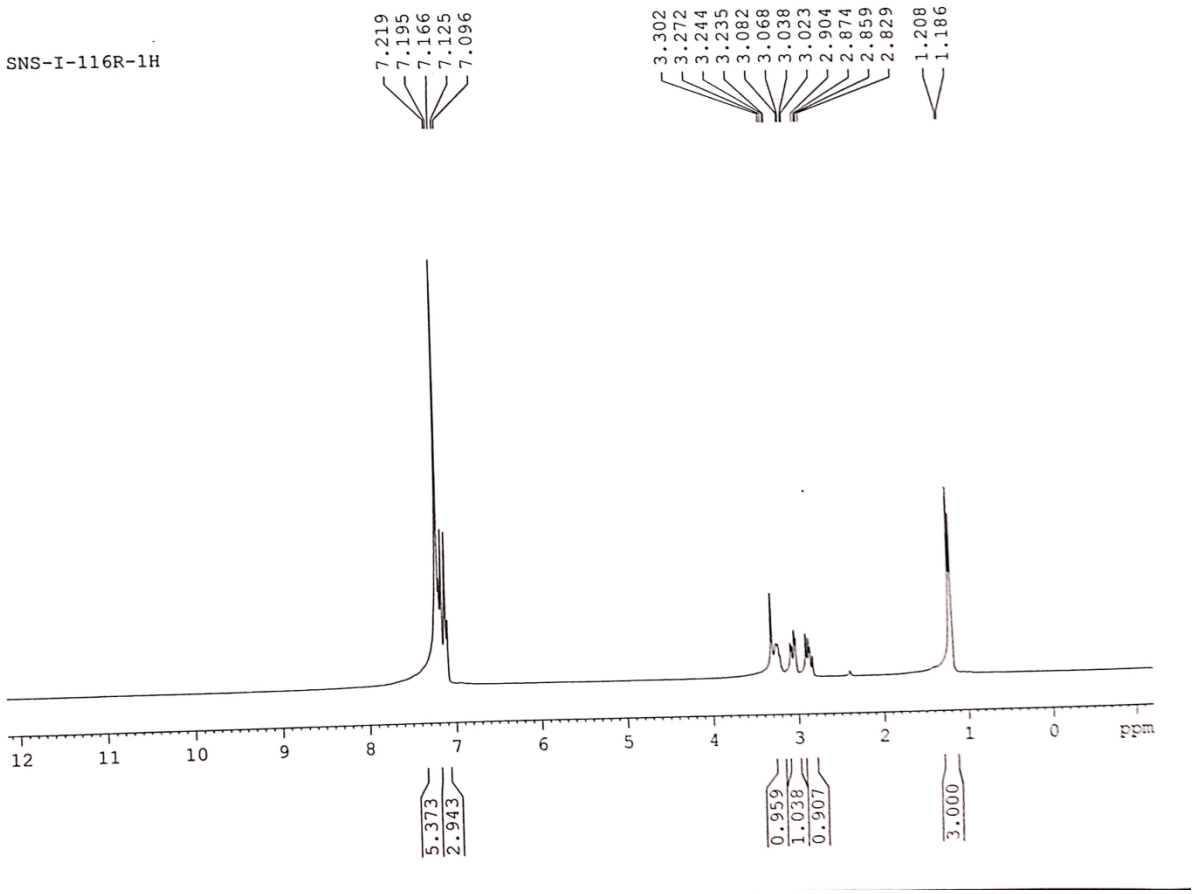

Figure III.6. *^{1}H NMR spectra of ligand 1–(1–(4–chlorophenylthio)propan–2–ylthio) –4–chlorobenzene (L)*

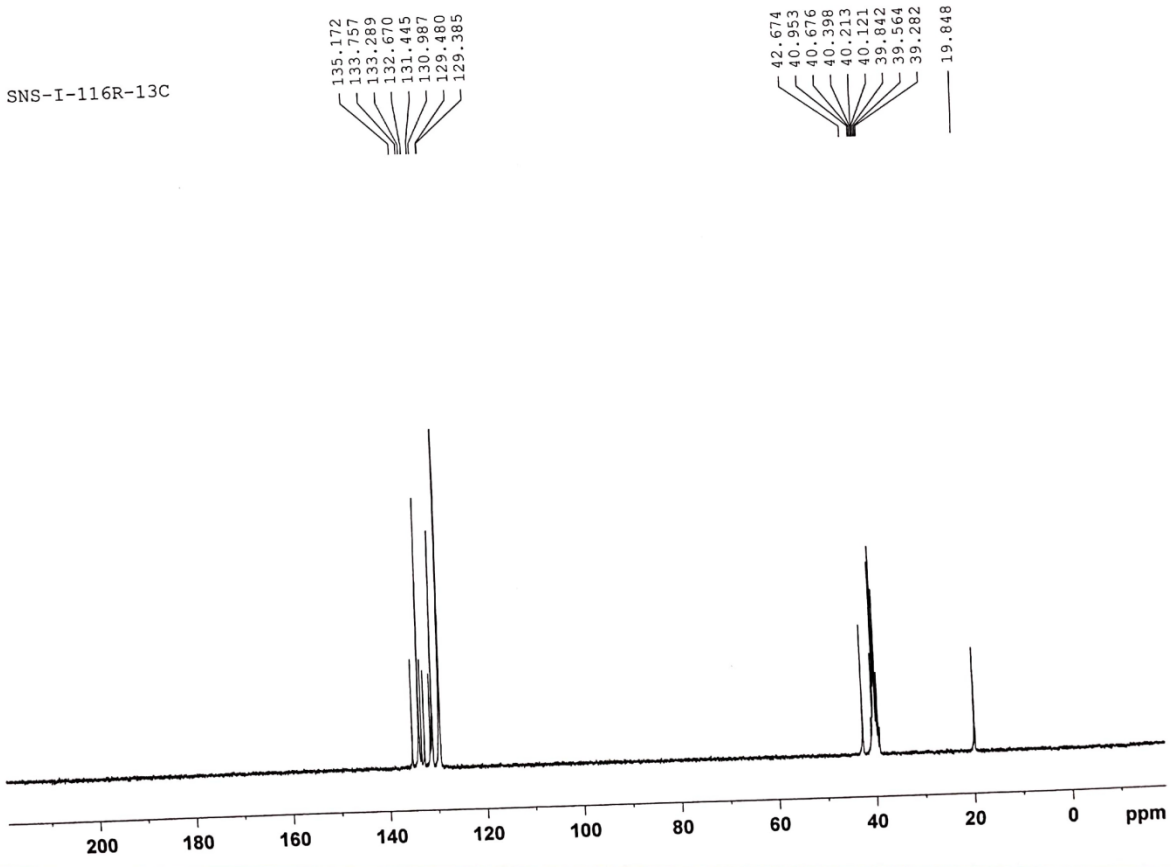

Figure III.7. *^{13}C NMR spectra of ligand 1–(1–(4–chlorophenylthio)propan–2–ylthio) –4–chlorobenzene (L)*

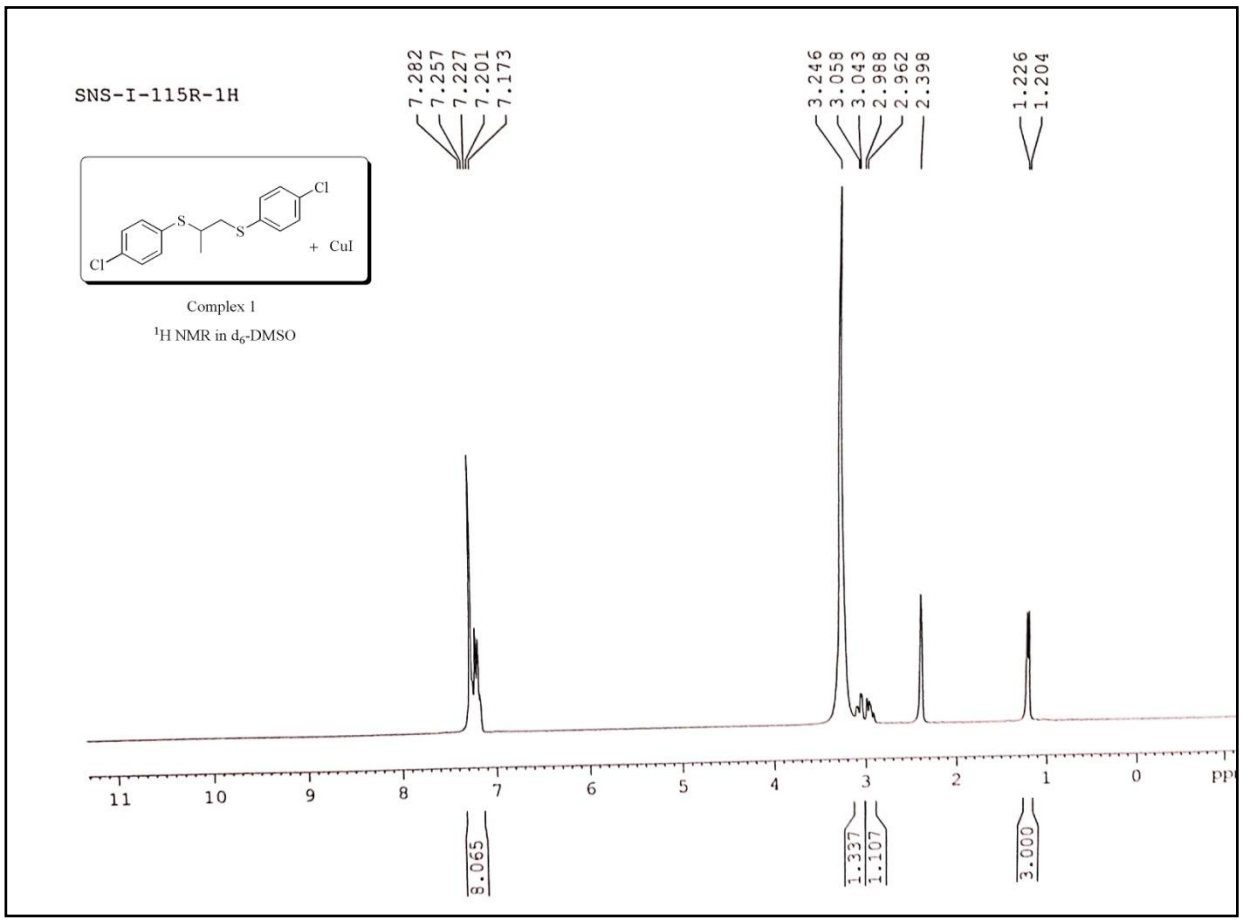

Figure III.8. *^{1}H NMR spectra of 1–(1–(4–chlorophenylthio)propan–2–ylthio)–4–chlorobenzene (L) ligated CuI–coordination complex (1)*

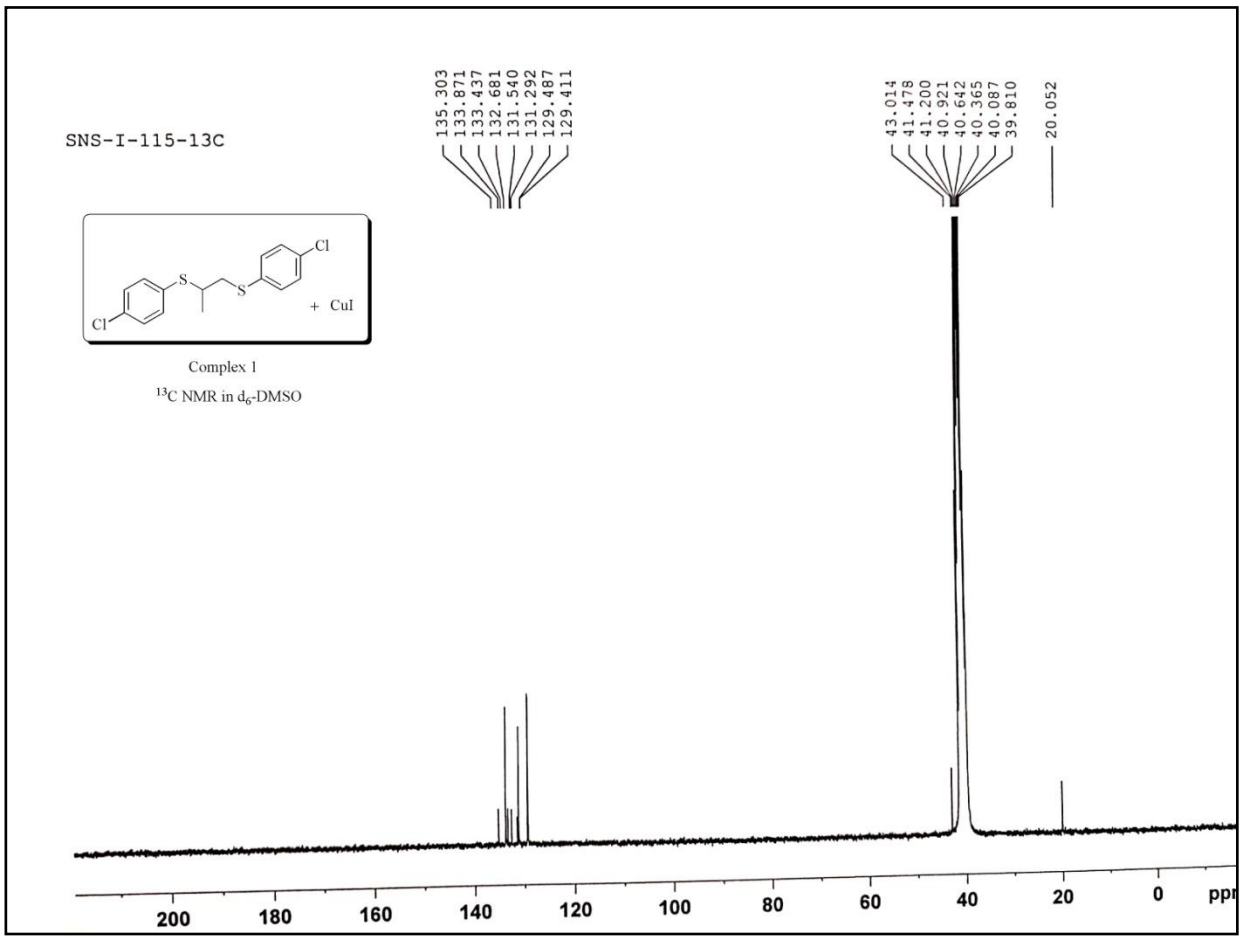

Figure III.9. *^{13}C NMR spectra of 1–(1–(4–chlorophenylthio)propan–2–ylthio)–4–chlorobenzene (L) ligated CuI–coordination complex (1)*

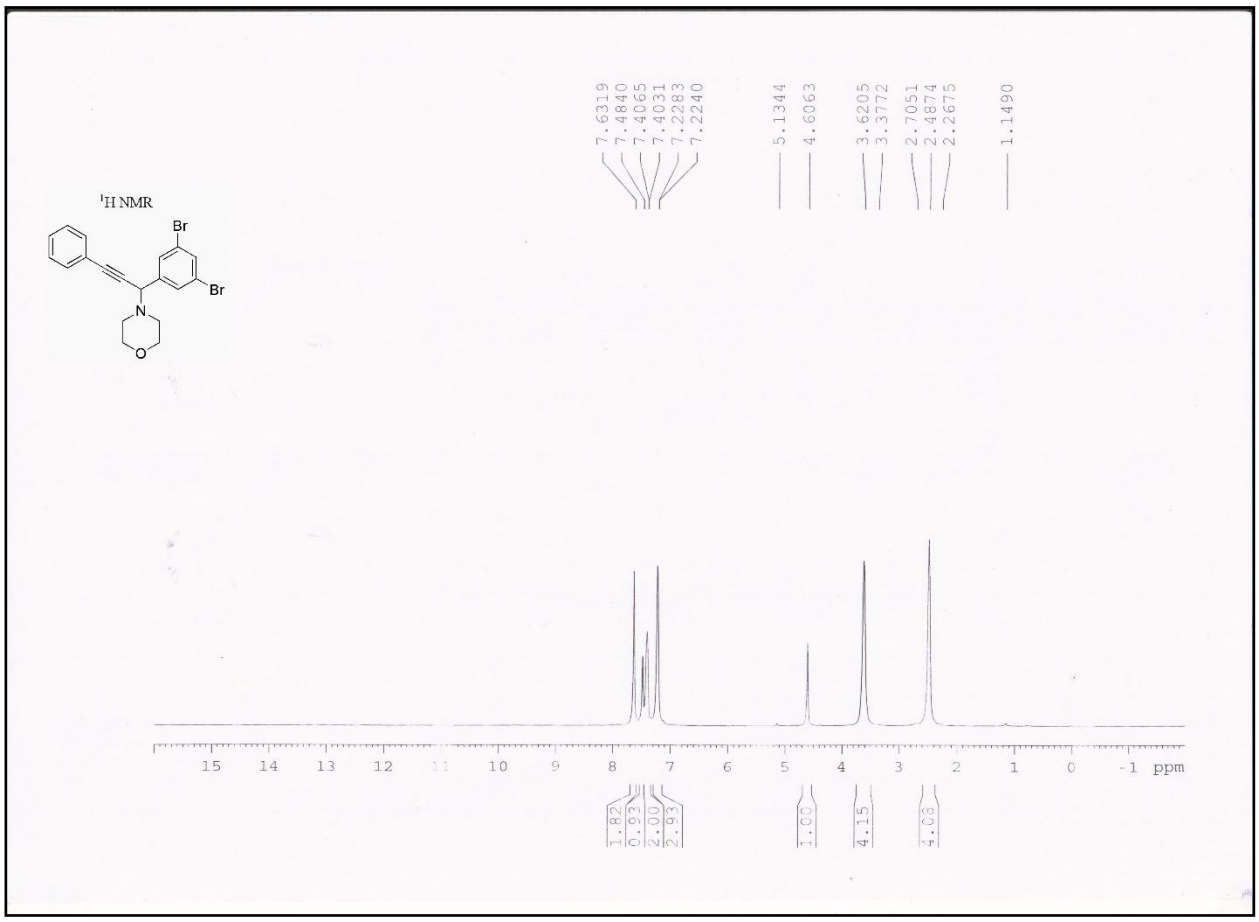

Figure III.10. *^{1}H NMR spectra of 4–(1–(3,5–dibromophenyl)–3–phenyl prop–2–ynyl)morpholine*

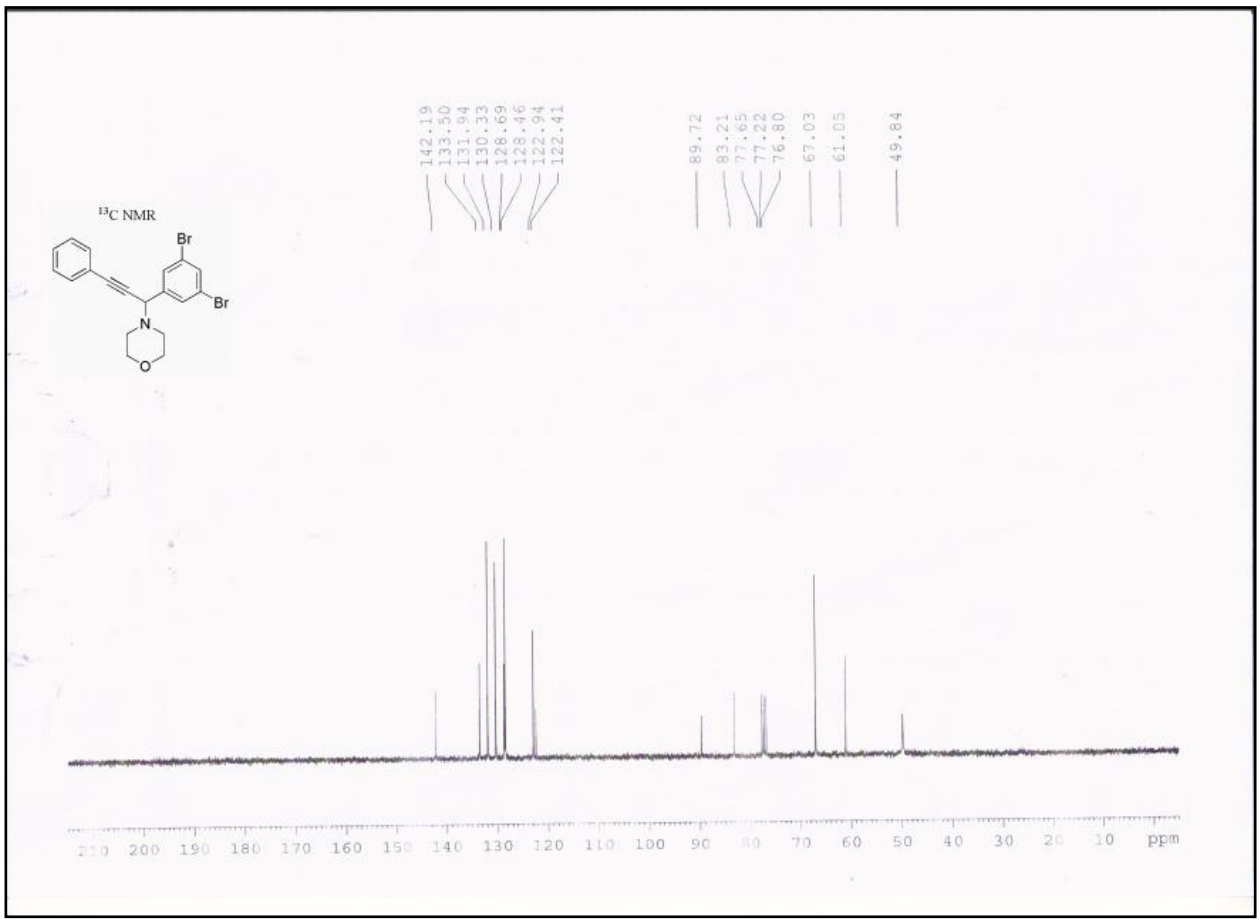

Figure III.11. *^{13}C NMR spectra of 4–(1–(3,5–dibromophenyl)–3–phenyl prop–2–ynyl)morpholine*

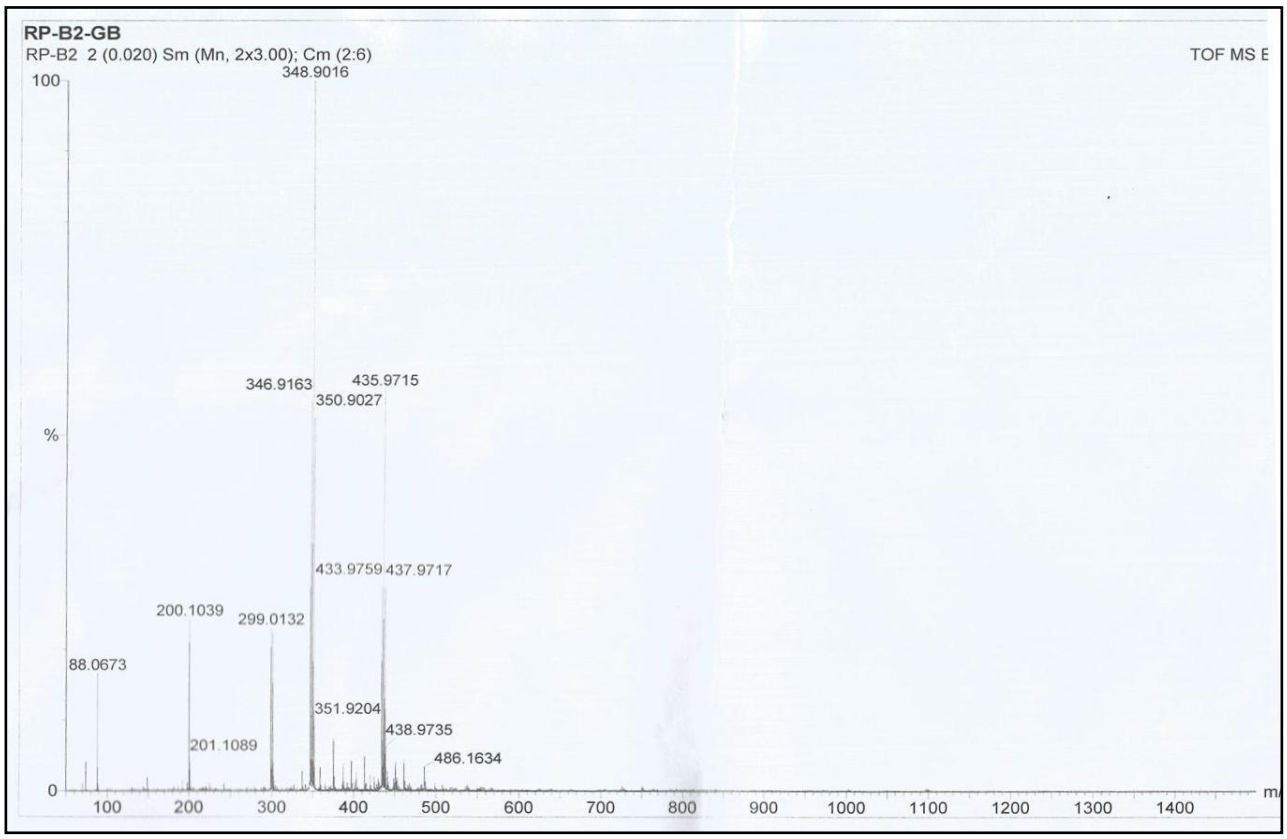

Figure III.12. *HRMS of of 4–(1–(3,5–dibromophenyl)–3–phenyl prop–2–ynyl)morpholine*

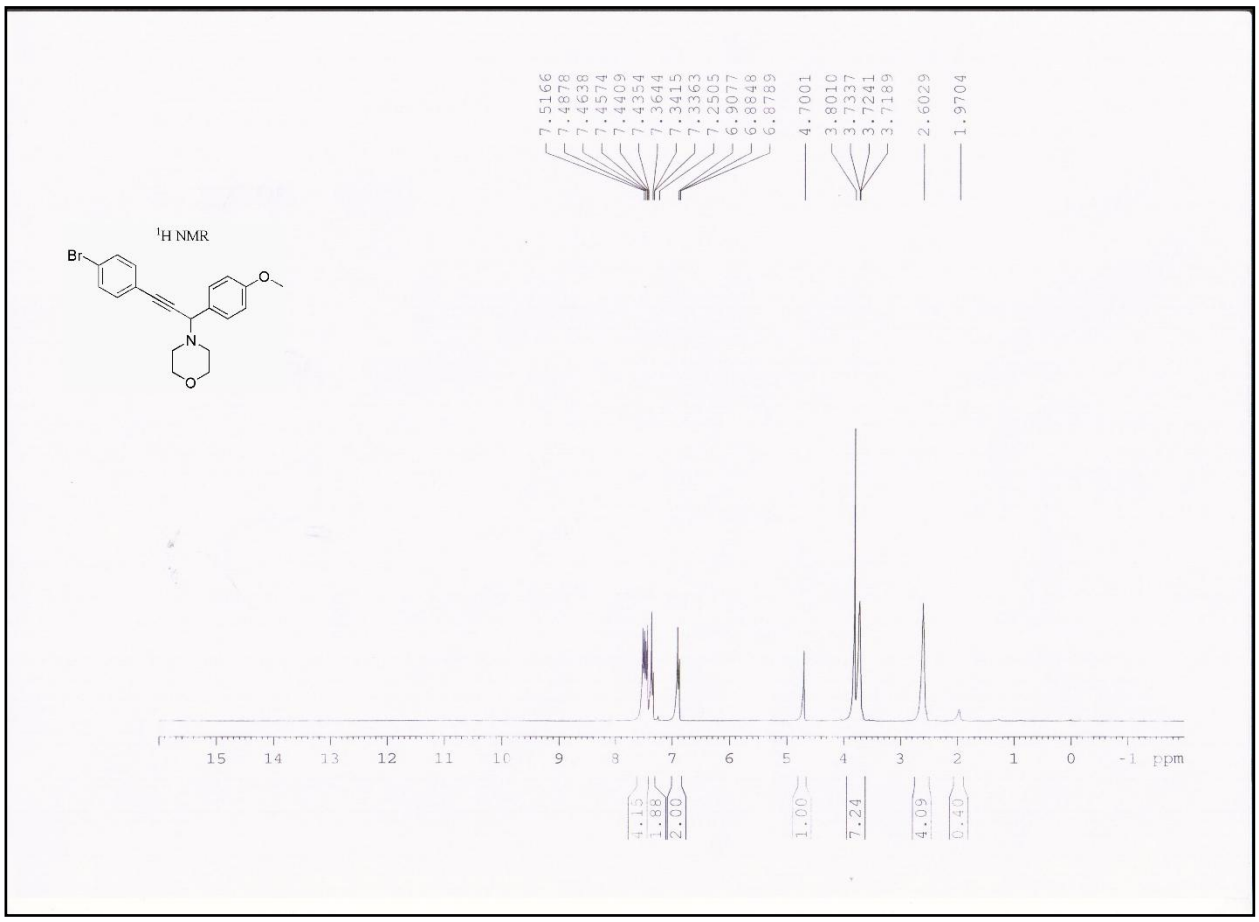

Figure III.13. *^{1}H NMR spectra of 4–(3–(4–bromophenyl)–1–(4–methoxyphenyl)prop–2–ynylmorpholine*

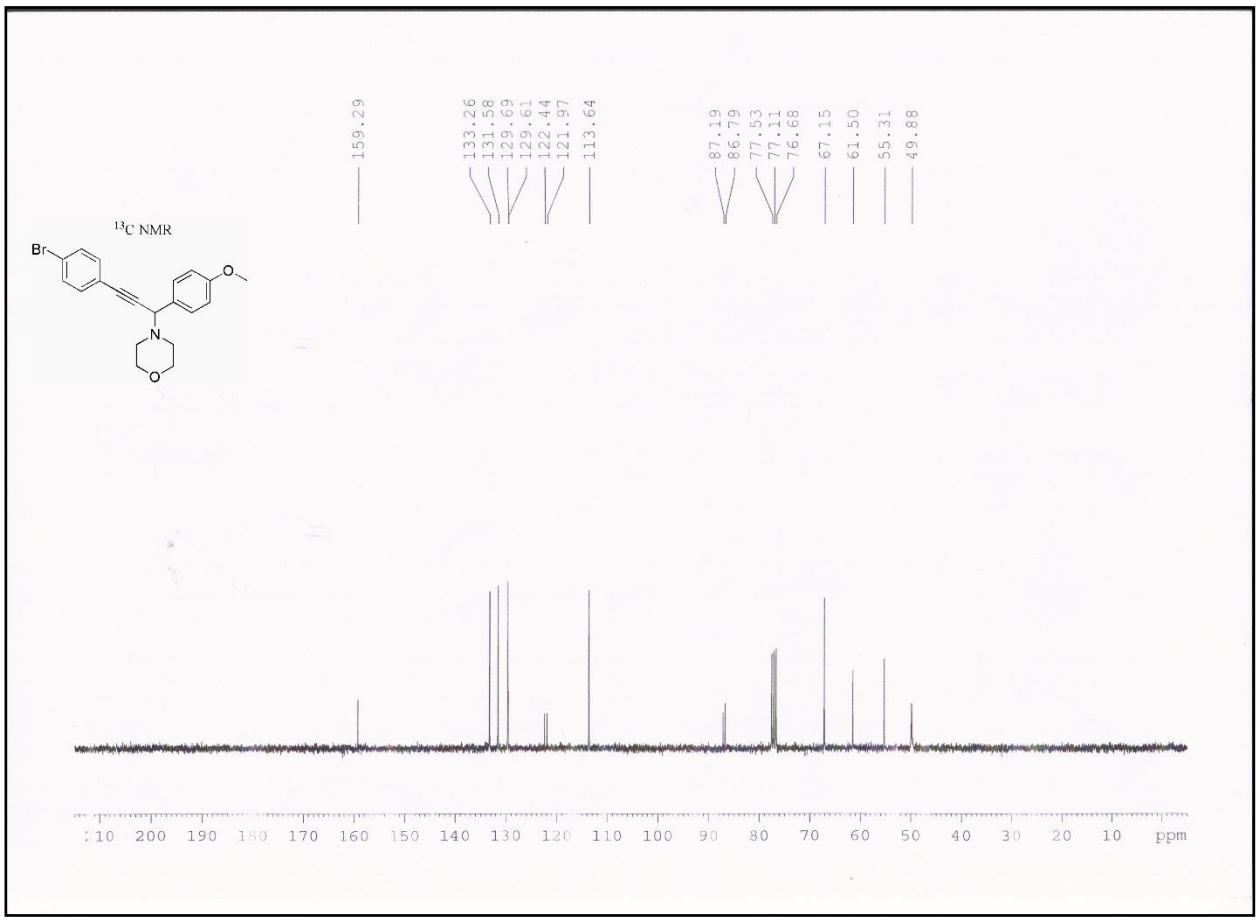

Figure III.14. *^{13}C NMR spectra of 4–(3–(4–bromophenyl)–1–(4–methoxyphenyl)prop–2–ynylmorpholine*

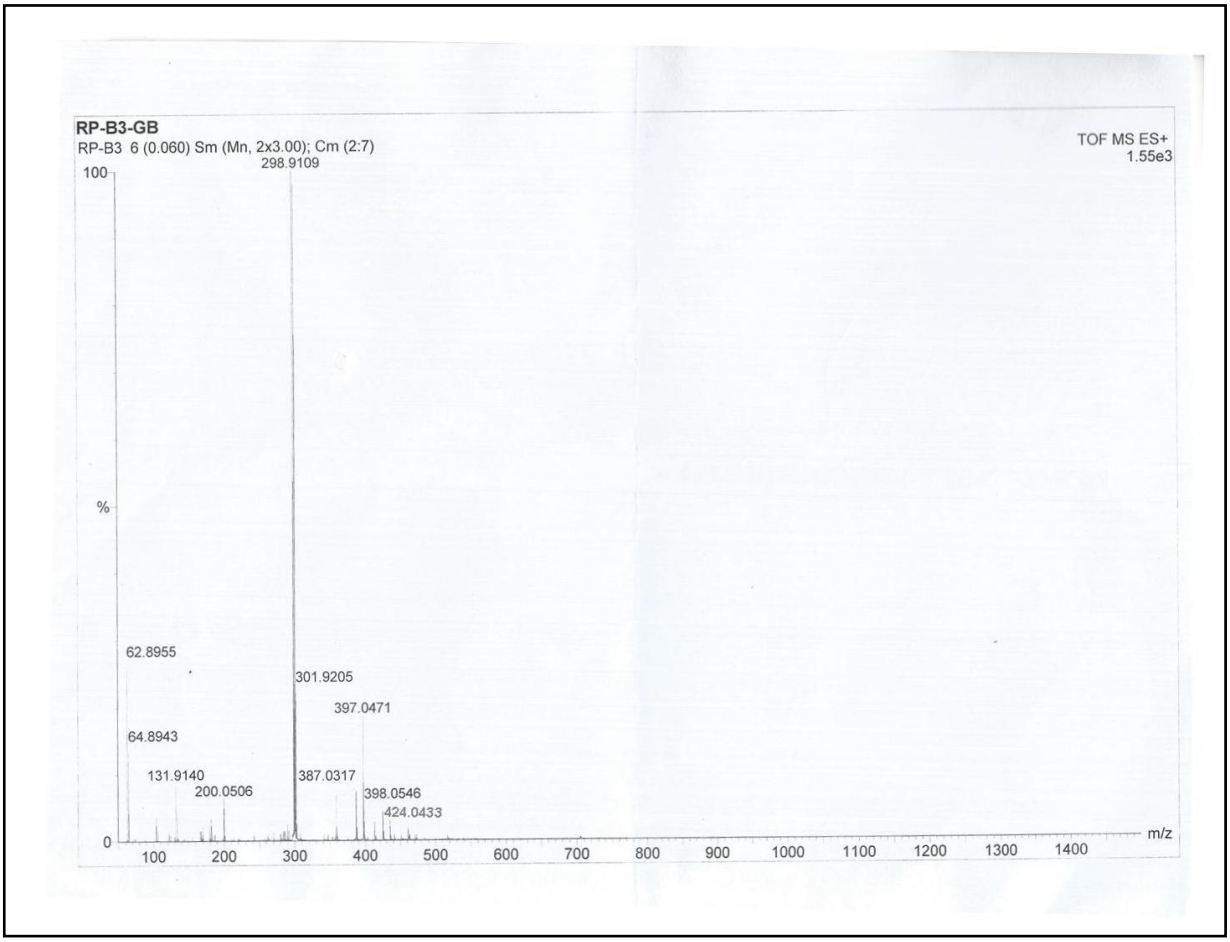

Figure III.15. *HRMS of 4–(3–(4–bromophenyl)–1–(4–methoxyphenyl)prop–2–ynylmorpholine*

III.6. References

References are given in BIBLIOGRAPHY under Chapter III page no. 136–139.

CHAPTER IV

Stabilized Cu_2O nanoparticles on macroporous poly–styrene resins (Cu_2O@ARF) as heterogeneous catalyst towards click reaction for the synthesis of triazoles in aqueous medium

IV.1. Introduction

1,2,3–1*H*–Triazoles have versatile applications in pharmaceuticals.[1] It also possess various biological properties like anticancer,[2–4] anti–HIV,[5,6] antibacterial,[7,8] antiallergic[9] antiplasmodial,[10] antiviral,[11] anti–inflammatory,[12,13] anti–Alzheimer,[14] H_1–antihistamine activity[15] etc. The activities further include fatty acid synthase,[16] anhydrase and protease inhibitors,[17,18] Vibrio cholera[19] inhibitors etc. 1,2,3–Triazole moieties are also found in herbicide, fungicide,[20] and in *α*–GalCer analogue (a potent agonistic antigen of the T cell receptors).[21] 2–Phenyl–oxazole–4–carboxamide tethered 1,2,3−triazole molecules show activity against several cancer cell lines.[22] Dithiocarbamate containing 1,2,3–triazole molecules possess antitumor activity.[1,23] It has also industrial applications in various fields like agrochemicals, optical brighteners, dyes, photo sensitizers, corrosion inhibitiors[1] etc. 1,4–disubstituted–1,2,3–1*H*–triazole molecules possessing biological activity are depicted in Figure IV.1

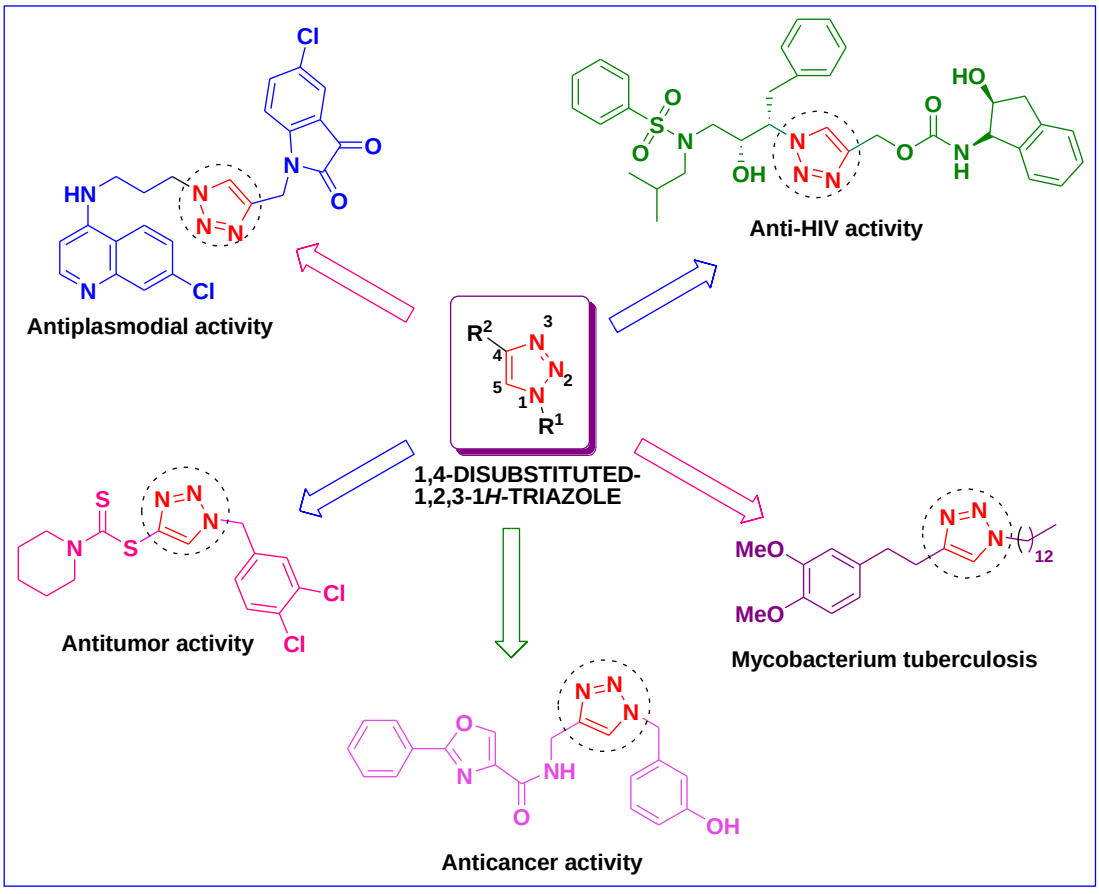

Figure IV.1. *Biologically active 1,4–disubstituted–1,2,3–1H–triazole molecules*

IV.2. Background and Objectives

1,2,3–triazoles was first synthesized by Han Von Pechmann during the synthesis of 'osotetrazone' derivatives of osazoes.[21,24,25] Another approach for the synthesis of 1,2,3–triazole was by Rolf Huisgen commonly known as Huisgen [3+2] cycloaddition reaction.[26] But high activation energy and slow reaction rate even at elevated temperatures are two major drawback of the process. Also the product possess lack of regioselectivity, both 1,4– as well as 1,5–disubstituted–1,2,3–triazoles are obtained as a mixture. Then the CuAAC (copper–catalyzed azide–alkyne cycloaddition) reaction was developed by Sharpless,[27,28] and Meldal,[29,30] independently which revealed that Cu(I) could assist regiospecific formation of 1,4–disubstituted–1,2,3–triazole under milder condition (Scheme IV.1) which is widely known as 'click' chemistry.

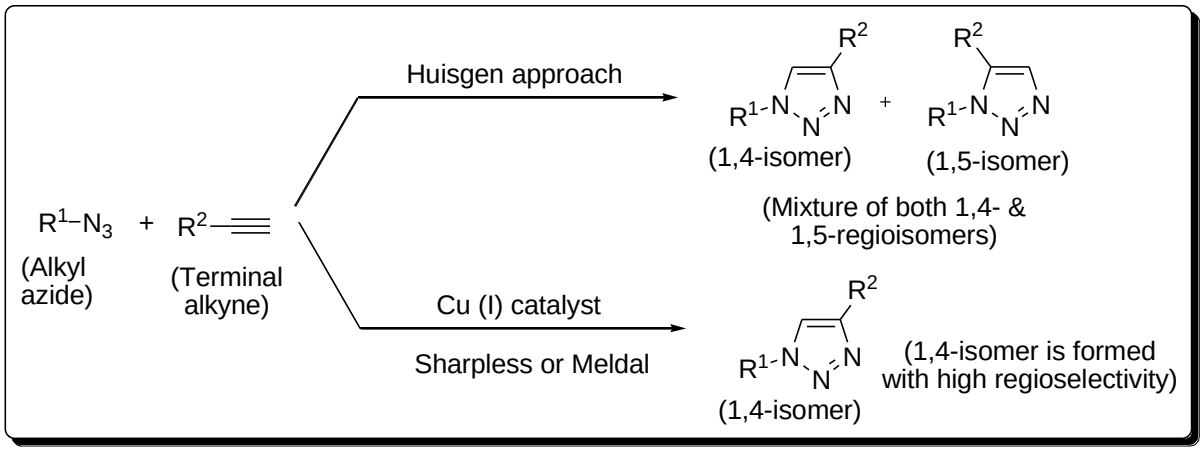

Scheme IV.1. *Huisgen and Sharpless or Meldal approach for 1,2,3–1H–triazole formation*

Since organyl azides are less common, toxic and hazardous organic compounds,[31] the three–component approach involving alkyl halide, sodium azide and terminal alkyne leading to selective synthesis of 1,4–disubstituted–1,2,3–triazole has been established as a robust 'click' protocol. Synthesis of triazoles both by three–component and two–component approach have been explored largely since last decade with homogeneous,[32,33] and heterogeneous[34,35] Cu–catalysts. However, heterogeneous copper catalysts are important now a days because of certain advantages like easy catalyst separation, recycling of the catalyst etc. Different heterogeneous nanostructured catalysts development is an interesting field of research.[36] Features like easy availability, high catalytic efficiency, high turn-over frequency, well selectivity, good recycling

ability without leaching of metal ions etc are important for commercial applications of these heterogeneous nanocatalysts. Control of the size, shape, stability of the nanocomposite etc. are some important features to acieve these.[37] On the other hand, for designing the nanocatalyst system the type of reaction and the reaction conditions need to be considered. Several heterogeneous supported Cu(I) and/or Cu(II) catalyst systems have been developed for the synthesis of 1,2,3–triazole.

Movassagh *et al.* synthesized polystyrene resin supported Cu(I) iodide–cryptand–22–complex (PS–C22–CuI) and used this heterogeneous catalyst for three–component click reaction (Scheme IV.2).[38]

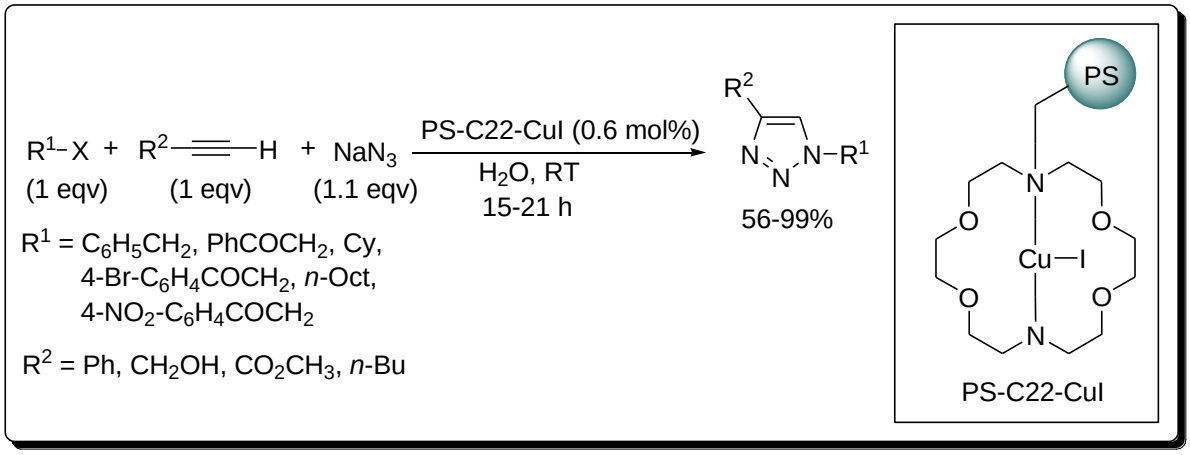

Scheme IV.2. *PS–C22–CuI–catalyzed three–component click reaction*

Lu *et al.* reported one–pot three–component click reaction of benzyl chloride, non activated terminal alkyne and sodium azide by magnetic $NiFe_2O_4$ supported glutamate–Cu catalyst at room temperature in water (Scheme IV.3).[39]

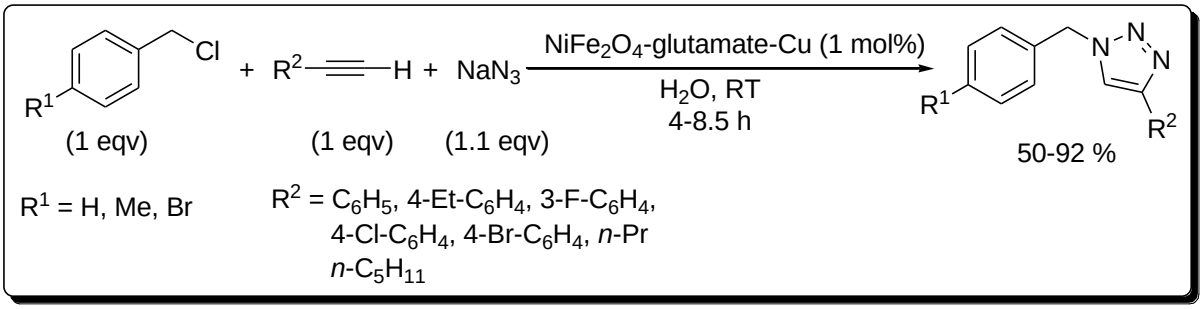

Scheme IV.3. *Three–component click reaction catalyzed by $NiFe_2O_4$–supported glutamate–Cu*

In another example three–component click reaction was achieved by water soluble copper *N*–heterocyclic chloride complex [Cu(NHC)Cl] of vitamin B_1 in water at room temperature and this work has been reported by Purohit *et al*. (Scheme IV.4).[40]

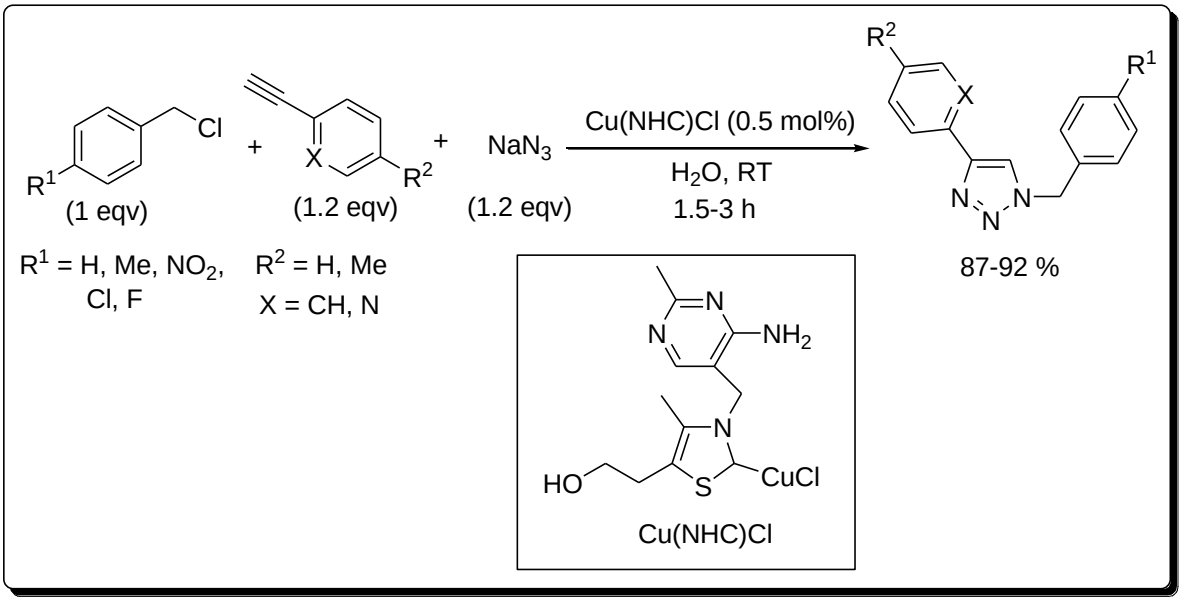

Scheme IV.4. *Three–component click reaction catalyzed by NHC–Cu(I) complex of vitamin* B_1

Using ammonium salt tagged SIPr–Cu(I) complex Wang *et al*. showed click reaction for the synthesis of 1,4–disubstituted–1,2,3–triazole under ambient reaction condition in aqueous medium. Water soluble NHC–Cu(I) catalyst could be reused at least four times with good yield of the products (Scheme IV.5).[41]

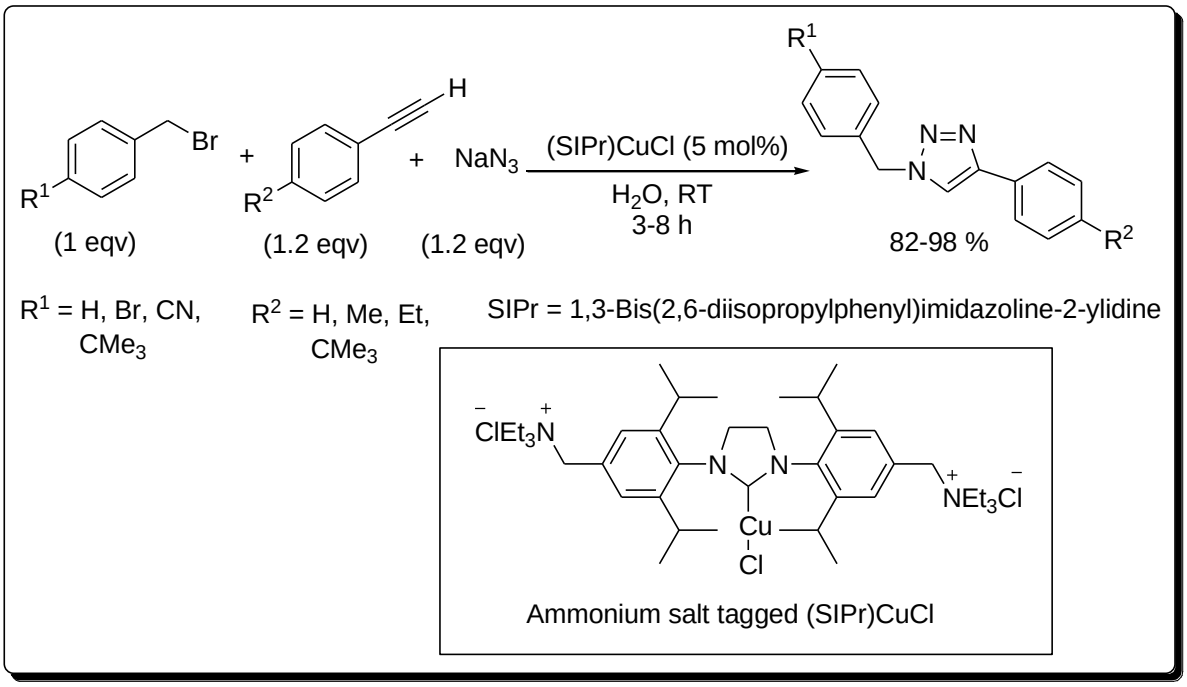

Scheme IV.5. *Three–component azide–alkyne click reaction catalyzed by NHC–Cu(I) complex*

Nemati *et al*. have used magnetic nano bimetallic catalyst $Fe_3O_4@TiO_2/Cu_2O$ for three–component click reaction under refluxing condition of water (Scheme IV.6).[42]

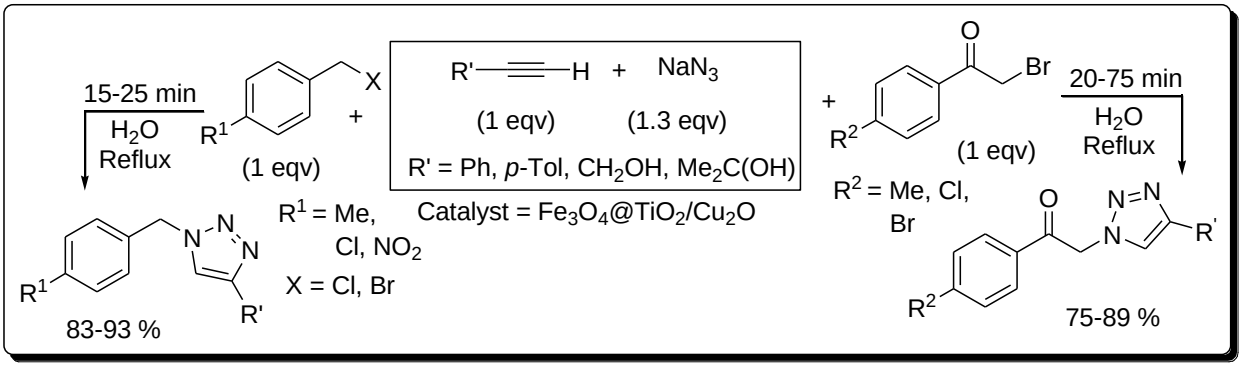

Scheme IV.6. *Three–component click reaction catalyzed by magnetic nano $Fe_3O_4@TiO_2/Cu_2O$*

Bhaumik *et al.* synthesized a new pyridine–imine functionalized mesoporus silica (SBA–15) heterogeneous reusable catalyst and found that the catalytic activity of Cu(II) containing mesoporous material, Cu@PyIm–SBA–15 was excellent towards the one pot click reaction between in situ formed azides from amines and acetylenes to form various 1,4–disubstituted 1,2,3–triazoles (Scheme IV.7).[43]

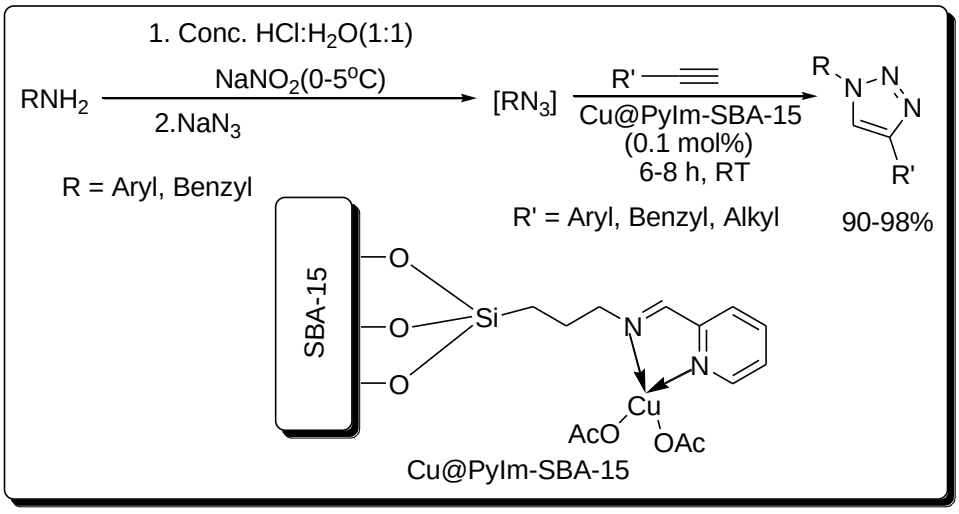

Scheme IV.7. *Cu@PyIm–SBA–15 catalyzed click reaction*

Pourjavadi *et al.* prepared heterogeneous Cu–catalyst based on poly (ionic liquid coated) magnetic nanoparticles and applied this heterogeneous catalyst for the synthesis of 1,4–disubstituted–1,2,3–triazole by three–component click reaction among 1° halide, terminal acetylene and sodium azide at room temperature in aqueous medium (Scheme IV.8).[44]

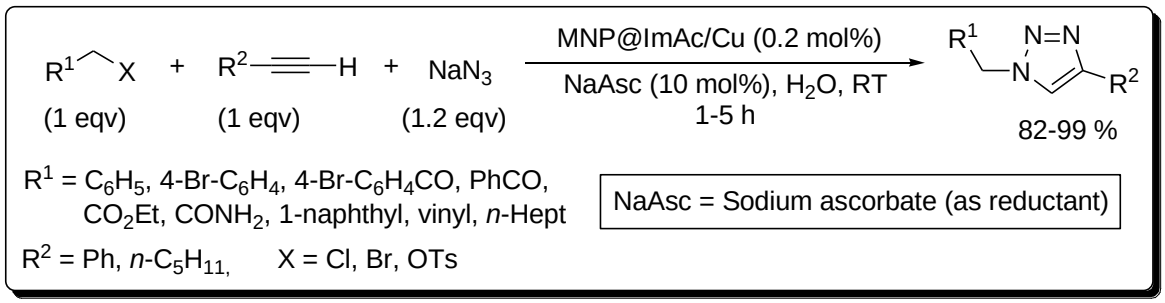

Scheme IV.8. *Three–component click reaction by MNP@ImAc/Cu*

D. Chattopadhyay *et al.* synthesized and characterized a reduced graphene oxide/cuprous oxide (RGO/Cu_2O) nanocomposite by *in situ* reduction method using a lactulose solution as reducing and stabilizing source. They found the RGO/Cu_2O nanocomposite as an excellent reusable heterogeneous catalyst for the 'click' reaction upto six conseceutive cycles (Scheme IV.9).[45]

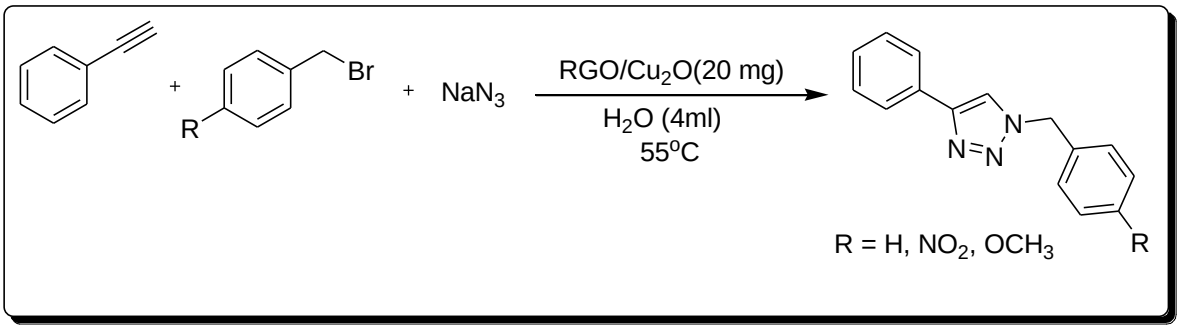

Scheme IV.9. *Three–component click reaction by (RGO/Cu_2O) nanocomposite*

Mohammadsaleh *et al.* prepared a poly vinyl alcohol stabilized Cu_2O particles. The PVA–Cu_2O composite was found to be an effective and recyclable heterogeneous catalyst for AAC reaction between terminal alkynes and azides to prepare 1,2,3–triazoles (Scheme IV.10).[46]

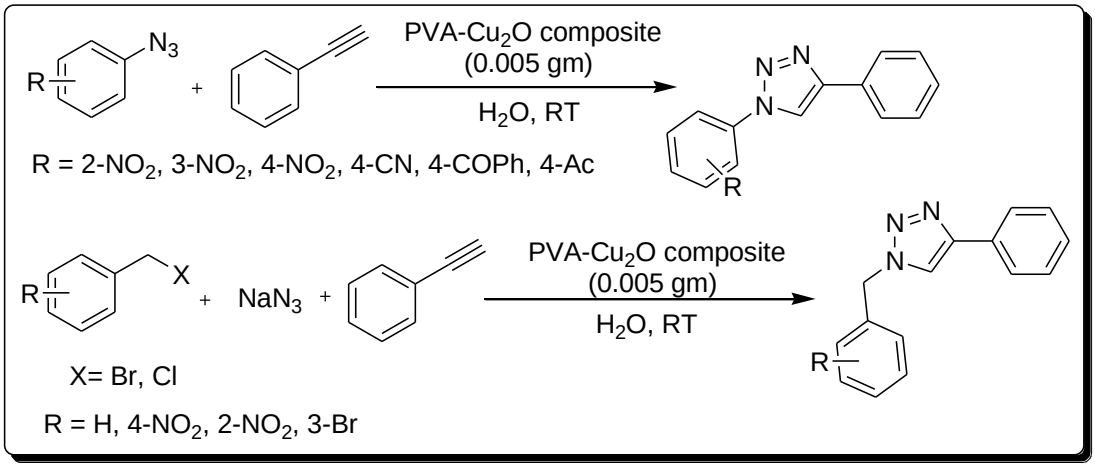

Scheme IV.10. *PVA–Cu_2O composite catalyzed three–component click reaction*

Polyvinyl poly(1–vinylpyrrolidin–2–one) (PVP), poly(4–vinylpyridine) (PVPy) supported Cu_2O have been also synthesized and used as catalyst in multicomponent click reaction.[47]

But most of these heterogeneous catalysts suffer from limitations like lower stability of Cu_2O, agglomeration of Cu_2O NPs, use of precious ligand–based heterogeneous supports, addition of extra reducing source with Cu(II) source, requirement of harsh reaction conditions, leaching of metal ions, lower recycling efficiency etc.[48] Very few examples of heterogeneous catalysts that work efficiently in water medium for AAC reaction are reported yet.[48] As a result, preparation of simple, stable and efficient catalytic system with stabilized Cu_2O NPs having vast applicability and reusability is an important field of study. Previously our group has developed polymer–supported transition metal (both mono– and bimetallic) catalysts with poly–styrene

resins as suitable support.[49] In the present work we have prepared a new heterogeneous catalyst Cu_2O@ARF which does not require such additional reagents either to stabilize Cu(I) oxide or to enhance its catalytic activity because here the polymeric resins with counter formate anions ($HCOO^-$) could not only reduce Cu(II) to Cu(I) species but also stabilized the Cu_2O NPs. The catalyst has been characterized by FT–IR spectroscopy, PXRD, XPS, HRTEM and ICP–AES and applied for three–component click reaction for the regioselective synthesis of 1,4–disubstituted–1,2,3–triazole. Here we have used water medium under ambient condition to afford triazole derivatives from alkyl halide, terminal alkyne and sodium azide (Scheme IV.11) The composite [Cu_2O@ARF] is stable, agglomeration–free and uniformly dispersed and exhibits excellent catalytic activity in three component AAC reaction for regioselective synthesis of 1,4–disubstituted–1,2,3–triazoles in water at room temperature. The as–synthesised catalytic system (Cu_2O@ARF) shows high TOF and efficient recyclability in on–water triazole synthesis, as compared to the other reported polymer–supported Cu(I) catalytic systems. Our work also finds application in the preparation of an antitumor drug molecule in aqueous medium which has significant commercial importance.[23]

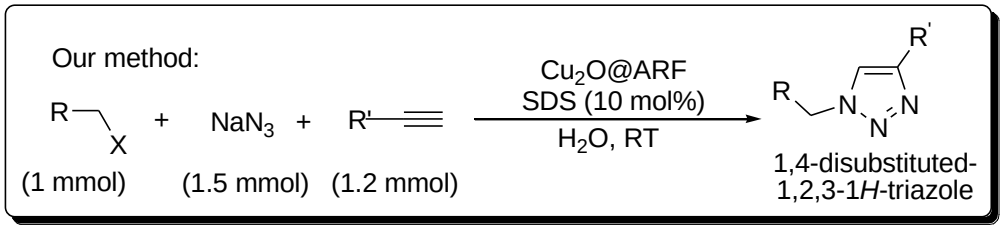

Scheme IV.11. *Cu_2O@ARF catalyzed three–component on–water click reaction at room temperature*

IV.3. Present Work: Result and Discussion

IV.3.1. Preparation of Cu_2O@ARF

ARF (Amberlite resin formate) was prepared according to the reported procedure.[50] At first 0.25 mmol $Cu(OAc)_2 \cdot H_2O$ (50 mg) in 5 mL dry distilled DMF was taken in a Teflon–capped sealed tube and was stirred at room temperature for 30 minutes. When all the $Cu(OAc)_2 \cdot H_2O$ was dissolved, 1 g ARF was added to it. It was then heated at 120 ^oC for 1 h with occasional gentle shaking. The supernatant liquid became completely colourless by this time and the white resin beads of ARF turned light brown. The mixture was then cooled at room temperature and the resin beads were filtered off and washed repeatedly with deionised water (4 x 5 mL) and

acetone (4 x 5 mL). After washing the resin beads were dried under vacuum before use (Figure IV.2).

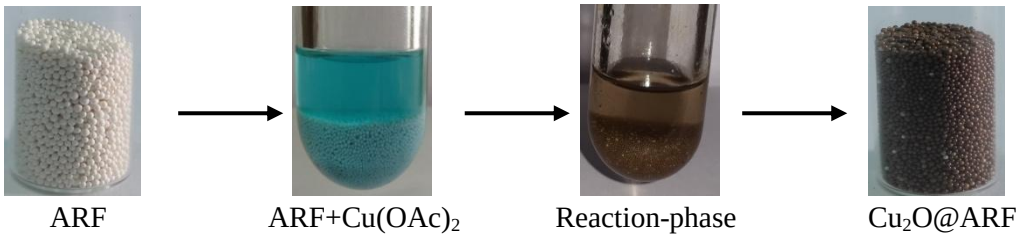

Figure IV.2. *Digital images of different steps during preparation of Cu_2O@ARF*

IV.3.2. Characterization of Cu_2O@ARF

IV.3.2.1. FT–IR spectroscopy

The FT–IR spectra of Cu_2O@ARF were recorded and compared with the ARF. The peaks at about 1348 cm^{-1} (symmetric) and 1596 cm^{-1} (anti–symmetric) were observed as unchanged in both ARF and Cu_2O@ARF species.

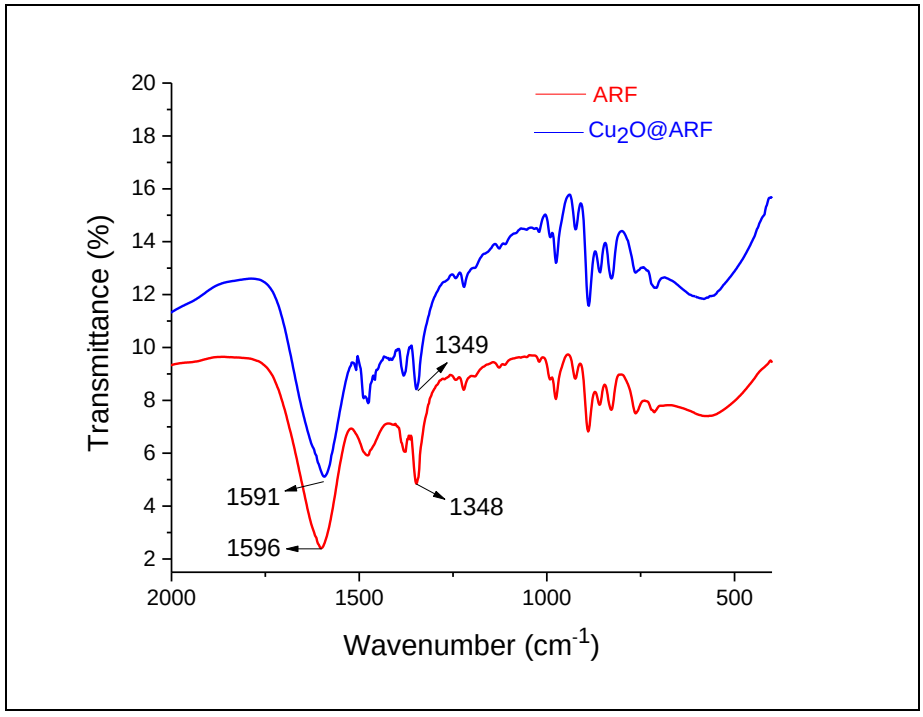

Figure IV.3. *FT–IR spectra of ARF and Cu_2O@ARF*

IV.3.2.2. Powder X–ray diffraction (P–XRD) pattern

The powder XRD patterns of Cu_2O@ARF composite (Figure IV.4) show amorphous hump, which indicates the presence of ARF. The presence of phase pure cuprous oxide (Cu_2O) is indicated by the Bragg diffraction patterns. The JCPDS peak positions of the Cu_2O@ARF composite is in the range of 30° to 80° that are nearly similar to the literature values for Cu_2O.[51,52] The distinguishable XRD peaks at (2θ values) 31.63°, 36.51°, 42.42°, 61.44° and 73.69° belong to (110), (111), (200), (220) and (311) planes of Cu_2O respectively (JCPDS card no. 01–073–6371, Phase: Cu_2O). We did not observe any signals related to Cu_2O in its X–ray diffraction as the ARF resins are amorphous in nature.[49]

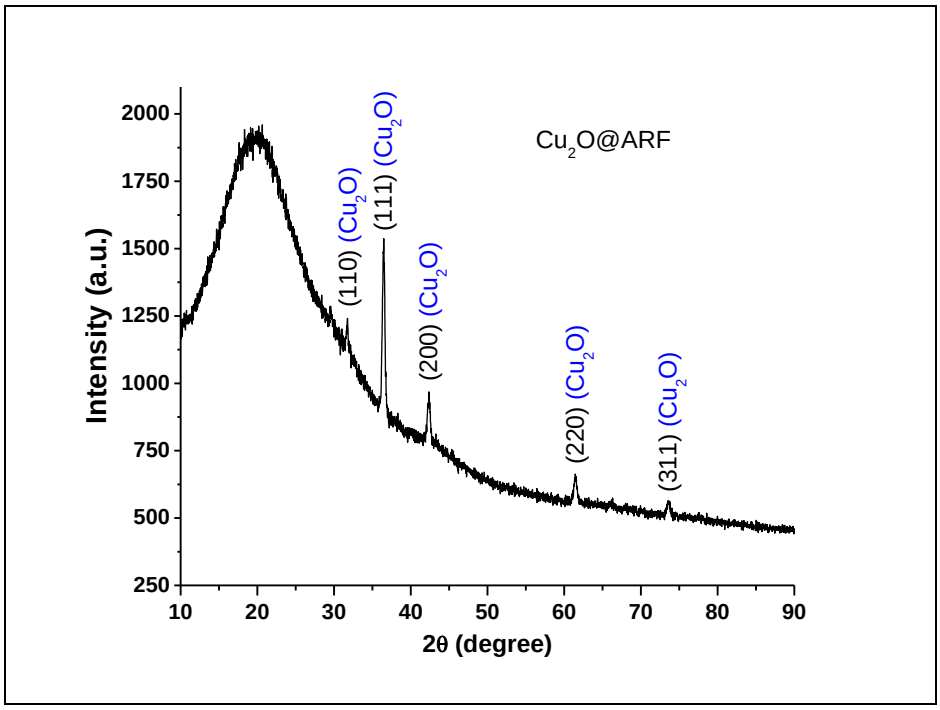

Figure IV.4. *P–XRD pattern of Cu_2O@ARF*

IV.3.2.3. TEM analysis

The presence of Cu_2O NPs embedded on the poly–ionic resin surface is confirmed by the HR–TEM analysis of the Cu_2O@ARF composite (Figure IV.5a). The homogeneous distribution of Cu_2O Nanoparticles with diameter of approximately ~5–7 nm in the Cu_2O@ARF composite is shown by high resolution TEM image (Figure IV.5b). The lattice fringes present with d = 0.29 nm (inset, Figure IV.5b) also confirms the (110) lattice plane of Cu_2O.[53]

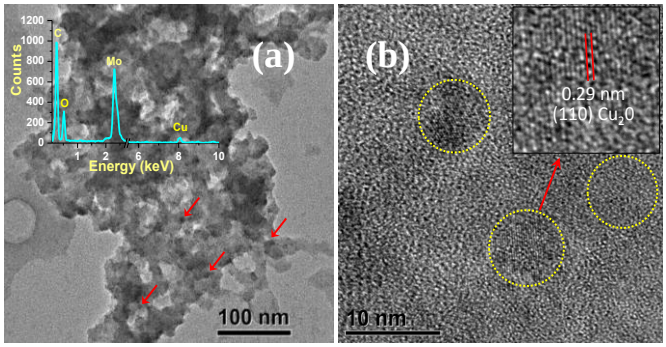

Figure IV.5 *(a) TEM image of the composite material showing the Cu_2O nanoparticles embedded in the resin. Inset of (a) shows the EDS pattern of the sample. It confirms presence of C, O and Cu from the sample; A part of C and Mo are coming from the carbon coated Mo grid used for TEM analysis. (b) HR–TEM showing the lattice fringes of Cu_2O nanoparticles. Magnified views of (110) lattice plane is shown in the inset of (b).*

IV.3.2.4. ICP–AES analysis

The copper content in resin composite, Cu_2O@ARF was determined by ICP–AES (Inductively coupled plasma–atomic emission spectroscopy) experiment. On analysis approximately 10.8 mg of copper was estimated in per gram of the resin composite (~1.08 wt% Cu). It means that 1 g resin nanocomposite (Cu_2O@ARF) contains 0.1699 mmol of copper metal.

IV.3.2.5. XPS analysis

The XPS analysis of the fresh catalyst confirms the presence of Cu_2O (Cu^+) only. The presence of two distinct peaks at 932.30 and 952.12 eV without any appearance of satellite peaks is observed by the high resolution Cu2p spectrum (Figure IV.6a) and the corresponding binding energies are indicating the Cu $2p_{3/2}$ and Cu $2p_{1/2}$ of Cu^+, respectively.[54,55] Also the peak located at 529.85 eV in the deconvoluted high resolution O1s spectrum (Figure IV.6b) assures the presence of Cu_2O state.[55,56] Moreover the peaks at 531.22 and 532.1 eV correspond (Figure IV.6b) to the adsorbed oxygen which is due to the surface OH groups and oxygenated functional groups that is $HCOO^-$ ions present in resin system.[55,56] Thus the XPS study fully appreciates the XRD patterns, that Cu_2O particles are in situ formed by the reduction of the soaked Cu^{2+} (Cu acetate) inside the ARF at 120 ºC.

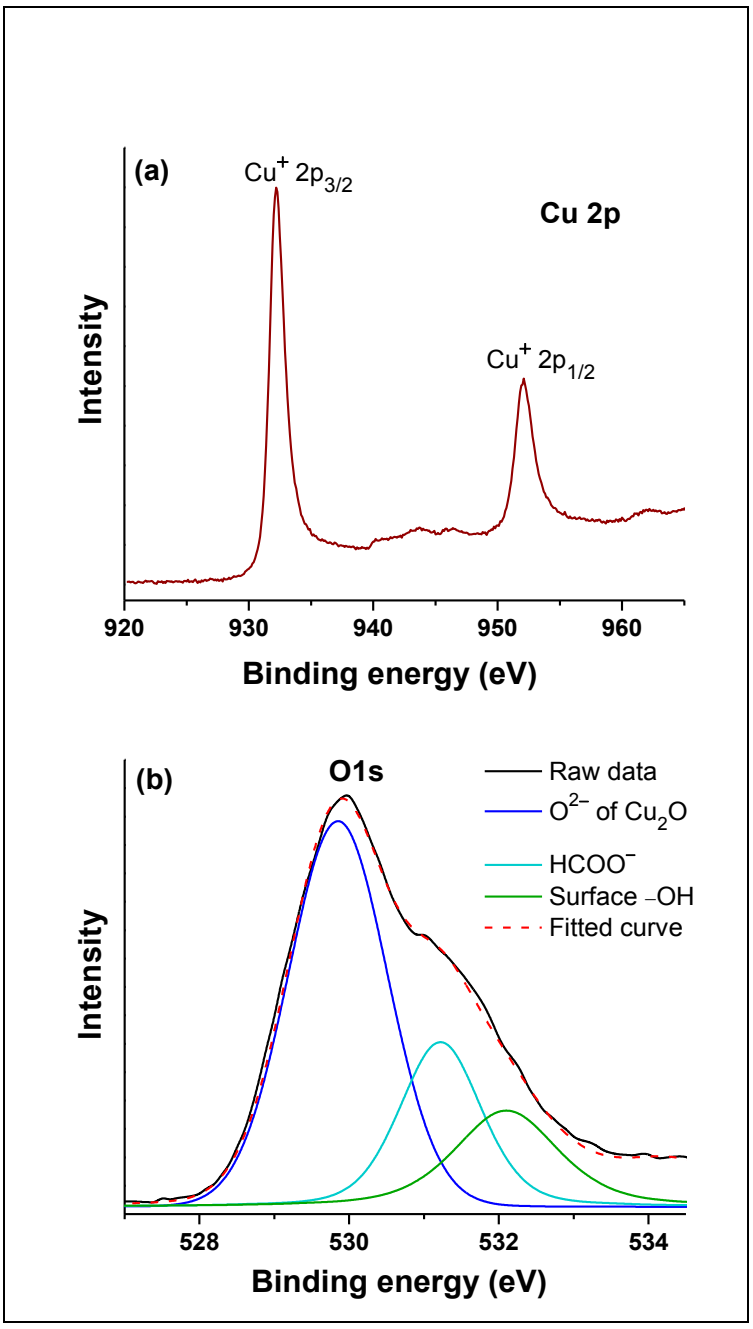

Figure IV.6*. XPS spectra of the fresh catalyst Cu_2O@ARF. (a) high resolution Cu2p spectrum showing two distinct peaks for Cu^+ and (b) deconvoluted high resolution O1s spectrum consistent with the presence of Cu_2O chemical state*

IV.3.3. Catalytic activity of Cu_2O@ARF nanocomposite in three–component click reaction

The three–component click reaction was optimized by using phenyl acetylene, benzyl bromide and sodium azide as the model reaction. At first the reaction was carried out in water at 60 ^oC in the presence of 50 mg of catalyst (Cu_2O@ARF). The isolated yield of the desired triazole was 75% (Table IV.1, entry 1). Then we tried the same reaction in a solvent system water:acetonitrile (v/v 1:1), assuming the poor solubility of reactant in water. The yield was 95% (entry 2). To overcome the solubility problem we tried a phase transfer agent, sodium dodecylsulfate (SDS) (entry 3). Now we tried the reaction with less quantity of the catalyst (25 mg) which afforded the triazole in same yield (entry 4). Further decrease in the catalyst amount (15 mg) resulted in lower yield (81%, entry 5). When the reaction was performed for 1 h keeping other aspects unchanged (25 mg of catalyst and temperature 60 ^oC), the yield of triazole obtained was 94% (entry 6). When the reaction temperature was kept at 40 ^oC, an excellent yield (92%, entry 7) was obtained within 1 h. Moreover the catalytic system was found highly efficient in carrying out the reaction even at room temperature to afford 92% product yield within 1 h (entry 8). The reaction furnished the product in only 18% yield in absence of catalyst indicates the prominent role of the heterogeneous catalyst Cu_2O@ARF (entry 9).

Table IV.1. Optimization of the reaction conditions for the synthesis of triazole[a]

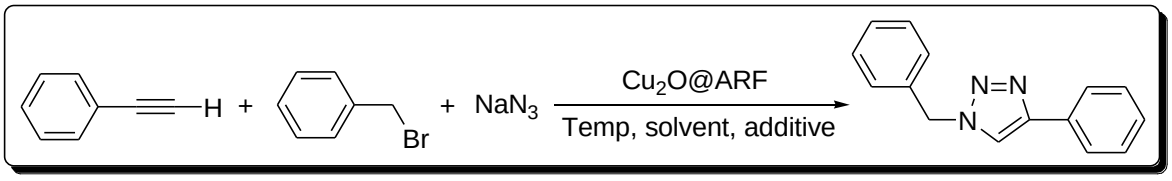

Entry	Solvent	Amount of SDS (mol%)	Temp (^oC)	Time (h)	Catalyst (mg)	Yield (%)[a]
1	Water	Nil	60	2	50	75
2	Water :CH_3CN (1:1)	Nil	60	2	50	95
3	Water	10	60	2	50	95
4	Water	10	60	2	25	95
5	Water	10	60	2	15	81
6	Water	10	60	1	25	94
7	Water	10	40	1	25	92
8	**Water**	**10**	**RT**	**1**	**25**	**92**
9[b]	Water	10	RT	10	Nil	18

[a]*Triazole obtained after purification by column chromatography.* [b]*Reaction performed without any catalyst Cu_2O@ARF.*

Due to high catalytic activity of the Cu_2O@ARF nanocomposite in three–component AAC reaction which leads to the 1,4–disubstituted triazoles selectively in aqueous medium, the optimized conditions (as in Table IV.1, entry 8) was extended to a series of terminal alkynes and alkyl halides. The products are presented in Table IV.2. Aromatic alkynes with benzyl bromide and sodium azide produced the corresponding triazole derivatives in good to excellent yields (**1a–1c** and **1e–1o**). The reactivity of the aliphatic alkyne was found to be somewhat lower than the aromatic alkynes (**1d**). The variation of the alkyl halide such as allyl bromide and cinnamyl bromide successfully produced corresponding triazole derivatives (product **1e** to **1i**). Using 2−bromo−1−(4–chlorophenyl)ethanone produced triazole derivative (**1j**) in 82% yield. In the case of 1–chloromethyl naphthalene the reaction required heating at 40 ^oC for 3 h (**1k**), as the reaction did not proceed at room temperature. Other substituted benzyl bromide bearing halides (bromo, iodo) in the benzene ring also produced the corresponding triazole derivatives in good yield (**1l–1o**). All triazole derivatives (**1a–1o**) were characterized by FT–IR, ^1H–NMR, ^{13}C–NMR spectra and also by checking melting points for solid compounds.

Table IV.2. Cu_2O@ARF catalyzed three–component click reaction in aqueous and aerobic conditions at room temperature[a]

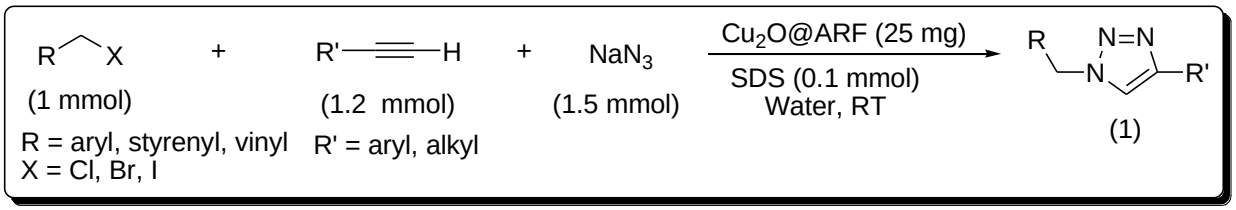

Entry	Alkyl Halide	Alkyne	Time (h)	Product	Yield [a] (%)
1	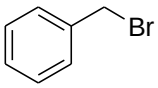	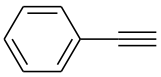	1	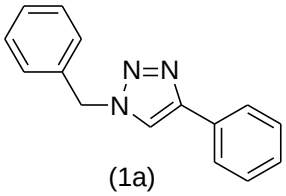 (1a)	92
2	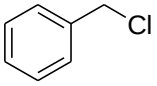	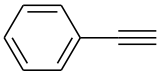	1.5	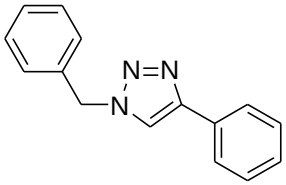	87
3	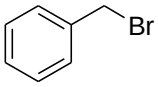		1	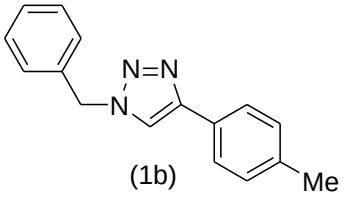 (1b)	87
4	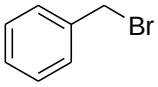	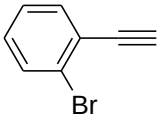	1.5	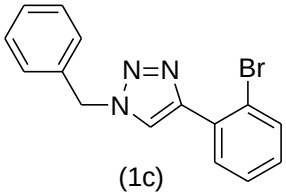 (1c)	88
5	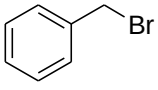	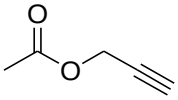	8	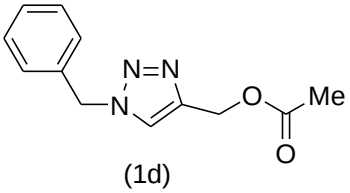 (1d)	68
6	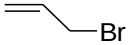	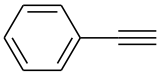	1	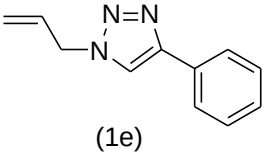 (1e)	83

7	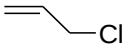	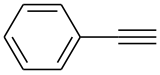	1.5	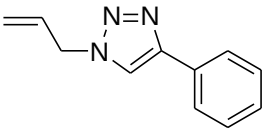	82
8	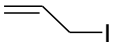	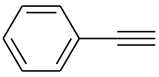	1	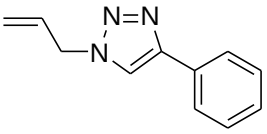	85
9	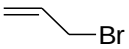		1	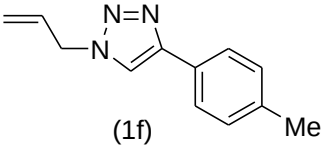 (1f)	82
10	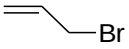	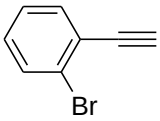	1.5	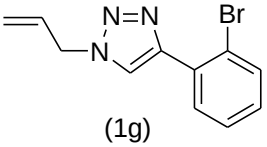 (1g)	86
11	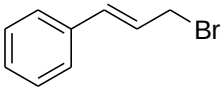	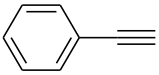	1	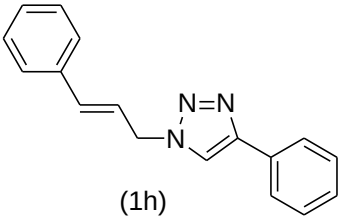 (1h)	84
12	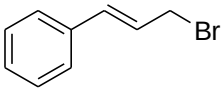		1	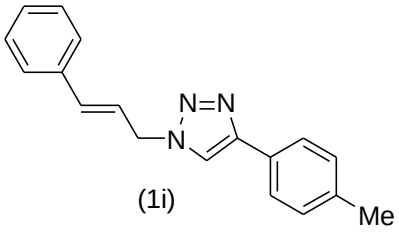 (1i)	82
13	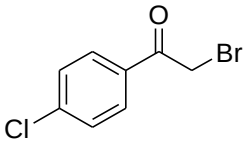	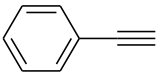	1	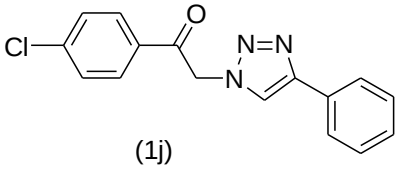 (1j)	82
14[b]	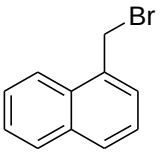	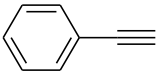	3	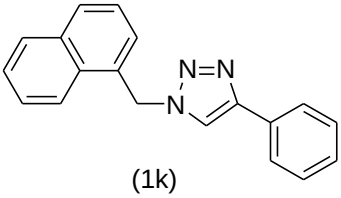 (1k)	79

15	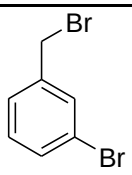	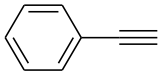	3	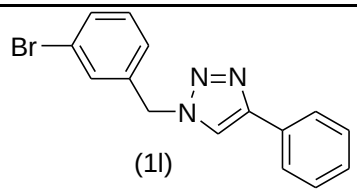 (1l)	78
16	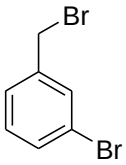	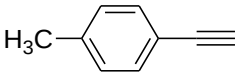	3	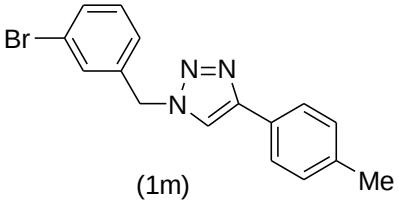 (1m)	76
17	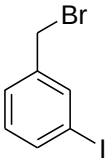	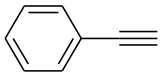	3	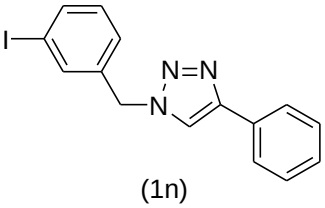 (1n)	76
18	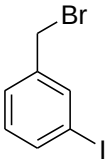		3	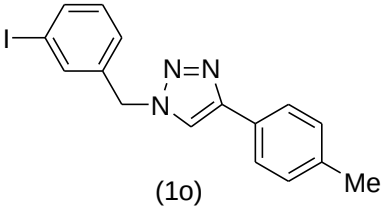 (1o)	74

(a) Isolated yield of the product after purification through column chromatography. (b) Initially alkyl chloride and sodium azide were stirred at 40 ^{o}C for 1 h and then alkyne was added and continued the reaction at room temperature for 2 h. [Entries 1a, 1b, 1c, 1d, 1e, 1f, 1h, 1i was synthesized by the presenting author and the rest of the entries were performed by the co–author S. Ghosh. The present author also extended the reaction scope towards the synthesis of bio–active triazole moiety (2).]

IV.3.4. Reusability and stability of Cu_2O@ARF.

We performed recycling experiments in the model click reaction of benzyl bromide, phenyl acetylene and sodium azide to check the reusability of the heterogeneous catalyst Cu_2O@ARF. To meet the purpose the reaction was carried out under the optimized reaction conditions i.e. Table IV.1, entry 8. The catalyst beads was filtered off, washed with water (4 x 5 mL) and acetone (3 x 5 mL) and dried under vacuum after completion of the reaction. Then the catalyst was reused for the second run. Figure IV.7 shows no significant drop in the yield of the product upto four consecutive runs. The copper content in Cu_2O@ARF before and after the recycle runs was measured by the ICP−AES analyses. Which shows the copper content in Cu_2O@ARF (25

mg) was 0.0042 mmol before the reaction, while that was found after the 1st and 3rd run 0.0039 and 0.0037 mmol respectively. Thus no significant leaching of copper has occurred from the polymeric resin surface during the reaction which supports its heterogeneous catalytic activity towards the reaction.

Table IV.3. Cu–content of fresh Cu_2O@ARF (25 mg) or recovered after 1st and 3rd run found by ICP−AES analyses

Sl No	Time (h)	Cu–content (mmol)
1st Run	1	0.0042
2nd Run	1	0.0039
3rd Run	1	–
4th Run	1	0.0037

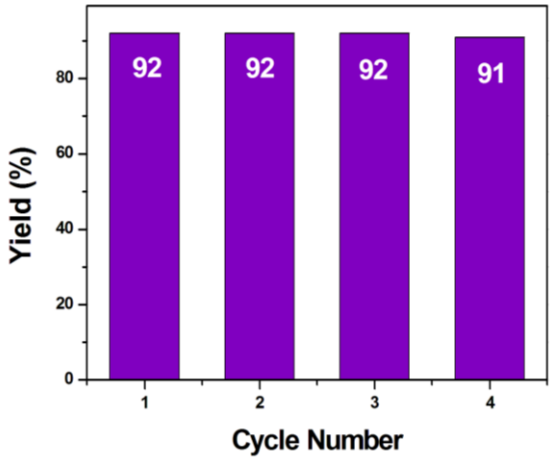

Figure IV.7. *Recyclability of the heterogeneous catalyst Cu_2O@ARF*

We performed mid–way filtration tests taking the reactants benzyl bromide, phenyl acetylene and sodium azide to establish about leaching of metallic species during the catalysis process, as done in case of various heterogeneous catalysis.[57] Here we at first carried out the reaction taking three sets of experiments with the catalyst for 10, 20 and 40 min. Then we filtered off the catalyst in each case and continued the reaction sets without the catalyst for 50, 40 and 20 min respectively. In each experiment, aliquots were taken at different times before and after filtering the catalyst. These were analyzed by HPLC to find the yield of triazole in each case. It

was found that while there was increasing conversion of triazole 34.63% (after 10 min), 53.80% (after 20 min) and 77.00% (after 40 min) in the presence of catalyst, whereas after removing the catalyst and carrying out the reaction for rest of 1h in all the three sets showed no appreciable changes in triazole conversion (Figure IV.8).

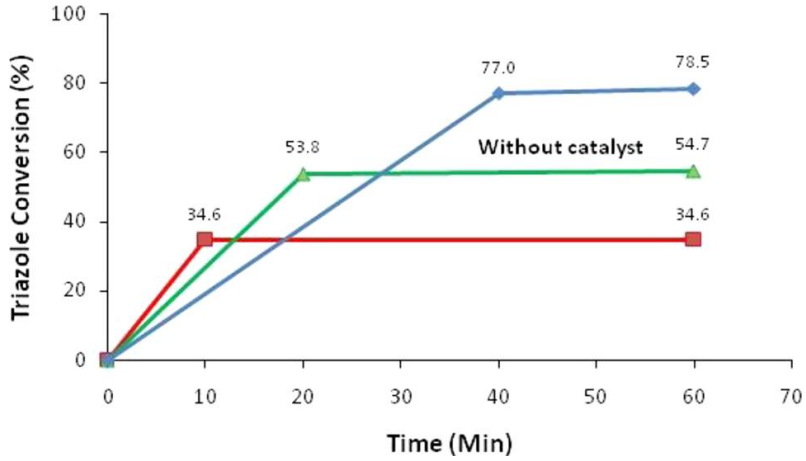

Figure IV.8. *Three sets of mid–way filtration test at different time intervals showing conversion of triazole with or without the catalyst*

The XRD pattern of the recovered catalysts after 1st and 4th run were found almost similar as observed in the fresh catalyst before the reaction which indicates no change in the nature of the composite during catalytic process (Figure IV.9). The peak positions with relative intensities of the recovered catalysts after 1st and 4th run are shown in blue and red lines, respectively.

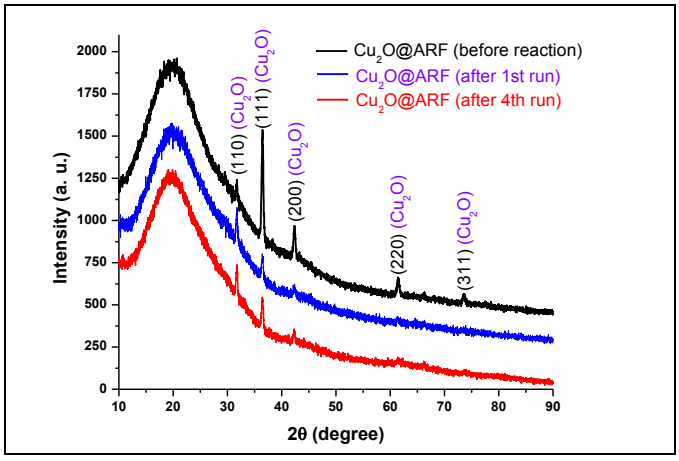

Figure IV.9. *Comparison of Powder XRD of Cu_2O@ARF before and after the reaction.*

IV.3.5. Plausible mechanism

The proposed mechanism of the click reaction is believed to be similar as illustrated for other Cu(I) catalysts.[58] The formation of alkynyl copper intermediate from alkyne in the presence of Cu(I) species of Cu_2O@ARF occurs which subsequently undergoes cycloaddition with the *in situ* formed alkyl azide from alkyl halide and sodium azide to form the intermediate (A) (Figure IV.10). Finally, the desired triazole product is formed by the protonation of C─Cu bond.[59]

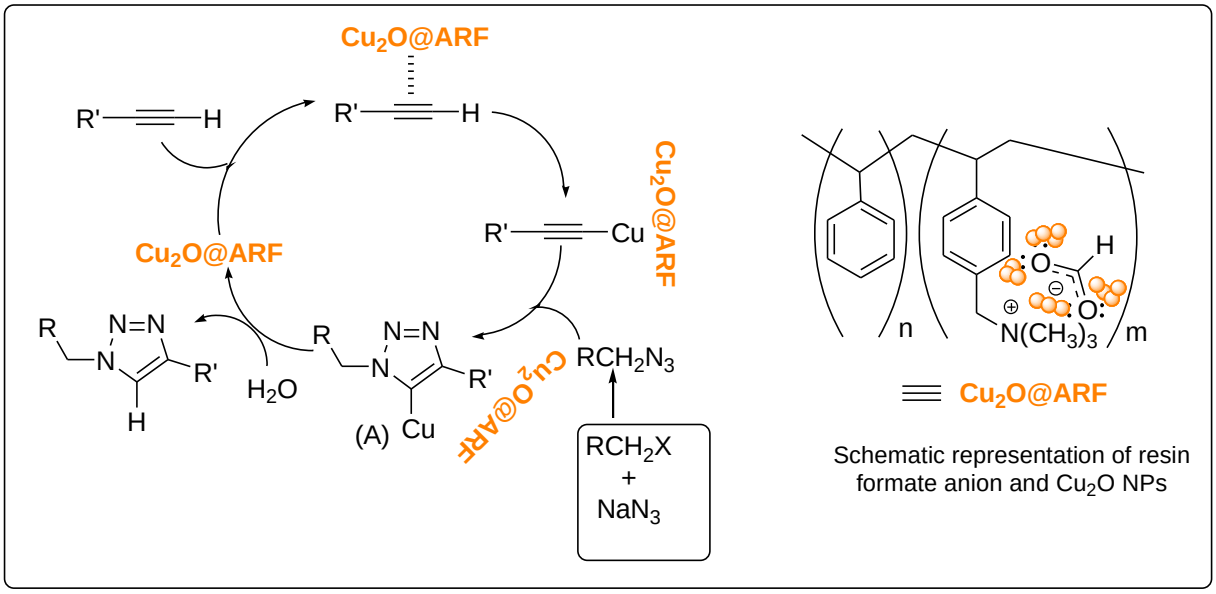

Figure IV.10. *Proposed mechanism of the three–component click reaction using Cu_2O@ARF.*

IV.3.6. Comparison of catalytic activity

Comparison of catalytic activity in terms of turn over frequency (TOF) was done. Other heterogeneous catalysts that are reported, performed three–component AAC reaction under same conditions (i.e, water as solvent system and room temperature). Our catalyst exhibits nearly double TOF (219 h^{-1}) value as compared to existing systems (maximum 120 h^{-1}) which is shown in Table IV.4. This is due to the availability of more active Cu_2O NPs available on the surface of amberlite resins which is stabilized by the formate ions.

Table IV.4. Comparison of on–water triazole synthesis using some Cu(I) catalytic systems and our catalyst at room temperature (without reducing source).

Entry	Catalyst	Mol% (Cu)	TOF (h^{-1})	Reference
1	PS–C22–CuI	0.6	11	38
2	Cu(NHC)Cl	0.5	120	40
3	H_4N^+–tagged SIPr–Cu(I)	5.0	6.53	41
4	**Cu_2O@ARF**	**0.42**	**219**	**Present work**

IV.3.7. Application towards the synthesis of bio–active 1,2,3–triazole

We further extended the scope of the catalyst to synthesize molecule possessing biological activity. Cu_2O@ARF was employed in a reaction to synthesize a triazole–based dithiocarbamate (**2**) moiety, which possess antitumor activity.[23] The reaction was conducted using a combination of benzyl bromide, pyrolidine–1–carbodithioate and sodium azide and Cu_2O@ARF as catalyst in aqueous medium at 35 ^oC, which formed compound (**2**) in 82% yield (Scheme IV.12). Thus our catalytic system Cu_2O@ARF can be also useful in the synthesis of triazole–based drug molecules.

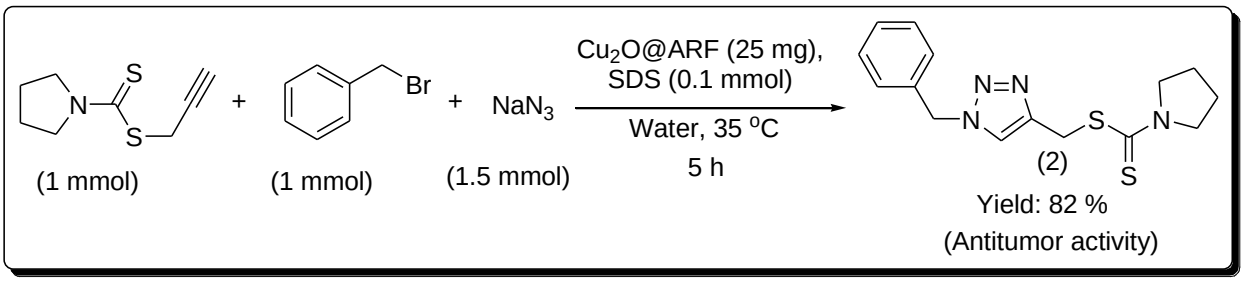

Scheme IV.12. *Synthesis of pharmaceutically active triazole compound (**2**) catalyzed by Cu_2O@ARF.*

IV.4. CONCLUSIONS

In conclusion we have demonstrated Cu_2O@ARF as an efficient heterogeneous catalyst for the one–pot synthesis of a wide variety of 1,4–disubstituted–1,2,3–triazole *via* three–component click reaction of alkyl halide, terminal alkyne and sodium azide in water at room temperature. Moreover, TOF value has been found to be significantly high for Cu_2O@ARF as compared to other Cu(I)–based catalytic systems that worked under identical conditions to synthesize triazole. The enhanced catalytic performance of our catalytic system is due to the high surface area of Cu_2O NPs of average size ~5–7 nm. Also the counter formate anion stabilizes the distributions of Cu_2O NPs on the macroporous resin matrices. Aqueous reaction media,

ambient reaction conditions, high yields, wide substrate scope, application in the synthesis of dithiocarbamate based bio–active triazole compound possessing antitumor activity, easy recovery and recyclability of the catalyst are some notable features of the work.

IV.5. EXPERIMENTAL SECTION

IV.5.1. General information

All the reagents were purchased from Sigma–Aldrich and used directly without further purification. The solvents were purchased from commercial suppliers and used after distillation. All the products were purified by column chromatography on 60–120 mesh silica gels (SRL, India). For tlc, Merck plates coated with silica gel 60, F_{254} were used. The ^{1}H & ^{13}C NMR spectra were recorded at 300 MHz and 75 MHz respectively on Bruker AV 300 spectrometer in $CDCl_3$. Splitting patterns of protons were described as s (singlet), d (doublet), t (triplet), dd (doublet of doublet) and m (multiplet). Chemical shifts were reported in parts per million (δ) relative to TMS as internal standard. *J* values (coupling constant) were reported in Hz (Hertz). ^{13}C NMR spectra were recorded with complete proton decoupling ($CDCl_3$: δ 77.0 ppm). The powder X–ray diffraction (PXRD) patterns were recorded using the Rigaku Smart Lab (9 kW) diffractometer using CuKα radiation. ICP–AES was measured in inductively coupled plasma atomic emission spectrometry of Spectro Ciros Vision, Germany. X–ray photoelectron spectroscopy (XPS) analysis was done with a PHI 5000 Versa probe II XPS system having a source of Al Kα and charge neutralizer at room temperature with a base pressure at 6 x 10^{-10} mbar. Transmission electron microscopy (TEM) of the samples was carried out with a Tecnai G2 30ST (FEI Company) operating at 300 kV and a JEOL JEM–2100F (FEG) operating at 200 kV. To prepare the TEM sample, a small amount of grinded sample was first dispersed in acetone. Then one small drop of this dispersion was applied to a carbon–coated molybdenum grid. HPLC analyses were carried out using HPLC of Agilent Technologies, 1260 Infinity series. Column: ZORBAX RX–SIL (5 μm, 4.6 x 150 mm). Eluent: 10% ethyl acetate in *n*–hexane (flow rate: 2 mL/minute).

IV.5.2. General procedure (GP1) for the synthesis of 1,2,3–triazole derivatives (1a–1o)

In a 25 mL round bottom flask, a mixture of alkyl halide (1 mmol), terminal alkyne (1.2 mmol), sodium azide (1.5 mmol), SDS (0.1 mmol), Cu_2O@ARF (25 mg) was taken and then 2 mL of water was added to it. The whole mixture was stirred at room temperature with a small

magnetic bar under open air. The reaction was monitored by tlc and after satisfactory conversion, the catalyst was filtered off, washed with ethyl acetate (3 x 5 mL). The organic part was separated out from the aqueous part and then collected by passing over anhydrous Na_2SO_4. Evaporation of the solvent afforded the crude product, which was purified by column chromatography over silica gel.

IV.5.3. Procedure for recovery and reusability of the catalyst [Cu_2O@ARF]

After completion of the reaction the reaction mixture was filtered off to separate the resin catalyst. Then ethyl acetate (3 x 5 mL) was passed through the filter paper and collected in the filtrate. The filtrate part was taken out and kept for product isolation. The partially washed resin beads in the filter paper were again subjected for washing with water (4 x 5 mL) and acetone (3 x 5 mL). The semidried resin beads were then completely dried under vacuum before applying in the next run.

IV.5.4. Procedure for the synthesis (GP2) of dithiocarbamate based triazole compound 2

In a 25 mL round bottom flask, a mixture of S–propargyl pyrrolidine–1–carbodithioate (1 mmol), benzyl bromide (1 mmol), sodium azide (1.5 mmol), SDS (0.1 mmol), Cu_2O@ARF (25 mg) was taken in water (2 mL) and stirred with bar magnet at 35 ^oC for 5 h under open air. At this tlc showed disappearance of starting material and therefore the reaction was stopped and the catalyst was filtered off as above. The resin beads were washed with ethyl acetate (3 x 5 mL) and combined organic layer, as above was separated out from water, dried over anhydrous Na_2SO_4. Evaporating the organic solvent afforded an oily residue which was purified by column chromatography over silica gel and eluting with light petroleum:ethyl acetate (4:1) afforded the desire triazole derivative (**2**) as a dark yellow solid, yield 82%, mp: 70–72 ^oC (lit.[23] 73–74 ^oC).

IV.5.5. Physical properties and spectroscopic data of triazole compounds

1–Benzyl–4–phenyl–1*H*–1,2,3–triazole (Table IV.2, entry 1a) [60]

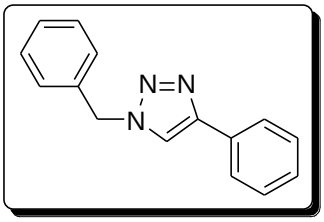

This compound was obtained by following the general procedure **GP1** in 92% yield as a white crystalline product having melting point 128−130 °C (lit.[60] 128−129 °C). The NMR data obtained are in quite agreement with that reported in the literature previously.[60] **^{1}H NMR ($CDCl_3$, 300 MHz)** δ 5.48 (s, 2H), 7.20–7.33 (m, 8H), 7.58 (s, 1H), 7.70–7.72 (m, 2H); **^{13}C NMR ($CDCl_3$, 75 MHz)** δ 54.1, 119.5, 125.6, 128.0, 128.1, 128.70, 128.73, 129.1, 130.5, 134.6, 148.1; **FT−IR (KBr)** ν_{max} 3127, 3029, 2925, 1638, 1465, 1358, 1226, 1074, 766, 729, 692 cm^{-1}.

1–Benzyl–4–(*p*–tolyl)–1*H*–1,2,3–triazole (Table IV.2, entry 1b)[61]

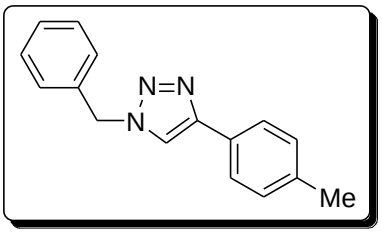

It was synthesized by following the general procedure **GP1** as a white crystalline solid having melting point 152–154 °C (lit.[61] 154–155 °C) and the yield obtained was 87%. The NMR data also corroborates that found in the literature.[61] **^{1}H NMR ($CDCl_3$, 300 MHz)** δ 2.26 (s, 3H), 5.44 (s, 2H), 7.10 (d, *J* = 7.8 Hz, 2H), 7.19–7.28 (m, 5H), 7.53 (s, 1H), 7.60 (d, *J* = 8.1 Hz, 2H); **^{13}C NMR ($CDCl_3$, 75 MHz)** δ 21.2, 54.1, 119.1, 125.5, 127.7, 128.0, 128.6, 129.0, 129.4, 134.7, 137.9, 148.2; **FT−IR (KBr)** ν_{max} 3143, 2921, 1631, 1496, 1431, 1224, 1047, 825, 794, 721, 510 cm^{-1}.

1–Benzyl–4–(2–bromophenyl)–1*H*–1,2,3–triazole (Table IV.2, entry 1c) [62]

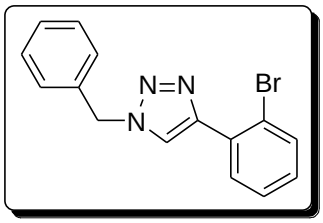

This compound was obtained by following the general procedure **GP1** in 88% yield as a pale yellow crystal having melting point 80–82 ^{o}C. The NMR data obtained are in quite agreement with that reported in the literature previously.[62] **^{1}H NMR ($CDCl_3$, 300 MHz)** δ 5.58 (s, 2H), 7.12–7.18 (m, 1H), 7.25–7.39 (m, 6H), 7.60 (d, *J* = 7.8, 1H), 8.08–8.15 (m, 2H); **^{13}C NMR ($CDCl_3$, 75 MHz)** δ 54.2, 121.2, 123.1, 127.7, 127.9, 128.7, 129.1, 129.4, 130.6, 131.3, 133.5, 134.7, 145.7; **FT−IR (KBr)** ν_{max} 3119, 3083, 2950, 1632, 1496, 1460, 1418, 1227, 1026, 831, 756, 730, 700 cm^{-1}.

(1–Benzyl–1*H*–1,2,3–triazol–4–yl) methyl acetate (Table IV.2, entry 1d) [63]

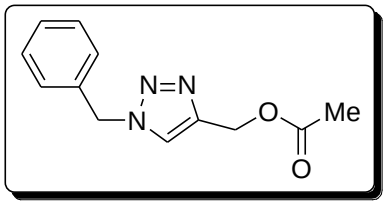

This compound was obtained by following the general procedure **GP1** in 68% yield as a light yellow viscous oil. The spectral data obtained are also in agreement with the literature.[63] **^{1}H NMR ($CDCl_3$, 300 MHz)** δ 2.20 (s, 3H), 5.16 (s, 2H), 5.51 (s, 2H), 7.26–7.36 (m, 5H), 7.72 (s, 1H); **^{13}C NMR ($CDCl_3$, 75 MHz)** δ 20.8, 54.1, 57.6, 123.7, 128.1, 128.7, 129.1, 134.5, 143.1, 170.7; **FT−IR (Neat)** ν_{max} 3143, 2960, 1740, 1643, 1455, 1367, 1230, 1035, 722 cm^{-1}.

1–Allyl–4–phenyl–1*H*–1,2,3–triazole (Table IV.2, entry 1e) [60]

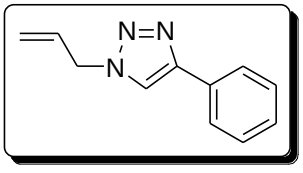

This compound was obtained by following the general procedure **GP1** in 83% yield as a white crystalline solid having melting point 62–64 ^{o}C (lit.[60] 57–58 ^{o}C). The NMR data obtained are in

quite agreement with that reported in the literature previously.[60] **^{1}H NMR ($CDCl_3$, 300 MHz)** δ 4.96 (d, *J* = 5.7 Hz, 2H), 5.26–5.34 (m, 2H), 5.95–6.08 (m, 1H), 7.28–7.42 (m, 3H), 7.76–7.83 (m, 3H); **^{13}C NMR ($CDCl_3$, 75 MHz)** δ 52.7, 119.7, 120.1, 125.7, 128.1, 128.8, 130.6, 131.3, 147.9; **FT−IR (KBr)** ν_{max} 3122, 3093, 2945, 1640, 1420, 1224, 1077, 991, 943, 763, 691 cm^{-1}.

1–Allyl–4–(*p*–tolyl)–1*H*–1,2,3–triazole (Table IV.2, entry 1f)[64]

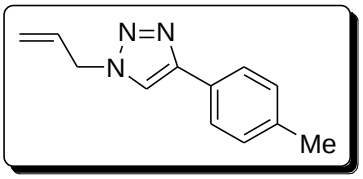

Obtained by following the general procedure **GP1** in 82% yield as a pale yellow solid having melting point 88–90 °C. The NMR data obtained are in quite agreement with that reported in the literature previously.[64] **^{1}H NMR ($CDCl_3$, 300 MHz)** δ 2.37 (s, 3H), 4.98–5.00 (m, 2H), 5.29–5.38 (m, 2H), 5.98–6.12 (m, 1H), 7.21–7.27 (m, 2H), 7.69–7.72 (m, 3H); **^{13}C NMR ($CDCl_3$, 75 MHz)** δ 21.3, 52.7, 119.1, 120.1, 125.6, 127.8, 129.5, 131.4, 138.0, 148.1; **FT−IR (KBr)** ν_{max} 3102, 3043, 2946, 1643, 1632, 1456, 1432, 1225, 1050, 947, 816, 776, 521 cm^{-1}.

1–Allyl–4–(2–bromophenyl)–1*H*–1,2,3–triazole (Table IV.2, entry 1g)

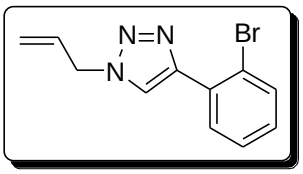

This compound was obtained by following the general procedure **GP1** as a viscous oil and the yield was 86%. **^{1}H NMR ($CDCl_3$, 300 MHz)** δ 5.04 (d, *J* = 6 Hz), 5.29–5.38 (m, 2H), 6.0–6.13 (m, 1H), 7.15–7.20 (m, 1H), 7.36–7.40 (m, 1H), 7.61–7.64 (m, 1H), 8.08–8.12 (m, 1H), 8.21 (s, 1H); **^{13}C NMR ($CDCl_3$, 75 MHz)** δ 52.7, 120.1, 121.2, 123.0, 127.7, 129.4, 130.6, 131.2, 131.3, 133.5, 145.5; **FT–IR (Neat)** ν_{max} 3154, 2930, 1646, 1466, 1420, 1225, 1050, 760 cm^{-1}.

1–(*E*)–Cinnamyl–4–phenyl–1*H*–1,2,3–triazole (Table IV.2, entry 1h)[65]

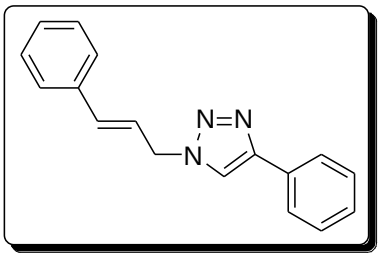

This compound was obtained by following the general procedure **GP1** in 84% yield as a white solid having melting point 136–138 ^{o}C (lit.[65] 132–134 ^{o}C). The NMR data obtained are in quite agreement with that reported in the literature previously.[65] **^{1}H NMR (CDCl$_3$, 300 MHz)** δ 5.12 (dd, *J* = 0.9 & 6.3 Hz, 2H), 6.29–6.41 (m, 1H), 6.66 (d, *J* = 15.9 Hz, 1H), 7.24–7.47 (m, 8H), 7.79–7.83 (m, 3H); **^{13}C NMR (CDCl$_3$, 75 MHz)** δ 52.4, 119.5, 121.9, 125.7, 126.8, 128.2, 128.6, 128.8, 128.9, 130.6, 135.4, 135.5, 148.1; **FT–IR (KBr)** ν_{max} 3132, 3022, 2951, 1608, 1464, 1449, 1220, 1075, 975, 760, 695 cm^{-1}.

1–(*E*)–Cinnamyl–4–(*p*–tolyl)–1*H*–1,2,3–triazole (Table IV.2, entry 1i)

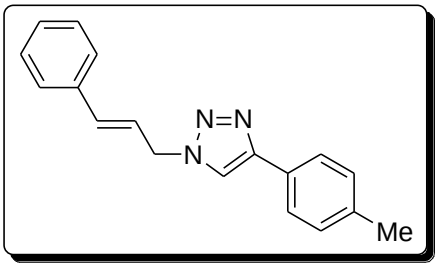

This compound was synthesized by following the general procedure **GP1** in 82% yield as a white solid having melting point 145–147 ^{o}C. **^{1}H NMR (CDCl$_3$, 300 MHz)** δ 2.35 (s, 3H), 5.12 (dd, *J* = 0.9 & 6.3 Hz, 2H), 6.30–6.39 (m, 1H), 6.67 (d, *J* = 15.6 Hz, 1H), 7.19–7.36 (m, 7H), 7.37–7.75 (m, 3H); **^{13}C NMR (CDCl$_3$, 75 MHz)** δ 21.3, 52.4, 119.1, 122, 125.6, 126.7, 127.8, 128.5, 128.7, 129.5, 135.3, 135.5, 138, 148.1; **FT–IR (KBr)** ν_{max} 3131, 2977, 1656, 1469, 1431, 1229, 1050, 823, 697 cm^{-1}.

1–(4–Chlorophenacyl)–4–phenyl–1*H*–1,2,3–triazole (Table IV.2, entry 1j) [66]

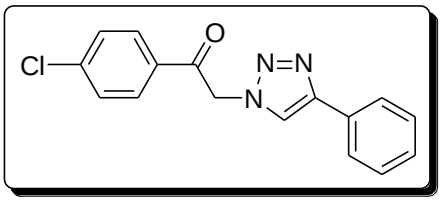

This compound was obtained by following the general procedure **GP1** in 82% yield as a white solid having melting point 104–106 ^{o}C (lit.[67] 106–109 ^{o}C). The NMR data obtained are in quite agreement with that reported in the literature previously.[66] **^{1}H NMR (d^{6}–DMSO, 300 MHz)** δ 6.24 (s, 2H), 7.35–7.37 (m, 1H), 7.44–7.49 (m, 2H), 7.67–7.69 (m, 2H), 7.86–7.89 (m, 2H), 8.10–8.12 (m, 2H); **^{13}C NMR (d^{6}–DMSO, 75 MHz)** δ 56.4, 123.5, 125.6, 128.4, 129.5, 129.6, 130.6, 131.1, 133.2, 139.7, 146.8, 191.8; **FT–IR (KBr)** ν_{max} 3147, 2953, 1710, 1587, 1400, 1230, 1090, 818, 763, 562 cm^{-1}.

1–(Naphthalen–1–ylmethyl)–4–phenyl–1*H*–1,2,3–triazole (Table IV.2, entry 1k) [44]

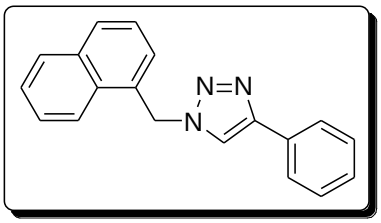

This compound was obtained by following the general procedure **GP1** as a white solid having melting point 135 ^{o}C and the yield was 79%. The NMR data obtained are in quite agreement with the literature.[44] **^{1}H NMR ($CDCl_3$, 300 MHz)** δ 5.96 (s, 2H), 7.22–7.35 (m, 3H), 7.38–7.51 (m, 5H), 7.70–7.72 (m, 2H), 7.87–7.89 (m, 2H), 7.97–7.99 (m 1H); **^{13}C NMR ($CDCl_3$, 75 MHz)** δ 54.4, 119.6, 123.9, 125.4, 125.7, 126.5, 127.4, 127.8, 128.1, 128.8, 129.0, 129.9, 130.1, 130.5, 131.2, 134.0, 148.0; **FT–IR (KBr)** ν_{max} 3118, 3088, 1632, 1511, 1400, 1214, 1083, 778, 693, 537 cm^{-1}.

1–(3–Bromobenzyl)–4–phenyl–1*H*–1,2,3–triazole (Table IV.2, entry 1l) [68]

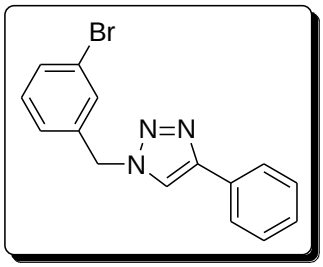

This compound was obtained by following the general procedure **GP1** in 78% yield as a light yellow solid having melting point 92–94 ^{o}C (lit.[68] 91–93 ^{o}C). The NMR data obtained are in quite agreement with that reported in the literature previously.[68] **^{1}H NMR ($CDCl_3$, 300 MHz)** δ 5.54 (s, 2H), 7.23–7.50 (m, 7H), 7.70–7.88 (m, 3H); **^{13}C NMR ($CDCl_3$, 75 MHz)** δ 53.5, 119.6, 123.1, 125.7, 126.6, 128.3, 128.9, 130.3, 130.7, 131.0, 132.0, 136.9, 148.5; **FT–IR (KBr)** ν_{max} 3079, 1656, 1632, 1572, 1417, 834, 751, 693 cm^{-1}.

1–(3–Bromobenzyl)–4–(*p*–tolyl)–1*H*–1,2,3–triazole (Table IV.2, entry 1m)

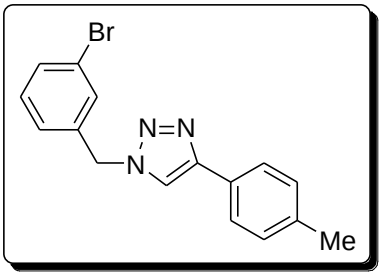

This compound was obtained by following the general procedure **GP1** in 76% yield as a light yellow solid having melting point 132–134 ^{o}C. **^{1}H NMR ($CDCl_3$, 300 MHz)** δ 2.37 (s, 3H), 5.53 (s, 2H), 7.20–7.28 (m, 4H), 7.46–7.51 (m, 2H), 7.65–7.71 (m, 3H); **^{13}C NMR ($CDCl_3$, 75 MHz)** δ 21.3, 53.4, 119.1, 123.1, 125.7, 126.5, 127.6, 129.5, 130.7, 131.0, 131.9, 137.0, 138.1, 148.6; **FT–IR (KBr)** ν_{max} 3041, 2951, 1656, 1650, 1628, 1422, 815, 761 cm^{-1}.

1–(3–Iodobenzyl)–4–phenyl–1*H*–1,2,3–triazole (Table IV.2, entry 1n)[67]

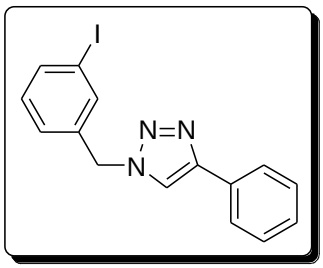

This compound was obtained by following the general procedure **GP1** in 76% yield as a white solid having melting point 120–122 ^{o}C (lit.[67] 122–124 ^{o}C). The NMR data obtained are in quite agreement with that reported in the literature previously.[67] **^{1}H NMR ($CDCl_3$, 300 MHz)** δ 5.50 (s, 2H), 7.08–7.13 (m, 1H), 7.24–7.35 (m, 2H), 7.38–7.43 (m, 2H), 7.67–7.70 (m, 3H), 7.79–7.82 (m, 2H); **^{13}C NMR ($CDCl_3$, 75 MHz)** δ 53.3, 94.8, 119.5, 125.8, 127.2, 128.3, 128.9, 130.4, 130.8, 136.8, 136.9, 137.9, 148.4; **FT–IR (KBr)** ν_{max} 3107, 2970, 2949, 1581, 1423, 1352, 1220, 1004, 786, 684 cm^{-1}.

1–(3–Iodobenzyl)–4–(*p*–tolyl)–1*H*–1,2,3–triazole (Table IV.2, entry 1o)

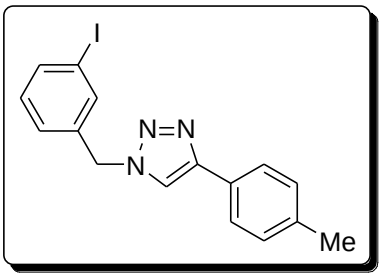

It was synthesized by following the general procedure **GP1** in 76% yield as a white solid having melting point 130 ^{o}C. **^{1}H NMR ($CDCl_3$, 300 MHz)** δ 2.37 (s, 3H), 5.50 (s, 2H), 7.08–7.13 (m, 1H), 7.20–7.26 (m, 3H), 7.65–7.71 (m, 5H); **^{13}C NMR ($CDCl_3$, 75 MHz)** δ 21.2, 53.3, 94.7, 119.1, 125.7, 127.2, 127.6, 129.5, 130.8, 136.9, 137, 137. 9, 138.1, 148.5; **FT–IR (KBr)** ν_{max} 3132, 2975, 2940, 1570, 1421, 1344, 1225, 1081, 820, 763 cm^{-1}.

(1–Benzyl–1*H*–1,2,3–triazol–4–yl)methyl pyrrolidine–1–carbodithioate (Scheme IV.12, Triazole compound 2) [23]

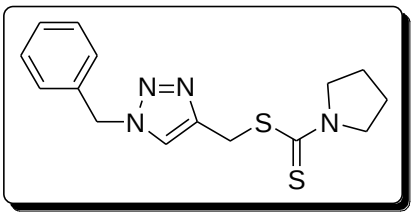

This compound was obtained by following the general procedure **GP2** in 74% yield as a dark yellow solid having melting point 70–72 ^{o}C (lit.[23] 73–74 ^{o}C). The NMR data obtained are in quite agreement with that reported in the literature previously.[23] **^{1}H NMR ($CDCl_3$, 300 MHz)** δ 1.98–2.08 (m, 4H), 3.62 (t, *J* = 6.6 Hz, 2H), 3.91 (t, *J* = 6.9 Hz, 2H), 4.67 (s, 2H), 5.48 (s, 2H),

7.25–7.27 (m, 2H), 7.34–7.37 (m, 3H), 7.63 (s, 1H); **^{13}C NMR ($CDCl_3$, 75 MHz)** δ 24.3, 26.1, 31.1, 50.6, 54.1, 55.2, 122.8, 128.0, 128.7, 129.1, 134.7, 144.8, 191.7; **FT–IR (KBr)** ν_{max} 3142, 2949, 1466, 1438, 1335, 1214, 1156, 1003, 955, 712 cm^{-1}.

IV.5.6. Scanned copies of ^{1}H NMR, ^{13}C NMR of Table IV.5, Entry 1d and triazole compound 2

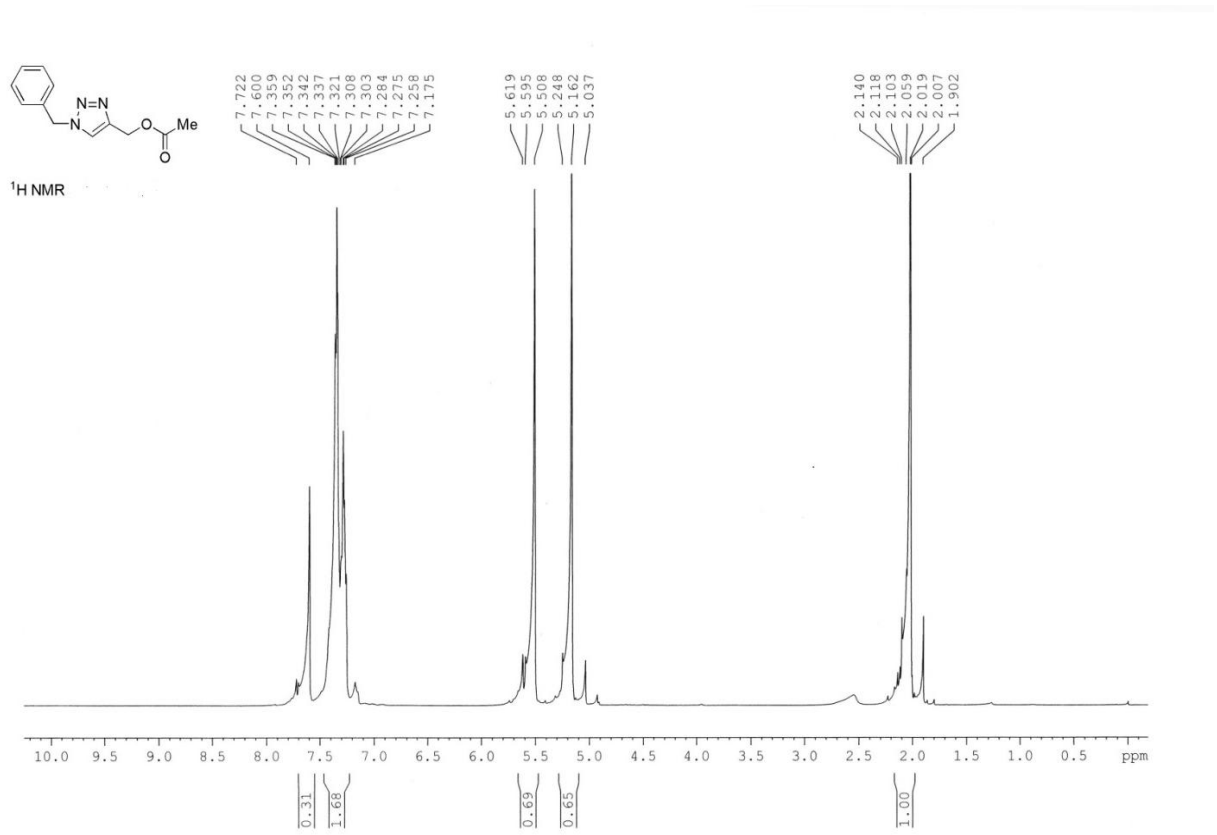

Figure IV.11. *^{1}H NMR spectra of (1–Benzyl–1H–1,2,3–triazol–4–yl) methyl acetate*

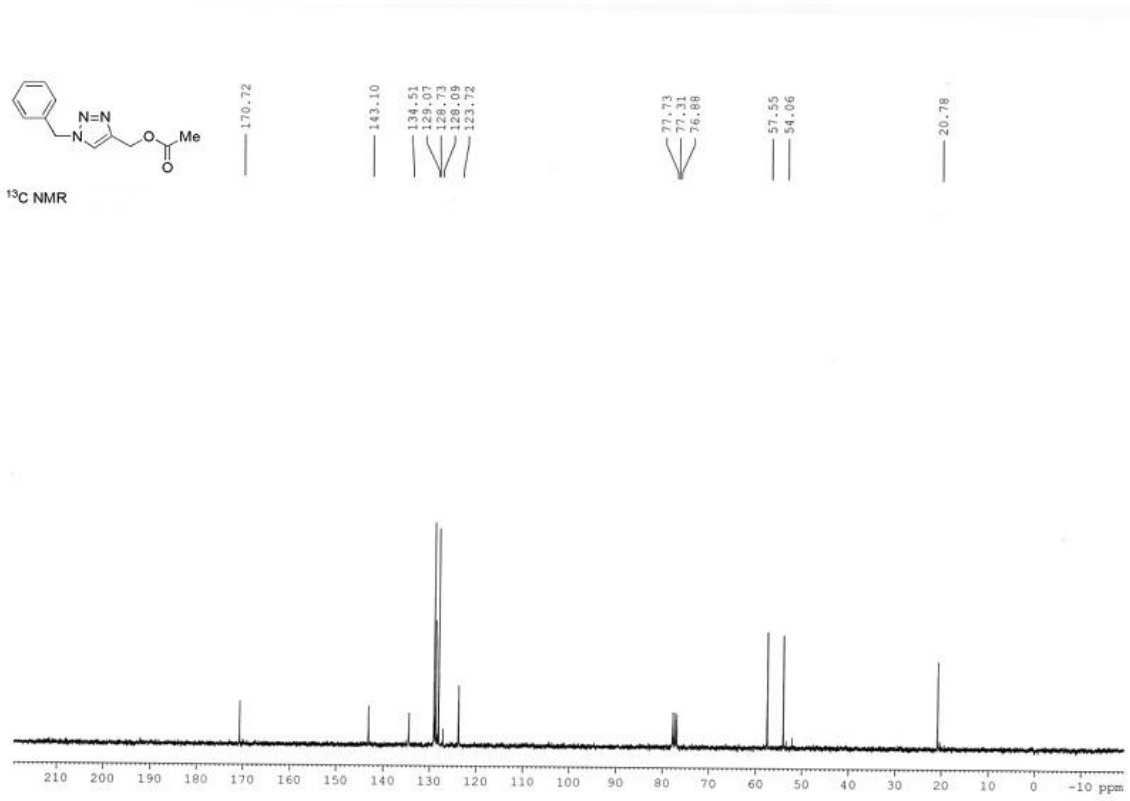

Figure IV.12. *^{13}C NMR spectra of (1–Benzyl–1H–1,2,3–triazol–4–yl) methyl acetate*

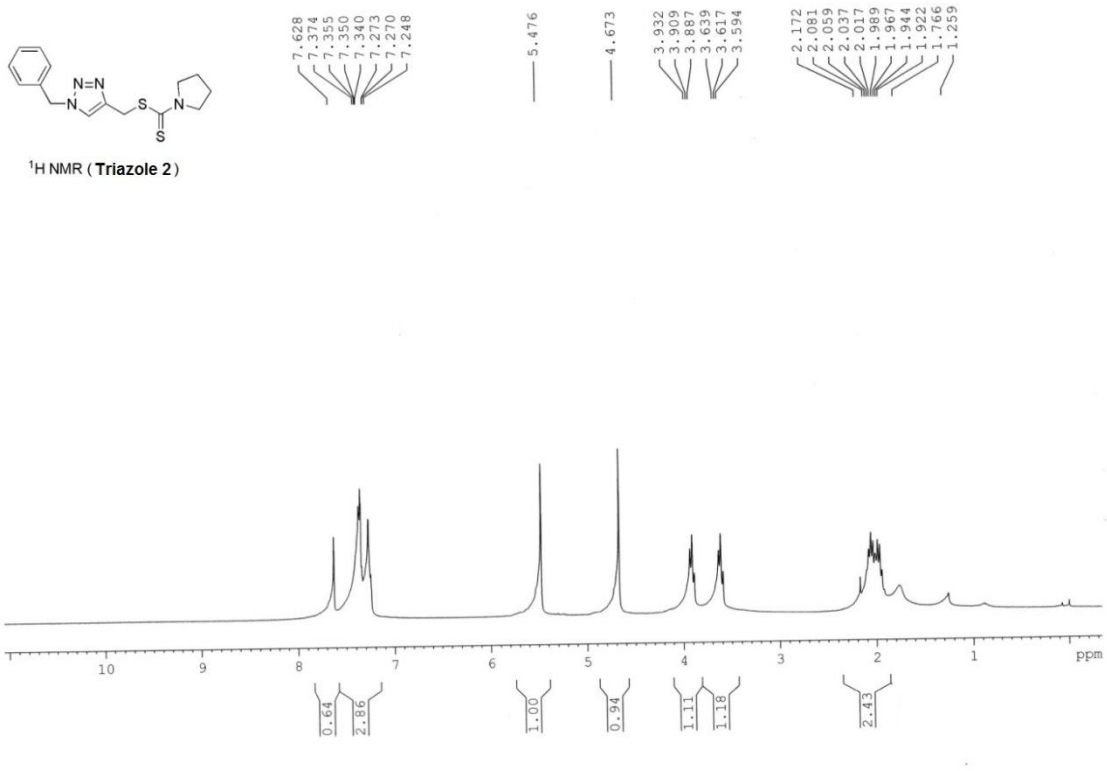

Figure IV.13. *[1]H NMR spectra of (1–Benzyl–1H–1,2,3–triazol–4–yl)methyl pyrrolidine–1–carbodithioate*

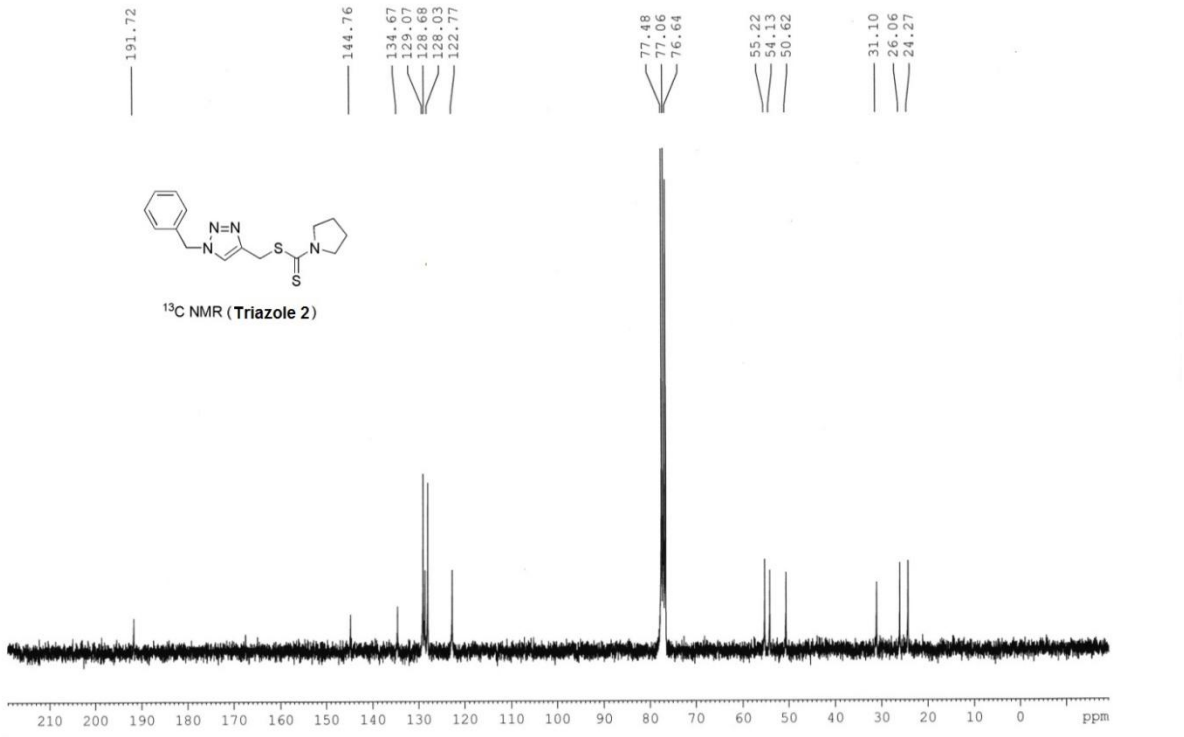

Figure IV.14. *^{13}C NMR spectra of (1–Benzyl–1H–1,2,3–triazol–4–yl)methyl pyrrolidine–1–carbodithioate*

IV.6. References

References are given in BIBLIOGRAPHY under Chapter IV page no. 139–143.

BIBLIOGRAPHY

CHAPTER I

1. a) J. R. Cremlyn, *An Introduction to Organosulfur Chemistry*, John Wiley and Sons: Chichester, 1996. b) W. W. Whittman, *Organosulfur Chemistry*, Oxford University Press: New York, 1995. c) C. B. P. Page, *Organosulfur Chemistry I* & II, Springer: Berlin, 1999.
2. E. M. Peach, S. Patai, Eds. *The Chemistry of the Thiol Group*, John Wiley & Sons: London, 1979, p 721.
3. P. D. Curran, M. B. Trost, I. Fleming, Eds. *Comprehensive Organic Synthesis*, Pergamon: New York, 1991; Vol. 4, pp 715–831.
4. F. R. Hartley, S. G. Murray, W. Levason, H. E. Soutter, C. A. McAuliffe, *Inorg. Chim. Acta*, 1979, **35**, 265–277.
5. T. Kondo, T. Mitsudo, *Chem. Rev.*, 2000, **100**, 3205–3220.
6. L. Wang, W. He, Z. Yu, *Chem. Soc. Rev.*, 2013, **42**, 599–621.
7. T. Kondo, S. Uenoyama, K. Fujita, T. Mitsudo, *J. Am. Chem. Soc*., 1999, **121**, 482.
8. Z. Jin, B. Xu, G. B. Hammond, *Eur. J. Org. Chem.*, 2010, 168–173.
9. S. Poulain, S. Julien, E. Dunach, *Tetrahedron Letters*, 2005, **46**, 7077–7079.
10. T. Kitamura, J. Matsuyuki, H. Taniguchi, *J. Chem. Soc. Perkin Trans.*, 1991, 1607–1608.
11. S. Usugi, H. Yorimitsu, H. Shinokubo, K. Oshima, *Org. Lett.*, 2004, **6**, 601–603.
12. N. Yamagiwa, Y. Suto, Y. Torisawa, *Bioorg. Med. Chem. Lett.*, 2007, **17**, 6197–6201.
13. S. Kundu, B. Roy, B. Basu, *Beilstein J. Org. Chem.*, 2014, **10**, 26–33.
14. A. M. Pasqualeti, P. –Y. Olu, M. Chatenet, F. H. B. Lima, *ACS Catal.*, 2015, **5**, 2778.
15. R. N. d'Alnoncourt, M. Friedrich, E. Kunkes, D. Rosenthal, F. Girgsdies, B. Zhang, L. Shao, M. Schuster, M. Behrens, R. Schlogl, *J. Catal*., 2014, **317**, 220.
16. H. Tsukamoto, R. Suzuki, Y. Kondo, *J. Comb. Chem.*, 2006, **8**, 289.
17. J. A. Murphy, S. Zhou, C. T. Tuttle, F. Schoenebeck, M. Mohan, S. R. Park, L. E. A. Berlouis, D. W. Thomson, *Angew. Chem. Int. Ed.*, 2007, **46**, 5178.
18. R. –J. Tang, Q. Heb, L. Yang, *Chem. Commun.*, 2015, **51**, 5925.

19. Y. Oudart, V. Artero, J. Pecaut, M. Fontecave, *Inorg. Chem.*, 2006, **45**, 4334–4336.
20. R. Kannan, N. Pillarsetty, H. Gali, J. T. Hoffman, L. C. Barnes, S. S. Jurisson, J. C. Smith, W. A. Volkert, *Inorg. Chem.*, 2011, **50**, 6210–6219.
21. M. Knorr, F. Guyon, A. Khatyr, C. Strohmann, M. Allain, M. S.Aly, A. Lapprand, D. Fortin, D. P. Harvey, *Inorg. Chem.*, 2012, **51**, 9917–9934.
22. J. –R. Li, X. –H. Bu, J. Jiao, W. –P. Du, X. –H. Xu, R. –H. Zhang, *Dalton Trans.*, 2005, 464–474.
23. W. Levason, G. Reid, W. Zhang, *Dalton Trans.*, 2011, **40**, 8491–8506.
24. M. Dieguez, A. Ruiz, C. Claver, M. M. Pereira, A. M. d'A. Rocha Gonsalves, *J. Chem. Soc*., *Dalton Trans*., 1998, 3517–3522.
25. A. Cohen, A. Yeori, I. Goldberg, M. Kol, *Inorg. Chem.*, 2007, **46**, 8114–8116.
26. A. Ishii, T. Toda, N. Nakata, T. Matsuo, *J. Am. Chem. Soc.*, 2009, **131**, 13566–13567.
27. G. –J. M. Meppelder, K. Beckerle, R. Manivannan, B. Lian, G. Raabe, T. P. Spaniol, J. Okuda, *Chem. Asian J.*, 2008, **3**, 1312 – 1323.
28. J. –P. Collin, D. Jouvenot, M. Koizumi, J. –P. Sauvage, *Inorganica Chimica Acta*, 2007, **360**, 923–930.
29. S. E. Dann, A. R. J. Genge, W. Levason, G. Reid, *J. Chem.* Soc., *Dalton Trans.*, 1996, 4471–4478.
30. X. –H. Bu, W. Chen, W. –F. Hou, M. Du, R. –H. Zhang, F. Brisse, *Inorg. Chem.*, 2002, **41**, 3477–3482.
31. M. O. Awaleh, F. Baril–Robert, C. Reber, A. Badia, F. Brisse, *Inorg. Chem.*, 2008, **47**, 2964–2974.
32. W. E. V. Zyl, J. M. Lopez–de-Luzuriaga, A. A. Mohamed, R. J. Staples, J. P. Fackler, *Inorg. Chem.*, 2002, **41**, 4579.
33. C. King, J. C.Wang, M. N. I. Khan, J. P. Fackler, *Inorg. Chem.*, 1989, **28**, 2145.
34. (a) M. A. Rawashdeh–Omary, M. A. Omary, H. H. Patterson, J. P. Fackler, *J. Am. Chem. Soc.*, 2001, **123**, 11237; (b) M. A. Rawashdeh–Omary, M. A. Omary, H. H. Patterson, *J. Am. Chem. Soc.*, 2000, **122**, 10371.
35. a) P. D. Harvey, M. Knorr, *Macromol. Rapid Commun.*, 2010, **31**, 808–826; b) A. Bonnot, C. Strohmann, M. Knorr, P. D. Harvey, *J Clust. Sci.*, 2014, **25**, 261–275; c) G. Rajput, M. K. Yadav, M. G. B. Drew, N. Singh, *Inorg. Chem.*, 2015, **54**, 2572−2579.

36. a) M. K. Rofouei, T. Hashempur, *Analytical Sciences*, 2008, **24**, x229–x230; b) R. Kinghat, M. Knorr, Y. Rousselin, M. M. Kubicki, *Acta Cryst.*, 2014, **E70**, 547–549; c) P. R. Martinez–Alanis, B. N. S. Eguia, V. M. Ugalde–Saldivar, I. Regla, P. Demare, G. Aullon, I. Castillo, *Chem. Eur. J.*, 2013, **19**, 6067–6079; d) J. P. Safko, J. E. Kuperstock, S. M. McCullough, A. M. Noviello, X. Li, J. P. Killarney, C. Murphy, H. H. Patterson, C. A. Baysec, R. D. Pike, *Dalton Trans.*, 2012, **41**, 11663–11674.
37. a) I. –H. Park, H. J. Kim, S. S. Lee, *Cryst. Eng. Comm.*, 2012, **14**, 4589; b) J. Zhang, Y. –S. Xue, Y. –Z. Li, H. –B. Du, X. –Z. You, *Cryst. Eng. Comm.*, 2011, **13**, 2578; c) T. H. Kim, Y. W. Shin, J. H. Jung, J. S. Kim, J. Kim, *Angew. Chem. Int. Ed.*, 2008, **47**, 685.
38. J. Zhou, G. –Q. Bian, J. Dai, Y. Zhang, Q. –Y. Zhu, W. Lu, *Inorg. Chem.*, 2006, **45**, 8486.
39. J. S. Filippo, L. E. Zyontz, J. Potenza, *Inorg. Chem.*, 1975, **14**, 166.
40. a) M. Knorr, F. Guyon, A. Khatyr, C. Strohmann, M. Allain, S. M. Aly, A. Lapprand, D. Fortin, P. D. Harvey, *Inorg. Chem.*, 2012, **51**, 9917–9934; b) J. –R. Li, X. –H. Bu, *Eur. J. Inorg. Chem.*, 2008, 27–40.
41. T. H. Kim, G. Park, Y. W. Shin, K. –M. Park, M. Y. Choi, J. Kim, *Bull. Korean Chem. Soc.*, 2008, **29**, 499.
42. C. Xie, L. Zhou, W. Feng, J. Wang, W. Chen, *J. Mol. Struct.*, 2009, **921**, 132.
43. H. N. Peindy, F. Guyon, A. Khatyr, M. Knorr, C. Strohmann, *Eur. J. Inorg. Chem.*, 2007, 1823–1828.
44. M. Knorr, F. Guyon, M. M. Kubicki, Y. Rousselin, S. M. Aly, P. D. Harvey, *New J. Chem.*, 2011, **35**, 1184.
45. A. Raghuvanshi, M. Knorr, L. Knauer, C. Strohmann, S. Boullanger, V. Moutarlier, L. Viau, *Inorganic Chemistry*, 2019, **58**, 5753–5775.
46. F. Wang, H. Fu, Y. Jiang, Y. Zhao, *Green Chem.*, 2008, **10**, 452–456.
47. S. Saha, K. Biswas, B. Basu, *Tetrahedron Lett.*, 2018, **59**, 2541–2545.

CHAPTER II

1. D. R. Buckle, C. J. M. Rockell, H. Smith, B. A. Spicer, *J. Med. Chem.*, 1986, **29**, 2269.

2. R. Alvarez, S. Velazquez, A. San–Felix, S. Aquaro, E. De Clercq, C. F. Perno, A. Karlsson, J. Balzarini, M. J. Camarasa, *J. Med. Chem*., 1994, **37**, 4185.
3. M. J. Genin, D. A. Allwine, D. J. Anderson, M. R. Barbachyn, D. E. Emmert, S. A. Garmon, D. R. Graber, K. C. Grega, J. B. Hester, D. K. Hutchinson, J. Morris, R. J. Reischer, C. W. Ford, G. E. Zurenko, J. C. Hamel, R. D. Schaadt, D. Stapert, B. H. Yagi, *J. Med. Chem.*, 2000, **43**, 953.
4. L. L. Brockunier, E. R. Parmee, H. O. Ok, M. R. Candelore, M. A. Cascieri, L. F. Colwell, L. Deng, W. P. Feeney, M. J. Forrest, G. J. Hom, D. E. MacIntyre, L. Tota, M. J. Wyvratt, M. H. Fisher, A. E. Weber, *Bioorg. Med. Chem. Lett.*, 2000, **10**, 2111.
5. R. Huisgen, 1,3–Dipolar Cycloaddition Chemistry; Padwa, A., Ed.; Wiley: New York, 198, Chapter 1, pp-1–176.
6. L. Liang, D. Astruc, *Coordination Chemistry Reviews*, 2011, **255**, 2933.
7. A. Taher, D. Nandi, R. U. Islam, M. Choudhury, K. Mallick, *RSC Adv*., 2015, **5**, 47275.
8. S. Brase, C. Gil, K. Knepper, V . Zimmerman, *Angew Chem. Int. Ed*., 2005, **44**, 5188.
9. E. Haldon, M. C. Nicasio, P. J. Perez, *Org. Biomol. Chem.*, 2015, **13**, 9528–9550.
10. J. C. Bayon, C. Claver, A. M. Masdeu–Bulto, *Coord. Chem. Re*v., 1999, **73**, 193–195.
11. Z. Mirjafarya, L. Ahmadib, M. Moradib, H. Saeidian, *RSC Adv*, **2015**, 5, 78038.
12. F. Wang, H. Fu, Y. Jiang, Y. Zhao, *Green. Chem*., 2008, **10**, 452.
13. S. –Q. Bai, L. L. Koh, T. S. A. Hor, *Inorg. Chem.*, 2009, **48**, 1207.
14. S. –Q. Bai, L. Jiang, J. –L. Zuo, T. S. A. Hor, *Dalton Trans*., 2013, **42**, 11319.
15. L. Jiang, Z. Wang, S. –Q. Bai , T. S. A. Hor, *Dalton Trans*., 2013, **42**, 9437.
16. (a) G. Rajput, M. K. Yadav, M. G. B. Drew, N. Singh, *Inorg. Chem*., 2015, **54**, 2572; (b) A. Bonnot, C. Strohmann, M. Knorr, P. D. Harvey, *J. Clust. Sci*., 2014, **25**, 261; (c) P. D. Harvey, M. Knorr, *Macromol. Rapid Commun.*, 2010, **31**, 808.
17. (a) M. Knorr, F. Guyon, A. Khatyr, C. Strohmann, M. Allain, S. M. Aly, A. Lapprand, D. L. Fortin, P. D. Harvey, *Inorg. Chem.*, 2012, **51**, 9917; (b) J. –R. Li, X. –H. Bu, *Eur. J. Inorg. Chem.*, 2008, 27.
18. (a) E. C. Brown, I. B. –Nahum, J. T. York, N. W. Aboelella, W. B. Tolham, *Inorg. Chem*., 2007, **46**, 486; (b) R. P. Houser, V. G. Young Jr., W. B. Tolman, *J. Am. Chem. Soc*., 1996, **118**, 2101.
19. S. Kundu, B. Roy, B. Basu, *Beilstein J. Org. Chem*., 2014, **10**, 26.
20. F. Alonso, Y. Moglie, G. Radivoy, M. Yusa, *Synlett*, 2012, **23**, A–D.

21. P. V. Chavan, K. S. Pandit, U. V. Desai, M. A. Kulkarnia, P. P. Wadgaonkar, *RSC Adv*., 2014, **4**, 42137.
22. F. Friscourt, G. –J. Boons, *Org. Lett*., 2011, **12**, 4936.
23. R. B. Nasir Baig, R. S. Varma, *Green Chem*., 2012, **14**, 625.
24. M. Liu, O. Reiser, *Org. Lett*., 2011, **13**, 1102.
25. J. –A. Shin, Y. –G. Lim, K. –H. Lee, *J. Org. Chem*., 2012, **77**, 4117.
26. B. Sreedhar, P. S. Reddy, *Synth. Commun*., 2007, **37**, 805.
27. Z. Ganda, Z. Novak, *Dalton Trans.*, 2010, **39**, 726–729.
28. Y. Zhou, T. Lecourt, L. Micouin, *Angew. Chem. Int. Ed.*, 2010, **49**, 2607–2610.
29. D. Wang, N. Li, M. Zhao, W. Shi, C. Ma, B. Chen, *Green Chem*., 2010, **12**, 2120–2123.
30. D. Mendoza–Espinosa, G. Negron–Silva, L. Lomas–Romero, A. Gutierrez–Carrillo, R. Santillan, *Synth. Commun.*, 2014, **44**, 807.

CHAPTER III

1. E. Vessally, *RSC Adv*., 2016, **6**, 18619–18631.
2. E. Vessally, L. Edjlali, A. Hosseinian, A. Bekhradnia, M. D. Esrafili, *RSC Adv.*, 2016, **6**, 49730–49746.
3. I. Matsuda, J. Sakakibara, H. Nagashima, *Tetrahedron Lett.*, 1991, **32**, 7431–7434.
4. a) M. Konishi, H. Ohkuma, T. Tsuno, T. Oki, G. D. Van Duyne, J. Clardy, *J. Am. Chem. Soc.*, 1990, **112**, 3715–3716; b) G. Dyker, *Angew. Chem. Int. Ed.*, 1999, **38**, 1698–1712.
5. P. H. Yu, B. A. Davis, A. A. Boulton, *J. Med. Chem.*, 1992, **35**, 3705–3713.
6. J. J. Chen, D. M. Swope, K. Dashtipour, *Clin Ther.*, 2007, **29**, 1825–1849.
7. M. Baranyi, P. F. Porceddu, F. Goloncser, *Mol Neurodegenerat.*, 2016, **11**, 6.
8. S. Ma, B. Wu, X. Jiang, *J. Org. Chem*., 2005, **70**, 2588–2593.
9. I. Matsuda, J. Sakakibara, H. Nagashima, *Tetrahedron Lett*., 1991, **50**, 7431–7434.
10. Y. Yamamoto, H. Hayashi, T. Saigoku, H. Nishiyama, *J. Am. Chem. Soc*., 2005, **127**, 10804–10805.
11. D. F. Harvey, D. M. Sigano, *J. Org. Chem*., 1996, **61**, 2268–2272.
12. A. Furstner, H. Szillat, F. Stelzer, *J. Am. Chem. Soc*., 2000, **122**, 6785–6786.
13. H. Li, J. Liu, B. Yan, Y. Li., *Tetrahedron Lett*., 2009, **50**, 2353–2357.

14. B. Yan, Y. Liu, *Org. Lett.*, 2007, **9**, 4323–4326.
15. D. S. Ermolat'ev, J. B. Bariwal, H. P. L. Steenackers, S. C. J. De Keersmaecker, E. V. V. Eycken, *Angew. Chem.*, 2010, **122**, 9655–9658.
16. E.–S. Lee, H.–S. Yeom, J.–H. Hwang, S. Shin, *Eur. J. Org. Chem.*, 2007, 3503–3507.
17. F. Xiao, Y. Chen, Y. Liu, J. Wang, *Tetrahedron*, 2008, **64**, 2755–2761.
18. J. B. Bariwal, D. S. Ermolat'ev, T. N. Glasnov, K. V. Hecke, V. P. Mehta, V. Meervelt, C. O. Kappe, E. V. V. Eycken, *Org. Lett.*, 2010, **12**, 2774–2777.
19. G. Magueur, B. Crousse, D. Bonnet–Delpon, *Tetrahedron Lett.*, 2005, **46**, 2219–2221.
20. P. Kaur, G. Shakya, H. Sun, Y. Pan, G. Li, *Org Biomol Chem.*, 2010, **8**, 1091–1096.
21. F. Colombo, M. Benaglia, S. Orlandi, F. Usuelli, G. Celentano, *J. Org. Chem.*, 2006, **71**, 2064–2070.
22. C. Wei, C. –J. Li, *J. Am. Chem. Soc.*, 2002, **124**, 5638–5639.
23. T. Murai, Y. Mutoh, Y. Ohta, M. Murakami, *J. Am. Chem.Soc.*, 2004, **126**, 5968–5969.
24. (a) L. Zani, S. Alesi, P. G. Cozzi, C. Bolm, *J. Org. Chem.*, 2006, **71**, 1558–1562; (b) G. Huang, Z. Yin, X. Zhang, *Chem.–Eur. J.*, 2013, **19**, 11992–11998; (c) G. Blay, E. Ceballos, A. Monle´on, J. R. Pedro, *Tetrahedron*., 2012, **68**, 2128–2134.
25. R. P. Herrera, E. Marques–Lopez, *Multicomponent Reactions: Concepts and Applications for Design and Synthesis, Hoboken, New Jersey: John Wiley & Sons Inc*., 2015, 94.
26. V. A. Peshkov, O. P. Pereshivko, E. V. V. Eycken, *Chem Soc Rev.*, 2012, **41**, 3790–3807.
27. S. B. Park, H. Alper, *Chem. Commun*., 2005, 1315–1317.
28. M. –T. Chen, O. Navarro, *Synlett*, 2013, **24**, 1190–1192.
29. C. Zhao, D. Seidel, *J. Am. Chem. Soc*., 2015, **137**, 4650–4653.
30. O. Prakash, H. Joshi, U. Kumar, A. K. Sharma, A. K. Singh, *Dalton Trans*., 2015, **44**, 1962–1968.
31. K. M. Reddy, N. S. Babu, I. Suryanarayana, P. S. Prasad, N. Lingaiah, *Tetrahedron Lett*., 2006, **47**, 7563–7566.
32. M. Trose, M. Dell'Acqua, T. Pedrazzini, V. Pirovano, E. Gallo, E. Rossi, A. Caselli, G. Abbiati, *J. Org. Chem*., 2014, **79**, 7311–7320.
33. A. Feiz, A. Barzgir, *Catal. Commun*., 2016, **73**, 88–92.

34. G. A. Price, A. K. Brisdon, K. R. Flower, R. G. Pritchard, P. Quayle, *Tetrahedron Lett*., 2014, **55**, 151–154.
35. M. Kidwai, V. Bansal, A. Kumar, S. Mozumdar, *Green Chem*., 2007, **9**, 742–745.
36. X. Huo, J. Li, B. Wang, H. Zhang, Z. Yang, X. She, P. Xi, *J. Mater. Chem. A*, 2013, **1**, 651–656.
37. T. Zeng, W. –W. Chen, C. M. Cirtiu, A. Moores, G. Sang, C. –J. Li, *Green Chem*., 2010, **12**, 570–573.
38. W. –W. Chen, H. –P. Bi, C. –J. Li, *Synlett*, 2010, 475–479.
39. K. Namitharan, K. Pitchumani, *Eur. J. Org. Chem*., 2010, 411–415.
40. J. S. Yadav, B. V. S. Reddy, A. V. H. Gopal, K. S. Patil, *Tettrahedron Lett.*, 2009, **50**, 3493–3496.
41. Y. Zhang, P. Li, M. Wang, L. Wang, *J. Org. Chem*., 2009, **74**, 4364–4367.
42. P. Li, L. Wang, *Chin. J. Chem*., 2005, **23**, 1076–1080.
43. E. –R., Bonfield, C. –J. Li, *Org. Biomol. Chem.*, 2007, **5**, 435–437.
44. S. Sakaguchi, T. Mizuta, M. Furuwan, T. Kubo, Y. Ishii, *Chem. Commun*., 2004, 1638–1639.
45. (a) W. L. Leong, J. J. Vittal, *Chem. Rev*., 2011, **111**, 688–764; (b) R. Mas–Balleste, J. Gomez–Herrero, F. Zamora, *Chem. Soc. Rev*., 2010, **39**, 4220–4233; (c) Z. Wang, G. Chen, K. Ding, *Chem. Rev*., 2009, **109**, 322–359.
46. (a) R. Peng, M. Li, D. Li, *Coord. Chem. Rev*., 2010, **254**, 1–18; (b) X. L. Wang, C. Qin, E. B. Wang, Z. M. Su, Y. G. Li, L. Xu, *Angew. Chem. Int. Ed*., 2006, **45**, 7411–7414; (c) A. J. Blake, N. R. Brooks, N. R. Champness, P. A. Cooke, A. M. Deveson, D. Fenske, P. Hubberstey, W. S. Li, M. Schroder, *J. Chem. Soc. DaltonTrans*., 1999, 2103–2110.
47. L. Jiang, Z. Wang, S. Q. Bai, T. S. A. Hor, *Dalton Trans.*, 2013, **42**, 9437–9443.
48. J. Rosales, J. M. Garcia, E. Ávila, T. González, D. S. Coll, E. Ocando–Mavárez, *Inorg. Chem Acta.*, 2017, **467**, 155–162.
49. N. –X. Zhu, C. –W. Zhao, J. Yang, X. –R. Wang, J. –P. Ma, Y. –B. Dong, *RSC Adv.*, 2016, **6**, 108645–108653.
50. E. Loukopoulos, M. Kallitsakis, N. Tsoureas, A. Abdul-Sada, N. F. Chilton, I. N. Lykakis, G. E. Kostakis, *Inorg. Chem.*, 2017, **56**, 4898−4910.

51. H. –B. Chen, Y. Zhaoa, Y. Liao, *RSC Adv*, 2015, **5**, 37737–37741.
52. S. Saha, K. Biswas, B. Basu, *Tetrahedron Lett.*, 2018, **59**, 2541–2545.
53. V. R. Akhmetova, N. S. Akhmadieva, G. M. Nurtdinovab, V. M. Yanybina, A. B. Glazyrinc, A. G. Ibragimova, *Russ. J. Gen. Chem.*, 2018, **88**, 1418–1424.
54. S. Kundu, B. Roy, B. Basu, *Beilstein J. Org. Chem*., 2014, **10**, 26.
55. M. Knorr, F. Guyon, A. Khatyr, C. Strohmann, M. Allain, S. M. Aly, A. Lapprand, D. Fortin, P. D. Harvey, *Inorg Chem*., 2012, **51**, 9917–9934.
56. H. N. Peindy, F. Guyon, A. Khatyr, M. Knorr, C. Strohmann, *Eur. J. Inorg. Chem.*, 2007, 1823.
57. J. –R. Li, X. – H. Bu, *Eur. J. Inorg. Chem.*, 2008, **27**.
58. J. Zhang, Y. –S. Xue, Y. –Z. Li, H. –B. Du, X. –Z. You, *Cryst Eng Comm.*, 2011, **13**, 2578–2585.
59. Bruker, *APEX3 and SAINT*, Bruker–Nonius AXS Inc., Madison, Wisconsin, USA, 2015.
60. G. M. Sheldrick, SHELXTL Version 2014/7.http://shelx.uniac.gwdg.de/SHELX/index.php.
61. B. Klaus, Diamond, Version 1.2c, University of Bonn, Germany, 1999.
62. J. S. Filipo Jr., L. E. Zyontz, J. Potenza, *Inorg. Chem*., 1975, **14**, 1667.
63. L. Shi, Y. –Q. Tu, M. Wang, F. –M. Zhang, C. A. Fan, *Org Lett.*, 2004, **6**, 1001.
64. S. Ghosh, K. Biswas, S. Bhattacharya, P. Ghosh, B. Basu, *Beilstein J. Org. Chem*., 2017, **13**, 552.
65. M. Gholinejad, F. Saadati, S. Shaybanizadeh, B. Pullithadathil, *RSC Adv.*, 2016, **6**, 4983.
66. H. –B. Chen, Y. Zhao, Y. Liao, *RSC Adv.*, 2015, **5**, 37737.
67. Y. Zhou, T. He, Z. Wang, *Arkivoc*, 2008, **xiii**, 80.

CHAPTER IV

1. S. G. Agalave, S. R. Maujan, V. S. Pore, *Chem. Asian. J*., 2016, **6**, 2696–2718.
2. C. –T. Zi, F. –Q. Xu, G. –T. Li, Y. Li, Z. –T. Ding, J. Zhou, Z. –H. Jiang, J. –M. Hu, *Molecules*, 2013, **18**, 13992–14012.
3. N. Pokhodylo, O. Shyyka, V. Matiychuk, *Med. Chem. Res*., 2014, **23**, 2426–2438.

4. M. J. Fray, D. J. Bull, C. L. Carr, *J. Med. Chem.*, 2001, **24**, 1951–1962.
5. R. Alvarez, S. Valazquez, A. San–Felix, S. Aquaro, E. D. Clercq, C. –F. Perno, A. Karlsson, J. Balzarini, M. J. Camarasa, *J. Med. Chem*., 1994, **37**, 4185–4194.
6. M. Whiting, J. Muldoon, Y. –C. Lin, S. M. Silverman, W. Lindstrom, A. J. Olson, H. C. Kolb, M. G. Fin, K. B. Sharpless, J. H. Elder, V. V. Fokin, *Angew. Chem. Int. Ed*., 2006, **45**, 1435–1439.
7. M. J. Genin, D. A. Allwine, D. J. Anderson, M. R. Barbachyn, D. E. Emmert, S. A. Garmon, D. R. Graber, K. C. Grega, J. B. Hester, D. K. Hutchinson, J. Morris, R. –J. Reischer, C. W. Ford, G. E. Zurneko, J. C. Hamel, R. D. Schaadt, D. Stapert, B. H. Yagi, *J. Med. Chem*., 2000, **43**, 953–970.
8. M. L. Conte, A. Marra, A. Chambery, S. S. Gurucha, G. S. Besra, A. Dondoni, *J. Org. Chem*., 2010, **75**, 6326–6336.
9. D. R. Buckle, D. J. Outred, C. J. M. Rockell, H. Smith, B. A. Spicer, *J. Med. Chem*., 1983, **26**, 251–254.
10. R. Raj, P. Singh, P. Singh, J. Gut, P. J. Rosenthal, V. Kumar, *Eur. J. Med. Chem*., 2013, **62**, 590–596.
11. M. Whiting, J. C. Trip, Y. –C. Lin, *J. Med. Chem*., 2006, **49**, 7697–7710.
12. G. Biagi, G. Dell'Omodarme, M. Ferretti, *Farmaco*., 1990, **45**, 1181–1192.
13. S. P. O. Assis, M. T. Silva, R. N. Oliveira, *Scientific World J*., 2012, 1–7.
14. C. J. Monceaux, C. Hirata–Fukae, P. C. H. Lam, M. M. Totrov, Y. Matsuoka, P. R. Carlier, *Biorg. Med. Chem. Lett*., 2011, **21**, 2992–3996.
15. J. L. Kelley, C. S. Kolbe, R. G. Davis, E. W. McLean, F. E. Soroko, B. R. Cooper, *J. Med. Chem*., 1995, **38**, 4131–4134.
16. A. Bahadoor, A. C. Castro, L. K. Chan, *U.S. Patent 0274654*, 2011.
17. S. –A. Poulsen, B. L. Willkinson, A. Innocenti, D. Vullo, C. T. Supuran, *Biorg. Med. Chem. Lett.*, 2008, **18**, 4624–4627.
18. R. Siles, Y. Kawasaki, P. Ross, E. Freire, *Biorg. Med. Chem. Lett.*, 2011, **21**, 5305–5309.
19. H. Hinou, R. Miyoshi, Y. Takasu, H. Kai, M. Kurogochi, S. Arika, X. –D. Gao, N. Miura, N. Fujitani, S. Omoto, T. Yoshinaga, T. Fujiwara, T. Noshi, H. Togame, H. Takemoto, S. –I. Nishimura, *Chem. Asian. J*., 2011, **6**, 1048–1056.
20. Z. Ke, H. –F. Chow, M. –C. Chan, Z. Liu, K. –H. Sze, *Org. Lett.*, 2012, **14**, 394–397.

21. H. H. Wamhoff, In *Comprehensive Heterocyclic Chemistry*; A. R. Katritzky, C. W. Rees, *Eds. Pergamon: Oxford*, 1984, **Vol. 5**, pp 669–732.
22. M. J. Miller, G. C. Morasaki, J. Stefely, *U.S. Patent 0021574A1*, 2011.
23. Q. –H. Li, Y. Ding, N. –W. Huang, *Chin. Chem. Lett.*, 2014, **25**, 1469–1472.
24. H. Von Pechmann, K. Wehsang, *Ber*., 1888, **21**, 2992–2993.
25. O. Baltzer, H. Von Pechmann, *Just. Lib. Ann. Chem*., 1891, **262**, 302–304.
26. R. Huisgen, In *1,3−Dipolar Cycloaddition Chemistry*; A. Padwa, *Ed. Wiley: New York*, 1984, **Chapter 1**, pp 1–176.
27. H. C. Kolb, M. G. Finn, K. B. Sharpless, *Angew. Chem. Int. Ed*., 2001, **40**, 2004–2021.
28. V. V. Rostovtsev, L. G. Green, V. V. Fokin, K. B. Sharpless, *Angew. Chem. Int. Ed*., 2002, **114**, 2708–2711.
29. C. W. Tornoe, M. Meldal, In *The Wave of the Future*; M. Leb, R. A. Houghten, *Eds. American Peptide Society and Kluwer Academic Publishers: San Diego*, 2001, pp 263–264.
30. C. W. Tornoe, C. Christensen, M. Meldal, *J. Org. Chem*., 2002, **67**, 3057–3064.
31. S. Brase, C. Gil, K. Knepper, V. Zimmerman, *Angew Chem. Int. Ed*., 2005, **44**, 5188–5240 and all references cited therein.
32. L. Jiang, Z. Wang, S. –Q. Bai, T. S. A. Hor, *Dalton. Trans*., 2013, **42**, 9437–9443.
33. D. P. Singh, B. K. Allam, K. N. Singh, V. P. Singh, *J. Mol. Catal. A. Chemical*, 2015, **398**, 158–163.
34. N. Mukherjee, S. Ahammed, S. Bhadra, B. C. Ranu, *Green Chem*., 2013, **15**, 389–397.
35. N. V. Sokolova, V. G. Nenajdenko, *RSC Adv*., 2013, **3**, 16212–16242.
36. M. Schmal, *Heterogeneous Catalysis and its Industrial Applications*, Springer: Switzerland, 2016.
37. C. M. Friend, B. Xu, *Acc. Chem. Res.*, 2017, *50*, 517–521.
38. B. Movassagh, N. Rezaei, *Tetrahedron*, 2014, **70**, 8885–8892.
39. J. Lu, E. –Q. Ma, Y. –H. Liu, Y. –M. Li, L. –P. Mo, Z. –H. Zhang, *RSC Adv*., 2015, **5**, 59167–59185.
40. V. B. Purohit, S. C. Karad, K. H. Patel, D. K. Raval, *RSC Adv*., 2014, **4**, 46002–46007.
41. W. Wang, J. Wu, C. Xia, F. Li, *Green Chem*., 2011, **13**, 3440–3445.
42. F. Nemati, M. M. Heravi, A. Elhampour, *RSC Adv*., 2015, **5**, 45775–45784.

43. S. Roy, T. Chatterjeec, M. Pramanik, A. Singha Roy, A. Bhaumik, Sk. M. Islam, *Journal of Molecular Catalysis A: Chemical*, 2014, **386**, 78–85.
44. A. Pourjavadi, M. Tajbakhsh, M. Farhang, S. H. Hosseini, *New. J. Chem*., 2015, **39**, 4591–4600.
45. I. Roy, A. Bhattacharyya, G. Sarkar, N. R. Saha, D. Rana, P. P. Ghosh, M. Palit, A. R. Das, D. Chattopadhyay, *RSC Adv.*, 2014, **4**, 52044–52052.
46. A. R. Hazipour, F. Mohammadsaleh, *J. Iran Chem. Soc.*, 2015, **12**, 1339–1345.
47. P. Abdulkina, Y. Moglie, B. R. Knappett, D. A. Jefferson, M. Yus, F. Alonso, A. E. H. Wheatley, *Nanoscale*, 2013, **5**, 342−350.
48. M. B. Gawande, A. Goswami, F. -X. Felpin, T. Asefa, X. Huang, R. Silva, X. Zou, R. Zbori, R. S. Varma, *Chem. Rev.*, 2016, **116**, 3722−3811.
49. D. Sengupta, J. Saha, G. De, B. Basu, *J. Mater. Chem. A*, 2014, **2**, 3986–3992.
50. B. Basu, S. Das, P. Das, B. Mandal, D. Banarjee, F. Almqvist, *Synthesis*, 2009, 1137–1146.
51. Z. Zhang, C. Dong, C. Yong, D. Hu, J. Long, L. Wang, H. Li, Y. Chen, D. Kang, *Adv. Synth. Catal*., 2010, **352**, 1600–1604.
52. K. Jayaramulu, V. M. Suresh, T. K. Maji, *Dalton Trans.*, 2015, **44**, 83–86.
53. B. Kumar, S. Saha, A. Ganguly, A. K. Ganguli, *RSC Adv.*, 2014, **4**, 12043–12049.
54. Y. Wang, Y. Lü, W. Zhan, Z. Xie, Q. Kuang, L. Zheng, *J. Mater. Chem. A*, 2015, **3**, 12796–12803.
55. M. Deo, S. Mujawar, O. Game, A. Yengantiwar, A. Banpurkar, S. Kulkarni, J. Jog, S. Ogale, *Nanoscale*, 2011, **3**, 4706–4712.
56. I. A. Khan, A. Badshah, M. A. Nadeem, N. Haider, M. A. Nadeem, *Int. J. Hydrogen Energy*, 2014, **39**, 19609–19620.
57. Y. Ji, S. Jai, R. J. Davis, *J. Phys. Chem. B*, 2005, ***109***, 17232–17238.
58. W. Zhang, B. Ren, Y. Jiang, Z. Hu, *RSC Adv.*, 2015, **5**, 12043–12047.
59. C. Wang, D. Ikhlef, S. Kahal, J. –Y. Saillard, D. Astruc, *Coord. Chem. Rev*., 2016, **316**, 1–20.
60. J. T. Fletcher, M. E. Keeney, S. E. Walz, *Synthesis*, 2010, 3339–3345.
61. J. –A. Shin, Y. –G. Lim, K. –H. Lee, *J. Org. Chem*., 2012, **77**, 4117–4122.
62. F. Friscourt, G. –J. Boons, *Org. Lett*., 2010, **12**, 4936–4939.
63. Z. Ganda, Z. Novak, *Dalton Trans*., 2010, **39**, 726–729.

64. B. Sreedhar, P. S. Reddy, *Synth. Commun*., 2007, **37**, 805–812.
65. M. d'Halluin, T. Mabit, N. Fairley, V. Fernandez, M. B. Gawande, E. L. Grognec, F. -X. Felpin, *Carbon*, 2015, **93**, 974–983.
66. P. S. Reddy, B. Sreedhar, *Synthesis*, 2009, 4203–4207.
67. A. Coelho, P. Diz, O. Caamano, E. Sotelo, *Adv. Synth. Catal*., 2010, **352**, 1179–1192.
68. C. Shao, X. Wang, Q. Zhang, S. Luo, J. Zhao, Y. Hu, *J. Org. Chem*., 2011, **76**, 6832–6836.

INDEX

A

A^3 53-62, 67-69, 72-73, 75

AAC reaction 19-23, 25, 31, 34, 35, 37, 58, 103, 104, 110, 116

Acetonitrile 25, 29, 30, 33, 37, 67, 68, 109

Allyl bromide 4, 31, 36, 75,110

Ambient 100, 104, 118

Anhydrous 37, 119

ARF 96, 104-109, 113-119

Azide 98-104, 109-114, 116-119

B

Benzyl bromide 29-31, 33,109-110, 113-114, 117, 119

C

Catalyst 2-6, 18-23, 25, 26, 29, 33, 35, 47, 55-61,63, 67, 73, 96, 98, 102, 107-110, 113, 116, 117

Characterization 1, 5, 9, 25, 37, 62, 73, 76, 105

Chromatography 30, 31, 33, 36, 37, 69, 72, 75, 110, 113, 118, 119

Click reaction 18, 19, 21-24, 29, 96, 99, 100-104, 109, 111, 113, 116, 117

Coordination polymer 4, 9, 11, 13-16, 18-20, 22, 35, 53, 58-62, 72, 73

Cycloaddition 18, 21-23, 25, 29, 35, 98, 116

D

Dichloromethane 56

Disulfide 3

Dithiocarbamate 97, 117, 118, 119

Dithioether 1-9, 11-15, 18-20, 24, 25, 34, 35, 53, 58, 59, 61, 62, 72, 73

DMF 3, 104

E

Eluent 118

H

Heterogeneous catalyst 22, 55, 59, 96, 98, 99, 101-104, 109, 113, 114, 116, 117

Homogeneous 22, 55, 60, 98, 106

HPLC 114, 118

I

ICP–AES 113, 114

M

Metallopolymer 26, 63

Methodology 2, 24, 25, 33, 35

Microwave 21, 22, 29, 30, 33, 58

MOF 4, 5, 15

Monoclinic 16, 26, 27

Morpholine 67, 69, 72, 74

Multicomponent 22, 23, 29, 33, 34, 35, 103

N

Nanoparticles 96, 102, 106, 107

NHC 22, 55, 100, 101, 117

O

Optimization 29, 68, 109

P

Phenyl acetylene 23, 30, 31, 67, 72, 109, 113, 114

Piperidine 69, 72, 74

Polymerization 6

Polystyrene 99

Propargylamine 53-57, 59-61, 69, 73, 75

PVP 103

PXRD 104, 118

Pyrrolidine 83, 119, 126, 130

Q

Quintet 26, 37

R

Radical 2

Recycling 98, 103, 113

Regioselectivity 21, 98

Resin 96, 99, 104-107, 116, 117, 119

Room temperature 99, 100, 102, 104, 109-111, 113, 116-118

S

SDS 109, 110, 118, 119

Secondary amine 69, 73, 75

Single crystal X-ray Diffraction 26, 63

Solvent free 21

Spacers 4

Stereoselectivity 2

T

TBAB 57

TEM 106, 107

Thiols 2

Triazole 33, 96-101, 103, 104, 109, 110, 113-119

Triclinic 16

Triplet 26, 36, 74, 118

X

XPS 104, 107, 108, 118

REPRINT OF PAPERS

Tetrahedron Letters 59 (2018) 2541–2545

Contents lists available at ScienceDirect

Tetrahedron Letters

journal homepage: www.elsevier.com/locate/tetlet

1-D copper(I) coordination polymer based on bidentate 1,3-dithioether ligand: Novel catalyst for azide-alkyne-cycloaddition (AAC) reaction

Sankar Saha [a], Kinkar Biswas [b,*], Basudeb Basu [a,*]

[a] Department of Chemistry, North Bengal University, Darjeeling 734013, India
[b] Department of Chemistry, Raiganj University, Raiganj 733134, India

ARTICLE INFO

Article history:
Received 6 April 2018
Revised 14 May 2018
Accepted 16 May 2018
Available online 19 May 2018

Keywords:
Click reaction
1-D Cu coordination complex
1,3-Dithioether
1,2,3-Triazole

ABSTRACT

A novel 1,3-bis(4-fluorophenylthio)-propane ligand based CuI 1-D polymeric coordination complex having formula ($[(CuI)_2\{ArS(CH_2)_3SAr\}_2]_n$, Ar = 4-F-$C_6H_4$) has been synthesized and characterized by ^{1}H NMR, ^{13}C NMR and single crystal XRD techniques. This complex has been employed for the first time as suitable catalyst for base-free one-pot three-component regioselective azide-alkyne cycloaddition (AAC) reaction. A novel 1,2,3-triazole compound with sulfur functionalized pendant arms has also been prepared using our catalytic system in a multicomponent manner via one-pot two-step reaction.

Introduction

The 1,2,3-triazoles are known to be an important heterocyclic scaffolds from biological and pharmaceutical viewpoints; such as anti-allergic,[1] anti-bacterial,[2] and anti-HIV activity,[3] and selective β3-adrenergic receptor agonism.[4] The atom-efficient 1,3-dipolar Huisgen cycloaddition reaction between alkynes and organyl azides (commonly known as AAC) is one of the most straightforward methods for the synthesis of 1,2,3-triazoles.[5] While AAC reaction gives a mixture of 1,4- and 1,5-disubstituted 1,2,3-triazoles, the use of Cu(I) catalysts under mild conditions selectively forms the 1,4-disubstituted 1,2,3-triazoles in excellent yields and this is commonly known as 'click reaction'. The simplest example of Cu (I) catalyzed click triazole synthesis was effectively achieved by excess of $CuSO_4$ and sodium ascorbate, where sodium ascorbate reduces the Cu(II) to Cu(I) and inhibits the aerobic oxidation of Cu(II) species.[6] For well-defined Cu(I) catalytic systems, various ligands like PPh_3, NHC, S- and N-based molecules have been used so far, though P-based ligands afford unwanted Staudinger reaction.[6–9] The coordination chemistry of sulfur ligands has been studied extensively and their copper complexes are attractive due to the reducing power of sulfur group as well as prevent further oxidation of Cu(I) to Cu(II) in the absence of any base.[10] This promoted the synthesis and application of Copper(I)-thioamide catalytic complex in AAC reaction.[11] Mononuclear complexes like $[CuX_2(SNS)]$ (X = Cl, Br), $[Cu(OTf)_2(H_2O)(SNS)]$ and 1-D Cu(I)-coordination polymer, $[Cu_2I_2(SNS)]_n$ have been used as effective catalyst for the AAC reaction.[12] Hybrid nitrogen-sulfur (NS) ligands supported Cu(I)/Cu(II) complexes have also been used for AAC reaction.[13] But in some cases, the hybrid SNS-based Cu(I) catalyst met with the problems of undesired alkyne-alkyne homocoupling reaction.[14]

Hor et al. reported the synthesis of novel pyridyl and thioether hybridised 1,2,3-triazole ligands based Cu(I) coordination polymers and its application in azide-alkyne cycloaddition reactions.[15] It opened a new dimension for the polymeric coordination complex catalyzed AAC reactions. Due to strong coordination power of sulfur atoms, sulfur containing ligands are generally used for the preparation of Cu(I)-coordination polymer.[16] Knorr et al. illustrated the coordination mode of aromatic dithioether ligands of the type $PhS(CH_2)_nSPh$.[16] Apart from the structural and photophysical properties, the catalytic activity of these types of dithioether based copper complexes in the AAC reaction has not been reported yet. Herein we report the synthesis, characterization of a new type of 1,3-dithioether based CuI coordination polymer and find its application to one pot azide-alkyne cycloaddition reaction in a multicomponent fashion. Our 1,3-bis(4-fluorophenylthio)-propane ligand based CuI coordination polymeric complex having molecular formula, $[(CuI)_2\{ArS(CH_2)_3SAr\}_2]_n$, Ar = 4-F-$C_6H_4$) was first synthesized and characterized by NMR and single crystal X-ray diffraction pattern. The catalyst works efficiently in AAC reaction under base-free condition in water/acetonitrile solvent mixture at 50 °C to afford selectively 1,4-disubstituted 1,2,3-triazole prod-

* Corresponding authors.
E-mail address: basu_nbu@hotmail.com (B. Basu).

https://doi.org/10.1016/j.tetlet.2018.05.040
0040-4039/

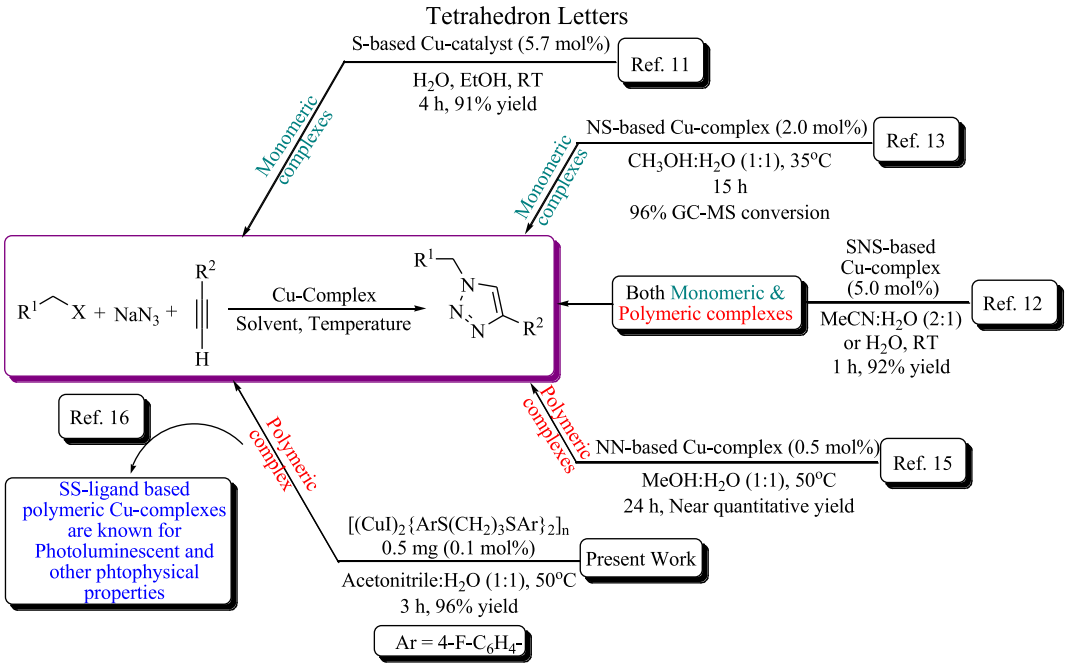

Scheme 1. Various ligand based copper complex catalyzed AAC reaction.

ucts. In Scheme 1, the AAC reaction performed by various Cu(I) complexes with S, NS and SNS ligand is presented. NN- and SNS-based polymeric Cu(I) complexes have been found as catalyzing the AAC reaction but interestingly, polymeric Cu(I) complex with SS-based bidentate ligands, used as AAC reaction is not found in literature.

Results and discussion

Synthesis of the copper complex

The 1,3-bis(4-fluorophenylthio)-propane ligand (L) was synthesized according to our previously reported procedure.[17] This compound was characterized by ^{1}H- and ^{13}C NMR spectroscopy. This ligand has been reacted with CuI in 1:2 metal to ligand ratio in acetonitrile solvent to obtain the desired 1-D polymeric CuI-1,3-dithioether complex. The as-synthesized Cu-complex was characterized by ^{1}H NMR, ^{13}C NMR and single crystal XRD techniques. The NMR spectra of bare ligand and copper(I) complex are given in Supplementary Materials.

This complex crystallizes in the monoclinic space group P $2_{1/c}$, and shows a polymeric propagation in the form of $[(CuI)_2\{ArS(CH_2)_3SAr\}_2]_n$ metallopolymer (Fig. 1). The 1D-network is built up upon dimeric Cu_2I_2 units which are interconnected via dithioether ligands. The framework consists of $Cu_2(\mu\text{-}I)_2$ prismatic part connected with the dithioether ligands. Within the cluster core, the Cu—I bond lengths range between 2.5867 (5) and 2.6443 (12) Å. The Cu...Cu distance between the two Cu (I) centers, 2.7812 (10) Å falls significantly below the sum of the vander Waals radius (2.8 Å). The mean Cu—S bond length of range between 2.3339 (11) to 2.3551 (12) Å similar to $[\{Cu(\mu\text{-}I)_2Cu\}_2\{\mu\text{-}PhS(CH_2)_3SPh\}_2]_n$ (2.3465 Å).[16a] The angle between Cu...I...Cu is 64.23° and I...Cu...I 115.77° in the metallocluster. The crystal data, data collection and structure refinement for the polymeric complex is given in the Supplementary Materials.

The catalytic activity of the copper complex

The catalytic activity of the complex towards one-pot multi-component AAC reaction under base-free conditions was optimized by the model reaction of benzyl bromide, NaN_3 and

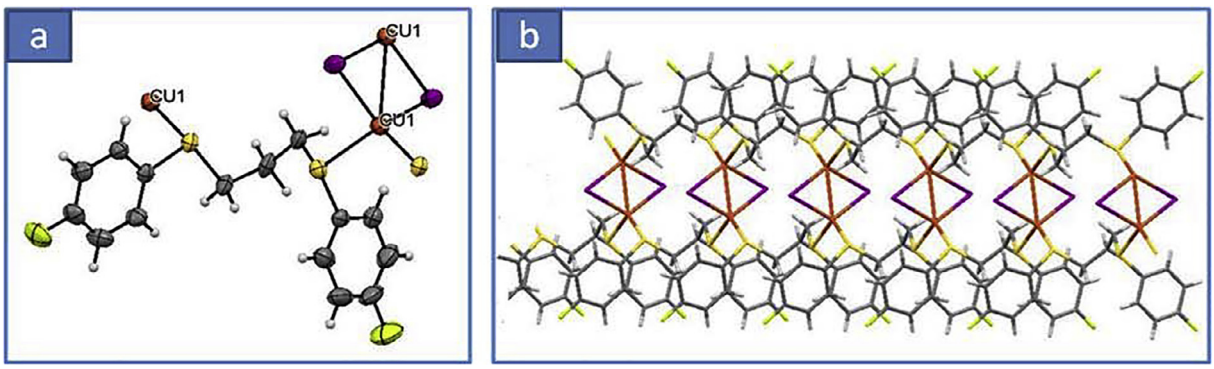

Fig. 1. View of (a) monomeric picture of the complex and (b) infinite 1-D chain of the complex incorporating dinuclear $Cu(\mu_2\text{-}I)_2Cu$ motifs along '*b*' axis.

Table 1
Optimization of reaction conditions for the Cu(I)-complex catalyzed one-pot three-component AAC reaction.

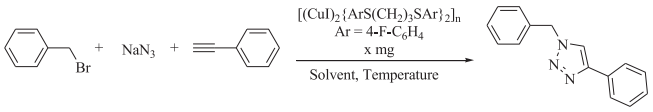

Entry	Solvent	Complex/CuI in (mg)	Temp. (°C)	Time (h)	Yield[a] (%)
1	Neat	5	60	5	84
2	Methanol	5	60	5	70
3	Acetonitrile	5	60	5	87
4	Water	5	60	8	80
5	Acetonitrile: water	5	60	3	97
6	Acetonitrile: water	5	60	0.5	92[b]
7	Acetonitrile: water	5	50	3	97
8	Acetonitrile: water	5	RT	5	85
9	Acetonitrile: water	3	50	3	97
10	Acetonitrile: water	1	50	3	96
11	Acetonitrile: water	0.5	50	3	96
12[c]	Acetonitrile: water	0.5	50	3	79
13[d]	Acetonitrile: water	0.5	50	4	65

Reaction conditions: Phenyl acetylene (1 mmol), NaN_3 (1.2 mmol) and benzyl bromide (1.1 mmol), Cu-complex [5.0 mg (1.0 mol%) to 0.5 mg (0.1 mol%)], Acetonitrile:H_2O (1:1, 2 mL).
[a] Isolated yield after purification through column chromatography by silica gel.
[b] Reaction tried on focused microwave reactor.
[c] CuI was used as catalyst.
[d] Phenyl acetylene (2 mmol), NaN_3 (2.4 mmol) and benzyl bromide (2.2 mmol).

phenylacetylene with varying catalyst loading under different temperature and solvent conditions (Table 1). The reaction was first studied at neat condition and higher temperature (60 °C) with 5 mg of the complex. After 5 h, 84% of the product was isolated under this condition (entry 1). When methanol was used as solvent relatively less conversion was achieved compared to the neat condition (70%, entry 2). Similarly the reactions in acetonitrile and water gave 87% and 80% yield of the product respectively (entry 3 & 4). A binary solvent mixture of acetonitrile and water (1:1) resulted excellent yield of the desired triazole product with lesser time (entry 5). The same experiment on microwave reactor yielded lesser amount of yield than conventional thermal heating (entry 6). Decreasing the temperature to 50 °C also gave excellent yield (97%) in 3 h (entry 7). The product conversion was dropped when the reaction was carried out at room temperature (entry 8). The catalyst loading was also performed from entry 8 to entry 10 and the catalytic activity has been found to be very effective with only 0.5 mg of the complex catalyst for this reaction (entry 11). While using CuI as the catalyst, the product was obtained in relatively lower yield (entry 12). Performing the reaction by doubling the reactants and keeping the catalyst quantity same (0.5 mg) also afforded the desired product in poor yield (entry 13).

The complex is air stable and can tolerate a range of benzyl, allyl, cinnamyl and alkyl halides under mild reaction conditions (Table 2). The terminal alkynes have participated in this reaction very smoothly (Table 2). Phenyl acetylene, 4-ethynyl toluene and 2-bromo phenyl acetylene gave excellent yield (entry 1 to 3). 4-nitro-phenyl acetylene also gave excellent yield but slightly lesser than the previous entries (entry 4). Apart from aromatic alkynes, aliphatic alkynes responded also to this reaction smoothly (entries 5, 13 and 14). Allyl bromide was found to be very reactive as a coupling partner in this AAC reaction (entry 6 and 7). Benzyl chlorides have been found to be reactive as benzyl bromides (entry 8 and 9). But the same reaction when carried out with diphenyl acetylene (internal alkyne) no reaction occurred even after 12 h (entry 10). This methodology has been also applied for cinnamyl chlorides (entry 11 and 12). *n*-Octyl iodide, an aliphatic halide also responded well to this cycloaddition reaction (entry 15). All the reactions proceeded without any difficulty and the products were isolated in good to excellent yields in high purity through column chromatography.

Mechanism

A probable mechanism for this multicomponent azide-alkyne-cycloaddition reaction was proposed in Scheme 2. It was presumed that the reaction was initiated by the metalation of phenylacetylene in the presence of the 1D-CuI dithioether polymeric complex giving copper acetylide. In the next step, benzyl/allyl/cinnamyl/alkyl azide was formed *in-situ* by the substitution reaction between benzyl/allyl/cinnamyl/alkyl halide and sodium azide. The polymeric copper acetylide moiety reacted with benzyl/allyl/cinnamyl/alkyl azide *via* cycloaddition fashion followed by elimination of the complex catalyst give rise to 1,4-disubstituted 1,2,3-triazoles as the main product.

Synthesis of sulfur functionalized 1,2,3-triazole

1,2,3-Triazoles containing diverse functional groups have strong potential as steel corrosion inhibitors or suitable ligands for transition-metal chemistry.[18] We have prepared sulfur functionalized pendant arms of 1,2,3-triazole compounds in a multicomponent approach via one-pot two-step reaction using our catalyst. Benzenethiol (1.1 mmol) was first reacted with propargyl bromide (1 mmol) in presence of triethyl amine (2 mmol) in water at room temperature. After 2 h, benzyl bromide (1.1 mmol) and sodium azide (1.2 mmol) and Cu(I)-complex (0.5 mg, 0.1 mol%) were added to the reaction mixture. The progress of the reaction was monitored by TLC and finally the desired product was isolated in column chromatography (82% yield). The preparation methodology is presented in Scheme 3.

Table 2
Catalytic activities of the Cu(I)-complex catalyzed one-pot three-component AAC reaction.

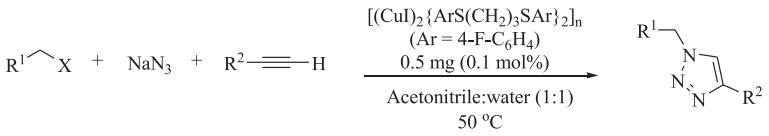

Entry	R^1CH_2X	R^2—≡—H	Time (h)	Product	Yield[a] (%)
1	$PhCH_2Br$	Ph—	3	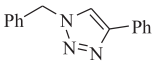 [2a]	97
2	$PhCH_2Br$	*p*-Tol—	3	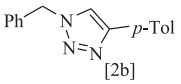 [2b]	96
3	$PhCH_2Br$	*o*-Br-Ph—	4	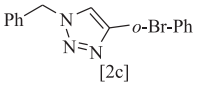 [2c]	96
4	$PhCH_2Br$	*p*-O_2N-Ph—	4	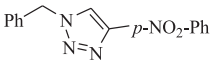 [2d]	91
5	$PhCH_2Br$	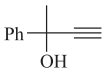	4	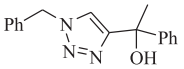 [2e]	90
6		Ph—	4	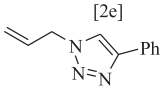 [2f]	81
7		*p*-Tol—	4	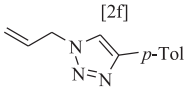 [2g]	83
8	$PhCH_2Cl$	Ph—	3.5	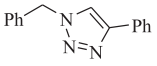 [2a]	95
9	$PhCH_2Cl$	*p*-Tol—	3.5	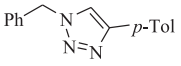 [2b]	94
10	$PhCH_2Br$	Ph—≡—Ph	12	NR	–
11	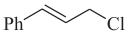	Ph—	4	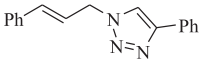 [2h]	84
12	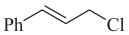	*p*-Tol—	4	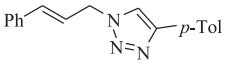 [2i]	85
13	$PhCH_2Br$	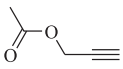	4	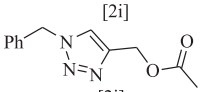 [2j]	72
14	$PhCH_2Br$	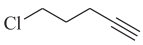	4	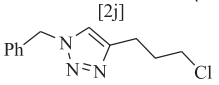 [2k]	81
15	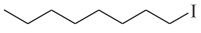	Ph—	4	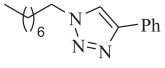 [2l]	76

Reaction conditions: Terminal alkynes (1 mmol), NaN_3 (1.2 mmol) and benzyl/allyl/cinnamyl/alkyl halide (1.1 mmol), Cu-complex (0.5 mg, 0.1 mol%), Acetonitrile:H_2O (1:1, 2 mL).
[a] Isolated yield after purification through column chromatography by silica gel.

Conclusion

In conclusion, we have synthesized a suitably designed Cu(I) coordination polymer based on dithioether ligands (SS, bidentate), which can be used as efficient catalyst for AAC reaction. The polymeric complex has been well characterized and applied in variety of substrates and the desired 1,4-disubstituted 1,2,3-triazole products are obtained in excellent yields. Low temperature and low cat-

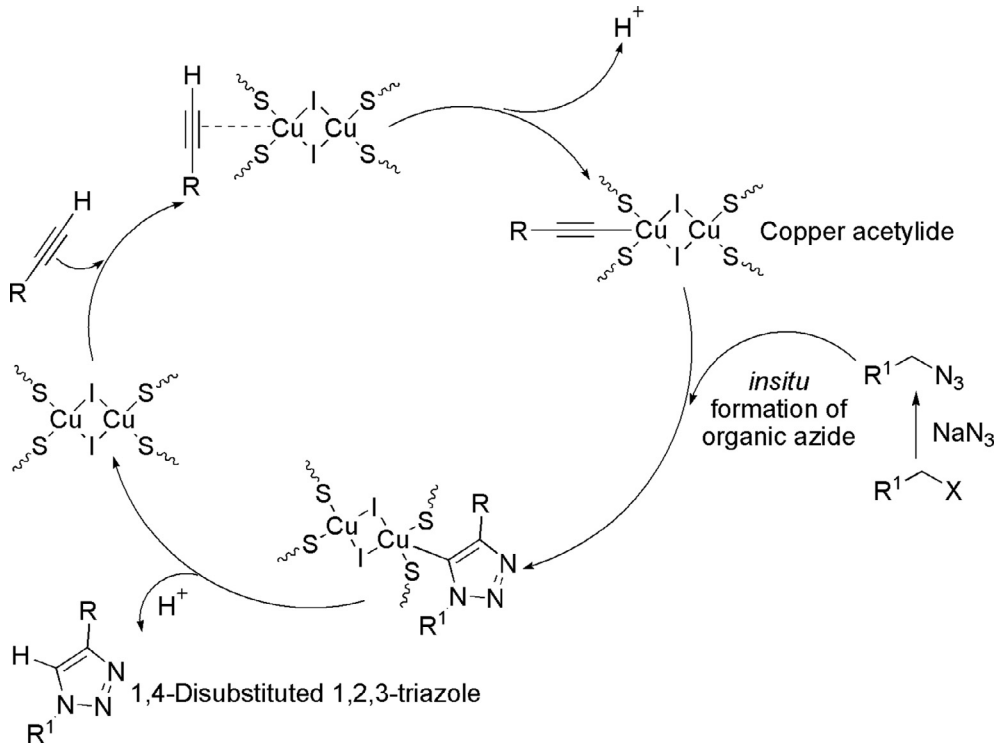

Scheme 2. A plausible mechanistic path for the Cu(I)-complex catalyzed one-pot three-component AAC reaction.

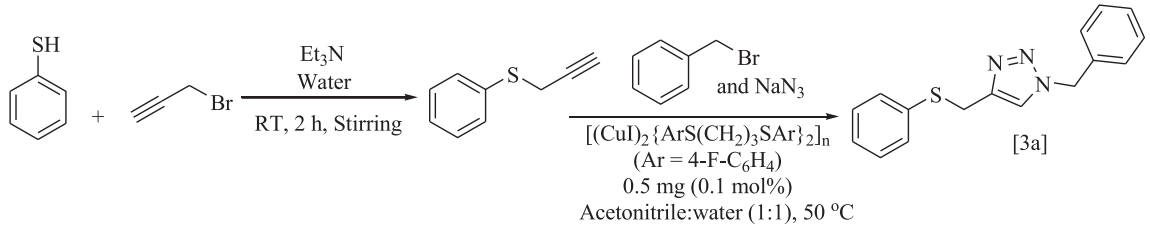

Scheme 3. One-pot two-step synthesis of sulfur functionalized 1,2,3-triazole derivative.

alyst loading for the reaction are noteworthy besides demonstrating the catalytic activity of S,S-based Cu(I) coordination polymer. Further application of the polymeric complex is under active pursuits.

Acknowledgement

This work was supported by Science and Engineering Research Board of India (Grant No. EMR/2015/000549).

A. Supplementary data

Supplementary data associated with this article can be found, in the online version, at https://doi.org/10.1016/j.tetlet.2018.05.040.

References

1. Buckle DR, Rockell CJM, Smith H, Spicer BA. *J Med Chem*. 1986;29:2262–2267.
2. Genin MJ, Allwine DA, Anderson DJ, et al. *J Med Chem*. 2000;43:953–970.
3. Alvarez R, Velazquez S, San-Felix A, et al. *J Med Chem*. 1994;37:4185–4194.
4. Brockunier LL, Parmee ER, Ok HO, et al. *Bioorg Med Chem Lett*. 2000;10:2111–2114.
5. Ding S, Jia G, Sun J. *Angew Chem Int Ed*. 2014;53:1877–1880.
6. Liang L, Astruc D. *Coord Chem Rev*. 2011;255:2933–2945.
7. (a) Díez-González S, Correa A, Cavallo L, Nolan SP. *Chem Eur J*. 2006;12:7558–7564;
   (b) Díez-González S, Escudero-Adán EC, Benet-Buchholz J, Stevens ED, Slawin SP, Nolan SP. *Dalton Trans*. 2010;39:7595–7606.
8. (a) Baig RBN, Varma RS. *Green Chem*. 2012;14:625–632;
   (b) Wan L, Cai C. *Catal Lett*. 2012;142:1134–1140.
9. Haldon E, Nicasio MC, Perez PJ. *Org Biomol Chem*. 2015;13:9528–9550.
10. Bayon JC, Claver C, Masdeu-Bulto AM. *Coord Chem Rev*. 1999;193–195:73–145.
11. Mirjafarya Z, Ahmadib L, Moradib M, Saeidian H. *RSC Adv*. 2015;5:78038–78046.
12. Bai S-Q, Koh LL, Hor TSA. *Inorg Chem*. 2009;48:1207–1213.
13. Bai S-Q, Jiang L, Zuo J-L, Hor TSA. *Dalton Trans*. 2013;42:11319–11326.
14. Tornøe CW, Christensen C, Meldal M. *J Org Chem*. 2002;67:3057–3064.
15. Jiang L, Wang Z, Bai S-Q, Hor TSA. *Dalton Trans*. 2013;42:9437–9443.
16. (a) Knorr M, Guyon F, Khatyr A, et al. *Inorg Chem*. 2012;51:9917–9934;
   (b) Li J-R, Bu X-H. *Eur J Inorg Chem*. 2008;27–40.
17. Kundu S, Roy B, Basu B. *Beilstein J Org Chem*. 2014;10:26–33.
18. Mendoza-Espinosa D, Negrón-Silva G, Lomas-Romero L, Gutiérrez-Carrillo A, Santillán R. *Synth Commun*. 2014;44:807–817.

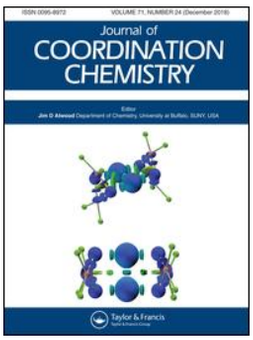

Journal of Coordination Chemistry

ISSN: 0095-8972 (Print) 1029-0389 (Online) Journal homepage: https://www.tandfonline.com/loi/gcoo20

New 1,2-dithioether based 2D copper(I) coordination polymer: from synthesis to catalytic application in A^3-coupling reaction

Sankar Saha, Kinkar Biswas, Pranab Ghosh & Basudeb Basu

To cite this article: Sankar Saha, Kinkar Biswas, Pranab Ghosh & Basudeb Basu (2019): New 1,2-dithioether based 2D copper(I) coordination polymer: from synthesis to catalytic application in A^3-coupling reaction, Journal of Coordination Chemistry, DOI: 10.1080/00958972.2019.1627339

To link to this article: https://doi.org/10.1080/00958972.2019.1627339

JOURNAL OF COORDINATION CHEMISTRY
https://doi.org/10.1080/00958972.2019.1627339

Taylor & Francis
Taylor & Francis Group

New 1,2-dithioether based 2D copper(I) coordination polymer: from synthesis to catalytic application in A^3-coupling reaction

Sankar Saha[a], Kinkar Biswas[b], Pranab Ghosh[a] and Basudeb Basu[a,b]

[a]Department of Chemistry, North Bengal University, Darjeeling, India; [b]Department of Chemistry, Raiganj University, Raiganj, India

ABSTRACT

A new 2D copper(I) coordination polymeric complex has been synthesized from CuI and 1-(1-{4-chlorophenylthio}propan-2-ylthio)-4-chlorobenzene ($[(CuI)_2\{ArSCH_2CH(CH_3)SAr\}_2]_n$, Ar = 4-$ClC_6H_4$) and characterized by high resolution mass spectrometry (HRMS) and single crystal X-ray diffraction techniques. The complex has been employed as a suitable catalyst for a solvent-free, one-pot, three-component A^3-coupling reaction. A variety of aromatic and aliphatic aldehydes, terminal alkynes and aliphatic cyclic secondary amines have been used to prepare a library of propargylamines using the 2D-Cu complex at significantly low concentration (0.2 mol%).

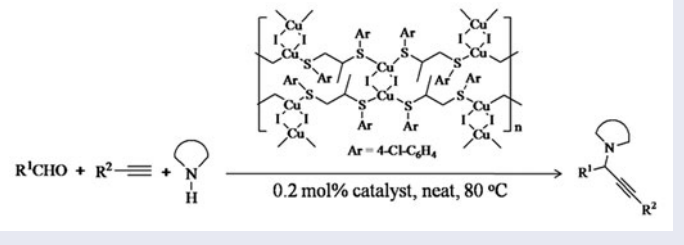

ARTICLE HISTORY
Received 12 February 2019
Accepted 21 May 2019

KEYWORDS
Coordination polymer; 2D-copper(I) complex; solvent-free; A^3-coupling; propargyl amine

1. Introduction

Coordination polymers of copper halides with infinite network structures composed with organic ligands are widely reported due to the presence of their enthralling physical and chemical properties [1]. For example, Cu(I) halide-based compounds have been widely explored due to their attractive structural characteristics and possible applications in luminescence-based sensors, photophysical phenomena, and biological probes [2]. They also find catalytic applications in various organic transformations [3–8]. *N*- and *P*-based ligands and Cu complexes are employed in catalytic applications

CONTACT Basudeb Basu basu_nbu@hotmail.com

Supplemental data for this article can be accessed https://doi.org/10.1080/00958972.2019.1627339.

[4–9]. Interestingly, metal complexes with 1,2-dithioether ligands are rarely synthesized and used as catalysts except for one recent report that describes the synthesis of a 1,2-dithioether and Cu(I) halide-based 2D complex and its catalytic application in aminomethylation of phenylacetylene. They have shown one example of catalytic use of the complex in the synthesis of propargylamine but the catalyst loading was high (5 mol%) [10]. Propargylamines are versatile building blocks for the preparation of various *N*-containing heterocyclic compounds as well as key intermediates for the synthesis of pharmaceuticals and natural products [11–13]. They also act as key intermediates for the construction of biologically active compounds such as β-lactams, oxotremorine substrates, conformationally restricted peptides, and therapeutic drug molecules [14]. Because of their importance, many synthetic methods have been developed [15–18].

The classical methodologies are less attractive due to their low tolerance of functional groups, harsh reaction conditions, and operational difficulty [19, 20]. However, the most direct and efficient method for the preparation of propargylamines can be achieved through transition-metal catalyzed three-component coupling between an aldehyde, an amine and a terminal alkyne, which is commonly known as an A^3-coupling reaction [21]. Among various synthetic methods, the copper-catalyzed A^3-coupling is the most common due to its easy availability, low cost, low toxicity, and high reactivity [22, 23].

Trivalent phosphorus ligands have been used to control the metal center that lead to metal catalysts with improved reactivity and stability. Garcia et al. reported a diallylphosphine-tetrameric copper(I) complex catalyzed A^3-coupling reaction for preparing propargylamine [4]. Apart from the phosphorous ligands, nitrogen-based Cu(I) compounds have also been used for A^3-coupling reaction. For example, a nitrogen-based 1-D Cu(I)-coordination polymer [5], a benzotriazole-based homogeneous and air-stable Cu-coordination compounds [6], and a dicopper (I) complex based on 2-picolyliminomethyl ligand [7] have been used in A^3-coupling reactions. A thioether-based Schiff base Cu(I) complex has been used as the catalyst for an asymmetric type A^3-coupling reaction [24]. Since the use of only CuI as catalyst requires prolonged times to complete the reaction, the presence of a co-catalyst or microwave irradiation is mandatory for facile A^3-coupling reactions [9, 25]. Interestingly, though the *S*-based copper complexes are widely known, their catalytic applications are quite limited as compared to the corresponding *N*- and *P*-based copper complexes. We report herein the synthesis of a new coordination polymer of CuI attached to the bidentate 1,2-dithioether [1-(1-(4-chlorophenylthio)propan-2-ylthio)-4-chlorobenzene] and characterize it by single crystal X-ray diffraction. The 2-D Cu(I)-1,2-dithioether coordination polymer catalyst works efficiently in A^3-coupling reactions under solvent-free condition at 80 °C to afford propargylamines in good to excellent yields. A summary of the previous catalytic A^3-coupling reactions along with the present work has been schematically presented in Scheme 1. This clearly shows the catalytic application of various Cu(I) monomeric and polymeric complexes based on *P*- and *N*-ligands in A^3-coupling reactions. However, to the best of our knowledge, there is no example of a polymeric 2D Cu(I) complex with 1,2-*SS*-based bidentate ligands used as the catalyst for the synthesis of propargylamines via A^3-coupling reaction. The present work thus demonstrates not only a new CuI-based complex as the catalyst for three-component reaction, but also shows the potentiality of using 1,2-dithioethers as the chelating ligands for making metal complexes and their catalytic applications in organic reactions.

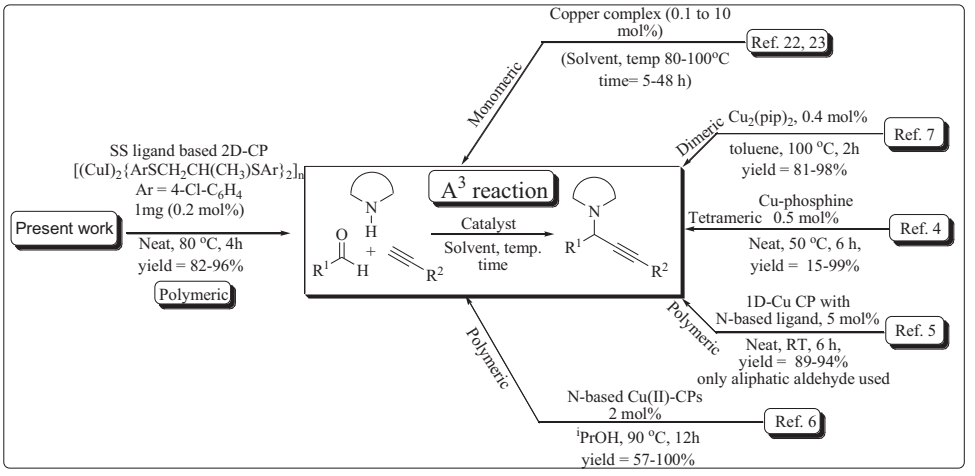

Scheme 1. Various copper complexes used as catalysts in A^3-coupling reaction.

2. Experimental

2.1. Materials and methods

Phenylacetylene, *p*-bromophenylacetylene, and cyclohexylcarboxaldehyde were purchased from Sigma – Aldrich and used directly as obtained. Benzaldehyde and salicylaldehyde were purchased from Merck and used without purification. All other aldehydes were purchased from SD Fine Chemical Limited, India. Morpholine, piperidine, and pyrrolidine were purchased from Lancaster and used after distillation. The solvents were purchased from Thomas Baker (Chemicals) Pvt. Ltd., India and used after distillation. All the products were purified by column chromatography on 60–120 mesh silica gels (SRL, India). For TLC, Merck plates coated with silica gel 60, F_{254} were used. The catalyst was weighed by using a Mettler-Toledo digital balance (0.1 mg sensitivity). FT-IR spectra were recorded with a FT-IR-8300 SHIMADZU spectrophotometer using a KBr pellet for solid compounds and neat for semi-solid or liquid compounds. ^{1}H and ^{13}C NMR spectra were recorded at 300 MHz and 75 MHz, respectively, on a Bruker AV 300 spectrometer in $CDCl_3$. Splitting patterns of protons were described as s (singlet), d (doublet), t (triplet), bs (broad singlet), dd (doublet of doublet), and m (multiplet). Chemical shifts (δ) were reported in parts per million (ppm) relative to TMS as internal standard. *J* values (coupling constant) were reported in Hz (Hertz). ^{13}C NMR spectra were recorded with complete proton decoupling ($CDCl_3$: δ 77.0 ppm). HRMS was performed by a Micromass Q-TOF Spectrometer under ESI (positive mode) at the Indian Association for the Cultivation of Science.

2.2. Crystal structure determination

Suitable crystals of the compound were obtained by slow evaporation of its saturated solution using the diffusion method. Single-crystal diffraction studies were carried out using a Bruker D8 Quest CMOS diffractometer with a Mo Kα (I = 0.71073 Å) sealed tube. The data frames were obtained using the program APEX3 and processed using the program SAINT in APEX3 [26]. The structures were solved by direct methods and

refined using the SHELXTL-2014/7 program [27]. The structures were refined by full-matrix least-squares (SHELXL2014-7) on F^2 [28]. Non-hydrogen atoms were refined with anisotropic displacement parameters. All hydrogens were positioned at their idealized positions using a riding model. The molecular structure figures were prepared using DIAMOND version 3.2 [29]. Table 1 provides the data collection and structure solving parameters for the compound. Selected bond distances and angles for the compound are given in Tables 2 and 3.

2.3. General procedure of preparing CuI-L (1,2-bis(4-chlorophenylthio)-propane)-coordination complex (1) Catena-poly [di-μ-iodido-bis[(1,2-bis(4-chlorophenylthio)-propane)-copper (I)]]

The dithioether ligand (**L**) was synthesized according to our previously reported procedure [30]. **L** (329 mg, 1.0 mmol) and CuI (95 mg, 0.5 mmol) in acetonitrile (2 mL) were

Table 1. Crystal data, data collection, and structure refinement for the complex.

Formula	$C_{15}H_{14}Cl_2CuIS_2$
Formula weight	519.73
Temperature/K	296(2)
Description	Block
Color	White
Crystal system	Orthorhombic
Space group	Pbca
a/Å	10.0087(5)
b/Å	15.4384(10)
c/Å	23.6978(14)
Cell angle (α)	90°
Cell angle (β)	90°
Cell angle (γ)	90°
Cell volume/Å^3	3661.7(4)
Cell formula units Z	8
Density (calculated) g/cm^3	1.886
θ Range for data collection/deg	2.42–27.48
F(000)	2016
Crystal size/mm	0.216, 0.284, 0.320
Absorption co-efficient (μ)	3.389
Index ranges	$-12 \leq h \leq 13$ $-20 \leq k \leq 20$ $-30 \leq l \leq 30$
Reflections collected	62648
Independent reflections	4182
Refinement method	Full-matrix least-squares on F^2
R-equivalents	0.0285
Sigma I/net I	0.0119

Table 2. Selected bond lengths.

Bond	Length
I3–Cu1	2.6119(4)
I3–Cu1	2.6182(4)
Cu1–S2	2.3539(7)
Cu1–S1	2.3990(7)
Cu1–I3	2.6182(4)
Cu1–Cu1	2.8979(8)
S1–C4	1.779(2)
S1–C1	1.828(2)
S1–Cu1	2.3990(7)

Table 3. Selected bond angles.

Bond	Angle
Cu1–I3–Cu1	67.296(15)
S2–Cu1–S1	96.07(2)
S2–Cu1–I3	123.28(2)
S1–Cu1–I3	110.344(19)
S2–Cu1–I3	102.56(2)
S1–Cu1–I3	110.42(2)
I3–Cu1–I3	112.705(15)

taken in a 25 mL round-bottomed flask. The mixture was stirred at room temperature for 4 h and then refluxed for 24 h. After cooling to room temperature, petroleum ether was added dropwise to the solution and the solution kept in a refrigerator. After two days, shining white crystals of the complex were separated by simple filtration, followed by washing with dry petroleum ether (2×5 mL), and finally dried in a vacuum desiccator. The 2-D polymeric complex compound (**1**) from CuI and 1,2-dithioether was found in 74% yield (384 mg).

2.4. General procedure for A^3-coupling reaction

A mixture of aldehyde (1.0 mmol), secondary amine (1.0 mmol), terminal acetylene (1.1 mmol), and the polymer catalyst ($\sim$1.0 mg) was magnetically stirred at 80 °C in an open reaction vessel for hours. The progress of the reaction was monitored by TLC. After completion of the reaction (disappearance of the alkyne spot on TLC), the reaction mixture was cooled to room temperature, dichloromethane (5 mL) was added, concentrated, and adsorbed on silica gel. The dry silica-adsorbed material was passed through a bed of silica gel in a column and elution with a light petroleum:ethyl acetate solvent mixture (in varying proportions) afforded the desired propargylamine.

3. Results and discussion

3.1. Characterization of the complex

The CuI-1,2-dithioether 2-D polymeric complex (**1**) was characterized by ^{1}H NMR, ^{13}C NMR spectroscopy, HRMS spectrometry (Supplementary Materials) and by single crystal X-ray diffraction (XRD) techniques. The δ values of proton and carbon in complex (**1**) were shifted downfield compared to the ligand (**L**) in both ^{1}H NMR and ^{13}C NMR spectra, indicating the formation of the complex. Single crystal XRD analysis (Table 1) revealed that **1** crystallizes in the orthorhombic *P*bca space group and shows a polymeric propagation in the form of the $[(CuI)_2\{ArSCH_2CH(CH_3)SAr\}_2]_n$ (Ar = 4-ClC_6H_4) metallopolymer (Figure 1) [31–33]. The ORTEP diagram of the complex is given in Figure 1(a). The 2D-network is built up of dimeric Cu_2I_2 units which are interconnected via dithioether ligands. Within the cluster core, the Cu–I bond lengths range between 2.6119(4) and 2.6182(4) Å. The interatomic distance between two Cu within the Cu_2I_2 cluster is 2.8979(8) Å, significantly larger than the sum of the van der Waals radius (2.80 Å) [34]. The mean Cu–S bond length, range between 2.3539(7) and 2.3990(7) Å, is a

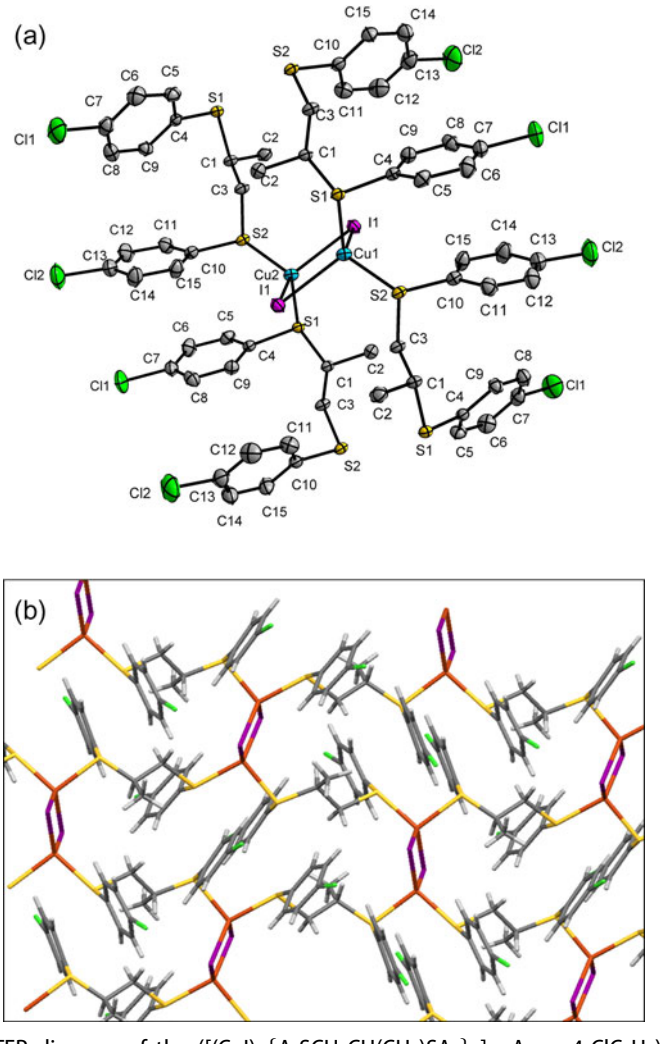

Figure 1. (a) ORTEP diagram of the ($[(CuI)_2\{ArSCH_2CH(CH_3)SAr\}_2]_n$, Ar = 4-$ClC_6H_4$) complex, **1**. (b) Two-dimensional framework of complex **1**.

little in excess of that seen in $[\{Cu(\mu\text{-}I)_2Cu\}_2\{\mu\text{-}PhS(CH_2)_3SPh\}_2]_n$ (2.3465 Å) and ($[(CuI)_2\{ArS(CH_2)_3SAr\}_2]_n$, Ar = 4-$FC_6H_4$); range between 2.3339(11) and 2.3551(12) Å) [31, 35]. The angle Cu … I … Cu is 67.296(15)° and the angle I … Cu … I is 112.705(15)° in the metallocluster. The polymeric framework of **1** is formed by the connection of Cu_2I_2 unit and four 1,2-dithioether linkers **L**. Each 1,2-dithioether coordinates via its *S*-donor atoms to two Cu_2I_2 units, while each Cu_2I_2 unit connects with four 1,2-dithioether ligands (**L**). This gives a 2-D shaped network matrix topology (Figure 1(b)). The crystal data, data collection, and structure refinement of the polymeric complex are given in Table 1. Selected bond lengths and angles of the complex are also given in the Tables 2 and 3, respectively. The refined bond length and angles are given in the Supplementary Materials (Tables S1 and S2, respectively, under 2.2).

3.2. The catalytic activity of copper complex 1

The catalytic activity of the complex towards A^3-coupling reactions was optimized in a model reaction of phenyl acetylene, benzaldehyde, and morpholine under varying catalyst loading, different temperatures and solvents (Table 4). Initially, the reaction of phenylacetylene (1.1 mmol), benzaldehyde (1.0 mmol), and morpholine (1.0 mmol) was performed in acetonitrile at 60 °C for 8 h using 5 mg of the complex as catalyst. A trace amount of conversion was achieved (entry 1). Raising the temperature of the medium from 60 to 80 °C gave 40% yield of the product (entry 2). Using polar hydroxylic solvents *e.g.* ethanol and water, the yield of the product was ~50% (entries 3 and 4). In a binary solvent mixture (acetonitrile:water = 1:1), the conversion was increased to 65% (entry 5). When the reaction was studied under neat conditions, the yield of the product was significantly increased to 91% (entry 6). Decreasing the amount of the catalyst from 5.0 mg to 3.0 and 1.0 mg (±0.1 mg) (approx. 0.2 mol%), respectively, did not affect the overall yield of the product (90% yield in both cases; entries 7 and 8). Reducing the reaction time did not show any significant drop in the yield of the desired product (entries 9 and 10). A reaction performed without any catalyst did not produce any desired product after 24 h (entry 11). On the other hand, conducting the experiment at room temperature showed traces of product after 24 h (entry 12). We also performed the reaction using CuI as the catalyst under similar reaction conditions affording the product in relatively lower yield (55%; entry 13). Among the different conditions attempted, the best condition was optimized as the presence of 1 mg

Table 4. Optimization of reaction conditions for the 2-D Cu(I)-polymeric complex catalyzed A^3-coupling reaction.

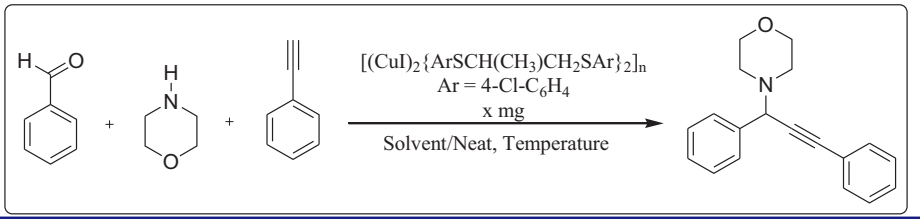

Entry	Solvent	Cu-catalyst (mg)	Temp. (°C)	Time (h)	Yield[a] (%)
1	Acetonitrile	5	60	8	Traces
2	Acetonitrile	5	80	8	40
3	Ethanol	5	80	8	52
4	Water	5	80	8	50
5	Acetonitrile:water	5	80	8	65
6	Neat	5	80	8	91
7	Neat	3	80	8	90
8	Neat	1	80	8	90
9	Neat	1	80	6	88
10	**Neat**	**1 ± 0.1 ~ 1[b]**	**80**	**4**	**88**
11	Neat	–	80	24	No reaction
12	Neat	1	RT	24	Traces
13[c]	Neat	1	80	4	55

Reaction conditions: phenyl acetylene (1.1 mmol), benzaldehyde (1.0 mmol) and morpholine (1.0 mmol), Cu-complex (5 mg to 1 mg), Neat.
[a]Isolated yield after purification through column chromatography over silica gel.
[b]Error in the measurement of the catalyst is ±0.1 mg.
[c]CuI was used as catalyst.
The bold values refer to the optimized reaction conditions used for the reaction.

(±0.1 mg) (approx. 0.2 mol%) catalyst under solvent-free and aerobic conditions at 80 °C (entry 10).

In order to explore the generality of the optimized reaction conditions, different types of substrates such as secondary amines with different types of aldehydes were allowed to react with terminal acetylenes. Very good to excellent isolated yields of the products have been achieved under this protocol (Table 5). In Table 5, it is clearly evident that various aldehydes including electron releasing or withdrawing groups such as OMe, OH, Br, Cl as well as benzaldehyde reacted smoothly with terminal alkynes (phenyl acetylene and 4-bromophenyl acetylene) and cyclic secondary amines (morpholine, piperidine and pyrrolidine). Furthermore, the reaction of an alicyclic aldehyde (cyclohexanecarboxaldehyde) and straight-chain aliphatic aldehyde (*n*-heptanal) with morpholine and phenylacetylene were performed efficiently and afforded the desired products in brilliant yields (entries 9 and 10).

3.3. Probable mechanism

The most possible mechanism of the A^3-coupling reaction is believed to proceed *via* the activation of the C_{sp}–H bond of the terminal alkyne by the copper catalyst (here the new coordination 2D polymer complex derived from CuI and 1,2-dithioether). The resulting four-coordinate alkynyl–Cu intermediate (3), formed by the dissociation of one thioether ligand, then reacts with the iminium ion generated *in situ* from aldehyde and secondary amine to produce the corresponding propargylamine product. The proposed mechanism is outlined in Scheme 2.

Table 5. Catalytic activities of the 2-D Cu(I)-polymeric complex catalyzed A^3-coupling reaction.

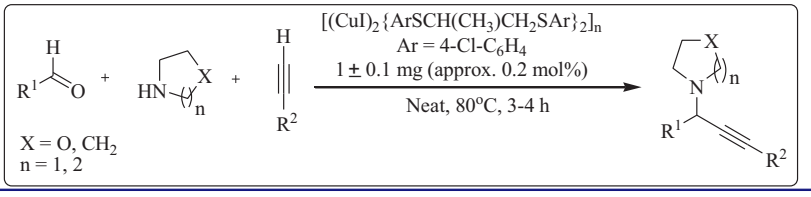

Sl No.	Aldehyde	2° Amine	Alkyne	Time (h)	Yield[a] (%)
1	4 − OMe−C_6H_4CHO	Morpholine	Ph—	4	87
2	4 − Br−C_6H_4CHO	Morpholine	Ph—	4	92
3	4 − C1−C_6H_4CHO	Morpholine	Ph—	4	96
4	2 − C1−C_6H_4CHO	Morpholine	Ph—	4	88
5	C_6H_5CHO	Morpholine	Ph—	4	88
6	3, 5−Br−C_6H_3CHO	Morpholine	Ph—	4	95
7	4−OMe−C_6H_4CHO	Morpholine	4−Br−C_6H_4—	4	92
8	2−OH−C_6H_4CHO	Morpholine	4−Br−C_6H_4—	3	85
9	Cy − CHO	Morpholine	Ph—	3.5	91
10	*n*−C_6H_{13} − CHO	Morpholine	Ph—	3.5	86
11	4−OMe−C_6H_4CHO	Piperidine	Ph—	4	93
12	2−OH−C_6H_4CHO	Piperidine	Ph—	3	90
13	4−OMe−C_6H_4CHO	Pyrrolidine	Ph—	4	82
14	2−OH−C_6H_4CHO	Pyrrolidine	Ph—	3	92
15	4−OMe−C_6H_4CHO	Pyrrolidine	4−Br−C_6H_4—	4	91

Reaction conditions: phenyl acetylene/4-bromo phenyl acetylene (1.1 mmol), aldehyde (1.0 mmol) and morpholine/piperidine/pyrrolidine (1.0 mmol), Cu-complex (1 ± 0.1 mg, approx. 0.2 mol%) in neat condition.
[a]Isolated yield after purification through column chromatography by silica gel.

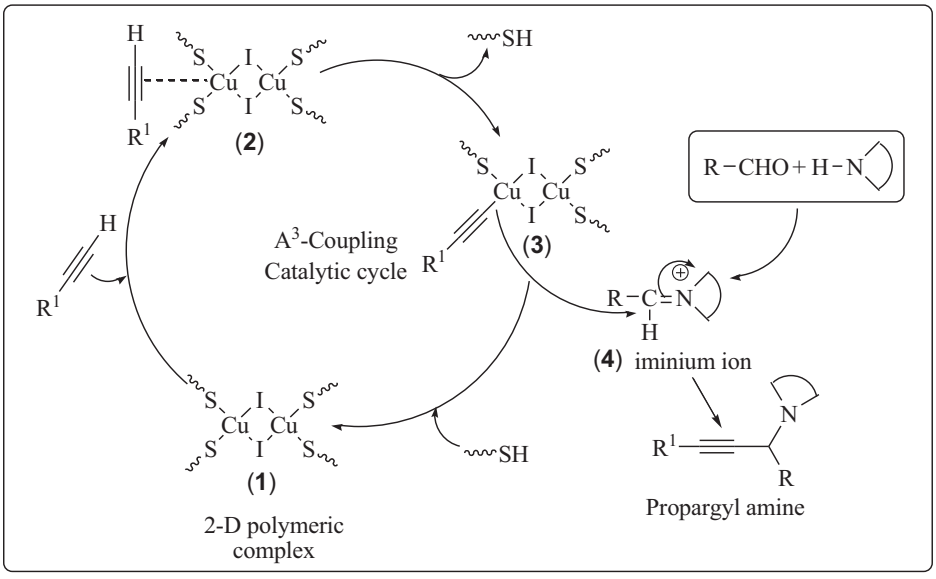

Scheme 2. A probable mechanism of Cu(I)-complex catalyzed A^3-coupling reaction.

4. Conclusion

We have demonstrated the synthesis and characterization of a new 2D-Cu(I) coordination polymer of 1,2-dithioether ligands (*SS*, bidentate) and its catalytic application in A^3-coupling reactions for the synthesis of various propargylamine derivatives under solvent-free conditions. Easy preparation of the copper complex, low catalyst loading (0.2 mol%), mild catalytic conditions and wider applicability to different reacting partners are notable features. The catalyst however performs better in the case of cyclic secondary amines. As the dithioether-based chelating ligands and corresponding copper complexes are less known in catalysis, we expect that the present work would encourage newer *S,S*-based copper complexes for catalytic applications. The choice of chloro-substituted ligands, however, does not carry any specific significance except physical parameters, easy characterization, *etc*.

Disclosure statement

No potential conflict of interest was reported by the authors.

Funding

This work was supported by the Science and Engineering Research Board of India under Grant Number EMR/2015/000549.

References

[1] (a) W.L. Leong, J.J. Vittal. *Chem. Rev.*, **111**, 688 (2011);(b) R. Mas-Balleste, J. Gomez-Herrero, F. Zamora. *Chem. Soc. Rev.*, **39**, 4220 (2010);(c) Z. Wang, G. Chen, K. Ding. *Chem. Rev.*, **109**, 322 (2009).

[2] (a) R. Peng, M. Li, D. Li. *Coord. Chem. Rev.*, **254**, 1 (2010);(b) X.L. Wang, C. Qin, E.B. Wang, Z.M. Su, Y.G. Li, L. Xu. *Angew. Chem. Int. Ed.*, **45**, 7411 (2006);(c) A.J. Blake, N.R. Brooks, N.R. Champness, P.A. Cooke, A.M. Deveson, D. Fenske, P. Hubberstey, W. S. Li, M. Schroder. *J. Chem. Soc., Dalton Trans.*, **13**, 2103 (1999).
[3] L. Jiang, Z. Wang, S.Q. Bai, T.S.A. Hor. *Dalton Trans.*, **42**, 9437 (2013).
[4] J. Rosales, J.M. Garcia, E. Ávila, T. González, D.S. Coll, E. Ocando-Mavárez. *Inorg. Chim. Acta*, **467**, 155 (2017).
[5] N.-X. Zhu, C.-W. Zhao, J. Yang, X.-R. Wang, J.-P. Ma, Y.-B. Dong. *RSC Adv.*, **6**, 108645 (2016).
[6] E. Loukopoulos, M. Kallitsakis, N. Tsoureas, A. Abdul-Sada, N.F. Chilton, I.N. Lykakis, G.E. Kostakis. *Inorg. Chem.*, **56**, 4898 (2017).
[7] H.-B. Chen, Y. Zhaoa, Y. Liao. *RSC Adv.*, **5**, 37737 (2015).
[8] G. Kumar, S. Pandey, R. Gupta. *Cryst. Growth Des.*, **18**, 2210 (2018).
[9] K. Lauder, A. Toscani, N. Scalacci, D. Castagnolo. *Chem. Rev.*, **117**, 14091 (2017).
[10] V.R. Akhmetova, N.S. Akhmadiev, G.M. Nurtdinova, V.M. Yanybin, A.B. Glazyrin, A.G. Ibragimov. *Russ. J. Gen. Chem.*, **88**, 1418 (2018).
[11] E. Vessally. *RSC Adv.*, **6**, 18619 (2016).
[12] E. Vessally, L. Edjlali, A. Hosseinian, A. Bekhradnia, M.D. Esrafili. *RSC Adv.*, **6**, 49730 (2016).
[13] I. Matsuda, J. Sakakibara, H. Nagashima. *Tetrahedron Lett.*, **32**, 7431 (1991).
[14] (a) M. Konishi, H. Ohkuma, T. Tsuno, T. Oki, G.D. Van Duyne, J. Clardy. *J. Am. Chem. Soc.*, **112**, 3715 (1990);(b) G. Dyker. *Angew. Chem. Int. Ed.*, **38**, 1698 (1999).
[15] G. Magueur, B. Crousse, D. Bonnet-Delpon. *Tetrahedron Lett.*, **46**, 2219 (2005).
[16] P. Kaur, G. Shakya, H. Sun, Y. Pan, G. Li. *Org. Biomol. Chem.*, **8**, 1091 (2010).
[17] F. Colombo, M. Benaglia, S. Orlandi, F. Usuelli, G. Celentano. *J. Org. Chem.*, **71**, 2064 (2006).
[18] C. Wei, C.-J. Li. *J. Am. Chem. Soc.*, **124**, 5638 (2002).
[19] T. Murai, Y. Mutoh, Y. Ohta, M. Murakami. *J. Am. Chem. Soc.*, **126**, 5968 (2004).
[20] (a) L. Zani, S. Alesi, P.G. Cozzi, C. Bolm. *J. Org. Chem.*, **71**, 1558 (2006);(b) G. Huang, Z. Yin, X. Zhang. *Chem. Eur. J.*, **19**, 11992 (2013);(c) G. Blay, E. Ceballos, A. Monleón, J.R. Pedro. *Tetrahedron*, **68**, 2128 (2012).
[21] R.P. Herrera, E. Marques-Lopez, *Multicomponent Reactions: Concepts and Applications for Design and Synthesis*, Vol. **94**, John Wiley & Sons Inc., Hoboken, New Jersey (2015).
[22] J.R. Cammarata, R. Rivera, F. Fuentes, Y. Otero, E. Ocando-Mavárez, A. Arce, J.M. Garcia. *Tetrahedron Lett.*, **58**, 4078 (2017).
[23] (a) M. Abdoli, H. Saeidian, A. Kakanejadifard. *Synlett.*, **27**, 2473 (2016);(b) H. Naeimi, M. Moradian. *Appl. Catal. A: Gen.*, **467**, 400 (2013);(c) B.M. Choudary, C. Sridhar, M.L. Kantam, B. Sreedhar. *Tetrahedron Lett.*, **45**, 7319 (2004).
[24] H. Naeimi, M. Moradian. *Tetrahedron: Asymmetry*, **25**, 429 (2014).
[25] L. Shi, Y.-Q. Tu, M. Wang, F.-M. Zhang, C.-A. Fan. *Org. Lett.*, **6**, 1001 (2004).
[26] Bruker, *APEX3 and SAINT*, Bruker–Nonius AXS Inc., Madison, Wisconsin, USA (2015).
[27] G.M. Sheldrick. *Acta Crystallogr., Sect. A Fundam. Crystallogr.*, **64**, 112 (2008).
[28] G.M. Sheldrick. *Acta Crystallogr., Sect. C Cryst. Struct. Commun.*, **71**, 3 (2015).
[29] B. Klaus, Diamond, version 3.2, University of Bonn, Germany (1999).
[30] S. Kundu, B. Roy, B. Basu. *Beilstein J. Org. Chem.*, **10**, 26 (2014).
[31] M. Knorr, F. Guyon, A. Khatyr, C. Strohmann, M. Allain, S.M. Aly, A. Lapprand, D. Fortin, P.D. Harvey. *Inorg Chem.*, **51**, 9917 (2012).
[32] H.N. Peindy, F. Guyon, A. Khatyr, M. Knorr, C. Strohmann. *Eur. J. Inorg. Chem.*, **2007**, 1823 (2007).
[33] J.-R. Li, X.-H. Bu. *Eur. J. Inorg. Chem.*, **2008**, 27 (2008).
[34] J. Zhang, Y.-S. Xue, Y.-Z. Li, H.-B. Du, X.-Z. You. *Cryst. Eng. Comm.*, **13**, 2578 (2011).
[35] S. Saha, K. Biswas, B. Basu. *Tetrahedron Lett.*, **59**, 2541 (2018).

I&EC research
Industrial & Engineering Chemistry Research

Article

Cite This: Ind. Eng. Chem. Res. 2017, 56, 11726-11733

pubs.acs.org/IECR

Stabilized Cu_2O Nanoparticles on Macroporous Polystyrene Resins [Cu_2O@ARF]: Improved and Reusable Heterogeneous Catalyst for On-Water Synthesis of Triazoles via Click Reaction

Sujit Ghosh,[†] Sankar Saha,[†] Debasish Sengupta,[†] Shreyasi Chattopadhyay,[‡] Goutam De,*[,‡] and Basudeb Basu*[,†]

[†]Department of Chemistry, North Bengal University, Darjeeling 734013, India

[‡]CSIR−Central Glass & Ceramic Research Institute, 196, Raja S. C. Mullick Road, Jadavpur, Kolkata 700032, India

Supporting Information

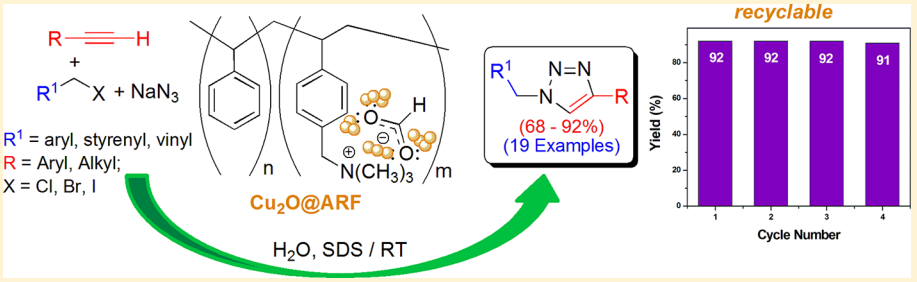

ABSTRACT: Amberlite resin formate (ARF) with a polyionic polar environment is successfully utilized as a unique support for immobilization of stabilized Cu_2O nanoparticles (NPs). The composite [Cu_2O@ARF] is characterized by FT−IR, XRD, XPS, HR−TEM, and ICP−AES analyses. The HR−TEM results confirm existence of fairly dispersed Cu_2O NPs with average diameter (∼5−7 nm) onto the resin surface, while ICP−AES analyses show loading of copper (10.8 mg) per gram of the resin composite (1.08 wt % of Cu). The ionic resin with counteranions ($HCOO^-$) could reduce precursor Cu(II) to Cu(I) and stabilize Cu_2O NPs. The as-synthesized composite acts as a robust, efficient, and recyclable catalyst for efficient construction of a 1,2,3-triazole ring under aqueous and aerobic conditions. The TOF (219 h^{-1}) is found significantly high as compared to that of some related existing catalysts (120 h^{-1}). The prowess of the catalyst is further demonstrated in the synthesis of a triazole-bearing antitumor drug molecule.

1. INTRODUCTION

The development of heterogeneous nanostructured catalysts for successful industrial applications is a rapidly growing field of research.[1] Primary objectives for commercial applications of heterogeneous nanocatalysts require certain features like cost-effective easy availability, high catalytic efficiency with turnover frequency, selectivity, significant recycling ability without leaching from the immobilizing surface, etc. In order to achieve this, precise control of the shape, size, and spatial distributions of nanoparticles (NPs) onto the surface as well as the stability of the nanocomposite remain as subtle features.[2] On the other hand, the type of reaction and conditions, where the nanocatalyst is being used, needs to be considered while designing and engineering the catalytic system. For example, the Cu-catalyzed azide−alkyne cycloaddition (CuAAC) reaction leading to the synthesis of 1,2,3-triazole represents an important reaction and finds applications in diverse technological fields including drug discovery.[3] A few examples of 1,4-disubstituted-1,2,3-1*H*-triazoles possessing diverse pharmacological activities are shown in Figure 1.

As a result, several heterogeneous-supported Cu(I) or Cu(II) catalysts have been developed to perform 1,2,3-triazole synthesis. A few among the myriad have been prepared and used as catalysts: polystyrene resin-supported CuI-cryptand-22-complex,[4] Cu(II) anchored with SBA-15,[5] Cu-loaded polymeric magnetic nanocatalyst,[6] $NiFe_2O_4$-glutamate-Cu,[7] magnetic nanobimetallic catalyst Fe_3O_4@TiO_2/Cu_2O,[8] NHC-based Cu(I) catalyst,[9,10] Cu_2On supported with reduced graphene oxide (RGO),[11] poly(vinyl alcohol) (PVA),[12] polyvinyl poly(1-vinylpyrrolidin-2-one) (PVP),[13] poly(4-vinylpyridine) (PVPy),[13] etc. However, most of the heterogeneous catalysts suffer from limitations. For example, lower stability of Cu_2O, agglomeration of Cu_2O NPs, use of precious ligand-based heterogeneous supports, addition of an extra reducing source while using a Cu(II) source, requirement of harsh reaction conditions for [3 + 2] cycloaddition, leaching of metal species, lower efficiency in recycling, etc. remain as major limitations.[14] Moreover, very few examples of heterogeneous catalysts are reported to work efficiently for on-water triazole synthesis.[14] As

Received: June 29, 2017
Revised: September 22, 2017
Accepted: September 26, 2017
Published: September 26, 2017

DOI: 10.1021/acs.iecr.7b02656
Ind. Eng. Chem. Res. 2017, 56, 11726−11733

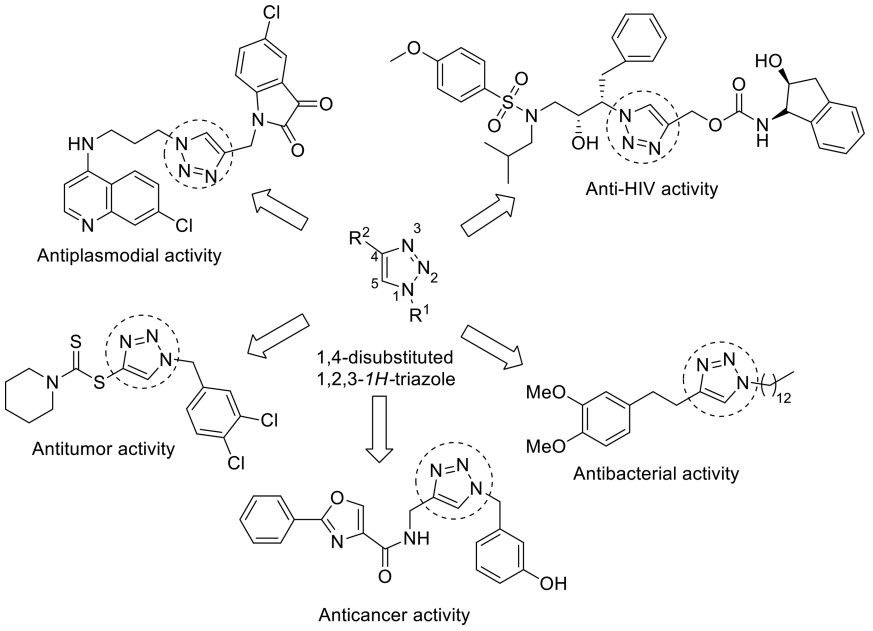

Figure 1. Representative biologically active pharmacophores bearing 1,4-disubstituted 1,2,3-triazole.

a result, the development of a simple, stable, and efficient catalytic system involving stabilized Cu_2O NPs with practical applicability and reusability to work under on-water and aerobic conditions is of immense interest as well as an important area of research for technological developments.

In connection with our interest in developing polymer-supported transition metal catalysts (both mono- and bimetallic) with the aid of polystyrene resins as suitable support,[15] here we demonstrate that unique polymeric resins with counter formate anions ($HCOO^-$) could not only reduce Cu(II) to Cu(I) species in a controlled manner but could also render necessary immobilizing ambiance through its polar microenvironment to stabilize Cu_2O NPs. Thus, no additional reductant, ligands, and capping agents are required. The as-synthesized stable composite [Cu_2O@ARF] with agglomeration-free uniformly dispersed Cu_2O NPs exhibits excellent catalytic performance in regioselective synthesis of 1,4-disubstituted-1,2,3-triazoles from alkyl halide, terminal alkyne, and sodium azide in water at room temperature. The prowess of the as-synthesized catalytic system [Cu_2O@ARF] as compared to other reported polymer-supported Cu(I) catalytic systems used in on-water triazole synthesis shows significantly high TOF and recyclability. The present work also demonstrates successful application of the catalytic system [Cu_2O@ARF] in the preparation of an antitumor drug molecule in aqueous medium, signifying commercial viability.

2. RESULTS AND DISCUSSION

2.1. Catalyst Preparation [Cu_2O@ARF]. Amberlite Resin Formate (ARF) was obtained according to a reported procedure.[15] Dry resin beads of ARF (1 g) were placed in a Teflon-capped sealed tube, and a solution of $Cu(OAc)_2{\cdot}H_2O$ (50 mg, 0.25 mmol) in 5 mL of dry distilled DMF was added to the ARF. The mixture was then heated at 120 °C for 1 h with occasional gentle shaking. The supernatant liquid became completely colorless by this time, and the white resin beads of ARF turned light brown. The color is expected because in the solid state of Cu_2O, the light of higher energy will only be absorbed. The resin beads were filtered off and washed repeatedly with DI water (4 mL × 5 mL) and acetone (4 mL × 5 mL) and then dried under vacuum to afford Cu_2O@ARF (Figure 2).

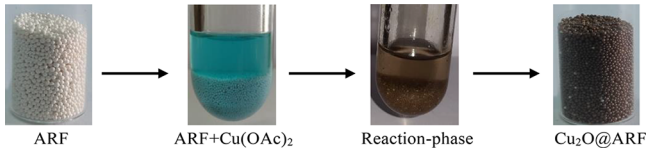

Figure 2. Digital images of different steps during preparation of Cu_2O@ARF.

2.2. Characterization of Cu_2O@ARF. The FT−IR spectra of Cu_2O@ARF were recorded and compared with the ARF. The peaks at about 1348 cm^{-1} (symmetric) and 1596 cm^{-1} (anti-symmetric) were observed in both ARF and Cu_2O@ARF species, which are attributed to the carboxylate anions ($HCOO^-$) of ARF (Figure S1, Supporting Information).

The powder XRD patterns of the Cu_2O@ARF composite (Figure 3) show an amorphous hump, which originated due to the presence of ARF. The Bragg diffraction patterns indicate the presence of phase-pure cuprous oxide (Cu_2O). The peak positions of the Cu_2O@ARF composite in the range from 30° to 80° are nearly similar to literature values for Cu_2O.[16,17] The distinguishable XRD peaks at (2θ values) 31.63°, 36.51°, 42.42°, 61.44°, and 73.69° belong to (110), (111), (200), (220), and (311) planes of Cu_2O respectively (JCPDS card no. 01-073-6371, Phase: Cu_2O). The ARF resins are amorphous in nature, and we did not observe any signals related to Cu_2O in its X-ray diffraction.[15]

The XPS analysis of the as-synthesized fresh catalyst confirms the existence of Cu_2O (Cu^+) only. The high resolution Cu 2p spectrum (Figure 4a) shows the presence of two distinct peaks at 932.30 and 952.12 eV without any appearance of satellite peaks, and the corresponding binding energies can be attributed to Cu $2p_{3/2}$ and Cu $2p_{1/2}$ of Cu^+, respectively.[18,19] Moreover, the peak located at 529.85 eV in the deconvoluted high resolution O 1s spectrum (Figure 4b) is also consistent with

DOI: 10.1021/acs.iecr.7b02656
Ind. Eng. Chem. Res. 2017, 56, 11726−11733

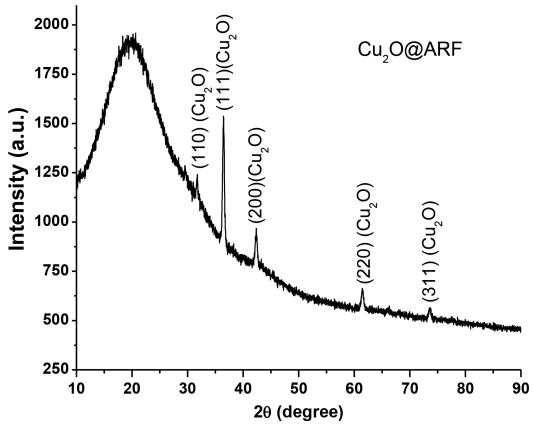

Figure 3. Powder XRD patterns of Cu_2O@ARF indicating the presence of Cu_2O.

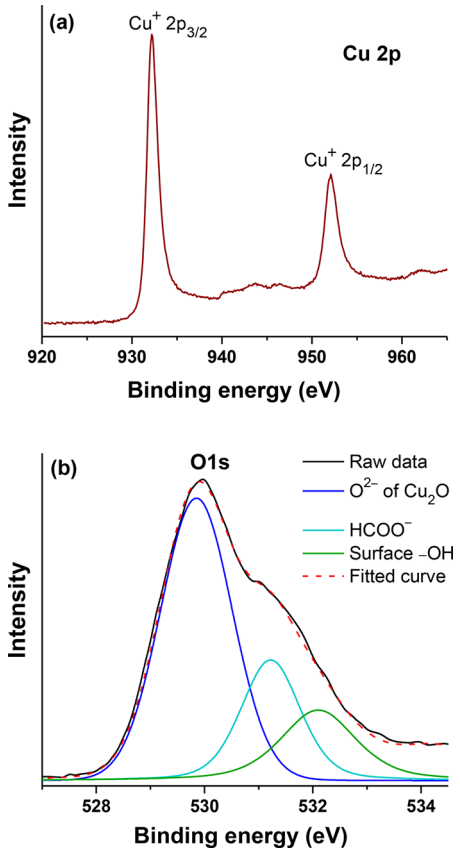

Figure 4. XPS spectra of fresh catalyst Cu_2O@ARF: (a) high resolution Cu 2p spectrum showing two distinct peaks for Cu^+ and (b) deconvoluted high resolution O 1s spectrum consistent with the presence of O associated with Cu_2O and ARF resin.

the presence of the Cu_2O chemical state.[19,20] In addition to that, peaks at 531.22 and 532.1 eV correspond (Figure 4b) to the adsorbed oxygen (surface OH) and oxygenated functional groups ($HCOO^-$) present in the resin system.[19,20] Thus, the XPS analysis fully corroborates the XRD result confirming that the Cu_2O particles have been formed by in situ reduction of the soaked Cu^{2+} salt (Cu acetate) inside the ARF at 120 °C.

HR−TEM analysis of the Cu_2O@ARF composite confirmed the presence of Cu_2O NPs embedded on the polyionic resin surface (Figure 5a). The high resolution TEM image (Figure 5b) shows the homogeneous distribution of Cu_2O NPs with

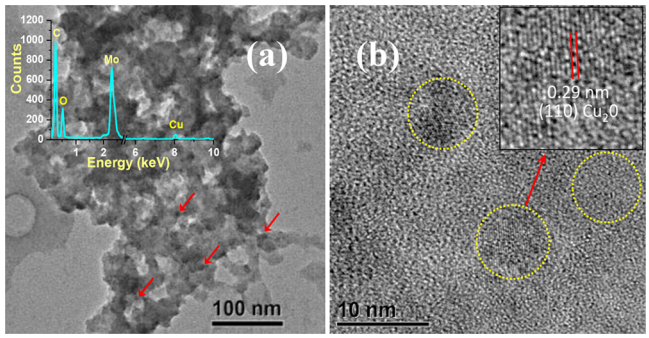

Figure 5. (a) TEM image of the composite material showing Cu_2O NPs embedded in the resin. Inset of (a) shows the EDS pattern of the sample. It confirms the presence of C, O, and Cu from the sample. Part of C and Mo are coming from the carbon-coated Mo grid used for TEM analysis. (b) HR-TEM showing the lattice fringes of Cu_2O nanoparticles. Magnified views of the (110) lattice plane are shown in the inset of (b).

diameters of ∼5−7 nm in the Cu_2O@ARF resin composite. Moreover, the lattice fringes present with d = 0.29 nm also (inset, Figure 5b) correspond to the (110) lattice of Cu_2O.[21]

The copper content in the resin composite, Cu_2O@ARF, was determined by ICP−AES analysis and found to be 10.8 mg of copper per gram of the resin composite (1.08 wt % of Cu). Thus, 1 g of resin nanocomposite (Cu_2O@ARF) contains 0.1699 mmol of copper.

2.3. Catalytic Activity of Cu_2O@ARF Nanocomposite in Triazole Synthesis by Three-Component Click Reaction. The three-component reaction methodology was optimized using benzyl bromide, phenyl acetylene, and sodium azide as the model reaction. The initial reaction was carried out in water at 60 °C in the presence of Cu_2O@ARF (50 mg $mmol^{-1}$ of alkyl halide) to afford the desired triazole in 75% isolated yield (Table 1, entry 1). Assuming the poor solubility

Table 1. Optimization of Reaction Conditions for Synthesis of Triazole

Entry	Solvent	Amount of SDS (mol %)	Temp (°C)	Time (h)	Catalyst (mg)	Yield (%)[a]
1	Water	Nil	60	2	50	75
2	Water:CH_3CN (1:1)	Nil	60	2	50	95
3	Water	10	60	2	50	95
4	Water	10	60	2	25	95
5	Water	10	60	2	15	81
6	Water	10	60	1	25	94
7	Water	10	40	1	25	92
8	**Water**	**10**	**RT**	**1**	**25**	**92**
9[b]	Water	10	RT	10	Nil	18

[a]Triazole obtained after purification by column chromatography. [b]Reaction performed without any catalyst Cu_2O@ARF.

of an organic compound in water, we tried the same reaction in a mixture of water:acetonitrile (v/v 1:1), which indeed gave excellent conversion (95%) (entry 2). The same problem could be overcome by using a phase transfer agent (sodium dodecyl sulfate; SDS) (entry 3). Decreasing the quantity of the catalyst (Cu_2O@ARF) to 25 mg afforded the triazole in same yield (entry 4). Further decreasing the amount of catalyst to 15 mg resulted in a lower yield (81%, entry 5). A much higher yield of

DOI: 10.1021/acs.iecr.7b02656
Ind. Eng. Chem. Res. 2017, 56, 11726−11733

Table 2. Cu_2O@ARF Catalyzed Three-Component Click Reaction in Aqueous and Aerobic Conditions at Room Temperature[a]

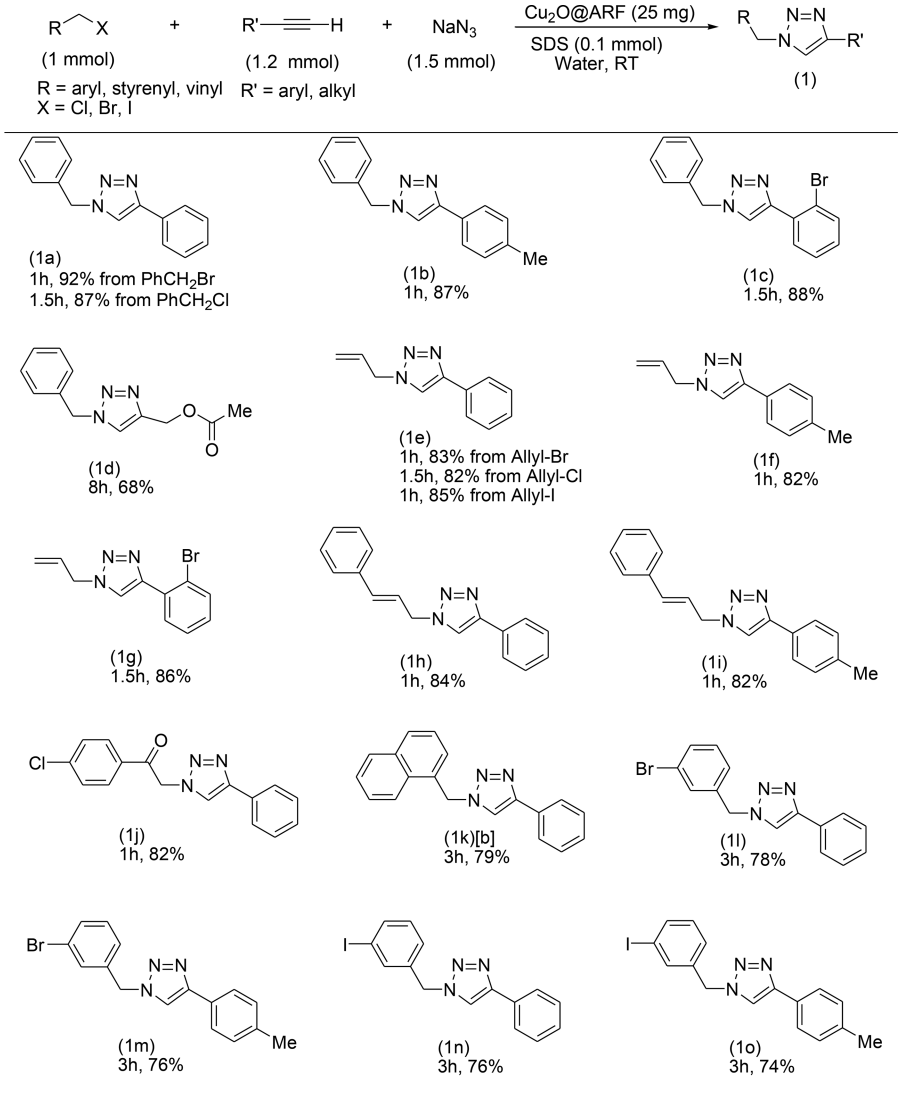

[a]Isolated yield of the product after purification through column chromatography. [b]Initially alkyl chloride and sodium azide were stirred at 40 °C for 1 h, and then, alkyne was added. The reaction continued at room temperature for 2 h.

triazole was obtained when the reaction was performed for 1 h keeping other aspects unchanged, i.e., 25 mg of catalyst and temperature 60 °C (94%, entry 6). Conducting the reaction at 40 °C also gave excellent yield within 1 h (92%, entry 7). The catalytic system is highly efficient as demonstrated in carrying out the reaction at room temperature to afford the product in 92% yield within 1 h (entry 8). In a control experiment, the reaction furnished the product in only 18% yield, signifying the prominent role of the heterogeneous catalyst (entry 9).

Encouraged by high catalytic activity of the resin-bound nanocomposite [Cu_2O@ARF] in the three-component reaction that leads to the substituted triazoles selectively under mild and aqueous conditions, we extended the optimized conditions (Table 1, entry 8) to a series of terminal alkynes and alkyl halides. The results are presented in Table 2 (see Experimental Section for general procedure of triazole synthesis). Aromatic alkynes afforded the corresponding triazole derivatives in good to excellent yields with benzyl bromide and sodium azide (**1a**−**1c** and **1e**−**1o**). However, the reactivity of aliphatic alkyne was somewhat lower than aromatic alkyne (**1d**). The variation of substrates in the alkyl halide was also tested. Other alkyl halides such as allyl bromide and cinnamyl bromide successfully produced corresponding olefin-substituted triazole derivatives. Another functionalized triazole derivative (**1j**) was prepared in 82% yield using 2-bromo-1-(4-chlorophenyl)ethanone. Besides alkyl bromide, other organic halides such as benzyl chloride, allyl chloride, and allyl iodide were also tested for this three-component click reaction affording successful conversion to triazole derivatives in good to excellent yields. In the case of 1-chloromethyl naphthalene, the three-component reaction did not proceed well at room temperature, which was however circumvented by heating the reaction mixture at 40 °C for 3 h (**1k**). Other representatives of benzyl bromide-bearing halides (bromo, iodo) also afforded the desired triazole derivatives in good yield (**1l**−**1o**) with aromatic alkyne in the presence of NaN_3. It is thus noteworthy that the catalyst was found to be quite active to a large variety of combinations affording the desired product in high yield under apparently mild and on-water conditions. All triazole derivatives (**1a**−**1o**) were characterized by FT−IR, ^{1}H−NMR, and ^{13}C−NMR spectral

DOI: 10.1021/acs.iecr.7b02656
Ind. Eng. Chem. Res. 2017, 56, 11726−11733

data and also by melting points for solid compounds (see characterization data (pp S2−S6) and scanned copy of NMR spectra of compounds **1a−1o** (pp S7−S38) in the Supporting Information).

2.4. Reusability and Stability of Cu_2O@ARF. To validate the reusability of the heterogeneous catalyst, we performed recycling experiments in the model click reaction of benzyl bromide, phenyl acetylene, and sodium azide. The reaction was carried out under the optimized conditions (Table 1, entry 8). After completion of the reaction, the catalyst (resin beads) was filtered off, washed with water (4 mL × 5 mL) and acetone (3 mL × 5 mL), and dried under vacuum and reused for the second run. The catalytic activity remains fairly consistent up to consecutive fourth run as tested without any significant drop in the yield of the product (Table 3). We measured the copper content in Cu_2O@ARF before and after the recycling runs. As shown by ICP−AES measurements, before the reaction, the copper content in Cu_2O@ARF (25 mg) was 0.0042 mmol, while those found after the first and third runs were 0.0039 and 0.0037 mmol, respectively. This indicates that no significant leaching of copper occurred from the polymeric resin surface during the reaction (see Experimental Section for recovery and reusability of the catalyst Cu_2O@ARF).

Table 3. Catalyst Recycling Experiments

Sl No	Time (h)	Yield (%)[a]	Cu content (mmol)[b]
first run	1	92	0.0042
second run	1	92	0.0039
third run	1	92	–
fourth run	1	91	0.0037

[a]Yield represents isolated after chromatography. [b]ICP−AES analyses of fresh Cu_2O@ARF (25 mg) or recovered after first and third runs.

In order to further establish about leaching of metallic species during the catalytic process, we performed midway filtration tests using the reaction partners benzyl bromide, phenyl acetylene, and sodium azide, as done in other reactions using a heterogeneous catalyst.[22] In this process, we carried out three sets of experiments using the catalyst [Cu_2O@ARF] for 10, 20, and 40 min, filtered off the catalyst in each case, and continued the reaction without the catalyst for 50, 40, and 20 min, respectively. Aliquots were taken at different times before and after filtering the catalyst in each experiment and analyzed by HPLC to quantify the formation of triazole in each case. As presented in Figure 6, it is shown that while there was conversion of triazole 34.6% (after 10 min), 53.8% (after 20 min), and 77.0% (after 40 min) in the presence of the catalyst, after removing the catalyst and carrying out the reaction for rest of 1 h showed no appreciable changes in conversion to triazole. These experiments indicate the heterogeneity of the catalyst during catalytic process (see Figures S2−S10 in the Supporting Information for HPLC chromatograms).

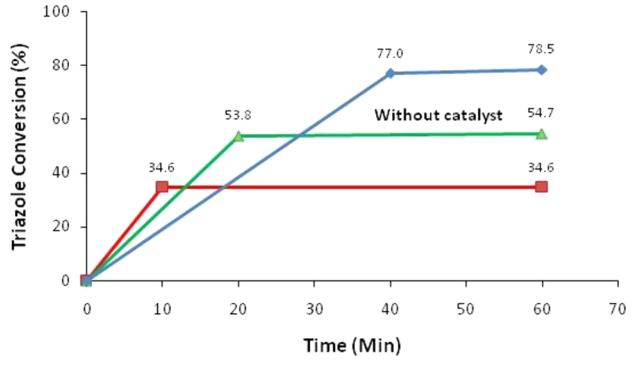

Figure 6. Three sets of midway filtration tests at different time intervals showing conversion of triazole with or without the catalyst.

The powder XRD of the recovered catalysts after the first and fourth runs were also undertaken to analyze any change in the composition that occurred after catalysis. The XRD patterns of these recovered catalysts (Figure 7) were found to be almost similar as observed in the fresh catalyst (Figure 3) before the reaction. This result indicates no significant change in the nature of the catalyst during the catalytic process.

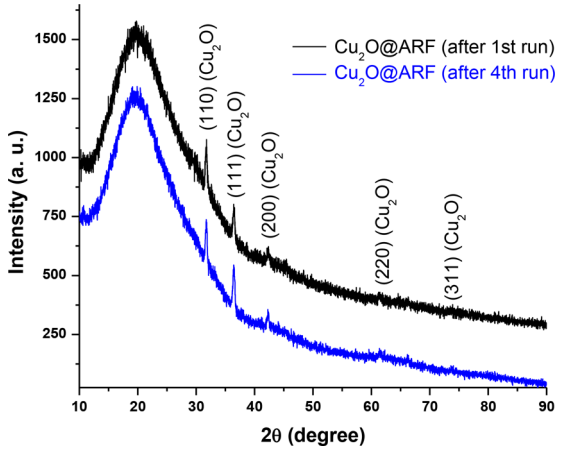

Figure 7. Powder XRD patterns of the recovered Cu_2O@ARF after the first and fourth cycles.

2.5. Plausible Mechanism. The proposed mechanism of the click reaction is believed to be similar as established for other Cu(I) catalysts.[23] The formation of an alkynyl copper intermediate from alkyne in the presence of Cu(I) species of Cu_2O@ARF undergoes cycloaddition with alkyl azide (in situ formed from alkyl halide and sodium azide) to form the intermediate (A). Finally, protonation of the C−Cu bond[24] affords the desired triazole product (Figure 8).

2.6. Comparison of Catalytic Activity. Comparison of catalytic activity with other reported heterogeneous catalytic systems that performed three-component triazole synthesis under on-water and room temperature conditions in terms of turn over frequency (TOF) was done, as shown in Table 4. Our catalytic system exhibits nearly double TOF (219 h^{-1}) as compared to existing systems (maximum 120 h^{-1}), which is attributed to the availability of more active Cu_2O NPs on the surface of Amberlite resins and stabilized by formate anions.

2.7. Broadening the Scope of the Catalyst. With a view to further extend the scope of the catalyst in a synthetic protocol, we employed Cu_2O@ARF in a reaction that leads to the synthesis of a triazole-based dithiocarbamate (**2**), which is known to exhibit antitumor activity.[25] We conducted the experiment using a combination of benzyl bromide, pyrolidine-1-carbodithioate and sodium azide in the presence of Cu_2O@ARF in aqueous medium at 35 °C, which gave rise to the formation of compound (**2**) in 82% yield (Scheme 1). This demonstrates that the present catalytic system could be technologically viable in constructing triazole-bearing drug molecules (see the Experimental Section for the synthesis of

DOI: 10.1021/acs.iecr.7b02656
Ind. Eng. Chem. Res. 2017, 56, 11726−11733

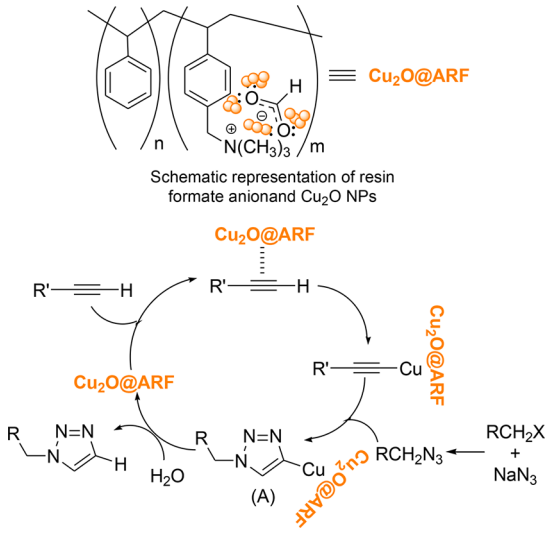

Figure 8. Proposed mechanism of the three-component click reaction using Cu_2O@ARF.

Table 4. Comparison of On-Water Triazole Synthesis Using Some Cu(I) Catalytic Systems and Our Catalyst at Room Temperature (without reducing source)

Entry	Catalyst	Mol% (Cu)	TOF (h^{-1})	Ref
1	PS−C22−CuI	0.6	11	4
2	Cu(NHC)Cl	0.5	120	9
3	H_4N^+-tagged SIPr−Cu(I)	5.0	6.53	10
4	**Cu_2O@ARF**	**0.42**	**219**	**Present work**

triazole compound (**2**); S2 and S3 in Supporting Information for the characterization data and scanned copy of NMR spectra).

3. CONCLUSIONS

In conclusion, we have developed a robust heterogeneous catalytic system [Cu_2O@ARF] and applied in the regioselective synthesis of diversely functionalized 1,2,3-triazoles via a three-component "click" reaction of alkyl halide, terminal alkyne, and sodium azide in water at room temperature. Aqueous reaction media, ambient reaction conditions, high yields, wide substrate scope, and easy recovery of the catalyst by simple filtration are some notable features. The catalytic system works efficiently in the synthesis of dithiocarbamate-containing triazole, a potential bioactive scaffold possessing antitumor activity, signifying its prospects in technological development. Moreover, the TOF has been found to be significantly high as compared to some other Cu(I)-based catalytic systems that work under on-water synthesis of triazoles. The enhanced catalytic performance and robustness of the catalytic system are due to the high surface area of Cu_2O NPs of average size ∼5−7 nm and their stabilized distributions on the macroporous resin matrices with the aid of counter formate anions.

4. EXPERIMENTAL SECTION

4.1. General Information. All the reagents were purchased from Sigma−Aldrich and used directly without further purification. The solvents were purchased from commercial suppliers and used after distillation. All the products were purified by column chromatography on 60−120 mesh silica gels (SRL, India). For tlc, Merck plates coated with silica gel 60, F_{254}, were used. The FT-IR spectra were recorded in Perkin Elmer, RXI spectrometer in KBr pellet for solid samples and in neat for liquid samples. The ^1H and ^{13}C NMR spectra were recorded at 300 and 75 MHz, respectively, on a Bruker AV 300 spectrometer in $CDCl_3$. Splitting patterns of protons were described as s (singlet), d (doublet), t (triplet), dd (doublet of doublet), and m (multiplet). Chemical shifts were reported in parts per million (δ) relative to TMS as the internal standard. J values (coupling constant) were reported in Hz (Hertz). ^{13}C NMR spectra were recorded with complete proton decoupling ($CDCl_3$: δ 77.0 ppm). The powder X-ray diffraction (PXRD) patterns were recorded using the Rigaku Smart Lab (9 kW) diffractometer using Cu Kα radiation. ICP−AES was measured in an inductively coupled plasma atomic emission spectrometry of Spectro Ciros Vision, Germany. X-ray photoelectron spectroscopy (XPS) analysis of the as-prepared catalyst was done with a PHI 5000 Versa probe II XPS system having a source of Al Kα and charge neutralizer at room temperature with a base pressure at 6×10^{-10} mbar. Transmission electron microscopy (TEM) of the samples was carried out with a Tecnai G2 30ST (FEI Company) operating at 300 kV and a JEOL JEM-2100F (FEG) operating at 200 kV. To prepare the TEM sample, a small amount of grinded sample was first dispersed in acetone. Then, one small drop of this dispersion was applied to a carbon-coated molybdenum grid. HPLC analyses were carried out using HPLC of the Agilent 1260 Infinity series and column: ZORBAX RX-SIL (5 μm, 4.6 mm × 150 mm), with an eluent of 10% ethyl acetate in n-hexane (flow rate: 2 mL/min).

4.2. General Procedure for Synthesis of 1,2,3-Triazole Derivative. In a 25 mL round-bottomed flask, a mixture of alkyl halide (1 mmol), terminal alkyne (1.2 mmol), sodium azide (1.5 mmol), SDS (0.1 mmol), and Cu_2O@ARF (25 mg) was taken, and then, 2 mL of water was added to it. The whole mixture was stirred at room temperature with a small magnetic bar under open air. The reaction was monitored by tlc, and after satisfactory conversion, the catalyst was filtered off and washed with ethyl acetate (3 mL × 5 mL). The organic part was separated from the aqueous part and then collected by passing over anhydrous Na_2SO_4. Evaporation of the solvent afforded the crude product, which was purified by column chromatography over silica gel.

Scheme 1. Synthesis of Pharmaceutically Active Triazole Compound (2) Catalyzed by Cu_2O@ARF

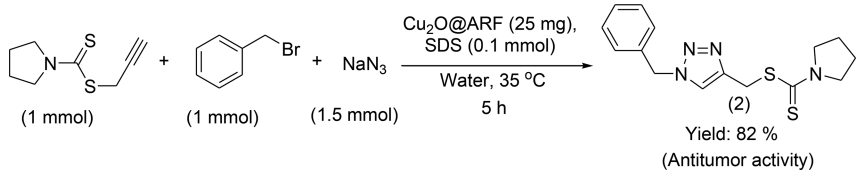

DOI: 10.1021/acs.iecr.7b02656
Ind. Eng. Chem. Res. 2017, 56, 11726−11733

4.3. Procedure for Recovery and Reusability of the Catalyst [Cu_2O@ARF]. As above, the catalyst resin beads left on the filter paper were washed successively with water (4 mL × 5 mL) and acetone (3 mL × 5 mL) and finally dried under a vacuum pump for further use in a recycled run. For each recycled experiment, a similar recovery procedure was followed.

4.4. Procedure for Synthesis of Dithiocarbamate-Based Triazole Compound (2). In a 25 mL round-bottomedf flask, a mixture of *S*-propargyl pyrrolidine-1-carbodithioate (1 mmol), benzyl bromide (1 mmol), sodium azide (1.5 mmol), SDS (0.1 mmol), and Cu_2O@ARF (25 mg) was taken in water (2 mL) and stirred with a bar magnet at 35 °C for 5 h under open air. With this, tlc showed a disappearance of starting material. Therefore, the reaction was stopped, and the catalyst was filtered off as above. The resin beads were washed with ethyl acetate (3 mL × 5 mL) and combined with an organic layer, then, as above, was separated out from the water and dried over anhydrous Na_2SO_4. Evaporating the organic solvent afforded an oily residue which was purified by column chromatography over silica gel, and eluting with light petroleum:ethyl acetate (4:1) afforded the desire triazole derivative (**2**) as a dark yellow solid: yield, 82%; mp, 70−72 °C (lit.[25] 73−74 °C).

■ ASSOCIATED CONTENT

Supporting Information

The Supporting Information is available free of charge on the ACS Publications website at DOI: 10.1021/acs.iecr.7b02656.

FT−IR spectra of ARF and Cu_2O@ARF (Figure S1), characterization data (melting point for solid compounds, FT−IR, ^1H and ^{13}C NMR), scanned copies of NMR spectra of all triazole compounds (**1a**−**1o** and **2**), chromatograms of HPLC analyses (Figure S2−S10), and references (Figure S5). (PDF)

■ AUTHOR INFORMATION

Corresponding Authors

*E-mail: gde@cgcri.res.in. Fax: +91 33 24730957. Tel: +91 33 23223403.

*E-mail: basu_nbu@hotmail.com. Fax: +91 353 2699001. Tel: +91 353 2776381.

ORCID

Goutam De: 0000-0003-0271-1634

Basudeb Basu: 0000-0002-7993-2964

Notes

The authors declare no competing financial interest.

■ ACKNOWLEDGMENTS

This work was supported by the Science and Engineering Research Board of India (Grant No. EMR/2015/000549). CSIR New Delhi (D.S.) and UGC (S.G. and S.C.) are thankfully acknowledged for the award of fellowships.

■ REFERENCES

(1) Schmal, M. *Heterogeneous Catalysis and its Industrial Applications*; Springer: Switzerland, 2016.

(2) Friend, C. M.; Xu, B. Heterogeneous catalysis: A central science for a sustainable future. *Acc. Chem. Res.* **2017**, *50*, 517−521.

(3) Totobenazara, J.; Burke, A. J. New click−chemistry methods for 1,2,3-triazoles synthesis: recent advances and applications. *Tetrahedron Lett.* **2015**, *56*, 2853−2859.

(4) Movassagh, B.; Rezaei, N. Polystyrene resin-supported CuI-cryptand-22-complex: a highly efficient and reusable catalyst for three-component synthesis of 1,4-disubstituted 1,2,3-triazoles under aerobic conditions in water. *Tetrahedron* **2014**, *70*, 8885−8892.

(5) Roy, S.; Chatterjee, T.; Pramanik, M.; Roy, A. S.; Bhaumik, A.; Islam, S. M. Cu(II)-anchored functionalized mesoporous SBA-15: An efficient and recyclable catalyst for the one-pot Click reaction in water. *J. Mol. Catal. A: Chem.* **2014**, *386*, 78−85.

(6) Pourjavadi, A.; Tajbakhsh, M.; Farhang, M.; Hosseini, S. H. Copper-loaded polymeric magnetic nanocatalysts as retrievable and robust heterogeneous catalysts for click reactions. *New J. Chem.* **2015**, *39*, 4591−4600.

(7) Lu, J.; Ma, E.-Q.; Liu, Y.-H.; Li, Y.-M.; Mo, L.-P.; Zhang, Z.-H. One-pot three-component synthesis of 1,2,3-triazoles using magnetic $NiFe_2O_4$−glutamate−Cu as an efficient heterogeneous catalyst in water. *RSC Adv.* **2015**, *5*, 59167−59185.

(8) Nemati, F.; Heravi, M. M.; Elhampour, A. Magnetic nano-Fe_3O_4@TiO_2/Cu_2O core-shell composite: an efficient novel catalyst for the regioselective synthesis of 1,2,3-triazoles using a click reaction. *RSC Adv.* **2015**, *5*, 45775−45784.

(9) Purohit, V. B.; Karad, S. C.; Patel, K. H.; Raval, D. K. Cu(N-heterocyclic carbene)chloride: an efficient catalyst for multicomponent click reaction for the synthesis of 1,2,3-triazoles in water at room temperature. *RSC Adv.* **2014**, *4*, 46002−46007.

(10) Wang, W.; Wu, J.; Xia, C.; Li, F. Reusable ammonium salt-tagged NHC−Cu(I) complexes: preparation and catalytic application in the three component click reaction. *Green Chem.* **2011**, *13*, 3440−3445.

(11) Roy, I.; Bhattacharyya, A.; Sarkar, G.; Saha, N. R.; Rana, D.; Ghosh, P. P.; Palit, M.; Das, A. R.; Chattopadhyay, D. In situ synthesis of a reduced graphene oxide/cuprous oxide nanocomposite: a reusable catalyst. *RSC Adv.* **2014**, *4*, 52044−52052.

(12) Hajipour, A. R.; Mohammadsaleh, F. Polyvinyl alcohol−stabilized cuprous oxide particles: efficient and recyclable heterogeneous catalyst for azide−alkyne cycloaddition in water at room temperature. *J. Iran. Chem. Soc.* **2015**, *12*, 1339−1345.

(13) Abdulkin, P.; Moglie, Y.; Knappett, B. R.; Jefferson, D. A.; Yus, M.; Alonso, F.; Wheatley, A. E. H. New routes to Cu(I)/Cu nanocatalysts for the multicomponent click synthesis of 1,2,3-triazoles. *Nanoscale* **2013**, *5*, 342−350.

(14) Gawande, M. B.; Goswami, A.; Felpin, F.-X.; Asefa, T.; Huang, X.; Silva, R.; Zou, X.; Zboril, R.; Varma, R. S. Cu and Cu-Based Nanoparticles: Synthesis and Applications in Catalysis. *Chem. Rev.* **2016**, *116*, 3722−3811.

(15) Sengupta, D.; Saha, J.; De, G.; Basu, B. Pd/Cu bimetallic nanoparticles embedded in macroporous ion-exchange resins: an excellent heterogeneous catalyst for the Sonogashira reaction. Pd/Cu bimetallic nanoparticles embedded in macroporous ion-exchange resins: an excellent heterogeneous catalyst for the Sonogashira reaction. *J. Mater. Chem. A* **2014**, *2*, 3986−3992.

(16) Zhang, Z.; Dong, C.; Yang, C.; Hu, D.; Long, J.; Wang, L.; Li, H.; Chen, Y.; Kong, D. Stabilized Copper(I) Oxide Nanoparticles Catalyze Azide-Alkyne Click Reactions in Water. *Adv. Synth. Catal.* **2010**, *352*, 1600−1604.

(17) Jayaramulu, K.; Suresh, V. M.; Maji, T. K. Stabilization of Cu_2O nanoparticles on a 2D metal−organic framework for catalytic Huisgen 1,3-dipolar cycloaddition reaction. *Dalton Trans.* **2015**, *44*, 83−86.

(18) Wang, Y.; Lü, Y.; Zhan, W.; Xie, Z.; Kuang, Q.; Zheng, L. Synthesis of Porous Cu_2O/CuO Cages using Cu-based Metal-Organic-Framework as Templates and their Gas-sensing Properties. *J. Mater. Chem. A* **2015**, *3*, 12796−12803.

(19) Deo, M.; Mujawar, S.; Game, O.; Yengantiwar, A.; Banpurkar, A.; Kulkarni, S.; Jog, J.; Ogale, S. Strong photo-response in a flip-chip nanowire p-Cu_2O/n-ZnO junction. *Nanoscale* **2011**, *3*, 4706−4712.

(20) Khan, I. A.; Badshah, A.; Nadeem, M. A.; Haider, N.; Nadeem, M. A. A copper based metal-organic framework as single source for the synthesis of electrode materials for high-performance super capacitors and glucose sensing applications. *Int. J. Hydrogen Energy* **2014**, *39*, 19609−19620.

DOI: 10.1021/acs.iecr.7b02656
Ind. Eng. Chem. Res. 2017, 56, 11726−11733

(21) Kumar, B.; Saha, S.; Ganguly, A.; Ganguli, A. K. A facile low temperature (350 °C) synthesis of Cu_2O nanoparticles and their electrocatalytic and photocatalytic properties. *RSC Adv.* **2014**, *4*, 12043−12049.
(22) Ji, Y.; Jain, S.; Davis, R. J. Investigation of Pd Leaching from Supported Pd Catalysts during the Heck Reaction. *J. Phys. Chem. B* **2005**, *109*, 17232−17238.
(23) Zhang, W.; Ren, B.; Jiang, Y.; Hu, Z. Carboxymethylpullulan promoted Cu_2O-catalyzed Huisgen-click reaction. *RSC Adv.* **2015**, *5*, 12043−12047.
(24) Wang, C.; Ikhlef, D.; Kahlal, S.; Saillard, J.-Y.; Astruc, D. Metal-catalyzed azide-alkyne "click" reactions: Mechanistic overview and recent trends. *Coord. Chem. Rev.* **2016**, *316*, 1−20.
(25) Li, Q.-H.; Ding, Y.; Huang, N.-W. Synthesis and biological activities of dithiocarbamates containing 1,2,3-triazoles group. *Chin. Chem. Lett.* **2014**, *25*, 1469−1472.

DOI: 10.1021/acs.iecr.7b02656
Ind. Eng. Chem. Res. 2017, 56, 11726−11733